Etude mathématique et numérique de quelques modèles cinétiques et de leurs asymptotiques : limites de diffusion et de diffusion anormale

Hélène Hivert

ANNÉE 2016

UNIVERSITÉ DE RENNES 1

UNIVERSITE BRETAGNE LOIRE

THÈSE / UNIVERSITÉ DE RENNES 1
sous le sceau de l'Université Bretagne Loire

pour le grade de

DOCTEUR DE L'UNIVERSITÉ DE RENNES 1

Mention : Mathématiques et applications

Ecole doctorale Matisse

présentée par

Hélène Hivert

Préparée à l'unité de recherche UMR 6625-IRMAR
Institut de recherche mathématiques de Rennes
UFR de mathématiques

Étude mathématique et numérique de quelques modèles cinétiques et de leurs asymptotiques : limites de diffusion et de diffusion anormale.

Thèse soutenue à Rennes le 5 octobre 2016

devant le jury composé de :

Vincent CALVEZ
Directeur de recherche CNRS, université de Lyon 1 / *rapporteur*

Axel KLAR
Professeur, université de Kaiserslautern / *rapporteur*

Florian MEHATS
Professeur, université de Rennes 1 / *examinateur*

Luc MIEUSSENS
Professeur, Institut polytechnique de Bordeaux / *examinateur*

Marjolaine PUEL
Professeur, université de Nice / *examinatrice*

Mohammed LEMOU
Directeur de recherche CNRS, université de Rennes 1 / *directeur de thèse*

Nicolas CROUSEILLES
Chargé de recherche Inria, Rennes / *co-directeur de thèse*

Remerciements

Tout d'abord, je tiens à remercier Florian Méhats, Luc Mieussens et Marjolaine Puel d'avoir accepté de faire partie de mon jury de thèse et Vincent Calvez et Axel Klar de l'avoir rapportée. J'ajoute que j'ai la chance d'avoir commencé un postdoc sous la direction de Vincent et je l'en remercie également. Je n'aurais pas pu faire ce travail sans l'encadrement et les conseils de mes deux directeurs, Nicolas Crouseilles et Mohammed Lemou. Je les remercie pour leur soutien, leur disponibilité, leur exigence, la confiance qu'ils m'ont accordée et pour l'autonomie qu'ils m'ont laissée en fin de thèse, tout cela a été très formateur. Je remercie également Julie et Marine, relectrices attentives et bénévoles de l'introduction de cette thèse.

Presque indépendamment de mes travaux de thèse, j'ai eu la chance de participer au CEMRACS 2015. Je remercie les organisateurs pour la qualité du séjour et de nous avoir ainsi permis de nous concentrer sur les seuls problèmes (de maths) auxquels nous avons été confrontés. Avec Andrea Bondesan et Colin Mietka, j'ai participé au projet proposé par le groupe CDMath. Je tiens à remercier Yohan Penel, Jonathan Jung et Stéphane Dellacherie pour leur implication dans la conduite du projet, leur patience face à nos erreurs et leur sympathie, ainsi que Gloria Faccanoni pour son aide.

Au cours de ma thèse, j'ai effectué mon monitorat à l'ENS Rennes dont je remercie toute l'équipe pour son accueil. Je tiens à remercier tout particulièrement Benjamin, collègue des plus agréables avec qui j'ai collaboré pour la quasi-totalité de mes missions d'enseignement. La vie du département de maths de l'ENS Rennes est rythmée par le groupe de travail du mercredi, et il faut bien dire que ~~la crêperie va~~ les exposés vont me manquer.

D'une manière un peu moins sérieuse (mais tout de même un peu, car c'est une personne très sérieuse), j'ai tellement de raisons de remercier Julie qu'elle va avoir le droit à un paragraphe à elle toute seule. Depuis cet instructif stage aux Pays-Bas dont nous sommes revenues avec un goût certain pour l'analyse numérique, et bien qu'elle m'ait abandonnée pour s'exiler de son plein gré dans la campagne normande, elle a été une indéfectible amie. Par exemple, elle m'a souvent rappelé de prendre mon manteau quand il faisait froid, me sauvant sans doute d'une mort atroce, froide et humide. Durant les trois ans que nous avons passé dans le même bureau (comme si ça ne suffisait pas que nous passions déjà quasiment toute notre vie ensemble...), elle s'est merveilleusement bien occupée de Vanna Scoma, Erwan, Tigrou, Pôv'Chérie et moi (j'omets volontairement PPN8, qui est aussi très joli tout sec). Bien qu'elle ne se l'avoue pas, elle adore mon humour et elle me soutient presque toujours quand mes blagues n'ont pas l'effet escompté. Je la remercie aussi pour toutes ces vacances passées ensemble, parce qu'elle aime les livres, les gâteaux et le thé (même si il est souvent vert), parce qu'elle est toujours au bout du téléphone quand il faut, parce que dans l'immédiat je n'arrive même pas à trouver un truc vache à dire tellement elle me manque et enfin parce qu'elle a fini par m'offrir cet éclair au chocolat !

Je tiens aussi à remercier les membres de l'IRMAR et particulièrement Marie-Aude, Chantal, Carole, Hélène, Nicole, Xhensila et le reste de l'équipe administrative dont l'efficacité transforme les mystères de l'administration en de simples formalités. J'ai fait partie de l'équipe INRIA IPSO, dont je remercie également l'équipe administrative. Je veux également remercier les organisateurs des journées Louis Antoine de m'avoir donné l'opportunité d'y présenter un exposé au cours de ma troisième année de thèse.

La vie à l'IRMAR ne serait pas complète sans les doctorants qui y pullulent. Par ordre d'apparition, je remercie mes cobureaux successifs Rania, Hassina et Gregory (qui m'a régulièrement prêté mon chargeur). Je remercie aussi tous les membres du Fat Day, qui ont ajouté

leur grain de sucre à nos thèses. Enfin, je veux remercier Florian #ôflo pour toutes les poules, les moutons et les lamas, Ophélie car elle a été bien plus efficace que moi pour co-organiser le séminaire Landau, Arnaud pour toutes les informations qu'il possède toujours, Blandine pour ses gâteaux, Maxime qui a un don extraordinaire pour les macarons, Jean-Philippe pour sa visite impromptue à Metz, Richard qui a presque réussi à me faire aimer l'Ice Tea, Christian et Federico pour leurs super soirées, Néstor pour son enthousiasme, Türkü qui m'a fait découvrir le Raki, Mac qui -je l'espère- sait maintenant faire du vélo, Axel parce qu'il a des goûts indiscutables quand il choisit un appartement, Alex parce qu'il a des goûts discutables quand il choisit un tee shirt, Yvan que je surveille de près, Vincent qui fait maintenant partie de ma famille, Basile et Coralie qui font des voyages qui font rêver, Adrien et Marine à qui je souhaite beaucoup de bonheur, Hélène H. qui me permet de donner un ton mégalo à ces remerciements (et j'adore ça), Damien et Charles qui sont pourtant à peu près d'accord en politique, Tristan pour les discussions poney, Salomé pour toutes nos discussions, Tristan qui a réussi à me faire trouver des p-adiques intéressants, et tous les autres doctorants que j'ai côtoyés, avec qui j'ai mangé (je n'irai pas jusqu'à remercier le RU) et que j'ai oubliés ici.

Je tiens aussi à remercier tous ceux que j'ai croisés durant mes études à Rennes, et en particulier l'agence matrimoniale Guillaume et Mama, Ludo avec qui j'ai toujours beaucoup de plaisir à parler de maths, Charlotte pour ses bons conseils littéraires et les souvenirs des Pays-Bas, Xavier pour son accueil à Bordeaux, Simon parce qu'on finit toujours par s'écrire, Victor pour son amitié et parce qu'il a eu la bonne idée d'habiter à Lyon et tous les gens qui ont participé à la belle aventure de la Compagnie Vert. Au CEMRACS, j'ai eu l'occasion de découvrir Clémentine qui est la meilleure coloc de tous les temps, Guillaume et Matthieu que je remercie de m'avoir invitée dans l'Est. Je remercie également Matteo car il va m'inviter à Barcelone bien qu'il ne le sache pas encore et Romain, Alexandre, Laura, Ranine, Nora et tous les autres participants pour les six semaines passées en bonne compagnie. Avant de commencer à remercier des gens qui ne font pas de maths -car, aussi étonnant que cela puisse paraître, il y en a- je veux remercier tous les profs de maths croisés au cours de ma scolarité. En particulier, je remercie M. Mounzil qui m'a convaincue d'oser me lancer dans tout ça.

J'ai fait de belles rencontres à Rennes, dont Fabien, Corentin, Xavier, Olivier et Clément. Je veux aussi remercier Perrine, Joanna, Sylvain, Charlotte, Estelle et tous ceux qui ont participé aux apéros bi-hebdomadaires d'après le poney. En remontant à plus loin, je remercie Alice d'avoir réussi à ne pas perdre le contact depuis nos années d'adolescence (qui a dit qu'elles étaient ingrates ?), et Jérémie qui a refait surface de la manière la plus inattendue qui soit. J'ai une pensée particulière pour Cécile avec qui je ne parle plus aux arbres mais que je connais depuis vingt ans tout juste, même si ça ne nous rajeunit pas du tout et pour Guillaume qui m'a fait découvrir, il y a longtemps maintenant, que le thé ne poussait pas forcément dans des sachets. Je tiens aussi à remercier l'ensemble de la Compagnie A Tout Va pour l'accueil chaleureux qu'ils me réservent toujours.

Je remercie Samy qui me supporte depuis déjà longtemps et qui a toujours réussi à remettre de l'insouciance, des grasses matinées et des gros dèj au milieu de toutes mes activités sérieuses. En plus de m'aider à engraisser la SNCF, il m'a permis de rencontrer un nombre incroyable de manceaux fort sympathiques et je salue au passage Kamal, Clément, Quentin et Anaïs. Je remercie aussi toute sa famille pour l'accueil qu'ils m'ont réservé.

Enfin, je tiens à remercier mes parents qui m'ont toujours poussée et encouragée dans mes études, ma ssœur qui est officiellement la seule à pouvoir me suivre dans un zoo ou un aquarium sans souffrir, ainsi que toute ma famille.

Table des matières

Résumé détaillé de la thèse

Équations cinétiques et limites de diffusion anormale

L'objet de cette thèse est l'étude de schémas *asymptotic preserving* pour les équations cinétiques avec limite de diffusion anormale. Les équations cinétiques décrivent l'évolution d'une distribution de particules qui dépend des variables de temps $t \geq 0$, d'espace $x \in \mathbb{R}^d$ et de vitesse $v \in V \subset \mathbb{R}^d$, où l'espace des vitesses V est supposé symétrique par rapport à l'origine. Les modèles cinétiques correspondent à une échelle intermédiaire entre les modèles microscopiques, où la description de la matière est effectuée à l'aide d'un grand nombre d'équations couplées, une par particule. Les modèles macroscopiques où seules les variables macroscopiques –qui font intervenir des variables mesurables expérimentalement, comme la densité du fluide, qui ne dépendent que du temps et de l'espace– sont considérées. Cette échelle intermédiaire est appelée *échelle mésoscopique*. L'étude théorique et numérique des modèles cinétiques possède de nombreuses applications en physique, chimie et biologie.

Comme les trois échelles peuvent être utilisées pour modéliser un même phénomène physique, il est naturel de rechercher une certaine cohérence entre eux. D'un point de vue mathématique, il est possible de dériver les modèles mésoscopiques à partir des modèles microscopiques. Il en va de même pour le passage de l'échelle mésoscopique à l'échelle macroscopique, qui peut être justifié par une analyse asymptotique des modèles cinétiques quand le libre parcours moyen des particules tend vers 0. Ainsi, il est par exemple possible de prouver qu'en utilisant un scaling approprié et l'opérateur de Boltzmann pour modéliser les collisions, l'équation cinétique dégénère en des équations fluides.

En notant $\varepsilon \in (0, 1]$ le nombre de Knudsen, qui est défini comme le quotient du libre parcours moyen des particules par une longueur caractéristique, nous considérons le *rescaling* suivant de l'équation cinétique

$$\Theta(\varepsilon)\partial_t f(t,x,v) + \varepsilon v \cdot \nabla_x f(t,x,v) = L(f)(t,x,v), \tag{0.0.1}$$

avec une condition initiale donnée $f(t=0,x,v) = f_{\text{in}}(x,v)$. La fonction $\Theta(\varepsilon)$ utilisée pour le scaling en temps vaut 1 pour $\varepsilon = 1$ et tend vers 0 quand ε tend vers 0. Elle est choisie en fonction des caractéristiques physiques du modèle pour permettre la dérivation des modèles macroscopiques lors de l'analyse asymptotique de (0.0.1). Enfin, l'opérateur L du membre de droite est choisi pour modéliser les collisions entre les particules et contient la physique du modèle. L'opérateur L est linéaire et de moyenne en vitesse nulle, ce qui assure la conservation de la masse au cours du temps. Dans cette thèse, nous considérons

$$L(f) = \int_V \big(\sigma(v,v')f(v') - \sigma(v',v)f(v)\big)\,\mathrm{d}v', \tag{0.0.2}$$

où σ qui désigne la section efficace des particules, est une grandeur liée à la probabilité qu'une particule ayant la vitesse v' prenne la vitesse v. Sous certaines hypothèses pour σ, qui seront toujours vérifiées dans cette thèse, le noyau de L est composé des fonctions de distributions de la forme $\rho(t,x)M(v)$, où l'équilibre M est une fonction de la variable v, paire, strictement positive, intégrable sur $\mathbb{R}^d$ et de moyenne 1. La condition de parité pour M assure que son moment d'ordre 1 est nul. L'existence des moments pairs d'ordre supérieur ou égal à 2 dépend des propriétés de l'équilibre. Un exemple important est le cas des équilibres dits *Maxwelliens*

$$M(v) = \frac{1}{(2\pi)^{d/2}} \mathrm{e}^{-\frac{|v|^2}{2}}, \quad v \in \mathbb{R}^d,$$

pour lesquels, en notant

$$\nu(v) = \int_V \sigma(v',v)\mathrm{d}v', \tag{0.0.3}$$

la fréquence de collision, le coefficient de diffusion

$$D = \int_V \frac{v \otimes v}{\nu(v)} M(v) \mathrm{d}v, \tag{0.0.4}$$

est fini si $\sigma(v, v') = M(v)$. On peut alors montrer qu'en prenant le scaling $\Theta(\varepsilon) = \varepsilon^2$, la solution de (0.0.1) dégénère, quand ε tend vers 0, vers une distribution à l'équilibre $\rho(t, x)M(v)$ où ρ est solution de l'équation de diffusion

$$\partial_t \rho - \nabla_x \cdot (D \nabla_x \rho) = 0,$$

avec condition initiale $\rho(0, x) = \langle f_{\text{in}}(x, v) \rangle$ ([7, 3, 22]). Ici, et dans toute la suite, les crochets désignent l'intégrale en vitesse.

Lorsque le coefficient de diffusion D donné par (0.0.4) n'est plus fini, la limite de diffusion ci-dessus tombe en défaut. Pour faire apparaître un modèle asymptotique non trivial pour (0.0.1), il est alors nécessaire de se placer sur une échelle de temps différente et donc de considérer un autre scaling $\Theta(\varepsilon)$ dans l'analyse asymptotique. Lorsque celui-ci ne s'écrit pas comme une puissance entière de ε, ce qui est le cas dans cette thèse, on parle de scaling anormal. Le choix d'un scaling anormal permet d'obtenir une équation de diffusion anormale quand ε tend vers zéro. Nous considérons dans cette thèse trois cas de limites anormales pour l'équation cinétique : dans les deux premiers, l'équation cinétique dégénère, quand ε tend vers 0, en une équation de diffusion fractionnaire alors que dans le dernier, le scaling anormal $\Theta(\varepsilon)$ entraîne une équation de diffusion normale à la limite.

Schémas *Asymptotic Preserving* (AP)

La résolution numérique de (0.0.1) est compliquée par les termes raides qui y apparaissent quand ε tend vers 0. Pour être valides dans ce contexte, les approches classiques de résolution numérique des EDP nécessitent des conditions sévères qui relient les paramètres de discrétisation à ε. Avec ces méthodes, les régimes asymptotiques sont donc difficilement accessibles car ils nécessitent un temps de calcul qui explose avec la diminution de ε. Les schémas *Asymptotic Preserving* (AP) ont été introduits pour pallier à ce problème ([37, 43, 44]). On peut expliquer leur principe avec un schéma

$$\begin{array}{ccc} P_\varepsilon & \xrightarrow[\varepsilon \to 0]{} & P_0 \\ {\scriptstyle h \to 0}\uparrow & & \uparrow{\scriptstyle h \to 0} \\ S_\varepsilon^h & \xrightarrow[\varepsilon \to 0]{} & S_0^h \end{array}$$

qui s'interprète ainsi : étant donné un problème P_ε qui dégénère en un problème P_0 quand ε tend vers 0, le schéma AP noté S_ε^h, dont les paramètres de discrétisation sont notés ici h, doit

- Être consistant avec le problème P_ε quand h tend vers 0 et ε est fixé.
- Dégénérer en un schéma S_0^h consistant avec le problème P_0 quand h est fixé et ε tend vers 0.

La contrainte supplémentaire de dégénérescence en un schéma consistant avec le problème limite permet à ces schémas d'être efficaces à la fois dans le régime mésoscopique, pour ε proche de

1, et dans les régimes proches du régime macroscopique, quand ε est petit. Les schémas AP peuvent, en outre, avoir la propriété supplémentaire d'uniforme précision (UA, pour *Uniform Accuracy*), ce qui signifie que la précision du schéma est indépendante du paramètre ε. La propriété UA permet de résoudre le problème du régime intermédiaire dans lequel le problème limite n'est pas valide, alors qu'il est déjà raide.

De tels schémas existent pour le cas des limites diffusives de l'équation cinétique ([12, 41, 58, 57]), mais ils ne peuvent pas être appliqués tels quels au cas, plus compliqué, des limites anormales. L'objectif de cette thèse est de construire des schémas AP et UA pour les limites anormales de (0.0.1). De tels schémas ont été construits dans le cas de la limite de diffusion, mais pas dans le cas de limites anormales. En effet, dans les cas que nous considérons l'analyse asymptotique formelle de (0.0.1) montre que les vitesses extrêmes (grandes et petites) jouent un rôle crucial dans la dérivation de l'équation limite. Pour assurer le caractère AP des schémas que nous proposons, nous développons donc une stratégie pour assurer leur prise en compte correcte dans les calculs numériques.

Organisation de la thèse

Le premier exemple que nous considérons est le cas d'un opérateur de collision de type BGK

$$L(f) = \rho M - f, \tag{0.0.5}$$

où $\rho = \langle f \rangle$, et dont l'équilibre est une fonction à queue lourde

$$M(v) \underset{|v|\to\infty}{\sim} \frac{m}{|v|^{d+\alpha}}, \tag{0.0.6}$$

où m est un coefficient de normalisation et $\alpha \in (0, 2)$. Dans ce cas, la fréquence de collision ν qui intervient dans la définition de D est égale à 1 et le poids important des grandes vitesses à l'infini rend le coefficient de diffusion (0.0.4) infini. En considérant le scaling $\Theta(\varepsilon) = \varepsilon^\alpha$, l'analyse asymptotique de (0.0.1) mène à une limite de diffusion fractionnaire ([55, 5]). Plus précisément, la fonction de distribution solution de (0.0.1) dégénère, quand ε tend vers 0, vers une distribution à l'équilibre $\rho(t, x)M(v)$ où ρ est solution de l'équation de diffusion fractionnaire, qui s'écrit en variable de Fourier

$$\partial_t \hat{\rho}(k) + \kappa |k|^\alpha \hat{\rho}(k) = 0, \tag{0.0.7}$$

avec la condition initiale $\hat{\rho}_{\text{in}}(k) = \left\langle \hat{f}_{\text{in}}(k, v) \right\rangle$ et

$$\kappa = \left\langle \frac{(v \cdot e)^2}{1 + (v \cdot e)^2} \frac{m}{|v|^{d+\alpha}} \right\rangle,$$

où e est un vecteur unitaire. Le laplacien fractionnaire qui y apparaît est un opérateur non local qui peut être défini par son symbole de Fourier

$$\left(\widehat{(-\Delta_x)^{\frac{\alpha}{2}} \rho} \right)(k) = |k|^\alpha \hat{\rho}(k),$$

mais a aussi une formulation intégrale

$$(-\Delta_x)^{\frac{\alpha}{2}} \rho(x) = c_{d,\alpha} P.V. \int_{\mathbb{R}^d} \frac{\rho(x + y) - \rho(x)}{|y|^{d+\alpha}} \mathrm{d}y,$$

dans laquelle $c_{d,\alpha}$ est une constante de normalisation et *P.V.* désigne la valeur principale. Cette limite de diffusion fractionnaire avec scaling anormal pour l'équation cinétique est une conséquence directe de l'importance des grandes vitesses de l'équilibre. D'un point de vue numérique, il est donc crucial d'être capable de capter leurs effets pour assurer aux schémas une dégénérescence vers des schémas qui résolvent l'équation limite. En outre, la non localité de l'opérateur de diffusion fractionnaire complique la résolution numérique du modèle asymptotique. Dans ce cadre, nous proposons trois schémas pour (0.0.1). Le premier est basé sur une formulation entièrement implicite de (0.0.1) en variable de Fourier. Pour le cas classique des limites diffusives, un tel schéma possède immédiatement le caractère AP. En revanche, la queue lourde de l'équilibre implique qu'une discrétisation naïve des vitesses fait perdre le caractère AP. Nous proposons donc une stratégie pour prendre en compte les grandes vitesses, et donc assurer le caractère AP du schéma. À partir de cette étude, nous sommes ensuite en mesure d'adapter l'approche des schémas micro-macro, écrits en variable d'espace, à cette asymptotique particulière ([50, 52]). Enfin, en utilisant une écriture intégrale de (0.0.1) en variable de Fourier, nous proposons un schéma pour (0.0.1) qui est UA en plus de posséder la propriété AP. Toutes les propriétés de nos schémas sont prouvées et illustrées par des tests numériques. Ces résultats ont été publiés dans [17].

Nous traitons ensuite un deuxième cas dans lequel (0.0.1) dégénère en une équation de diffusion fractionnaire quand ε tend vers 0. Cette fois, nous nous plaçons sur un espace de vitesses $V = \{v \in \mathbb{R}^d, |v| \leq v_{\max}\}$ borné et nous considérons le cas d'un équilibre constant $M(v) = m$ avec l'opérateur de collision (0.0.2) dans un cadre simplifié dans lequel la section efficace

$$\sigma(v, v') = a(v)a(v')M(v),$$

où $a \in L^1_{\text{loc}}\left(\mathbb{R}^d\right)$ vérifie $a(v) = a(-v)$, est telle que la fréquence de collision (0.0.3) est fortement dégénérée à l'origine

$$\nu(v) \underset{|v|\to 0}{\sim} \nu_0 |v|^{d+2+\beta},$$

pour $\beta > 0$. Sous ces hypothèses, le coefficient de diffusion (0.0.4) est infini à cause de la singularité en 0 de l'intégrande. Pour faire apparaître un modèle asymptotique non trivial pour (0.0.1), il est donc nécessaire de prendre en compte les effets importants des petites vitesses dans l'analyse asymptotique. Il a été prouvé dans [4] que, sous ces hypothèses, la fonction de distribution solution de (0.0.1) tend vers une distribution à l'équilibre $\rho(t, x)M$ dans laquelle la densité ρ vérifie (0.0.7) avec

$$\kappa = \frac{\nu_0^{1-\alpha}}{d+1+\beta} \left\langle \frac{(v \cdot e)^2}{1 + (v \cdot e)^2} \frac{m}{|v|^{d+\alpha}} \right\rangle.$$

Du point de vue des schémas numériques, il faut donc s'assurer que les petites vitesses sont correctement prises en compte pour que les schémas dégénèrent vers le bon modèle limite quand ε tend vers 0. Comme dans le premier chapitre, nous adaptons les schémas implicites, micro-macro et basé sur la formulation intégrale de (0.0.1) au cas de la fréquence de collision dégénérée. Dans ce chapitre, bien que nous nous soyons placés dans un cadre simplifié, la non-localité de l'opérateur de collision complique la résolution numérique de (0.0.1). Nous proposons donc une stratégie pour contourner cette difficulté et pour prendre en compte les petites vitesses de manière adéquate. Nous prouvons ensuite que les schémas ont les mêmes propriétés que ceux du premier chapitre, ce que nous illustrons par des tests. Ces résultats ont été annoncés dans [16] puis publiés dans [18].

En revenant au cas d'un équilibre à queue lourde avec opérateur BGK (0.0.5), nous considérons dans le troisième chapitre le cas limite $\alpha = 2$ dans (0.0.6). Dans ce cadre, le coefficient de diffusion (0.0.4) est encore infini. Il a été montré dans [55] qu'en considérant le scaling anormal $\Theta(\varepsilon) \underset{\varepsilon\to 0}{\sim} \varepsilon^2 |\ln(\varepsilon)|$, la fonction de distribution solution de (0.0.1) tend quand ε tend vers 0 vers une distribution à l'équilibre $\rho(t,x)M(v)$ avec ρ solution de l'équation de diffusion

$$\partial_t \rho - c_d m \Delta_x \rho = 0, \tag{0.0.8}$$

où c_d ne dépend que de la dimension et prend les valeurs $c_1 = 2, c_2 = \pi$ et $c_3 = 8\pi/3$. Il s'agit d'un modèle asymptotique de diffusion normale qui se distingue des limites diffusives usuelles par le scaling $\Theta(\varepsilon)$ anormal. Celui-ci est, encore une fois, une conséquence directe de l'importance des grandes vitesses de l'équilibre dans l'analyse asymptotique, ce qui impose un traitement spécifique des vitesses dans les calculs numériques. De plus, nous prouvons que la dégénérescence de (0.0.1) vers (0.0.8) est très lente, en $1/\left(1 + |\ln(\varepsilon)|\right)$, ce qui rend le modèle asymptotique *a priori* difficile à atteindre numériquement. Nous sommes cependant en mesure de préciser le comportement asymptotique de (0.0.1) au cours de cette très lente dégénérescence. En effet, nous prouvons que la solution de (0.0.1) dégénère avec le taux bien plus rapide $\varepsilon\sqrt{1 + |\ln(\varepsilon)|}$ vers une distribution à l'équilibre dont la densité vérifie, en variable de Fourier,

$$\partial_t \hat{\rho} + a_\varepsilon(k)\hat{\rho} = 0, \tag{0.0.9}$$

où le coefficient $a_\varepsilon(k)$ ne dépend que de ε et de k et dégénère avec la vitesse $1/\left(1 + |\ln(\varepsilon)|\right)$ vers le symbole en variable de Fourier de la diffusion (0.0.8) $c_d m|k|^2$. Nous adaptons les trois schémas proposés dans les premiers chapitres pour que, en plus de posséder la propriété AP, ils respectent la dynamique de cette convergence en dégénérant à la vitesse $\varepsilon\sqrt{1 + |\ln(\varepsilon)|}$ en un schéma pour (0.0.9). Toujours en considérant le même équilibre, nous nous plaçons ensuite dans le cadre d'un opérateur de collision non local (0.0.2) et, en nous basant sur [49], nous proposons un schéma micro-macro relaxé possédant la propriété AP pour l'asymptotique de diffusion anormale traitée dans ce chapitre. Les propriétés des schémas sont prouvées et nous proposons de nombreux tests numériques pour les illustrer. Ces résultats seront soumis prochainement [33].

Enfin, nous proposons dans le quatrième chapitre une généralisation du cas de la limite de diffusion fractionnaire pour l'équation cinétique du premier chapitre au cas d'un opérateur de collision non local dont la section locale dépend de l'espace

$$L(f) = \int_{R^d} \left(\sigma(x,v,v')f(v') - \sigma(x,v',v)f(v)\right) \mathrm{d}v'.$$

Dans ce contexte, traité dans [53], l'analyse asymptotique de l'équation cinétique ne peut pas être effectuée en variable de Fourier. Les schémas implicites et basés sur une formulation intégrale de (0.0.1) ne peuvent donc pas être écrits dans ce cas. Nous proposons une adaptation du schéma micro-macro relaxé de la fin du troisième chapitre, qui possède la propriété AP pour l'asymptotique de diffusion fractionnaire. Des tests numériques sont ensuite présentés pour valider l'approche.

Liste des publications

Dans le cadre de la thèse :

- H. Hivert. Numerical schemes for kinetic equations with diffusion limit and anomalous time scale. *Preprint*, 2016.
- N. Crouseilles, H. Hivert, et M. Lemou. Numerical schemes for kinetic equations in the anomalous diffusion limit. Part II : the case of degenerate collision frequency. *SIAM, J. Sc. Comput.*, 38(4) :A2464-A2491, 2016.
- N. Crouseilles, H. Hivert, et M. Lemou. Numerical schemes for kinetic equations in the anomalous diffusion limit. Part I : the case of heavy-tailed equilibrium. *SIAM, J. Sc. Comput.*, 38(2) : A737-A764, 2016.
- N. Crouseilles, H. Hivert, et M. Lemou. Multiscale numerical schemes for kinetic equations in the anomalous diffusion limit. *C. R. Math. Acad. Sci. Paris*, 353(8) : 755-760, 2015.

CEMRACS 2015 :

- A. Bondesan, S. Dellacherie, H. Hivert, J. Jung, V. Lleras, C. Mietka, and Y. Penel. Study of a depressurisation process at low Mach number in a nuclear reactor core. *Hal-01258397* (submitted), 2016.

Extended abstract

Introduction

We are interested in the construction of asymptotic preserving schemes for kinetic equations in the anomalous diffusion limit. The anomalous asymptotic behavior of kinetic equations comes from stiffness arising with the properties of the equilibrium, and of the collision frequency. Three cases are considered: in the first one, we deal with a constant collision frequency, and an heavy-tailed equilibrium leading to a fractional diffusion equation. Still in the case of a fractional diffusion limit, we then consider the case of a degenerate collision frequency. Eventually, a critical heavy-tailed equilibrium, for which the limit of the model is a diffusion equation, is considered.

Anomalous diffusion limit of kinetic equations

Kinetic equations describe the evolution of a distribution function of particles depending on the time, the space and the velocity. This corresponds to an intermediate model between the microscopic description of a particles system, given by a large number of coupled equations -one for each particle- and the macroscopic modeling where the unknowns only depend on time and space. The theoretical and numerical study of kinetic equations is a very active field of research and has major applications in plasma physics, galactic dynamic, chemotaxis and biological models.

We are interested in the following scaling of the kinetic equation satisfied by the distribution function $f = f(t, x, v)$

$$\theta(\varepsilon)\partial_t f + \varepsilon v \cdot \nabla_x f = \nu(v) L f, \tag{0.0.10}$$

where ν is a collision frequency and the operator L describes the interactions between particles, is linear and acts only on the velocities. The distribution function f depends on the time $t > 0$, the space $x \in \mathbb{R}^d$ and the velocity $v \in V \subset \mathbb{R}^d$, with a symmetric velocity space V. It is well-known that when $\theta(\varepsilon) = \varepsilon^2$, the asymptotic analysis of (0.0.10) leads to a diffusion asymptotic (see [7, 3, 22]). In this limit, the distribution function f tends to an equilibrium $\rho(t, x)M(v)$ where ρ solves a diffusion equation. The diffusion coefficient in this equation is essentially a second order moment in v of $\nu^{-1}M$, which is finite in the particular case ν constant, and M Maxwellian. Unfortunately, for some equilibrium M, this moment may be infinite. This happens for instance when ν is constant and M is heavy-tailed

$$M(v) \underset{|v|\to+\infty}{\sim} \frac{m}{|v|^\beta}, \beta \in (d, d+2), \tag{0.0.11}$$

(d is the dimension of the space). In this case, the appropriate scaling is no longer $\theta(\varepsilon) = \varepsilon^2$, but $\theta(\varepsilon) = \varepsilon^{\beta-d}$. The asymptotic analysis when $\varepsilon \to 0$ in this case leads to a fractional diffusion equation (see [5, 55, 53]). A fractional diffusion limit also arises when the collision frequency ν is degenerated at $v = 0$, the equilibrium M being constant or Maxwellian ([4]). Note that the critical case $\beta = d + 2$, with a heavy-tailed equilibrium leads to a classical diffusion limit with an anomalous scaling $\theta(\varepsilon) = \varepsilon^2 |\ln(\varepsilon)|$ (see [55]).

In comparison to the usual diffusion limit, the numerical resolution of (0.0.10) in the anomalous diffusion limits is complicated by the specificities of the collision frequency ν, and of the equilibrium M that are considered. In what follow, we detail the strategy we use to construct asymptotic preserving schemes for (0.0.10) when the equilibrium is heavy-tailed, when the collision frequency is degenerated at $v = 0$, and in the critical case of the heavy-tailed equilibrium.

Asymptotic Preserving (AP) schemes

The difficulties when numerically solving (0.0.10) with an anomalous diffusion limit come from two stiffness of different nature. The first one is related to the scaling $\theta(\varepsilon)$, which tends to 0 when ε becomes small, and the second one comes from the infinite second order moment of $\nu^{-1}M$. Efficient numerical schemes have already been proposed for the diffusion limit of (0.0.10) (see [37, 43, 44, 12, 41, 58, 57]). They are designed to deal with the difficulties arising from the stiffness in ε, but not to the ones linked to the infinite character of $\langle v \otimes v\nu^{-1}M \rangle$.

To get rid of the first difficulty, numerical schemes which are uniformly stable when the stiffness parameter ε goes to 0 are constructed. The aim of an AP scheme is the following: being consistent with the ε-dependent problem for all fixed ε and degenerating in a scheme solving the limit equation when ε goes to 0. An AP scheme can also enjoy the stronger property of being Uniformly Accurate (UA), meaning that its precision does not depend on the stiffness parameter ε. Because of the presence of an additional stiffness, the existing schemes for the case of the diffusion limit cannot be applied to the more intricate case of the anomalous diffusion limit. Up to our knowledge, no scheme exists in this framework; then, we started to find a strategy to extend AP schemes for the diffusion case to the anomalous diffusion case. Indeed, in the anomalous diffusion limit cases, difficulties arise since one has to take into account the large (or small) velocities of the heavy-tailed equilibrium M (or the degenerate collision frequency). The non locality of the fractional diffusion equation, as well as the complexity of the asymptotic analysis are other difficulties of the problem.

Publications

About fractional diffusion limit of kinetic equation [17, 16, 18]

In the cases of the heavy-tailed equilibrium and of the degenerate collision frequency leading to a fractional diffusion limit, we considered the BGK operator $Lf = \rho M - f$ with $\rho = \int f \mathrm{d}v$ and we constructed three numerical schemes solving (0.0.10) and enjoying the AP property. In each of them, we managed to take into account the specificities of the anomalous diffusion limits of (0.0.10), such as the effects of the large (or low) velocities of the problem. The first one is based on a fully implicit scheme in time, using the Fourier variable in space. In this case both the transport and the collision operator are considered implicit. It can be shown easily that this fully implicit scheme is AP in the diffusion case, but not in the anomalous diffusion case. Before discretization in v, we perform a suitable change of variables to capture the effects of large velocities, and then to ensure the good behavior of the scheme when $\varepsilon \to 0$. Although this new scheme is AP, it has some drawbacks. Indeed, its fully implicit character may induce a huge computational cost, especially when dealing with multi-dimensional problems. Therefore, we proposed a strategy based on a suitable micro-macro decomposition of (0.0.10), in which the transport operator becomes explicit in time. It is known that such a strategy directly leads to an AP scheme in the diffusion case, but the fractional diffusion case requires more care to capture the effects of the large and small velocities. The last strategy we proposed is based on a Duhamel formulation of (0.0.10) in Fourier variable in space. The Duhamel formulation has an interesting advantage: it provides a closed equation for the density ρ. Moreover, we proved that this strategy ensures that the scheme enjoys the UA property.

The construction of our numerical schemes is based on adequate reformulation of the problem at the continuous level, in which transformations are made to make the fractional diffusion operator appear in the reformulated model. These transformations have been also useful for us

to derive the explicit convergence rate (in ε) of (0.0.10) to the fractional diffusion limit. The numerical tests we propose highlight this convergence rate. The case of the heavy-tailed equilibrium is treated in [17] and the case of the degenerate collision frequency has been announced in [16] and developed in [18] where all the properties of the schemes are proved and illustrated by several tests.

About diffusion limit of kinetic equation with anomalous time scale [33]

The critical case $\beta = d+2$ in (0.0.11) leads to a classical diffusion limit with anomalous scaling $\theta(\varepsilon) = \varepsilon^2 |\ln(\varepsilon)|$. In numerical computations, a numerical diffusion, which does not match with the expected one, occurs when the classical AP schemes for diffusion are applied to this problem. The derivation of AP schemes for this case brings the same difficulties as in the case of the fractional diffusion equation coming from an heavy-tailed equilibrium. In addition, the speed of the degeneracy of (0.0.10) towards the diffusion limit is very slow, in $1/(1+|\ln(\varepsilon)|)$, which makes the asymptotic model hard to reach numerically. However, we proved that (0.0.10) degenerates towards an intermediate model, still dependent of ε, with rate $\varepsilon\,(1+|\ln(\varepsilon)|)$. To take into account the high velocities in the numerical computations, we use the strategy we developed for the case of the fractional diffusion limit, and we adapt the three previous schemes to this case of anomalous diffusion limit. We ensure that they enjoy an interesting property: in addition to the AP property, they respect the dynamics of degeneracy towards the asymptotic equation. Indeed, they degenerate with the proper rate $\varepsilon\,(1+|\ln(\varepsilon)|)$ into schemes solving the intermediate model, and into schemes for limit model with rate $1/\,(1+|\ln(\varepsilon)|)$.

Still in the context of the normal diffusion limit with anomalous time scale, we then consider the case of (0.0.10), supplied with a more general integral collision operator. We propose a relaxed micro-macro scheme based on [49] which enjoys the AP property. These results are presented in [33], where numerical tests enable to validate the approach are proposed.

Fractional diffusion limit and non local collision operator

The fourth chapter presents a generalization of the relaxed micro-macro scheme proposed in the case of the diffusion limit with anomalous time scale, to the case of (0.0.10) with (0.0.11) with a fractional diffusion limit and a general collision operator

$$L(f) = \int_{\mathbb{R}^d} \big(\sigma(x,v,v')f(v') - \sigma(x,v',v)f(v)\big)\,\mathrm{d}v'.$$

In this context, which has been treated in [53], the asymptotic analysis of (0.0.10) can not be done in the Fourier variable. As a consequence, the numerical treatment of the fractional laplacian has to be done in the space variable.

Introduction

Contexte général

L'objet de cette thèse est la construction de schémas *Asymptotic Preserving* (AP) pour des équations cinétiques, qui sont une classe d'équations aux dérivées partielles notamment utilisées en théorie cinétique des gaz. La modélisation de l'évolution d'un ensemble de particules -comme un gaz- peut être réalisée à plusieurs échelles. La plus détaillée est l'échelle *microscopique*, dans laquelle chaque particule est étudiée séparément. On applique alors les lois de Newton à chacune des particules, ce qui mène à l'étude de systèmes d'équations couplées avec autant d'inconnues que de particules. Cependant, le nombre de particules est souvent très grand, de sorte qu'une telle étude devient extrêmement compliquée théoriquement et numériquement. L'échelle des quantités observables expérimentalement du système physique est l'échelle *macroscopique*. On y considère des quantités physiquement mesurables associées au système, comme sa densité, sa vitesse moyenne, sa température ou sa pression. Cela revient à considérer un ensemble continu de particules décrit par des quantités macroscopiques, qu'on peut voir comme des moyennes de leurs équivalents microscopiques et qui définissent l'état du système physique dans sa globalité. Ces quantités dépendent des variables de temps et d'espace et ne peuvent donc différencier les particules autrement que par leur localisation spatiale et temporelle. Une échelle intermédiaire est l'échelle *mésoscopique*, qui consiste en une description continue des systèmes physiques qui prend en compte plus de paramètres que ceux qui sont effectivement observables physiquement. Du point de vue de la modélisation, ce sont les modèles cinétiques qui sont utilisés à cette échelle. Avec cette approche, c'est une distribution statistique des particules qui est considérée, qui dépend non seulement du temps et de l'espace, mais aussi de la vitesse des particules. Les quantités macroscopiques, et donc observables, du système peuvent être obtenues comme des moyennes en vitesse de quantités mésoscopiques.

Le choix d'une modélisation (miscroscopique, mésoscopique, macroscopique) dépend de l'échelle à laquelle le problème est considéré. D'autre part, les trois approches se doivent d'être cohérentes les unes avec les autres puisqu'elles sont supposées décrire des systèmes physiques identiques. D'un point de vue mathématique, la dérivation de modèles cinétiques à partir des modèles particulaires a été étudié notamment par O. E. Lanford en 1975. Dans [47], un gaz raréfié de sphères dures est considéré et l'équation de Boltzmann en est dérivée pour des temps courts. Ses résultats ont ensuite été précisés, notamment dans des travaux de Gallagher, Saint-Raymond et Texier [29] et de Pulvirenti, Saffirio et Simonella [66]. Le passage de l'échelle mésoscopique à l'échelle macroscopique se fait en considérant la limite du modèle cinétique lorsque le nombre de Knudsen, qui est proportionnel au libre parcours moyen des particules, devient très petit. Cette limite implique qu'il y a beaucoup de collisions entre les particules et que la répartition en vitesse relaxe vers un équilibre. En 1912, Hilbert a proposé un développement formel de l'équation de Boltzmann en puissances du nombre de Knudsen dans le cas d'une limite hydrodynamique. En 1917, Chapman et Enskog ont proposé une méthode perturbative pour réaliser ce développement, ainsi qu'une méthode systématique pour dériver les quantités macroscopiques à partir des interactions microscopiques. En fonction des propriétés du modèle, de nombreuses limites macroscopiques peuvent être considérées, les plus importantes d'entre elles sont les limites hydrodynamiques et les limites diffusives. Les limites hydrodynamiques de l'équation cinétique ont ensuite été prouvées rigoureusement et dans un cadre général par Bardos, Golse et Levermore en 1991–1993 [1, 2]. Les limites diffusives pour les équations cinétiques, qui sont plus proches de l'objet de cette thèse, ont été étudiées d'abord d'un point de vue physique, par exemple par Wigner [70] ou par Larsen et Keller [48], puis d'un point de vue mathématique par Bensoussan, Lions et Papanicolaou [7], Bardos, Santos et Sentis [3], ou encore dans des travaux plus récents [22]. Mais d'autres limites existent, comme par exemple

les limites de diffusion fractionnaire de l'équation cinétique, qui sont étudiées dans cette thèse. On peut citer les travaux de N. Ben Abdallah, A. Mellet, S. Mischler, C. Mouhot et M. Puel [55, 4, 5, 53].

Dans toute la suite, nous considérerons le *rescaling* suivant de l'équation cinétique

$$\Theta(\varepsilon)\partial_t f + \varepsilon v \cdot \nabla_x f = L(f). \tag{0.0.12}$$

Il s'agit d'une équation aux dérivées partielles dont l'inconnue est une fonction de distribution f qui dépend du temps $t > 0$, de la variable d'espace $x \in \mathbb{R}^d$ et de la vitesse $v \in V \subset \mathbb{R}^d$, où l'espace des vitesses V est supposé symétrique par rapport à l'origine. La condition initiale $f(0, x, v) = f_{\text{in}}(x, v)$ est donnée. Le paramètre $\varepsilon \in (0, 1]$ désigne le nombre de Knudsen et $\Theta(\varepsilon)$ est une fonction de ε qui vaut 1 pour $\varepsilon = 1$ et tend vers 0 quand ε tend vers 0. Le choix de $\Theta(\varepsilon)$ dépend des caractéristiques physiques du modèle, et permet la dérivation des modèles macroscopiques lors de l'analyse asymptotique de (0.0.12). Par exemple, le cas des limites hydrodynamiques correspond à $\Theta(\varepsilon) = \varepsilon$ et le cas des limites diffusives apparaît lorsque $\Theta(\varepsilon) = \varepsilon^2$. Ces deux fonctions de ε, qui s'écrivent comme des puissances entières du paramètre ε sont opposées aux *scalings* dits *anormaux*, qui s'écrivent comme des fonctions plus compliquées de ε. La fonction $\Theta(\varepsilon)$ est alors l'échelle de temps à choisir pour obtenir un modèle asymptotique non trivial pour (0.0.12). Dans la suite, nous considérerons des *scalings* qui ne s'écrivent pas comme une puissance entière de ε :

$$\Theta(\varepsilon) = \varepsilon^\alpha, \quad \alpha \in (0, 2),$$

ou

$$\Theta(\varepsilon) = \varepsilon^{\frac{2d+2+\beta}{d+1+\beta}}, \quad \beta > 0,$$

et le cas

$$\Theta(\varepsilon) = \varepsilon^2(1 + |\ln(\varepsilon)|).$$

Avec les propriétés du modèle considéré, les deux premiers choix de $\Theta(\varepsilon)$ permettent de faire apparaître une équation de diffusion fractionnaire comme modèle asymptotique de (0.0.12) quand ε tend vers 0. Le dernier cas correspond à une limite de diffusion normale, mais avec un scaling anormal.

Le membre de droite dans (0.0.12) est un opérateur linéaire qui modélise les collisions auxquelles sont soumises les particules et qui contient la physique du modèle. Le cas le plus général traité dans cette thèse s'écrit

$$L(f)(v) = \int_V \left[\sigma(v, v')f(v') - \sigma(v', v)f(v)\right] \mathrm{d}v', \tag{0.0.13}$$

où σ, qui désigne la section efficace des particules, est une grandeur liée à la probabilité d'interaction de la particule ayant la vitesse v avec celles ayant la vitesse v'. L'opérateur L est de moyenne nulle, ce qui traduit la conservation de la masse

$$\langle L(f) \rangle = 0,$$

où, $\langle \cdot \rangle$ désigne l'intégration en vitesse. Dans toute la suite, l'intégrale par rapport à la variable v sur un domaine $\mathcal{D}$ sera notée par

$$\langle f \rangle_{\mathcal{D}} := \int_{\mathcal{D} \subset \mathbb{R}^d} f(v) \mathrm{d}v,$$

et la mention de l'ensemble d'intégration sera omise lorsqu'il s'agira de l'espace entier V. En notant ρ la densité associée à la fonction de distribution f

$$\rho(t,x) = \langle f(t,x,\cdot)\rangle\,,$$

la propriété de conservativité de l'équation cinétique, c'est à dire la conservation de la masse au cours du temps

$$\int_{\mathbb{R}^d} \rho(t,x)\mathrm{d}x = \int_{\mathbb{R}^d} \rho(0,x)\mathrm{d}x,\ \ \forall t>0,$$

est une conséquence directe de la moyenne nulle de l'opérateur de collision L.

L'opérateur L peut être réécrit sous la forme

$$L(f) = K(f) - \nu f,$$

où

$$K(f) = \int_{\mathbb{R}^d} \sigma(v,v')f(v')\mathrm{d}v',$$

et

$$\nu(v) = \int_{\mathbb{R}^d} \sigma(v',v)\mathrm{d}v'.$$

Par la suite, on appellera ν la fréquence de collision, qui sera supposée positive, localement intégrable dans $\mathbb{R}^d$ et telle que $\nu(-v) = \nu(v)$, pour tout $v \in \mathbb{R}^d$ dans la suite. Sous des hypothèses supplémentaires sur la section efficace σ (voir [22]), le noyau de l'opérateur L est composé des fonctions de distributions de la forme $\rho(t,x)M(v)$, où la fonction M est l'équilibre associé à l'opérateur de collision. Comme précisé dans [55], ces hypothèses sont notamment satisfaites lorsque σ vérifie le principe de micro-réversibilité, c'est à dire lorsqu'il existe une fonction $b \in L^1_{\mathrm{loc}}\left(\mathbb{R}^{2d}\right)$, symétrique, telle que

$$\sigma(v,v') = b(v,v')M(v),$$

ce qui est le cas traité dans ce manuscrit. L'équilibre M est une fonction de la variable v, symétrique

$$M(-v) = M(v),\ \ \forall v \in V,$$

strictement positive, intégrable sur $\mathbb{R}^d$ et de moyenne 1

$$\langle M\rangle = 1.$$

La condition de symétrie assure le fait que ses moments d'ordre impairs sont nuls, en particulier $\langle vM\rangle = 0$. Par contre, l'existence de ses moments pairs d'ordre supérieurs ou égaux à 2 dépend de l'équilibre M considéré. Parmi les équilibres utilisés dans les applications, on citera les équilibres maxwelliens

$$M(v) = \frac{1}{(2\pi)^{d/2}}\mathrm{e}^{-|v|^2/2}, v \in \mathbb{R}^d, \tag{0.0.14}$$

qui sont utilisés dans l'écriture des noyaux de collisions lorsque, au niveau microscopique, les mouvements des particules peuvent être représentés par des mouvements browniens. L'opérateur de collision L peut alors être utilisé pour modéliser des applications du domaine de la physique [51, 70], de la biologie [67], ou des sciences économiques et humaines [62, 60]. Cependant, cette modélisation est insuffisante pour prendre en compte la diversité des situations

physiques, et d'autres équilibres doivent alors être considérés. Lorsque, au niveau microscopique, le mouvement des particules est modélisé par un processus de Levy, des équilibres dits *à queue lourde* apparaissent. Ce type d'équilibres interviennent physiquement dans l'étude des milieux granulaires [8, 27, 9], des plasmas astrophysiques [68, 56] ou de problèmes liés à la modélisation des tokamaks [23]. Dans le domaine des sciences sociales et économiques, les équilibres à décroissance polynomiale ont été introduits au XIX$^{\text{ème}}$ siècle par V. Pareto [63]. En raison de l'importance qu'ils donnent aux événements extrêmes (les grandes vitesses), ils sont souvent préférés aux équilibres maxwelliens pour des applications à la modélisation de l'économie, des répartitions de richesse mais aussi pour la modélisation de comportements humains et de mouvements collectifs. On pourra se référer à [60] pour de nombreux exemples.

Limite de diffusion pour l'équation cinétique

Les limites de diffusion anormale, diffusion fractionnaire ou diffusion usuelle avec un scaling anormal $\Theta(\varepsilon)$ qui sont étudiées dans cette thèse, constituent un cas proche de la limite de diffusion pour les équations cinétiques. Afin de mettre en lumière les particularités inhérentes aux limites anormales qui seront étudiées dans la suite, cette partie propose de rappeler le cas de la limite de diffusion usuelle $\Theta(\varepsilon) = \varepsilon^2$. Pour cela, nous proposons une approche formelle de l'analyse asymptotique de (0.0.12)-(0.0.13) quand ε tend vers 0. Nous supposerons que la section locale σ vérifie

$$\sigma(v, v') = a(v)a(v')M(v),$$

où $a \in L^1_{\text{loc}}\left(\mathbb{R}^d\right)$ vérifie $a(v) = a(-v)$, et M est une maxwellienne de la forme (0.0.14). L'opérateur de collision L peut donc être réécrit

$$L(f) = Ka(v)\left(\rho_a M - f\right), \tag{0.0.15}$$

où $K = \langle aM \rangle$, et

$$\rho_a = \frac{\langle af \rangle}{\langle aM \rangle}.$$

La densité modifiée ρ_a coïncide avec la densité usuelle $\rho = \langle f \rangle$ lorsque la fonction de distribution est à l'équilibre. Dans un cadre plus général, l'étude de la limite de la solution de (0.0.12) vers une fonction de distribution à l'équilibre dont la densité résout une équation de diffusion peut être faite rigoureusement, par exemple dans [7, 22, 3]. Nous proposons ici une approche formelle de la dérivation de cette asymptotique. Nous supposerons donc que $a > 0$ est suffisamment régulier pour assurer que les quantités $\langle aM \rangle$, $\langle af \rangle$ et $\langle v \otimes vM/a(v) \rangle$ sont bien définies. Nous allons montrer formellement que, quand ε tend vers 0, la solution de (0.0.12)-(0.0.15) converge vers une distribution à l'équilibre $f_0 = \rho_0 M$ où ρ_0 résout l'équation de diffusion

$$\partial_t \rho_0 - \nabla_x \cdot (D \nabla_x \rho_0) = 0, \tag{0.0.16}$$

avec condition initiale $\rho_0(0, x) = \langle f_{\text{in}}(x, \cdot) \rangle$, et où le coefficient de diffusion est donné par

$$D = \frac{1}{\langle aM \rangle} \int_{\mathbb{R}^d} \frac{v \otimes v}{a(v)} M(v) \mathrm{d}v. \tag{0.0.17}$$

Dans toute la suite, la transformée de Fourier par rapport à la variable d'espace de la fonction de distribution f sera notée $\hat{f}$. Elle est définie par

$$\hat{f}(t, k, v) = \int_{\mathbb{R}^d} \mathrm{e}^{-\mathrm{i}k \cdot x} f(t, x, v) \mathrm{d}x,$$

et les notations $\hat{\rho}, \hat{\rho}_a$ et $\hat{\rho}_0$ seront utilisées pour désigner les transformées de Fourier des fonctions ρ, ρ_a et ρ_0. En variable de Fourier, l'équation cinétique (0.0.12)-(0.0.15) se réécrit

$$\Theta(\varepsilon)\partial_t \hat{f} + \varepsilon \mathrm{i} k \cdot v \hat{f} = Ka \left(\hat{\rho}_a M - \hat{f} \right), \tag{0.0.18}$$

ce qui donne une expression de $\hat{f}$

$$\hat{f} = \frac{Ka}{Ka + \varepsilon \mathrm{i} k \cdot v} \hat{\rho}_a M - \Theta(\varepsilon) \frac{\partial_t \hat{f}}{Ka + \varepsilon \mathrm{i} k \cdot v}. \tag{0.0.19}$$

Comme $\Theta(\varepsilon)$ tend vers 0 quand ε tend vers 0, en supposant que la dérivée $\partial_t \hat{f}$ est bornée (il s'agit toujours de calculs formels), l'expression précédente montre que $\hat{f}$ tend vers $\hat{\rho}_a M$ quand ε tend vers 0. Ainsi, à la limite, les densités usuelle ρ et modifiée ρ_a de f coïncident

$$\rho \underset{\varepsilon \to 0}{=} \rho_a. \tag{0.0.20}$$

Intégrer (0.0.18) en vitesse permet de trouver une équation vérifiée par $\hat{\rho}$ quand ε tend vers 0

$$\partial_t \hat{\rho} + \frac{1}{\Theta(\varepsilon)} \left\langle \varepsilon \mathrm{i} k \cdot v \hat{f} \right\rangle = 0. \tag{0.0.21}$$

En injectant (0.0.19) dans (0.0.21) on obtient

$$\partial_t \hat{\rho} + \frac{1}{\Theta(\varepsilon)} \left\langle \frac{\varepsilon \mathrm{i} k \cdot v}{Ka + \varepsilon \mathrm{i} k \cdot v} KaM \right\rangle \hat{\rho}_a - \left\langle \frac{\varepsilon \mathrm{i} k \cdot v \partial_t \hat{f}}{Ka + \varepsilon \mathrm{i} k \cdot v} \right\rangle = 0. \tag{0.0.22}$$

Toujours en supposant que $\partial_t \hat{f}$ est bornée, le dernier terme de l'égalité précédente tend vers 0 quand ε tend vers 0. Pour trouver la limite du second terme, l'intégrale en vitesse peut être transformée en utilisant la parité de M et a

$$\frac{1}{\Theta(\varepsilon)} \left\langle \frac{\varepsilon \mathrm{i} k \cdot v}{Ka + \varepsilon \mathrm{i} k \cdot v} KaM \right\rangle = \frac{1}{\Theta(\varepsilon)} \left\langle \frac{\varepsilon^2 (k \cdot v)^2}{(Ka)^2 + \varepsilon^2 (k \cdot v)^2} KaM \right\rangle.$$

Cette écriture implique qu'il faut choisir $\Theta(\varepsilon) = \varepsilon^2$ pour que l'expression précédente ait une limite finie non nulle quand ε tend vers 0. Avec ce choix, qui correspond bien à un scaling diffusif, on a alors

$$\frac{1}{\Theta(\varepsilon)} \left\langle \frac{\varepsilon^2 (k \cdot v)^2}{(Ka)^2 + \varepsilon^2 (k \cdot v)^2} KaM \right\rangle \underset{\varepsilon \to 0}{=} \frac{1}{K} \left\langle \frac{(k \cdot v)^2}{a} M \right\rangle,$$

où les hypothèses faites sur a et la forme de M assurent qu'il s'agit d'une limite finie. Ainsi, en utilisant (0.0.20), on obtient à partir de (0.0.22) une équation fermée sur $\hat{\rho}$

$$\partial_t \hat{\rho} + \frac{1}{K} \left\langle \frac{(k \cdot v)^2}{\nu} M \right\rangle \hat{\rho} = 0,$$

qui correspond bien à l'écriture en variable de Fourier de (0.0.16).

Dans le cas des limites de diffusion anormale qui font l'objet de cette thèse, les propriétés de l'équilibre M et/ou de la fréquence de collision Ka n'assurent pas le caractère fini du coefficient de diffusion (0.0.17). Ainsi, la limite de diffusion classique tombe alors en défaut et le scaling $\Theta(\varepsilon)$ doit être adapté pour faire apparaître une équation asymptotique non triviale pour ρ.

Limites anormales pour l'équation cinétique

Les limites de diffusion anormale pour les équations cinétiques ont été introduites pour modéliser le comportement d'un gaz raréfié entre deux plaques métalliques rapprochées, dans [10] puis [25, 30, 26]. Dans ce cas, comme le coefficient de diffusion classique (0.0.17) est infini, le scaling $\Theta(\varepsilon) = \varepsilon^2$ ne peut plus être considéré. En utilisant le scaling anormal $\Theta(\varepsilon) \sim \varepsilon^2 |\ln(\varepsilon)|$, une équation de diffusion peut toutefois être dérivée de l'équation cinétique quand ε tend vers 0. Les limites de diffusion fractionnaire pour les équations cinétiques ont été introduites bien plus récemment, dans [55] et, avec des méthodes très différentes, dans [36]. Ces travaux ont ensuite été précisés dans [4, 5, 53], et la limite de diffusion fractionnaire pour les équations cinétique a aussi pu être prouvée dans un cadre stochastique [20]. Mathématiquement, il s'agit d'un domaine toujours très actif, car de nombreux problèmes restent ouverts comme la prise en compte de conditions de bord, ou l'utilisation d'autres opérateurs de collision que ceux de type intégral (0.0.13).

En revenant aux calculs formels proposés dans la partie précédente pour mettre en évidence la limite de diffusion de l'équation cinétique (0.0.12), dans le cas d'un équilibre à queue lourde, montrons que la limite de diffusion peut tomber en défaut. En effet, en considérant le cas simple de l'opérateur de collision

$$L(f) = \rho M - f, \tag{0.0.23}$$

avec $\rho = \langle f \rangle$, qui s'écrit comme (0.0.15) avec $a = 1$, et un équilibre M tel que

$$M(v) \underset{|v|\to\infty}{\sim} \frac{m}{|v|^{d+\alpha}},$$

où m est un coefficient de normalisation, le coefficient de diffusion (0.0.17) est infini dès que $\alpha \leq 2$. La condition d'intégrabilité de M impose de plus $\alpha > 0$. Ainsi lorsque $\alpha \in (0, 2]$, l'étude de la limite de (0.0.12)-(0.0.23) quand ε tend vers 0 nécessite une analyse plus poussée. De la même manière que dans le cas diffusion, l'écriture en Fourier de (0.0.12)-(0.0.23) donne l'expression suivante pour $\hat{f}$

$$\hat{f} = \frac{1}{1 + \varepsilon \mathrm{i} k \cdot v} \hat{\rho} M - \Theta(\varepsilon) \frac{\partial_t \hat{f}}{1 + \varepsilon \mathrm{i} k \cdot v},$$

qui indique que $\hat{f}$ tend vers une distribution à l'équilibre $\hat{\rho} M$ quand ε tend vers 0. On peut aussi en déduire une expression pour $\hat{\rho}$

$$\partial_t \hat{\rho} + \frac{1}{\Theta(\varepsilon)} \left\langle \frac{\varepsilon \mathrm{i} k \cdot v}{1 + \varepsilon \mathrm{i} k \cdot v} M \right\rangle \hat{\rho} - \left\langle \frac{\varepsilon \mathrm{i} k \cdot v}{1 + \varepsilon \mathrm{i} k \cdot v} \partial_t \hat{f} \right\rangle = 0, \tag{0.0.24}$$

dans laquelle le dernier terme s'annule à la limite si on suppose $\partial_t \hat{f}$ bornée. Le second terme peut être réécrit comme suit

$$\frac{1}{\Theta(\varepsilon)} \left\langle \frac{\varepsilon \mathrm{i} k \cdot v}{1 + \varepsilon \mathrm{i} k \cdot v} M \right\rangle = \frac{\varepsilon^2}{\Theta(\varepsilon)} \left\langle \frac{(k \cdot v)^2}{1 + \varepsilon^2 (k \cdot v)^2} M \right\rangle.$$

Cependant, comme $\left\langle (k \cdot v)^2 M \right\rangle$ est infini, la limite du terme ci-dessus quand ε tend vers 0 n'est pas immédiate. Pour trouver un équivalent de cette expression quand ε tend vers 0, on peut effectuer le changement de variables $w = \varepsilon |k| v$ dans l'intégrale en vitesse, on obtient alors

$$\frac{\varepsilon^2}{\Theta(\varepsilon)} \int_{\mathbb{R}^d} \frac{(k \cdot v)^2}{1 + \varepsilon^2 (k \cdot v)^2} M \, \mathrm{d}v \underset{\varepsilon\to 0}{\sim} \frac{\varepsilon^\alpha}{\Theta(\varepsilon)} |k|^\alpha \int_{\mathbb{R}^d} \frac{(w \cdot e)^2}{1 + (w \cdot e)^2} \frac{m}{|w|^{d+\alpha}} \mathrm{d}w, \tag{0.0.25}$$

où e est un vecteur unitaire. Si $\alpha \in (0,2)$, l'intégrale est finie. Dans ce cas, en posant $\Theta(\varepsilon) = \varepsilon^\alpha$, on observe formellement que lorsque ε tend vers 0, $\hat{f}$ converge vers $\hat{\rho}M$, où la la densité $\hat{\rho}$ résout, en variable de Fourier,

$$\partial_t \hat{\rho} + \kappa |k|^\alpha \hat{\rho} = 0, \quad \hat{\rho}(0,k) = \left\langle \hat{f}_{\text{in}}(k,\cdot) \right\rangle, \tag{0.0.26}$$

où

$$\kappa = \left\langle \frac{(w\cdot e)^2}{1+(v\cdot e)^2} \frac{m}{|v|^{d+\alpha}} \right\rangle,$$

est le coefficient de la diffusion anormale. L'équation (0.0.26) est appelée équation de diffusion fractionnaire. Le laplacien fractionnaire qui y apparaît par son symbole de Fourier est un opérateur non local

$$\left(\widehat{(-\Delta_x)^{\frac{\alpha}{2}} \rho} \right)(k) = |k|^\alpha \hat{\rho}(k),$$

mais il a aussi une définition intégrale

$$(-\Delta_x)^{\frac{\alpha}{2}} \rho(x) = c_{d,\alpha} P.V. \int_{\mathbb{R}^d} \frac{\rho(x+y)-\rho(x)}{|y|^{d+\alpha}} \mathrm{d}y,$$

où $P.V.$ désigne la valeur principale et $c_{d,\alpha}$ une constante de normalisation de la forme

$$c_{d,\alpha} = \frac{\alpha \Gamma\left(\frac{d+\alpha}{2}\right)}{2\pi^{\frac{d}{2}+\alpha} \Gamma\left(1-\frac{\alpha}{2}\right)},$$

dans laquelle Γ désigne la fonction Γ usuelle

$$\Gamma(x) = \int_0^{+\infty} t^{x-1} e^{-t} \mathrm{d}t.$$

Une étude détaillée de cet opérateur est proposée dans [65]. Le cas d'un équilibre à queue lourde avec $\alpha \in (0,2)$ est traité dans [55, 5] et fait l'objet du premier chapitre de ce manuscrit.

Quand $\alpha = 2$, le coefficient κ défini précédemment est encore infini. En l'état, l'expression (0.0.25) ne fournit donc pas d'équivalent utilisable pour l'analyse asymptotique formelle de l'équation cinétique. On peut cependant la transformer, par exemple en utilisant un changement de variables en coordonnées polaires ou sphériques (selon la dimension) puis une intégration par parties. On obtient l'équivalent suivant pour le second terme de (0.0.24)

$$\frac{\varepsilon^2}{\Theta(\varepsilon)} \left\langle \frac{(k\cdot v)^2}{1+(k\cdot v)^2} M \right\rangle \underset{\varepsilon\to 0}{\sim} \frac{\varepsilon^2 |\ln(\varepsilon)|}{\Theta(\varepsilon)} c_d m |k|^2,$$

où m est la constante de normalisation de l'équilibre et c_d dépend uniquement de la dimension ($c_1 = 2, c_2 = \pi, c_3 = 8\pi/3$). Dans ce cas, en choisissant un scaling *anormal* $\Theta(\varepsilon)$ tel que $\Theta(\varepsilon) \sim \varepsilon^2 |\ln(\varepsilon)|$, l'équation vérifiée par la densité à la limite est une équation de diffusion

$$\partial_t \hat{\rho} + c_d m |k|^2 \hat{\rho} = 0, \quad \hat{\rho}(0,k) = \left\langle \hat{f}_{\text{in}}(k,\cdot) \right\rangle.$$

L'étude théorique de ce cas est détaillée dans un cadre plus général dans [55], son étude numérique fait l'objet du troisième chapitre de ce manuscrit.

Les limites de diffusion anormales pour l'équation cinétique ne sont pas uniquement le fait des équilibres à queue lourde. En effet, dans [4], l'équation (0.0.12)-(0.0.15) dont l'équilibre M est une fonction constante sur V (remarquons que la démarche de [4] peut être adaptée pour

le cas M maxwellien) est considérée et une limite de diffusion fractionnaire y est étudiée. En supposant que l'équilibre est constant égal à m sur V, mais en considérant la fréquence de collision Ka fortement dégénérée à l'origine

$$Ka(v) \underset{|v|\to 0}{\sim} K|v|^{d+2+\beta}, \tag{0.0.27}$$

où $\beta > 0$, le coefficient de diffusion (0.0.17) est infini. Ceci est dû, à la non intégrabilité de l'intégrande pour les petites vitesses. De la même manière que précédemment, l'analyse asymptotique formelle de (0.0.12) conduit à chercher la limite quand ε tend vers 0 du deuxième terme de (0.0.22). On a alors

$$\frac{1}{\Theta(\varepsilon)}\left\langle \frac{\varepsilon \mathrm{i} k\cdot v}{Ka+\varepsilon \mathrm{i} k\cdot v} KaM\right\rangle = \frac{1}{\Theta(\varepsilon)}\left\langle \frac{\frac{\varepsilon^2(k\cdot v)^2}{K^2a^2}}{1+\frac{\varepsilon^2(k\cdot v)^2}{K^2a^2}}\frac{M}{Ka}\right\rangle.$$

Pour trouver un équivalent quand ε tend vers 0 du terme précédent, on peut effectuer le changement de variables $w = \varepsilon|k|v/\left(K|v|^{d+2+\beta}\right)$ dans l'intégrale en vitesse. On a alors

$$\frac{1}{\Theta(\varepsilon)}\left\langle \frac{\frac{\varepsilon^2(k\cdot v)^2}{K^2a^2}}{1+\frac{\varepsilon^2(k\cdot v)^2}{K^2a^2}}\frac{M}{Ka}\right\rangle \underset{\varepsilon\to 0}{\sim} \frac{\varepsilon^{\frac{2d+2+\beta}{d+1+\beta}}}{\Theta(\varepsilon)}\frac{K^{1-\alpha}}{d+1+\beta}|k|^{\alpha}\left\langle \frac{(w\cdot e)^2}{1+(w\cdot e)^2}\frac{m}{|v|^{d+\alpha}}\right\rangle,$$

ce qui permet de trouver l'équation vérifiée par $\hat{\rho}$ à la limite, en posant $\Theta(\varepsilon) = \varepsilon^{\frac{2d+2+\beta}{d+1+\beta}}$.

Le type de fréquences de collisions fortement dégénérées à l'origine qui sont considérées ici intervient dans la modélisation de certaines chaînes d'oscillateurs. Dans [54], les auteurs considèrent une chaîne d'atomes dans un cristal uni-dimensionnel. Ils utilisent une modélisation cinétique pour représenter les vibrations du réseau, responsables du transport de la chaleur dans le cristal, dans laquelle une fréquence de collision dégénérée apparaît, ce qui induit une asymptotique de diffusion fractionnaire pour l'équation cinétique. Le chapitre 2 de ce manuscrit traite du cas de l'asymptotique de diffusion fractionnaire pour l'équation cinétique en se plaçant dans le cadre de [4].

Enfin, en suivant les idées développées dans [55], il est possible de considérer un opérateur de collision dans lequel l'équilibre M est à queue lourde et la fréquence de collision ν se comporte comme une puissance à l'infini, mais est régulière à l'origine. En fonction des poids respectifs de M et de ν, le comportement asymptotique de l'équation cinétique peut être soit de la diffusion normale, soit de la diffusion fractionnaire ou encore une diffusion normale avec scaling anormal. Une approche numérique pour ce dernier cas est proposée à la fin du troisième chapitre de ce manuscrit.

Ainsi, les asymptotiques de diffusion anormale pour les équations cinétiques qui sont considérées dans ce manuscrit se distinguent de l'asymptotique de diffusion classique par l'existence de deux raideurs de nature distincte : $\varepsilon \to 0$ et $\left\langle v\otimes v\nu^{-1}M\right\rangle = +\infty$. D'un point de vue numérique, la résolution de (0.0.12) dans l'asymptotique de diffusion anormale nécessite de gérer ces deux raideurs en même temps, ce qui n'avait jamais été réalisé auparavant. Comme la seconde raideur vient du rôle important des grandes ou petites vitesses, il sera essentiel de capturer numériquement les vitesses extrêmes, qui interviennent naturellement dans l'analyse asymptotique formelle, pour qu'un schéma puisse respecter les limites de diffusion fractionnaire.

Schémas *Asymptotic Preserving* (AP) pour les équations cinétiques

Comme indiqué au début de l'introduction, l'objet de cette thèse est la construction de schémas numériques pour l'équation cinétique (0.0.12) qui respectent les asymptotiques de diffusion anormales qui ont été introduites dans la partie précédente. Quelle que soit l'asymptotique considérée, la construction de schémas numériques pour (0.0.12) est compliquée si le paramètre ε est amené à devenir petit. En effet, quand ε tend vers 0, l'équation cinétique devient un problème raide. D'un point de vue numérique, la résolution de tels problèmes nécessite l'utilisation de méthodes spécifiques, puisque les méthodes naïves font apparaître des contraintes fortes liant les paramètres de discrétisation et la raideur. Ainsi, si résoudre numériquement l'équation cinétique est relativement aisé quand ε est proche de 1, considérer des ε plus petits impose la réduction des paramètres de discrétisation proportionnellement à ε (voire à une puissance de ε), et donc l'explosion des temps de calculs quand ε tend vers 0. À cette difficulté s'ajoute l'apparition fréquente de phénomènes de diffusion numérique dans les schémas, qui viennent de l'utilisation de trop petits paramètres numériques qui entraînent la propagation des erreurs numériques. Pour résoudre numériquement des problèmes raides typiques, il est commun d'utiliser des méthodes spécifiques, souvent basées sur une implicitation des termes raides.Cependant, l'application de telles méthodes peut s'avérer insuffisante dans le cas des équations cinétiques. La première raison à cela est que les méthodes implicites sont inadaptées aux problèmes en grande dimension, à cause du coût en temps de calcul des inversions. Or, dans le contexte cinétique, la présence de la variable v en plus de la variable d'espace augmente automatiquement la dimension des problèmes à résoudre. D'autre part, il est nécessaire de s'assurer que le modèle résolu par la méthode numérique quand ε tend vers 0 est le modèle limite voulu. En effet, si l'indépendance des paramètres numériques par rapport à ε est assurée, l'équation résolue par le schéma quand ε tend vers 0 n'est pas forcément l'équation limite attendue.

Dans le contexte des équations cinétiques, où se posent à la fois des problèmes liés au nombre de variables et au respect de la limite du modèle par le schéma quand ε tend vers 0, l'écriture de schémas aptes à respecter ces contraintes est donc cruciale. Les schémas *Asymptotic Preserving* (AP) ont été introduits pour répondre à la question de la précision de la solution numérique quand ε tend vers 0. Leur principe est souvent expliqué avec le diagramme suivant

$$\begin{array}{ccc} P_\varepsilon & \xrightarrow[\varepsilon\to 0]{} & P_0 \\ \uparrow{\scriptstyle h\to 0} & & \uparrow{\scriptstyle h\to 0} \\ S_\varepsilon^h & \xrightarrow[\varepsilon\to 0]{} & S_0^h \end{array}$$

qui s'interprète ainsi : étant donné un problème P_ε qui tend vers un problème P_0 quand ε tend vers 0, le schéma AP noté S_ε^h, dont les paramètres de discrétisation sont notés ici h, doit

- Être consistant avec le problème P_ε quand h tend vers 0 et ε est fixé.
- Tendre vers un schéma S_0^h consistant avec le problème P_0 quand h est fixé et ε tend vers 0.

La contrainte supplémentaire de convergence vers un schéma consistant avec le problème limite permet à ces schémas d'être efficaces à la fois dans le régime mésoscopique, pour ε proche de

1, et dans les régimes proches du régime macroscopique, quand ε est petit. On peut demander aux schémas AP d'avoir la propriété supplémentaire d'uniforme précision (UA, pour *Uniform Accuracy*), qui implique alors que la précision du schéma est indépendante du paramètre ε. La propriété d'uniforme précision permet de traiter le régime intermédiaire pour lesquels le problème est déjà raide mais pas encore proche du problème limite. Par contre, en raison des résonances entre les paramètres de discrétisation et ε, un schéma AP mais pas UA peut rencontrer des difficultés à approcher ce régime.

Des schémas respectant des asymptotiques de l'équation cinétique ont été proposés par A. Klar dans [43, 44], puis le principe des schémas AP a été introduit par S. Jin dans [37]. La notion a ensuite été largement étudiée et appliquée aux différentes asymptotiques de l'équation cinétique, comme la limite de diffusion [58, 41, 12, 52, 50, 57] ou les limites hydrodynamiques [6, 49]. Il n'existait pas –à notre connaissance– de schémas AP pour les limites de diffusion anormale des équations cinétiques lorsque cette thèse a commencé. Une approche basée sur une décomposition micro-macro de la fonction de distribution f et un calcul numérique précis des intégrales à queue lourde a été proposée en 2016 par L. Wang et B. Yan dans [69] pour le cas d'un équilibre M de type heavy-tail avec $\alpha \in (1, 2)$.

À cause de la raideur supplémentaire $\left\langle v \otimes v\nu^{-1}M \right\rangle = +\infty$, les schémas AP de la littérature pour la limite diffusive de (0.0.12) ne respectent pas les asymptotiques de diffusion anormale. Par exemple, même un schéma entièrement implicite écrit en variable de Fourier en espace ne capture pas les limites de diffusion anormale de (0.0.12)-(0.0.23), alors qu'il possède la propriété AP pour la limite de diffusion. Pour assurer le caractère AP des schémas dans le cas des limites de diffusion anormale, il faut s'assurer que les grandes (ou petites) vitesses qui sont responsables de l'anormalité de l'asymptotique sont correctement prises en compte. En effet, les approches numériques pour la limite de diffusion utilisent le plus souvent un espace numérique des vitesses tronqué puisque l'équilibre Maxwellien (0.0.14) décroit exponentiellement vite vers 0. Dans le cas d'un équilibre à queue lourde, tronquer l'espace des vitesses ne permet pas de capturer l'effet des grandes vitesses. En effet, en se plaçant en dimension 1 et en considérant une discrétisation $v_j, 1 \leq j \leq N_v$ à pas constant Δv de l'espace des vitesses tronqué $\{v \in V, |v| \leq v_{\max}\}$, le coefficient de diffusion (0.0.17) s'écrit,

$$D_{\text{discret}} = \Delta v \sum_{j=1}^{N_v} \frac{v_j^2}{a(v_j)} M(v_j), \tag{0.0.28}$$

qui est une somme finie de termes finis. Ainsi, le coefficient de diffusion qui devrait être infini dans les cas de diffusion anormale devient fini, bien que grand, dans les calculs numériques. En s'inspirant des calculs formels proposés pour la dérivation des limites de diffusion et de diffusion anormale, il apparaît qu'en considérant cette discrétisation en vitesse l'équation cinétique tend vers une équation de diffusion normale dont le coefficient de diffusion est D_{discret} quand ε tend vers 0. Le même problème se pose, en considérant les vitesses infiniment petites, dans le cas de la limite de diffusion fractionnaire induite par une fréquence de collision fortement dégénérée à l'origine. La prise en compte correcte des grandes et petites vitesses dans les schémas numérique est donc cruciale pour assurer le caractère AP des schémas pour (0.0.12) considérée dans ses limites de diffusion anormale.

L'approche développée dans ce manuscrit consiste à écrire tout d'abord des schémas semi-discrets en temps-espace, mais continus en vitesse, à identifier les termes qui permettent d'obtenir à la limite $\varepsilon \to 0$ la diffusion fractionnaire, et à modifier ces termes analytiquement avant d'appliquer la discrétisation en vitesse. La modification analytique de ces termes est effectuée de sorte que la consistance des schémas ne soit pas altérée.

Par rapport à la limite de diffusion, une difficulté s'ajoute lorsque le cas des limites de diffusion fractionnaires est considéré. En effet, comme il s'agit d'un opérateur non local, la discrétisation de l'équation limite est relativement délicate, alors que la discrétisation de l'équation de la chaleur ne pose *a priori* pas de problèmes particuliers. Lorsque les schémas sont écrits en variable de Fourier, la forme simple du laplacien fractionnaire permet de se libérer de cette contrainte. Lorsque les schémas sont écrits dans la variable d'espace, ce qui peut éventuellement être nécessaire pour éviter l'augmentation des coûts de calcul numérique, nous avons choisi dans un premier temps d'écrire tout de même les termes correspondant à l'asymptotique de diffusion fractionnaire en variable de Fourier dans les schémas. Avec des modifications mineures, qui sont indiquées à chaque fois aux endroits concernés, il est possible de les remplacer par une discrétisation en variable d'espace du laplacien fractionnaire. Un schéma AP pour l'équation cinétique avec limite de diffusion fractionnaire dans un cas où l'opérateur de collision est non local est proposé dans le quatrième chapitre de ce manuscrit. Dans ce cadre, l'écriture du problème en variable de Fourier n'est pas plus simple que le problème de départ, nous proposons donc une méthode numérique utilisant la variable d'espace, en nous basant sur des méthodes numériques existantes pour la discrétisation du laplacien fractionnaire [65].

En plus de la nécessité de la prise en compte des grandes et petites vitesses et du caractère non local de l'équation de diffusion fractionnaire, une autre difficulté spécifique aux asymptotiques de diffusion anormale surgit lors de l'écriture de schémas AP pour (0.0.12) dans les cas de diffusion anormale. En effet, nous avons mis en évidence, dans les trois cas considérés dans ce manuscrit, que le taux de convergence de l'équation cinétique vers l'équation asymptotique peut être lent. Par exemple, dans le cas critique de l'équilibre à queue lourde qui induit une limite de diffusion normale avec scaling anormal, la convergence de la solution de (0.0.12) vers la distribution limite se fait à la vitesse $1/|\ln(\varepsilon)|$. Le taux, extrêmement lent, rend difficile l'exploration et la validation numérique du régime intermédiaire. Néanmoins, dans ce cas nous avons pu mettre en évidence que la dynamique de la convergence vers l'équation de diffusion se fait en deux étapes :

- Une convergence rapide vers une distribution à l'équilibre dont la densité intermédiaire est solution d'une équation plus simple que l'équation cinétique,
- Une convergence lente de cette densité intermédiaire vers la densité solution de l'équation de diffusion limite.

Ainsi, pour capter la dynamique de cette convergence, nous proposons des schémas AP qui ont de plus la propriété de résoudre le problème intermédiaire dans l'intervalle de ε concernés. Comme pour les schémas AP, leur principe peut-être résumé par le diagramme suivant

$$\begin{array}{ccccc} P_\varepsilon & \xrightarrow[\varepsilon \text{ diminue}]{\gamma_1} & \tilde{P}_\varepsilon & \xrightarrow[\varepsilon\to 0]{\gamma_2} & P_0 \\ \uparrow{\scriptstyle h\to 0} & & \uparrow{\scriptstyle h\to 0} & & \uparrow{\scriptstyle h\to 0} \\ S_\varepsilon^h & \xrightarrow[\varepsilon \text{ diminue}]{\gamma_1} & \tilde{S}_\varepsilon^h & \xrightarrow[\varepsilon\to 0]{\gamma_2} & S_0^h \end{array}$$

Cette fois, le problème P_ε tend, avec le taux de convergence en temps $\gamma_1 = \varepsilon\,(1 + |\ln(\varepsilon)|)$, vers un problème $\tilde{P}_\varepsilon$ lequel tend plus lentement, avec le taux $\gamma_2 = 1/\,(1 + |\ln(\varepsilon)|)$, vers le modèle asymptotique P_0. Pour respecter la dynamique de cette asymptotique, le schéma S_ε^h doit être consistant avec le problème P_ε quand ε est fixé, et quand les paramètres de discrétisation (notés

ici h) sont fixés, tendre, avec le taux γ_1 en ε, vers un schéma $\tilde{S}^h_\varepsilon$ consistant avec le problème $\tilde{P}_\varepsilon$. Enfin, toujours quand les paramètres de discrétisation sont fixés, le schéma $\tilde{S}^h_\varepsilon$ doit tendre avec le taux γ_2 vers un schéma S^h_0 consistant avec P_0 quand ε tend vers 0. Dans le cas de la limite de diffusion normale avec scaling anormal traité dans le troisième chapitre de ce manuscrit, les schémas AP ont été améliorés pour respecter le diagramme. Ainsi, ils s'avèrent plus performants dans le régime intermédiaire où l'équation cinétique est difficile à résoudre. Pour prendre en compte les grandes vitesses à l'origine de l'asymptotique de diffusion anormale considérée, il est ensuite nécessaire d'appliquer la même méthodologie que dans les deux premiers chapitres pour assurer la convergence du schéma en un schéma consistant avec l'équation limite et éviter une limite de diffusion numérique de coefficient (0.0.28).

Approche numérique

Les schémas AP pour l'équation cinétique (0.0.12) avec limite de diffusion anormale présentés dans ce manuscrit ont été construits à partir de schémas possédant la propriété AP pour la limite de diffusion. La prise en compte de conditions de bord pour les équations cinétiques avec limite de diffusion fractionnaire étant toujours un problème ouvert, nous avons choisi de résoudre (0.0.12) sur le tore en x. Du point de vue des schémas numériques, ceci permet aussi l'utilisation de la transformée de Fourier discrète. Comme les opérateurs de collision (0.0.23) et (0.0.15) ont une écriture simple en variable de Fourier, considérer (0.0.12) munie de ces opérateurs permet d'écrire des schémas AP utilisant la variable de Fourier.

Nous proposons trois schémas dans ce manuscrit :

- Un schéma entièrement implicite pour (0.0.12)-(0.0.23)-(0.0.15) en variable de Fourier en espace, dont nous verrons qu'il nécessite une modification pour être AP.
- Un schéma micro-macro qui permet de s'affranchir de l'utilisation de la variable de Fourier en espace et qui peut être adapté aux cas d'opérateurs de collision généraux (0.0.13).
- Un schéma basé sur une formulation intégrale de (0.0.12)-(0.0.23)-(0.0.15), dont nous verrons qu'il est UA.

La première approche que nous proposons est basée sur une formulation entièrement implicite de l'équation cinétique en variable de Fourier. Comme (0.0.12) s'écrit comme une équation différentielle ordinaire

$$\Theta(\varepsilon)\partial_t \hat{f} + \varepsilon \mathrm{i} k \cdot v \hat{f} = L(\hat{f}),$$

où L désigne (0.0.23) ou (0.0.15), il est possible d'écrire un schéma d'Euler implicite pour la résoudre numériquement. Étant donnée la forme simplifiée de l'opérateur L que nous considérons, l'inversion de l'opérateur peut être réalisée analytiquement et ne pose donc pas de problème particulier. Dans le cas de la limite de diffusion classique, il est bien connu qu'un tel schéma possède la propriété AP. Néanmoins, comme indiqué dans la partie précédente, ce n'est pas vrai dans le cas de la diffusion anormale et il est nécessaire de prendre en compte correctement l'influence des grandes et petites vitesses pour assurer son caractère AP. Ceci est fait en modifiant dans l'expression du schéma, le terme qui génère la diffusion fractionnaire quand ε tend vers 0, qui s'exprime comme une intégrale en vitesse. L'idée consiste à faire apparaître explicitement la diffusion fractionnaire grâce à un changement de variables dans l'intégrale en vitesse continue, avant de discrétiser. Après cette manipulation, le schéma est d'ordre 1, conserve la masse et possède la propriété AP.

Pour s'affranchir d'un schéma implicite pour le transport et de l'utilisation (restrictive) de la variable de Fourier, il peut être nécessaire de considérer un schéma AP utilisant la variable d'espace pour (0.0.12). Dans ce manuscrit, nous proposons une deuxième classe de schéma basée sur une décomposition micro-macro de la fonction de distribution f, comme dans [52, 50]. En notant

$$f = \rho M + g,$$

où $\rho = \langle f \rangle$ et $g = f - \rho M$ vérifie $\langle g \rangle = 0$, on peut écrire un système couplé vérifié par ρ et g

$$\begin{cases} \partial_t \rho + \dfrac{\varepsilon}{\Theta(\varepsilon)} \langle v \cdot \nabla_x g \rangle = 0 \\ \partial_t g + \dfrac{\varepsilon}{\Theta(\varepsilon)} v \cdot \nabla_x \rho M + \dfrac{\varepsilon}{\Theta(\varepsilon)} (I - \Pi)\,(v \cdot \nabla_x g) = \dfrac{1}{\Theta(\varepsilon)} L(g), \end{cases}$$

où Π désigne la projection sur le noyau de L

$$\Pi(f) = \langle f \rangle\, M.$$

La discrétisation en temps de ce système doit alors être effectuée de manière à assurer le caractère AP du schéma. Dans le cas des opérateurs de collision simplifiés (0.0.23) et (0.0.15) pour lesquels L peut être inversé analytiquement, on procède en implicitant les termes les plus raides. Dans le cas le plus général, où l'inversion de l'opérateur de collision (0.0.13) est plus compliquée, on applique une stratégie dite de relaxation pour l'équation sur g (voir[49]). L'équation en ρ est aussi discrétisée en implicitant le terme $\langle v \cdot \nabla_x g \rangle$, qui est le terme le plus raide de l'équation. Cependant, assurer que ρ résout l'équation de diffusion anormale quand ε tend vers 0 est moins immédiat. En effet, réinjecter l'expression de g trouvée avec l'étape précédente ne suffit pas à assurer le caractère AP du schéma, puisque les grandes et petites vitesses ne sont pas prises en compte. D'autre part, l'opérateur de transport qui intervient de manière cruciale dans l'analyse, n'est pas inversé. Pour faire apparaître l'inverse du transport, on procède en injectant une formulation implicite de (0.0.12) dans le flux macroscopique $\langle v \cdot \nabla_x g \rangle = \langle v \cdot \nabla_x f \rangle$. Ensuite, l'expression obtenue peut être simplifiée de manière consistante et le terme qui tend vers la limite de diffusion anormale est traité comme indiqué dans la partie précédente pour assurer la prise en compte correcte des petites et grandes vitesses. Une fois ces manipulations réalisées, le schéma est toujours d'ordre 1, préserve la masse et possède le caractère AP. De plus, le transport y est traité explicitement.

Enfin, dans les cas d'opérateurs de collision simplifiés (0.0.23) et (0.0.15), nous proposons un troisième schéma AP pour l'équation cinétique avec limite de diffusion anormale, qui possède de plus la propriété UA. Il est basé sur une formulation intégrale de (0.0.12) en variable de Fourier et sa construction est proche de celle des schémas exponentiels proposés dans [34]. Pour expliquer plus simplement son principe, plaçons-nous dans le cas de l'opérateur (0.0.23). L'équation cinétique se réécrit

$$\hat{f}(t,k,v) = A_0(t,k,v) + \int_0^{\frac{t}{\Theta(\varepsilon)}} \mathrm{e}^{-s(1+\varepsilon \mathrm{i} k\cdot v)} \hat{\rho}(t - \Theta(\varepsilon)s, k) M(v) \mathrm{d}s, \tag{0.0.29}$$

où A_0 est un terme de couche initiale donné par $A_0 = \mathrm{e}^{-t(1+\mathrm{i}\varepsilon k\cdot v)} \hat{f}_{\mathrm{in}}(k,v)$. Une expression fermée en $\hat{\rho}$ est obtenue en intégrant (0.0.29) par rapport à v

$$\hat{\rho}(t_{n+1},k) = \langle A_0(t_{n+1},k,v) \rangle + \sum_{j=0}^{n} \int_{\frac{t_j}{\Theta(\varepsilon)}}^{\frac{t_{j+1}}{\Theta(\varepsilon)}} \left\langle \mathrm{e}^{-s(1+\varepsilon \mathrm{i} k\cdot v)} M(v) \right\rangle \hat{\rho}(t_{n+1} - \Theta(\varepsilon)s, k) \mathrm{d}s,$$

où la discrétisation en temps est définie par $t_n = n\Delta t, 0 \leq n \leq N, N\Delta t = T$. À partir de cette expression, un schéma numérique peut être écrit en considérant dans chaque intégrale en temps une quadrature d'ordre 2 de $\hat{\rho}(t_{n+1} - \Theta(\varepsilon)s, k)$. En supposant que ρ et ses dérivées en temps sont régulières, l'erreur commise dans cette quadrature ne dépend pas de ε, ce qui indique que l'approximation effectuée est valide aussi bien dans le régime mésoscopique que dans le régime macroscopique. Une fois cette quadrature effectuée, les intégrales en temps peuvent être calculées et il ne reste plus qu'à discrétiser les intégrales en vitesse qui apparaissent dans les coefficients de la somme. Pour assurer le caractère AP du schéma, on procède comme précédemment, en transformant analytiquement les termes qui tendent vers la limite de diffusion anormale pour faire apparaître explicitement leur limite, avant de discrétiser les vitesses. En plus de fournir un schéma uniformément précis d'ordre 1, cette approche permet d'écrire un schéma satisfait par $\hat{\rho}$, ce qui allège les coûts de calcul en réduisant la dimension du problème. Néanmoins, la fonction de distribution peut être calculée avec une approche similaire sur (0.0.29) si nécessaire. Ce schéma et la preuve de son uniforme précision sont détaillés, dans tous cas de diffusion fractionnaire que nous considérons, dans les trois premiers chapitres de ce manuscrit.

Organisation du manuscrit

Le manuscrit est organisé en quatre parties dans lesquelles nous détaillons la construction des schémas numériques présentées dans la partie précédente dans les trois cas de diffusion anormale introduits dans la partie . Le premier chapitre est consacré au cas de la limite de diffusion fractionnaire pour l'équation cinétique dans le cas d'un équilibre à queue lourde M avec

$$M(v) \underset{|v|\to\infty}{\sim} \frac{m}{|v|^{d+\alpha}}, \tag{0.0.30}$$

où $\alpha \in (0, 2)$. En considérant le cas d'un opérateur de collision de type (0.0.23), nous proposons une dérivation formelle de l'asymptotique de diffusion fractionnaire qui permet d'introduire le principe des schémas numériques que nous construisons par la suite. Nous mettons ensuite en place les trois approches numériques détaillées dans la section précédente : schéma implicite en variable de Fourier, schéma basé sur une décomposition micro-macro et schéma basé sur une écriture intégrale de (0.0.12) en variable de Fourier. Ces schémas sont tous trois d'ordre 1, préservent la masse et possèdent le caractère AP. Ces propriétés sont soigneusement prouvées et nous montrons également que le dernier schéma possède en outre la propriété d'uniforme précision. Enfin, nous proposons des tests numériques pour illustrer les propriétés des schémas dans le cadre que nous considérons. Ces résultats ont été publiés dans [17].

Dans la continuité du premier chapitre, nous étudions alors un autre cas d'asymptotique de diffusion fractionnaire pour l'équation cinétique. En se plaçant dans le cadre de [4], l'opérateur de collision considéré est de la forme (0.0.15), avec une fréquence de collision fortement dégénérée à l'origine, comme dans (0.0.27). Cette fois encore, nous proposons une analyse formelle de l'asymptotique diffusion fractionnaire qui prépare l'écriture des schémas introduits ensuite. Nous étudions aussi formellement le taux de convergence de l'équation cinétique vers son modèle limite en fonction de ε. Comme dans le premier chapitre, nous adaptons les schémas implicites, micro-macro et basés sur la formulation intégrale de (0.0.12) au cas spécifique de la fréquence de collision dégénérée. Par rapport au cas *heavy-tail*, des difficultés spécifiques à la fréquence de collision dégénérée surgissent. En premier lieu, au lieu des grandes vitesses ce sont les petites vitesses qui nécessitent une attention particulière dans ce cas. Ensuite, l'opérateur de

collision (0.0.15) fait intervenir une densité renormalisée, différente de la densité usuelle, qu'il faut traiter spécifiquement. Enfin, nous montrons que le taux de convergence de l'équation cinétique vers le modèle limite est lent, ce qui implique que le régime intermédiaire est étendu et complique les calculs numériques. Nous proposons donc une stratégie pour contourner ces difficultés, et nous prouvons ensuite que les schémas ont les mêmes propriétés que ceux du premier chapitre. Les tests numériques illustrent les propriétés des schémas et montrent que la solution numérique de (0.0.12) tend vers la solution du modèle limite avec la vitesse de convergence attendue. Ces résultats ont été annoncés dans [16], puis acceptés dans [18].

Le troisième chapitre est dédié à l'étude de la limite de diffusion normale avec scaling anormal qui apparaît dans le cas critique $\alpha = 2$ des opérateurs de collision heavy-tail (0.0.30) étudiés dans le premier chapitre. Dans ce cadre, il n'y a plus de difficulté liée au caractère non local de l'équation limite. En revanche, la lenteur de la vitesse de convergence de (0.0.12) vers le modèle limite implique qu'atteindre numériquement le régime asymptotique est difficile. En considérant l'opérateur de collision (0.0.23), nous commençons par prouver que la convergence vers le modèle asymptotique fait intervenir deux dynamiques : l'une rapide vers un modèle intermédiaire et l'autre lente vers l'équation de diffusion limite. Nous adaptons les trois schémas proposés dans les deux premiers chapitres pour que, en plus de posséder la propriété AP, ils respectent la dynamique de cette convergence. Toujours en considérant le même équilibre, nous nous plaçons ensuite dans le cadre d'un opérateur de collision non local de type (0.0.13). Nous proposons alors, en nous basant sur les travaux précédents et sur [49], un schéma micro-macro relaxé possédant la propriété AP pour l'asymptotique de diffusion anormale traitée dans ce chapitre. Toutes les propriétés des schémas sont soigneusement prouvées, et nous proposons de nombreux tests numériques pour les illustrer. Ces résultats seront soumis prochainement [33].

Enfin, nous proposons dans le quatrième chapitre une généralisation du cas de la limite de diffusion fractionnaire pour l'équation cinétique du premier chapitre au cas d'un opérateur de collision non local dont la section locale dépend de l'espace

$$L(f) = \int_{R^d} \big(\sigma(x, v, v')f(v') - \sigma(x, v', v)f(v)\big)\, \mathrm{d}v'.$$

Dans ce contexte, traité mathématiquement dans [53], l'analyse asymptotique de l'équation cinétique ne peut pas être effectuée en variable de Fourier. Les schémas implicite et basé sur une formulation intégrale de (0.0.12) ne peuvent donc pas être écrits dans ce cas. Nous proposons alors une adaptation du schéma micro-macro relaxé de la fin du troisième chapitre. Le schéma ainsi obtenu possède la propriété AP pour l'asymptotique de diffusion fractionnaire. Des tests numériques sont ensuite présentés pour illustrer cette propriété.

Chapter 1

Numerical schemes for kinetic equations in the anomalous diffusion limit: the case of heavy-tailed equilibrium

1.1 Introduction

The modeling and numerical simulation of particles systems is a very active field of research. Indeed, they provide the basis for applications in neutron transport, thermal radiation, medical imaging or rarefied gas dynamics. According to the physical context, particles systems can be described at different scales. When the mean free path of the particles (*i.e.* the crossed distance between two collisions) is large compared to typical macroscopic length, the system is described at a microscopic level by kinetic equations; kinetic equations consider the time evolution of a distribution function which gives the probability of a particle to be at a given state in the six dimensional phase space at a given time. Conversely, when the mean free path is small, a macroscopic description (such as diffusion or fluid equations) can be used. It makes evolve macroscopic quantities which depends only on time and on the three dimensional spatial variable. In some situations, this description can be sufficient and leads to faster numerical simulations.

Mathematically, the passage from kinetic to macroscopic models is performed by asymptotic analysis. From a numerical point of view, considering a small mean free path, the kinetic equation then contains stiff terms which make the numerical simulations very expensive for stability reasons. In fact, a typical example is the presence of multiple spatial and temporal scales which intervene in different positions and at different times. These behaviors make the construction of efficient numerical methods a real challenge.

In this work, we are interested in the time evolution of the distribution function f which depends on the time $t \geq 0$, the space variable $x \in \Omega \subset \mathbb{R}^d$ and the velocity $v \in \mathbb{R}^d$, with $d = 1, 2, 3$. Particles undergo the effect of collisions which are modelized here by a linear operator L acting on f through

$$L(f)(t,x,v) = \rho(t,x)M_\beta(v) - f(t,x,v),$$

where

$$\rho(t,x) = \langle f(t,x,v)\rangle =: \int_{\mathbb{R}^d} f(t,x,v)\mathrm{d}v,$$

and where the equilibrium M_β is defined by

$$M_\beta(v) = \begin{cases} \dfrac{1}{(2\pi)^{d/2}} \exp\left(-|v|^2/2\right) & \text{if } \beta = 2+d, \\ \underset{|v|\to\infty}{\sim} \dfrac{m}{|v|^\beta} & \text{if } \beta \in (d, d+2), \end{cases} \tag{1.1.1}$$

where m is a normalization factor. In the sequel, we will always denote by brackets the integration over v. In order to capture a nontrivial asymptotic model, a suitable scaling has to be considered. The good scaling of the kinetic equation (see [55, 53, 5]) satisfied by the distribution function f is given by

$$\varepsilon^\alpha \partial_t f + \varepsilon v \cdot \nabla_x f = L(f), \quad \text{with} \quad \alpha = \beta - d \in (0, 2], \tag{1.1.2}$$

where $\varepsilon > 0$ is the Knudsen number (ratio between the mean free path and a typical macroscopic length). With the equilibrium M_β defined in (1.1.1), the case $\alpha = 2$ refers to the classical diffusion limit whereas the case $\alpha \in (0, 2)$ refers to the anomalous diffusion limit. Although our analysis could be applied to general operators L, we will consider for a sake of simplicity a BGK type operator. We suppose that M_β given by (1.1.1) is an even positive function such

that $\langle M_\beta(v)\rangle = 1$ and $\langle vM_\beta(v)\rangle = 0$. Equation (1.1.2) has to be supplemented with an initial condition $f(0,x,v) = f_0(x,v)$ and spatial periodic boundary conditions are considered.

The main goal of this work is to construct numerical schemes for (1.1.2) which are uniformly stable along the transition from kinetic to macroscopic regime (*i.e.* for all $\varepsilon > 0$). More precisely, we consider here the asymptotic of anomalous diffusion ($\alpha \in (0,2)$). We shall also consider the asymptotic of diffusion ($\alpha = 2$) to highlight the differences between the two cases. For the diffusion limit, several numerical schemes have already been proposed but in the anomalous diffusion limit, to the best of author's knowledge, the only other approach was proposed in [69] for the case $\alpha \in (1,2)$ at the same time this paper was submitted. Here, we deal with $\alpha \in (0,2)$ and the method we propose is robust enough to deal with other cases giving fractional diffusion, such as the case of a degenerate collision frequency which will be detailed in [18]. The results we present here were announced in [16].

Mathematically, the derivation of diffusion type equation from kinetic equations such as (1.1.2) when $\alpha = 2$ was first investigated in [70], [7], [48] or [22]. When M_β decreases quickly enough for large $|v|$, the solution f of (1.1.2) converges, when ε goes to zero, to an equilibrium function $f(t,x,v) = \rho(t,x)M_\beta(v)$ where $\rho(t,x)$ is solution of the diffusion equation

$$\partial_t \rho(t,x) - \nabla_x \cdot (D\nabla_x \rho(t,x)) = 0, \tag{1.1.3}$$

and where the diffusion matrix D is given, in the simple case of the BGK operator, by the formula

$$D = \int_{\mathbb{R}^d} v \otimes v M_\beta(v) \mathrm{d}v. \tag{1.1.4}$$

In particular, a crucial assumption on M_β for D to be finite is that

$$\int_{\mathbb{R}^d} |v|^2 M_\beta(v) \mathrm{d}v < +\infty;$$

this is the case when M_β is Maxwellian (first case of (1.1.1)).

Hence, if the equilibrium has no finite second order moment, the asymptotic of rescaled kinetic equation with $\alpha = 2$ is not able to capture a nontrivial dynamics and the value of α should be tuned with M_β in order to recover this macroscopic equation when $\varepsilon \to 0$. Typically, let M_β be a heavy-tailed distribution function, corresponding to the second case of (1.1.1). In the sequel, we will consider as an example of such a distribution function $M_\beta(v) = \frac{m}{1+|v|^\beta}$ with m chosen such that $\langle M_\beta(v)\rangle = 1$ and $\beta = d + \alpha,\ \alpha \in (0,2)$.

In the case of astrophysical plasmas, it often occurs that the equilibrium M_β is a heavy-tailed distribution of particles which typically generates an anomalous diffusion behaviour (see [56, 68]). In particular, the diffusion matrix D is no longer well-defined and this requires to adapt the value of α in terms of the tail decreasing rate β, in order to capture a nontrivial dynamics.

When ε goes to 0, the solution of this equation with BGK operator converges to $\rho(t,x)M_\beta(v)$ where ρ is the solution of the anomalous diffusion equation which can be written in Fourier variable

$$\partial_t \hat{\rho}(t,k) = -\kappa |k|^\alpha \hat{\rho}(t,k), \tag{1.1.5}$$

where $\hat{\rho}$ stands for the space Fourier variable of ρ, k is the Fourier variable and κ is a constant which depends only on the size of the tail of the equilibrium $M_\beta(v)$ and is defined by

$$\kappa = \int_{\mathbb{R}^d} \frac{(w\cdot e)^2}{1+(w\cdot e)^2} \frac{m}{|w|^\beta} \mathrm{d}w, \tag{1.1.6}$$

for any $e \in \mathbb{R}^d$ such that $|e| = 1$ (note that κ does not depend on e). The anomalous diffusion equation can also be written in the space variable

$$\partial_t \rho(t,x) = -\frac{m\Gamma(\alpha+1)}{c_{d,\alpha}} (-\Delta_x)^{\frac{\alpha}{2}} \rho(t,x), \tag{1.1.7}$$

where m is the normalization factor of M_β in (second case in 1.1.1), Γ is the usual function defined by

$$\Gamma(x) = \int_0^{+\infty} t^{x-1} \mathrm{e}^{-t} \mathrm{d}t,$$

and $c_{d,\alpha}$ is a normalization constant given by

$$c_{d,\alpha} = \frac{\alpha\Gamma\left(\frac{d+\alpha}{2}\right)}{2\pi^{\frac{d}{2}+\alpha}\Gamma\left(1-\frac{\alpha}{2}\right)}. \tag{1.1.8}$$

The fractional operator of the anomalous diffusion is easily defined by its Fourier transform

$$\widehat{\left((-\Delta_x)^{\frac{\alpha}{2}} \rho\right)}(k) = |k|^\alpha \hat{\rho}(k),$$

but has also an integral definition

$$(-\Delta_x)^{\frac{\alpha}{2}} \rho(x) = c_{d,\alpha} P.V. \int_{\mathbb{R}^d} \frac{\rho(x+y)-\rho(x)}{|y|^{d+\alpha}} \mathrm{d}y, \tag{1.1.9}$$

where *P.V.* denotes the principal value of the integral.

The anomalous diffusion occurs not only in astrophysical plasmas but also in the study of granular media (see [27, 9, 8]), tokamaks (see [23]) or even in economy or social science: as detailed in [46], the Pareto distribution is a power tail distribution that satisfies the second case of (1.1.1). This kind of distribution is a common object used to modelise the repartition of sizes in a given set (asteroïds, cities, income, opinions...). At a microscopic level, these velocity distributions arise when the motion of the particles is no longer governed by a brownian process but by a Levy process (see [20], [21]).

In this work, we want to construct a numerical scheme over the kinetic equation using a heavy-tailed distribution equilibrium, which is robust when the stiffness parameter ε goes to 0. Asymptotic Preserving (AP) schemes already exist in the case of the diffusion limit where the equilibrium is a Maxwellian (see [37, 11, 12, 40, 43, 52, 41, 58]) but the strategy used to obtain them cannot be rendered word for word to the anomalous diffusion case. As in the diffusion case, the difficulties when numerically solving the kinetic equation in the case of anomalous diffusion come from the stiff terms which require a severe condition on the numerical parameters. But in the anomalous diffusion case, there is an additional difficulty since one needs to take into account the large velocities arising in the equilibrium M_β. Indeed, the role of these high velocities is crucial and they have to be captured numerically in order to produce the anomalous diffusion operator when $\varepsilon \to 0$.

To derive a numerical scheme which enjoys the AP property, different strategies are investigated in this work. The first one is based on a fully implicit scheme in time (both the transport and the collision term are considered implicit). Using this *brute force* strategy, the so-obtained numerical scheme is obviously AP in the diffusion limit but not in the anomalous diffusion one. Therefore, a suitable transformation of this implicit scheme is proposed in this work and leads to a scheme enjoying the AP property in the anomalous diffusion limit.

From a computational point of view, a fully implicit scheme may be very expensive especially if one deals with high-dimensional problems. To avoid this implicitation, we propose another strategy which is based on a micro-macro decomposition. The distribution function f is written as a sum of an equilibrium part ρM_β plus a remainder g. A model equivalent to (1.1.2) is then derived, composed of a kinetic equation satisfied by g and a macroscopic equation satisfied by ρ. The macroscopic flux is then reformulated to obtain a numerical scheme which enjoys the AP property and which does not require the implicitation of the transport term.

The last strategy proposed in this work is based on a Duhamel formulation of the equation from which a AP numerical scheme solving the kinetic equation is obtained, this approach bears similarities with [34]. This numerical scheme is efficient for the diffusion case and has to be adapted also to get an AP scheme in anomalous diffusion limit. Moreover, there are two main advantages in using such strategy. First we derive a closed equation on ρ and the computation of the full distribution function is not needed at any time. Second, this strategy ensures that the numerical scheme has uniform accuracy in ε. Eventually, it would be easier to construct high order (in time) schemes on this formulation.

The paper is organized as follows. In the next section we shall start with formal computations recalling how the anomalous diffusion limit can be obtained from the kinetic equation. Section 1.3 is devoted to the derivation of the different numerical schemes: a fully implicit scheme, a micro-macro scheme and a scheme based on a Duhamed formulation of (1.1.2). After the theoretical study of their properties, several numerical tests are presented in Section 1.4 in a one-dimensional case with periodic boundary conditions in space to illustrate and compare the efficiency of the various numerical schemes.

1.2 A closed equation for the density and its diffusion asymptotics

This section is devoted to the derivation from (1.1.2) of a closed equation satisfied by ρ. This equation will be the basic equation from which we formally derive the anomalous diffusion equation. Of course, the formal derivation of anomalous diffusion equation is classical but, for a sake of clarity, we present one way (among many others) to perform such derivation. In particular, the formal computation below will drive the construction of a class of our numerical schemes. We recall here the hypothesis on the equilibrium $M_\beta(v)$ introduced in (1.1.1): it is an even function such that $\langle M_\beta(v)\rangle = 1, \langle vM_\beta(v)\rangle = 0$. Then we will consider the two following cases mentioned in (1.1.1): $\alpha = 2$ and $0 < \alpha < 2$ with the following equilibrium functions

Case 1.1. $\langle v \otimes vM_{d+2}(v)\rangle < +\infty$ and $\alpha = 2$. We will consider

$$M_{d+2}(v) = \frac{1}{(2\pi)^{d/2}} \mathrm{e}^{-\frac{|v|^2}{2}}.$$

Case 1.2. $\langle v \otimes vM_\beta(v)\rangle = \infty$ and $\alpha \in (0, 2)$. We will consider the heavy-tailed function M_β defined by

$$M_\beta(v) = \frac{m}{1 + |v|^\beta}, \qquad \beta = d + \alpha, \tag{1.2.1}$$

with a positive normalization factor m ensuring $\langle M_\beta\rangle = 1$.

1.2.1 Space Fourier transform based computations

Starting from (1.1.2), we propose here a method based on spatial Fourier transform to formally derive the asymptotic equation in both diffusion and anomalous diffusion limits. It will also be the basis of the numerical methods we set in Section 1.3.3.

Eventually, we remind that we denote by $\hat{f}(t,k,v)$ (resp. $\hat{\rho}(t,k)$)

$$\hat{f}(t,k,v) = \int_{\mathbb{R}^d} \mathrm{e}^{-\mathrm{i}k\cdot x} f(t,x,v)\mathrm{d}x,$$

the space Fourier transform of $f(t,x,v)$ (resp. $\rho(t,x)$). We have

Proposition 1.1. *1. Equation (1.1.2) formally implies the following exact equation on $\hat{\rho}$*

$$\hat{\rho}(t,k) = \left\langle \mathrm{e}^{-\frac{t}{\varepsilon^\alpha}(1+\mathrm{i}\varepsilon k\cdot v)} \hat{f}(0,k,v) \right\rangle + \int_0^{\frac{t}{\varepsilon^\alpha}} \mathrm{e}^{-s} \left\langle \mathrm{e}^{-\mathrm{i}\varepsilon s k\cdot v} M_\beta(v) \right\rangle \hat{\rho}(t-\varepsilon^\alpha s,k)\mathrm{d}s. \quad (1.2.2)$$

2. In case 1.2 (anomalous diffusion scaling), when $\varepsilon \to 0$, $\hat{\rho}$ solves the anomalous diffusion equation

$$\partial_t \hat{\rho}(t,k) = -\kappa\,|k|^\alpha\,\hat{\rho}(t,k),$$

with κ defined by (1.1.6) and $\beta - d = \alpha$.

Proof.

1. **Formal derivation of the expression (1.2.2) from (1.1.2)**
   We start by taking the Fourier transform of (1.1.2)

$$\partial_t \hat{f} + \mathrm{i}\varepsilon^{1-\alpha} v\cdot k\hat{f} = \frac{1}{\varepsilon^\alpha}\left(\hat{\rho}M_\beta - \hat{f}\right).$$

   We solve in $\hat{f}$ (assuming $\hat{\rho}$ is given)

$$\hat{f}(t,k,v) = \mathrm{e}^{-\frac{t}{\varepsilon^\alpha}(1+\mathrm{i}\varepsilon k\cdot v)}\hat{f}(0,k,v) + \frac{1}{\varepsilon^\alpha}\int_0^t \mathrm{e}^{-\frac{t-s}{\varepsilon^\alpha}(1+\mathrm{i}\varepsilon k\cdot v)}\hat{\rho}(s,k)M_\beta(v)\mathrm{d}s,$$

   which can be written after a change of variables $s \to (t-s)/\varepsilon^\alpha$

$$\hat{f}(t,k,v) = \mathrm{e}^{-\frac{t}{\varepsilon^\alpha}(1+\mathrm{i}\varepsilon k\cdot v)}\hat{f}_0 + \int_0^{\frac{t}{\varepsilon^\alpha}} \mathrm{e}^{-s(1+\mathrm{i}\varepsilon k\cdot v)}\hat{\rho}(t-\varepsilon^\alpha s,k)M_\beta(v)\mathrm{d}s.$$

   Still denoting by brackets the integration over the velocity space, we can integrate the previous expression with respect to v to get (1.2.2). Then, we can write it to make the limit equation appear

$$\begin{aligned}\hat{\rho} =& \hat{A}_0(t,k) + \int_0^{\frac{t}{\varepsilon^\alpha}} \mathrm{e}^{-s}\left\langle \mathrm{e}^{-\mathrm{i}\varepsilon s k\cdot v} M_\beta \right\rangle \mathrm{d}s\hat{\rho} \\ &+ \varepsilon^\alpha \int_0^{\frac{t}{\varepsilon^\alpha}} s\mathrm{e}^{-s}\frac{\hat{\rho}(t-\varepsilon^\alpha s,k)-\hat{\rho}(t,k)}{\varepsilon^\alpha s}\left\langle \mathrm{e}^{-\mathrm{i}\varepsilon s k\cdot v} M_\beta(v) \right\rangle \mathrm{d}s, \end{aligned} \quad (1.2.3)$$

   where

$$\hat{A}_0(t,k) = \left\langle \mathrm{e}^{-\frac{t}{\varepsilon^\alpha}(1+\mathrm{i}\varepsilon k\cdot v)}\hat{f}_0 \right\rangle, \quad (1.2.4)$$

   denotes the initial layer term.

   Here, in case 1.1, Taylor expansions of the exponentials and of $\hat{\rho}$ with respects to ε formally leads to the asymptotic diffusion equation (1.1.3) in Fourier variable. In case 1.2 (anomalous diffusion case) a finer analysis must be done to find the asymptotic equation.

2. **The anomalous diffusion limit**

Now we will show that when M_β fulfills the conditions of case 1.2 (anomalous diffusion scaling), the solution of (1.1.2) converges to the solution of the anomalous diffusion equation when ε goes to zero.

At first, let us remark that the first term has exponential decay when ε goes to zero, $\hat{A}_0 = o(\varepsilon^\infty)$, for all $t > 0$. With assumptions of smoothness in time for $\hat{\rho}$, we get the following behaviour for the third term of (1.2.3)

$$\int_0^{\frac{t}{\varepsilon^\alpha}} s\mathrm{e}^{-s} \frac{\hat{\rho}(t-\varepsilon^\alpha s,k)-\hat{\rho}(t,k)}{\varepsilon^\alpha s} \left\langle \mathrm{e}^{-\mathrm{i}\varepsilon s k\cdot v} M_\beta \right\rangle \mathrm{d}s \underset{\varepsilon\to 0}{\sim} -\partial_t\hat{\rho}(t,k) + o(1).$$

We now have to make appear the fractional diffusion in the second term of (1.2.3). Since the moment of order 2 of M_β is not finite, we cannot expand the exponential term into a power series in ε anymore. We decompose this term as

$$\int_0^{\frac{t}{\varepsilon^\alpha}} \mathrm{e}^{-s} \left\langle \mathrm{e}^{-\mathrm{i}\varepsilon s k\cdot v} M_\beta \right\rangle \mathrm{d}s = \int_0^{\frac{t}{\varepsilon^\alpha}} \mathrm{e}^{-s}\mathrm{d}s + \int_0^{\frac{t}{\varepsilon^\alpha}} \mathrm{e}^{-s} \left\langle \left(\mathrm{e}^{-\mathrm{i}\varepsilon s k\cdot v} - 1\right) M_\beta \right\rangle \mathrm{d}s,$$

and we focus on the second term on the right hand side of this last equality.

Here we still suppose that $M_\beta(v) = \frac{m}{1+|v|^\beta}$, where m is chosen to ensure that $\langle M_\beta\rangle = 1$. Still, the general case dealing with $M_\beta \underset{|v|\to\infty}{\sim} \frac{m}{|v|^\beta}$ is a bit more tedious but can be done similarly, the details of the computations are proposed in the supplementary materials of this paper.

We consider the integral $\left\langle \left(\mathrm{e}^{-\mathrm{i}\varepsilon s k\cdot v} - 1\right) M_\beta \right\rangle$ and, for nonzero k, we perform the change of variables $w = \varepsilon|k|v$

$$\left\langle \left(\mathrm{e}^{-\mathrm{i}\varepsilon s k\cdot v} - 1\right) \frac{m}{1+|v|^\beta} \right\rangle = (\varepsilon|k|)^{\beta-d} \int_{\mathbb{R}^d} \left(\mathrm{e}^{-\mathrm{i}s\frac{k}{|k|}\cdot w} - 1\right) \frac{m}{(\varepsilon|k|)^\beta + |w|^\beta}\mathrm{d}w.$$

Since the last integral has rotational symmetry, for any unitary vector e of $\mathbb{R}^d$ we have

$$\begin{aligned} \left\langle \left(\mathrm{e}^{-\mathrm{i}\varepsilon s k\cdot v} - 1\right) \frac{m}{1+|v|^\beta} \right\rangle &= (\varepsilon|k|)^{\beta-d} \int_{\mathbb{R}^d} \left(\mathrm{e}^{-\mathrm{i}s e\cdot w} - 1\right) \frac{m}{(\varepsilon|k|)^\beta + |w|^\beta}\mathrm{d}w \\ &= (\varepsilon|k|)^{\beta-d}\,\mathcal{C}(s) + (\varepsilon|k|s)^{\beta-d}\,R(\varepsilon,s,k), \end{aligned} \tag{1.2.5}$$

where

$$\mathcal{C}(s) = \int_{\mathbb{R}^d} \left(\mathrm{e}^{-\mathrm{i}s e\cdot w} - 1\right) \frac{m}{|w|^\beta}\mathrm{d}w, \tag{1.2.6}$$

and

$$R(\varepsilon,s,k) = -m\,(\varepsilon s|k|)^\beta \int_{\mathbb{R}^d} \left(\mathrm{e}^{-\mathrm{i}e\cdot w} - 1\right) \frac{1}{|w|^\beta\left((\varepsilon s|k|)^\beta + |w|^\beta\right)}\mathrm{d}w.$$

In particular, $R(\varepsilon,s,k)$ tends to 0 when ε go to zero and is bounded. If we set $R(\varepsilon,s,0) = 0$, equality (1.2.5) is also true for $k = 0$.

From (1.2.3) and (1.2.5), we have to set $\alpha = \beta - d$ to get the fractional diffusion equation when $\varepsilon \to 0$ and then we get

$$\hat{\rho} \underset{\varepsilon\to 0}{=} \hat{\rho} + \varepsilon^\alpha|k|^\alpha \int_0^{+\infty} \left(\int_{w\in\mathbb{R}^d} \left(\mathrm{e}^{-isw\cdot e} - 1\right) \frac{m}{|w|^\beta}\mathrm{d}w\right) \mathrm{e}^{-s}\mathrm{d}s\hat{\rho} - \varepsilon^\alpha\partial_t\hat{\rho} + o(\varepsilon^\alpha),\ \forall t > 0.$$

From the equality

$$\int_0^{+\infty}\left(\int_{w\in\mathbb{R}^d}\left(\mathrm{e}^{-isw\cdot e}-1\right)\frac{m}{|w|^\beta}\mathrm{d}w\right)\mathrm{e}^{-s}\mathrm{d}s=-\int_{w\in\mathbb{R}^d}\frac{(w\cdot e)^2}{1+(w\cdot e)^2}\frac{m}{|w|^{d+\alpha}}\mathrm{d}w:=-\kappa,$$

we derive, when ε goes to 0, the fractional diffusion equation (1.1.5) given in [55, 5].

□

1.2.2 Computations in the space variable

The aim of this section is to generalize the previous computations to the original space variable. We have the following proposition

Proposition 1.2. *1. Equation (1.1.2) formally implies the following exact equation on ρ*

$$\rho(t,x)=\left\langle \mathrm{e}^{-\frac{t}{\varepsilon^\alpha}}f_0(x-\varepsilon^{1-\alpha}tv,v)\right\rangle+\int_0^{\frac{t}{\varepsilon^\alpha}}\mathrm{e}^{-s}\left\langle\rho(t-\varepsilon^\alpha s,x-\varepsilon sv)M_\beta(v)\right\rangle\mathrm{d}s. \quad (1.2.7)$$

2. In case 1.2 (anomalous diffusion scaling), when $\varepsilon\to 0$, ρ solves the anomalous diffusion equation

$$\partial_t\rho(t,x)=-\frac{m\Gamma(\alpha+1)}{c_{d,\alpha}}\left(-\Delta_x\right)^{\frac{\alpha}{2}}\rho(t,x),$$

where Γ is the usual Euler Gamma function, m the normalization constant appearing in the expression of the equilibrium M_β, $c_{d,\alpha}$ is defined by (1.1.8) and $\beta-d=\alpha$.

Proof.

1. **Formal derivation of the expression (1.2.7) from (1.1.2)**

   As in the previous section, we can integrate (1.1.2) to get

   $$\rho=A_0+\int_0^{\frac{t}{\varepsilon^\alpha}}\mathrm{e}^{-s}\left\langle\rho(t-\varepsilon^\alpha s,x-\varepsilon sv)M_\beta\right\rangle\mathrm{d}s,$$

   with

   $$A_0(t,x)=\left\langle\mathrm{e}^{-\frac{t}{\varepsilon^\alpha}}f_0(x-\varepsilon^{1-\alpha}tv,v)\right\rangle. \quad (1.2.8)$$

   Once again, in case 1.1, the diffusion equation can be derived from the (1.2.7) with Taylor expansions with respect to ε in the expression of ρ, whereas in case 1.2 the asymptotic equation is more complicated to obtain because of the infinite moment of order 2 of M_β.

2. **The anomalous diffusion limit**

   To find the limit equation in the case of the anomalous diffusion limit, we rewrite (1.2.7) as follows

   $$\begin{aligned}\rho(t,x)=A_0(t,x)&+\varepsilon^\alpha\int_0^{\frac{t}{\varepsilon^\alpha}}s\mathrm{e}^{-s}\left\langle\frac{\rho\left(t-\varepsilon^\alpha s,x-\varepsilon vs\right)-\rho\left(t,x-\varepsilon vs\right)}{\varepsilon^\alpha s}M_\beta(v)\right\rangle\mathrm{d}s\\&+\int_0^{\frac{t}{\varepsilon^\alpha}}\mathrm{e}^{-s}\left\langle\left(\rho(t,x-\varepsilon vs)-\rho(t,x)\right)M_\beta(v)\right\rangle\mathrm{d}s+\int_0^{\frac{t}{\varepsilon^\alpha}}\mathrm{e}^{-s}\mathrm{d}s\left\langle M_\beta(v)\right\rangle\rho(t,x).\end{aligned} \quad (1.2.9)$$

Under smoothness assumptions on ρ, the first integral of (1.2.9) becomes, for small ε

$$\int_0^{\frac{t}{\varepsilon^\alpha}} s\mathrm{e}^{-s} \left\langle \frac{\rho\left(t-\varepsilon^\alpha s, x-\varepsilon v s\right)-\rho\left(t, x-\varepsilon v s\right)}{\varepsilon^\alpha s} M_\beta(v) \right\rangle \mathrm{d}s = -\partial_t \rho(t,x) + o(1).$$

Since the last term of (1.2.9) can be explicitly computed, let us focus on the second integral of (1.2.9). As in the Fourier variable, we cannot expand ρ with respect to ε since M_β has an infinite moment of order 2. Hence, we must refine the analysis to find the limit of this term. We perform the change of variables $y = x - \varepsilon v s$ in the integral over v and exchanging the integrals in t and y to get

$$\int_0^{\frac{t}{\varepsilon^\alpha}} \mathrm{e}^{-s} \left\langle \left(\rho(t, x-\varepsilon v s)-\rho(t,x)\right) M_\beta(v) \right\rangle \mathrm{d}s = \int_{\mathbb{R}^d} \frac{\rho(t,y)-\rho(t,x)}{|x-y|^\beta} a(\varepsilon, x-y)\mathrm{d}y, \tag{1.2.10}$$

where

$$a(\varepsilon, z) = \int_0^{\frac{t}{\varepsilon^\alpha}} |z|^\beta \frac{\mathrm{e}^{-s}}{(\varepsilon s)^d} M_\beta\left(\frac{z}{\varepsilon s}\right) \mathrm{d}s. \tag{1.2.11}$$

Now, we want to find an equivalent of $a(\varepsilon, z)$ for small values of ε. Here we consider the equilibrium $M_\beta(v) = \frac{m}{1+|v|^\beta}$. Once again, the general case with M_β satisfying (1.2.1) can be done similarly, we refer for the supplementary materials of this article for more details. The integral a becomes

$$a(\varepsilon, z) = m \int_0^{\frac{t}{\varepsilon^\alpha}} |z|^\beta \frac{(\varepsilon s)^\beta}{(\varepsilon s)^\beta + |z|^\beta} \frac{\mathrm{e}^{-s}}{(\varepsilon s)^d} \mathrm{d}s,$$

and we consider, for a nonzero z, the following quantity

$$\begin{aligned} a(\varepsilon, z) - m\varepsilon^{\beta-d}\Gamma(\beta-d+1) = &-m \int_0^{+\infty} (\varepsilon s)^{\beta-d} \mathrm{e}^{-s} \frac{(\varepsilon s)^\beta}{(\varepsilon s)^\beta + |z|^\beta} \mathrm{d}s \\ &- m \int_{\frac{t}{\varepsilon^\alpha}}^{+\infty} |z|^\beta \frac{(\varepsilon s)^\beta}{(\varepsilon s)^\beta + |z|^\beta} \frac{\mathrm{e}^{-s}}{(\varepsilon s)^d} \mathrm{d}s. \end{aligned}$$

Then, for almost every $z \in \mathbb{R}^d$, $\frac{1}{\varepsilon^{\beta-d}}\left(a(\varepsilon, z) - m\varepsilon^{\beta-d}\Gamma(\beta-d+1)\right)$ converges to 0 when ε goes to zero. We also have the following estimation

$$\left| a(\varepsilon, z) - m\varepsilon^{\beta-d}\Gamma(\beta-d+1) \right| \leq K\left(\varepsilon^{\beta-d} + \varepsilon^{\beta-d}\mathrm{e}^{-\frac{t}{2\varepsilon^\alpha}}\right). \tag{1.2.12}$$

Let us remark that for a reasonable regularity of ρ, the integral appearing in (1.2.10) is well defined as a principal value because $\beta \in (d, d+2)$

$$P.V. \int_{\mathbb{R}^d} \frac{\rho(t,y)-\rho(t,x)}{|y-x|^\beta} \mathrm{d}y = \int_{\mathbb{R}^d} \frac{\rho(t,y)-\rho(t,x)-(y-x)\cdot\nabla_x\rho(t,x)}{|y-x|^\beta} \mathrm{d}y.$$

Hence, using (1.2.12) we obtain that for almost all $y \in \mathbb{R}^d$

$$\left| \frac{1}{\varepsilon^{\beta-d}} \frac{\rho(t,y)-\rho(t,x)-(y-x)\cdot\nabla_x\rho(t,x)}{|y-x|^\beta} \left(a(\varepsilon, z) - m\varepsilon^{\beta-d}\Gamma(\beta-d+1)\right) \right|,$$

is dominated by an integrable function. We also obtained that for almost all $y \in \mathbb{R}^d$ it tends to zero when ε goes to zero, by using the dominated convergence theorem for this function.

We have, from (1.2.10)

$$\int_0^{\frac{t}{\varepsilon^\alpha}} \mathrm{e}^{-s} \left\langle \left(\rho(t, x - \varepsilon v s) - \rho(t,x)\right) M_\beta(v) \right\rangle \mathrm{d}s$$
$$= \int_{\mathbb{R}^d} \frac{\rho(t,y) - \rho(t,x) - (y-x)\cdot \nabla_x \rho(t,x)}{|x-y|^\beta} a(\varepsilon, x-y) \mathrm{d}y,$$

where we used that a is even. So we have

$$\int_0^{\frac{t}{\varepsilon^\alpha}} \mathrm{e}^{-s} \left\langle \left(\rho(t, x - \varepsilon v s) - \rho(t,x)\right) M_\beta(v) \right\rangle \mathrm{d}s$$
$$\underset{\varepsilon\to 0}{\sim} m\varepsilon^{\beta-d}\Gamma(\beta - d + 1) \int_{\mathbb{R}^d} \frac{\rho(t,y) - \rho(t,x) - (y-x)\nabla_x \rho(t,x)}{|y-x|^\beta} \mathrm{d}y$$
$$\underset{\varepsilon\to 0}{\sim} m\varepsilon^{\beta-d}\Gamma(\beta - d + 1) P.V. \int_{\mathbb{R}^d} \frac{\rho(t,y) - \rho(t,x)}{|y-x|^\beta} \mathrm{d}y.$$

We remark that we have to set $\beta - d = \alpha$ to recover the limit equation, so we get

$$\rho(t,x) \underset{\varepsilon\to 0}{=} -\varepsilon^\alpha \partial_t \rho(t,x) + m\varepsilon^\alpha \Gamma(\alpha+1) P.V. \int_{\mathbb{R}^d} \frac{\rho(t,y) - \rho(t,x)}{|y-x|^{\alpha+d}} \mathrm{d}y + \rho(t,x) + o\left(\varepsilon^\alpha\right),$$

that is when ε goes to 0

$$\partial_t \rho(t,x) = -m\Gamma(\alpha+1) P.V. \int_{\mathbb{R}^d} \frac{\rho(t,x) - \rho(t,y)}{|y-x|^{\alpha+d}} \mathrm{d}y,$$

which is the expected anomalous diffusion equation.

□

1.3 Numerical schemes

This section is devoted to the presentation of appropriate numerical schemes to capture the solution of (1.1.2). We want these schemes to be Asymptotic Preserving (AP), that is, for arbitrary initial condition f_0

- to be consistent with the kinetic equation (1.1.2) when the time step Δt tends to 0, with a fixed ε,
- to degenerate into a scheme solving the asymptotic equation (here, anomalous diffusion) when ε goes to 0 with a fixed time step Δt.

In the sequel, three different numerical schemes are presented: a fully implicit scheme, a micro-macro decomposition based scheme and a Duhamel based scheme. We will consider a time discretization $t_n = n\Delta t, n = 0, \ldots, N$ such that $N\Delta t = T$ where T is the final time and we will set $f^n \simeq f(t_n)$.

As we used Fourier transform in the previous formal computations, we will consider a bounded domain Ω for the spatial domain with periodic conditions. Hence, we will be able to

use the discrete Fourier transform in the algorithm. The schemes we present in this section are semi-discrete-in-time schemes. However, in the section devoted to the numerical tests, we will consider the following discretization for the space and velocity

- The space domain will be $\Omega = [-1, 1]$, discretized with N_x points such that, denoting $\Delta x = \frac{2}{N_x}$,
$$x_i = -1 + (i-1)\Delta x, \;\; 1 \leq i \leq Nx. \tag{1.3.1}$$
The discrete Fourier transform will be computed with the modes
$$-\frac{N_x}{2} \leq k \leq \frac{N_x}{2}, \;\; k \in \mathbb{Z}. \tag{1.3.2}$$

- For the velocities, we want to compute the integrals with very simple discretization. Here, we consider the bounded velocity space $V = [-v_{max}, v_{max}]$ and $2N_v + 1$ points of discretization such that denoting $\Delta v = \frac{v_{max}}{N_v}$, we define the points
$$v_j = -v_{max} + j\Delta v, \;\; 0 \leq j \leq 2N_v, \tag{1.3.3}$$
to ensure the symmetry property of the discretization. The numerical integration in v will be denoted by $\langle \cdot \rangle_{N_v}$. In the case $d = 1$ with (1.3.3), we will consider
$$\langle g(v) \rangle_{N_v} = \Delta v \sum_{j=0}^{2N_v} g(v_j). \tag{1.3.4}$$

1.3.1 Implicit scheme

The first idea to design a scheme for the kinetic equation (1.1.2) is to set an implicit scheme over the Fourier formulation of the kinetic equation. It is known that in the case of the diffusion limit, it preserves easily the asymptotic equation. But in the case of the anomalous diffusion limit, the effect of large velocities must be taken into account to obtain the good asymptotic and this needs a suitable modification of this fully implicit scheme.

We start with (1.1.2) written in the spatial Fourier variable and consider a fully implicit time discretization

$$\frac{\hat{f}^{n+1} - \hat{f}^n}{\Delta t} + \frac{1}{\varepsilon^\alpha}\left(1 + \mathrm{i}\varepsilon k \cdot v\right)\hat{f}^{n+1} = \frac{1}{\varepsilon^\alpha}\hat{\rho}^{n+1} M_\beta.$$

We have
$$\hat{f}^{n+1} = \frac{1-\lambda}{1 + \mathrm{i}\lambda\varepsilon k \cdot v}\hat{f}^n + \frac{\lambda}{1 + \mathrm{i}\lambda\varepsilon k \cdot v}\hat{\rho}^{n+1} M_\beta, \tag{1.3.5}$$
with
$$\lambda = \frac{\Delta t}{\varepsilon^\alpha + \Delta t}. \tag{1.3.6}$$
Note that $0 < \lambda < 1, \lambda \underset{\Delta t \to 0}{\longrightarrow} 0$ and that $\lambda \underset{\varepsilon \to 0}{\to} 1$.

To compute $\hat{f}^{n+1}$ from (1.3.5), $\hat{\rho}^{n+1}$ has to be determined first. To do that we integrate (1.3.5) with respect to v at the discrete level to get

$$\hat{\rho}^{n+1} = \lambda \left\langle \frac{M_\beta}{1 + \mathrm{i}\lambda\varepsilon k \cdot v} \right\rangle_{N_v} \hat{\rho}^{n+1} + (1-\lambda) \left\langle \frac{\hat{f}^n}{1 + \mathrm{i}\lambda\varepsilon k \cdot v} \right\rangle_{Nv}, \tag{1.3.7}$$

that is

$$\hat{\rho}^{n+1} = \left\langle \frac{\hat{f}^n}{1+\mathrm{i}\lambda\varepsilon k\cdot v} \right\rangle_{N_v} \frac{1}{\left\langle \frac{M_\beta}{1+\mathrm{i}\lambda\varepsilon k\cdot v}\right\rangle_{N_v} + \frac{1}{1-\lambda}\left\langle \frac{\mathrm{i}\lambda\varepsilon k\cdot v M_\beta}{1+\mathrm{i}\lambda\varepsilon k\cdot v}\right\rangle_{N_v}}. \tag{1.3.8}$$

In case 1.1 of the diffusion scaling, this scheme is consistent with the kinetic equation and degenerates into a scheme solving the diffusion equation when ε becomes small.

In case 1.2 of anomalous diffusion scaling, the equilibrium M_β is heavy-tailed and $D = \langle v\otimes v M_\beta(v)\rangle = +\infty$. Hence, at the continuous level, the limit of

$$\left\langle \frac{\mathrm{i}\lambda\varepsilon k\cdot v M_\beta}{1+\mathrm{i}\lambda\varepsilon k\cdot v}\right\rangle = -\varepsilon^2\lambda^2\left\langle \frac{(k\cdot v)^2 M_\beta}{1+\varepsilon^2\lambda^2(k\cdot v)^2}\right\rangle,$$

which appears in (1.3.8) is not obvious but uses similar calculations as in proof of Prop. 1.1. It reads

$$\lim_{\varepsilon\to 0}\frac{1}{\varepsilon^\alpha}\left\langle \frac{\varepsilon^2(k\cdot v)^2\lambda^2}{1+\lambda^2\varepsilon^2(k\cdot v)^2}M_\beta(v)\right\rangle \hat{\rho}^{n+1} = |k|^\alpha\,\kappa\hat{\rho}^{n+1},$$

with κ defined in (1.1.6). Unfortunately, as we want to use a discretization of the velocities using a bounded domain for v, a quadrature of the integral involved in this limit does not capture the heavy tail of the equilibrium. It means that the effect of large velocities is completely missed. Namely, once computed with (1.3.4), the above integral in velocity reads

$$\varepsilon^{2-\alpha}\Delta v\sum_{j=0}^{2N_v}\frac{k^2v_j^2\lambda^2}{1+\lambda^2\varepsilon^2k^2v_j^2}M_\beta(v_j) \underset{\varepsilon\to 0}{\sim} \varepsilon^{2-\alpha}\Delta v\ k^2\sum_{j=0}^{2N_v}v_j^2M_\beta(v_j).$$

In fact, with a finite N_v, the discretized coefficient $\sum_{j=0}^{2N_v} v^2M_\beta(v)$ might be large but is finite. Thus,

$$\lim_{\varepsilon\to 0}\varepsilon^{2-\alpha}\Delta v\ k^2\sum_{j=0}^{2N_v}v_j^2M_\beta(v_j) = 0,$$

and then, when ε goes to zero the implicit kinetic scheme we wrote in (1.3.5)-(1.3.8) degenerates into the following scheme

$$\hat{\rho}^{n+1} = \hat{\rho}^n,\quad \hat{f}^{n+1} = \hat{\rho}^{n+1}M_\beta,$$

which is not the correct asymptotics. Hence we have to transform its expression to make the right limit clearly appear in the scheme. The scheme is presented in the following proposition.

Proposition 1.3. *In the case 1.2 (anomalous diffusion scaling), we consider the following scheme defined for all k and for all time index $0\le n\le N, N\Delta t = T$ by*

$$\begin{cases} \hat{\rho}^{n+1}(k) = \dfrac{\left\langle \dfrac{\hat{f}^n}{1+\mathrm{i}\lambda\varepsilon k\cdot v}\right\rangle_{N_v}}{\left\langle \dfrac{M_\beta}{1+\mathrm{i}\lambda\varepsilon k\cdot v}\right\rangle_{N_v} + \dfrac{(\varepsilon\lambda|k|)^\alpha}{1-\lambda}\left\langle \dfrac{m}{(\varepsilon\lambda|k|)^{\alpha+d}+|v|^{\alpha+d}}\dfrac{(v\cdot e)^2}{1+(v\cdot e)^2}\right\rangle_{N_v}} \\ \hat{f}^{n+1} = \dfrac{1}{1+\mathrm{i}\lambda\varepsilon k\cdot v}\left[(1-\lambda)\hat{f}^n + \lambda\hat{\rho}^{n+1}M_\beta\right], \end{cases}$$

with $\lambda = \Delta t/(\varepsilon^\alpha+\Delta t)$, where e is any unitary vector and with the initial condition $\hat{f}^0(k,v) = \hat{f}_0(k,v)$. This scheme has the following properties:

1. *The scheme is of order* 1 *for any fixed* ε *and preserves the total mass*

$$\forall n \in [\![1, N]\!], \hat{\rho}^n(0) = \hat{\rho}^0(0).$$

2. *The scheme is AP: for a fixed* Δt*, the scheme solves the anomalous diffusion equation when* ε *goes to zero*

$$\frac{\hat{\rho}^{n+1}(k) - \hat{\rho}^n(k)}{\Delta t} = -\kappa |k|^\alpha \hat{\rho}^{n+1}(k), \tag{1.3.9}$$

where κ*, defined by (1.1.6), is computed with* (1.3.4)*.*

Proof. As (i) is straightforward, let us prove (ii). We start by considering the expression of $\hat{\rho}^{n+1}$ given in (1.3.8) with continuous integrations in v, and more precisely the integral

$$\left\langle \frac{\mathrm{i}\varepsilon\lambda k \cdot v \; M_\beta}{1 + \mathrm{i}\varepsilon\lambda k \cdot v} \right\rangle = \int_{\mathbb{R}^d} M_\beta(v) \frac{\varepsilon^2\lambda^2 (k \cdot v)^2}{1 + \varepsilon^2\lambda^2 (k \cdot v)^2} \mathrm{d}v.$$

As in the previous section, we perform the change of variables $w = \varepsilon\lambda|k|v$ to obtain

$$\begin{aligned} \int_{\mathbb{R}^d} M_\beta(v) \frac{\varepsilon^2\lambda^2 (k \cdot v)^2}{1 + \varepsilon^2\lambda^2 (k \cdot v)^2} \mathrm{d}v &= (\varepsilon\lambda|k|)^{-d} \int_{\mathbb{R}^d} M_\beta\left(\frac{w}{\varepsilon\lambda|k|}\right) \frac{\left(w \cdot \frac{k}{|k|}\right)^2}{1 + \left(w \cdot \frac{k}{|k|}\right)^2} \mathrm{d}w, \\ &= (\varepsilon\lambda|k|)^{-d} \int_{\mathbb{R}^d} M_\beta\left(\frac{w}{\varepsilon\lambda|k|}\right) \frac{(w \cdot e)^2}{1 + (w \cdot e)^2} \mathrm{d}w, \end{aligned} \tag{1.3.10}$$

with $e = k/|k|$; note that the last integral does not depend on this unitary vector e thanks to its rotational invariance.

We consider explicitly the case $M_\beta(v) = \frac{m}{1+|v|^{\alpha+d}}$ with m such that $\langle M_\beta \rangle = 1$ and with $\alpha \in]0, 2[$. We have

$$\left\langle M_\beta \frac{\varepsilon^2\lambda^2 (k \cdot v)^2}{1 + \varepsilon^2\lambda^2 (k \cdot v)^2} \right\rangle = (\varepsilon\lambda|k|)^\alpha \int_{\mathbb{R}^d} \frac{m}{(\varepsilon\lambda|k|)^{\alpha+d} + |w|^{\alpha+d}} \frac{(w \cdot e)^2}{1 + (w \cdot e)^2} \mathrm{d}w,$$

where e is any unitary vector. Inserting this formula in (1.3.8) with discrete integration, we get the expression for $\hat{\rho}^{n+1}$. The equation satisfied by $\hat{f}^{n+1}$ in (1.3.5) is unchanged, then the numerical scheme of the proposition is derived. Now, it remains to show that this scheme enjoys the AP property. From the following form of the equation on $\hat{\rho}^{n+1}$

$$\begin{aligned} \frac{\hat{\rho}^{n+1} - \hat{\rho}^n}{\Delta t} = -\lambda^\alpha |k|^\alpha &\left\langle \frac{m}{(\varepsilon\lambda|k|)^{\alpha+d} + |v|^{\alpha+d}} \frac{(v \cdot e)^2}{1 + (v \cdot e)^2} \right\rangle_{N_v} \hat{\rho}^{n+1} \\ &- \left\langle \frac{\mathrm{i}\lambda\varepsilon k \cdot v}{1 + \mathrm{i}\lambda\varepsilon k \cdot v} \frac{\hat{f}^n}{\Delta t} \right\rangle_{N_v}, \end{aligned} \tag{1.3.11}$$

we easily observe that it degenerates when ε goes to zero to an implicit scheme for the anomalous diffusion equation. This concludes the proof.

□

1.3.2 Scheme based on a micro-macro decomposition

In the previous part, we constructed a fully implicit scheme enjoying the AP property. The implicit character of the transport may induce a high computational cost. Therefore, we propose another scheme, which is based on a micro-macro decomposition of the kinetic equation and in which the transport part is explicit in time. In the diffusion case, such a scheme has been set in [52]. We first recall here the way to derive it. Then, we consider more precisely the case of the anomalous diffusion and show how to take into account the effect of the large velocities induced by the heavy-tailed structure of the equilibrium $M_\beta(v)$.

The distribution f is decomposed as

$$f = \langle f \rangle M_\beta + g = \rho M_\beta + g,$$

where $\langle g \rangle = 0$. Injecting this decomposition into (1.1.2), we have

$$\partial_t \rho M_\beta + \partial_t g + \frac{\varepsilon}{\varepsilon^\alpha} v \cdot \nabla_x \rho M_\beta + \frac{\varepsilon}{\varepsilon^\alpha} v \cdot \nabla_x g = -\frac{1}{\varepsilon^\alpha} g. \tag{1.3.12}$$

To derive an equation on ρ, we integrate with respect to v to obtain

$$\partial_t \rho + \frac{\varepsilon}{\varepsilon^\alpha} \langle v \cdot \nabla_x g \rangle = 0. \tag{1.3.13}$$

Now we replace $\partial_t \rho$ in (1.3.12) to get an equation satisfied by g

$$\partial_t g + \frac{\varepsilon}{\varepsilon^\alpha} v \cdot \nabla_x \rho M_\beta + \frac{\varepsilon}{\varepsilon^\alpha} \left(v \cdot \nabla_x g - \langle v \cdot \nabla_x g \rangle M_\beta \right) = -\frac{1}{\varepsilon^\alpha} g. \tag{1.3.14}$$

From this formulation the semi-implicit scheme proposed in [52] writes

$$\begin{cases} \dfrac{\rho^{n+1} - \rho^n}{\Delta t} + \dfrac{\varepsilon}{\varepsilon^\alpha} \left\langle v \cdot \nabla_x g^{n+1} \right\rangle_{N_v} = 0 \\ \dfrac{g^{n+1} - g^n}{\Delta t} + \dfrac{\varepsilon}{\varepsilon^\alpha} v \cdot \nabla_x \rho^n M_\beta + \dfrac{\varepsilon}{\varepsilon^\alpha} \left(v \cdot \nabla_x g^n - \left\langle v \cdot \nabla_x g^n \right\rangle_{N_v} M_\beta \right) = -\dfrac{1}{\varepsilon^\alpha} g^{n+1}, \end{cases} \tag{1.3.15}$$

which is of order 1 for any fixed ε and preserves the asymptotic of diffusion equation when considered in case 1.1. However, as in the last section, when case 1.2 is considered, formulation (1.3.15) does not work because the fractional laplacian does not appear when ε goes to 0. We then have to modify the micro-macro scheme. As M_β is even and the discrete velocities are symmetrically spread around 0 we have

$$\left\langle v \cdot \nabla_x g^{n+1} \right\rangle_{N_v} = \left\langle v \cdot \nabla_x \rho^{n+1} M_\beta \right\rangle_{N_v} + \left\langle v \cdot \nabla_x g^{n+1} \right\rangle_{N_v} = \left\langle v \cdot \nabla_x f^{n+1} \right\rangle_{N_v},$$

and so the first equation of (1.3.15) can be rewritten as

$$\frac{\rho^{n+1} - \rho^n}{\Delta t} + \frac{\varepsilon}{\varepsilon^\alpha} \left\langle v \cdot \nabla_x f^{n+1} \right\rangle_{N_v} = 0.$$

Now we use an implicit formulation of the kinetic equation to express f^{n+1}

$$\varepsilon^\alpha \frac{f^{n+1} - f^n}{\Delta t} + \varepsilon v \cdot \nabla_x f^{n+1} = \rho^{n+1} M_\beta - f^{n+1}.$$

As we did in the previous part we introduce the variable λ defined by (1.3.6) and write this last equation as

$$(I + \varepsilon \lambda v \cdot \nabla_x) f^{n+1} = \lambda \rho^{n+1} M_\beta + (1 - \lambda) f^n,$$

that is

$$f^{n+1} = \lambda \left(I + \varepsilon\lambda v \cdot \nabla_x\right)^{-1} \rho^{n+1} M_\beta + (1-\lambda)\left(I + \varepsilon\lambda v \cdot \nabla_x\right)^{-1} f^n.$$

As $\lambda \underset{\Delta t \to 0}{=} O(\Delta t)$, we will use the following approximated expression for f^{n+1}

$$f^{n+1} = \lambda \left(I + \varepsilon\lambda v \cdot \nabla_x\right)^{-1} \rho^{n+1} M_\beta + (1-\lambda)\left(I - \varepsilon\lambda v \cdot \nabla_x\right) f^n + O(\Delta t),$$

to avoid a costly inversion of the transport operator. As we will use a bounded domain for the velocities in the numerical computations, this approximation induces an error of order $O(\Delta t)$. However, since we are writing an order 1 scheme, its accuracy is not changed. In this expression, the terms we removed also vanish when ε goes to zero, independently of Δt. Scheme (1.3.15) can be rewritten in the anomalous diffusion limit as

$$\left\{\begin{array}{ll} \dfrac{\rho^{n+1}-\rho^n}{\Delta t} & + \dfrac{\varepsilon}{\varepsilon^\alpha}\lambda \left\langle v \cdot \nabla_x \left(I + \varepsilon\lambda v \cdot \nabla_x\right)^{-1} \rho^{n+1} M_\beta \right\rangle_{N_v} \\ & + \dfrac{\varepsilon}{\varepsilon^\alpha}(1-\lambda)\left\langle v \cdot \nabla_x \left(I - \varepsilon\lambda v \cdot \nabla_x\right) f^n \right\rangle_{N_v} = 0, \\ \dfrac{g^{n+1}-g^n}{\Delta t} & + \frac{\varepsilon}{\varepsilon^\alpha} v \cdot \nabla_x \rho^n M_\beta + \frac{\varepsilon}{\varepsilon^\alpha}\left(v \cdot \nabla_x g^n - \left\langle v \cdot \nabla_x g^n \right\rangle_{N_v} M_\beta\right) = -\frac{1}{\varepsilon^\alpha} g^{n+1}. \end{array}\right. \tag{1.3.16}$$

We can make additional simplifications. First, we remark that,

$$\left\langle v \cdot \nabla_x \left(I - \varepsilon\lambda v \cdot \nabla_x\right) f^n \right\rangle_{N_v} = \left\langle v \cdot \nabla_x f^n \right\rangle_{N_v} + O(\Delta t) = \left\langle v \cdot \nabla_x g^n \right\rangle_{N_v} + O(\Delta t),$$

where we used $\langle v M_\beta \rangle_{N_v} = 0$ and $\lambda = O(\Delta t)$ at fixed ε. When performing this approximation, we removed terms of order $O(\Delta t)$. It is consistent with the kinetic equation, since the magnitude of the numerical error is not changed. Moreover, this simplification is also valid when considering the AP character of the scheme. Indeed, for a fixed Δt the terms we removed can also be neglected in the small ε limit. As the fractional diffusion limit of the scheme is now ensured (at the semi-discrete level), all the other terms of order Δt can also be neglected with no incidence on the precision and on the AP character of the scheme. Then, the last term in the first line of the scheme (1.3.16) can be replaced by $\varepsilon^{1-\alpha}(1-\lambda)\left\langle v \cdot \nabla_x g^n \right\rangle_{N_v}$. Second, we will reformulate the second term of the first line of the scheme (1.3.16) (which produces the fractional diffusion when ε goes to zero) in order to get the right limit when $\varepsilon \to 0$ when the integrals in v are computed with (1.3.4). To simplify the presentation, we present the reformulation using the Fourier variable (because of the non-local character of the fractional laplacian in the space coordinates, the case in these coordinates is more delicate). The second term of (1.3.16) writes in the Fourier variable and with continuous integration in v

$$\frac{\varepsilon}{\varepsilon^\alpha}\lambda \left\langle \frac{\mathrm{i}k \cdot v}{1 + \mathrm{i}\varepsilon\lambda k \cdot v} M_\beta \right\rangle \hat{\rho}^{n+1}(k) = \frac{1}{\varepsilon^\alpha} \left\langle \frac{\varepsilon^2\lambda^2 (k \cdot v)^2}{1 + \varepsilon^2\lambda^2 (k \cdot v)^2} M_\beta \right\rangle \hat{\rho}^{n+1}(k).$$

Here, as in the previous section, we remark that this term degenerates into the fractional laplacian $\kappa|k|^\alpha \hat{\rho}^{n+1}(k)$ with κ defined in (1.1.6) for small ε. However, once again, the passage to the numerical integration misses the high velocities effects. To make the fractional diffusion appear in the scheme, we then make the change of variables $w = \varepsilon\lambda|k|v$ in the above expression before discretizing in velocity. Hence, denoting e any unitary vector and $\mathcal{F}^{-1}$ the inverse of the Fourier transform, the following proposition holds:

Proposition 1.4. *In case 1.2 (anomalous diffusion scaling), we introduce the following micro-macro the scheme defined for all $x \in \Omega$, $v \in \mathbb{R}^d$ and all time index $0 \leq n \leq N, N\Delta t = T$ by*

$$\left\{ \begin{array}{ll} \dfrac{\rho^{n+1}-\rho^n}{\Delta t} & +\lambda^\alpha \mathcal{F}^{-1}\left(|k|^\alpha \left\langle \dfrac{(v\cdot e)^2}{1+(v\cdot e)^2} \dfrac{m}{(\varepsilon\lambda|k|)^\beta + |v|^\beta} \right\rangle_{N_v} \hat{\rho}^{n+1}(k) \right) \\ & +\dfrac{\varepsilon}{\varepsilon^\alpha + \Delta t} \langle v\cdot \nabla_x g^n \rangle_{N_v} = 0 \\ \dfrac{g^{n+1}-g^n}{\Delta t} & +\dfrac{\varepsilon}{\varepsilon^\alpha} v\cdot\nabla_x \rho^n M_\beta + \dfrac{\varepsilon}{\varepsilon^\alpha}\left(v\cdot\nabla_x g^n - \langle v\cdot\nabla_x g^n\rangle_{N_v} M_\beta \right) = -\dfrac{g^{n+1}}{\varepsilon^\alpha}, \end{array} \right. \tag{1.3.17}$$

where e is any unitary vector, and where initial conditions are $\rho^0(x) = \rho(0,x)$ and $g^0(x,v) = f(0,x,v) - \rho(0,x)M_\beta$. This scheme has the following properties:

1. *The scheme is of order 1 for any fixed ε and preserves the total mass*

$$\forall n \in [\![1, N]\!], \hat{\rho}^n(0) = \hat{\rho}^0(0).$$

2. *The scheme is AP: for a fixed Δt, the scheme solves the diffusion equation when ε goes to zero*

$$\frac{\hat{\rho}^{n+1}(k) - \hat{\rho}^n(k)}{\Delta t} = -\kappa|k|^\alpha \hat{\rho}^{n+1}(k),$$

where κ, defined by (1.1.6), is computed with (1.3.4).

Proof.

Remark 1.5. In the macro part of (1.3.17), for a fixed ε, we have

$$\left\langle \frac{(v\cdot e)^2}{1+(v\cdot e)^2} \frac{m}{(\varepsilon\lambda|k|)^\beta + |v|^\beta} \right\rangle_{N_v} = \left\langle \frac{(v\cdot e)^2}{1+(v\cdot e)^2} \frac{m}{|v|^\beta} \right\rangle_{N_v} + O(\Delta t^\beta).$$

Hence, as $\beta > 1$, we could have replaced directly the term treated in Fourier variable by its asymptotics for small ε with no impact on the accuracy of the scheme neither on its AP property. This rewriting permits to write a micro-macro scheme with no use of the Fourier variable. Since the discretization of the fractional laplacian in the space variable is a consequent piece of work, we decided, for a sake of simplicity, to present here the strategy in Fourier variable.

The proof of (i) is immediate, let us prove (ii). We have when ε goes to zero with a fixed Δt, the scheme solves the anomalous diffusion equation. The equation on g gives, when ε goes to zero.

$$g^{n+1} = O(\min(\varepsilon, \varepsilon^\alpha)).$$

The equation on ρ gives, in the Fourier variable

$$\frac{\hat{\rho}^{n+1} - \hat{\rho}^n}{\Delta t} + \lambda^\alpha |k|^\alpha \left\langle \frac{(v\cdot e)^2}{1+(v\cdot e)^2} \frac{m}{(\varepsilon\lambda|k|)^\beta + |v|^\beta} \right\rangle_{N_v} \hat{\rho}^{n+1} = O(\min(\varepsilon^2, \varepsilon^{1+\alpha})).$$

Thanks to the following relations,

$$\lambda^\alpha = \left(\frac{\Delta t}{\varepsilon^\alpha + \Delta t} \right)^\alpha = 1 + O(\varepsilon^\alpha), \quad \text{and} \quad \frac{m}{(\varepsilon\lambda|k|)^\beta + |v|^\beta} = \frac{m}{|v|^\beta} + O(\varepsilon^{\alpha+d}),$$

we get the implicit discretization of the anomalous diffusion equation (1.3.9) when $\varepsilon \to 0$. Hence the scheme solves the anomalous diffusion equation when ε goes to zero with a fixed Δt.

□

1.3.3 Scheme based on an integral formulation of the equation

In the previous parts, we wrote two AP schemes solving (1.1.2) in the case of anomalous diffusion limit, both of them were of order 1 in time. Here we present a scheme based on a Duhamel formulation of (1.1.2) which has uniform accuracy in ε. This approach bears similarities with the UGKS scheme (see [71, 57]). As in the previous parts, the case of the classical diffusion gives easily an AP scheme but the large velocities effects require a specific treatment for the anomalous diffusion case.

Considering in a first time that the integrals in velocity are done continuously, we start from (1.2.2)

$$\hat{\rho}(t,k) = \left\langle \mathrm{e}^{-\frac{t}{\varepsilon^\alpha}(1+\mathrm{i}\varepsilon k\cdot v)}\hat{\rho}(0,k,v)\right\rangle + \int_0^{\frac{t}{\varepsilon^\alpha}} \mathrm{e}^{-s}\left\langle \mathrm{e}^{-\mathrm{i}\varepsilon s k\cdot v} M_\beta(v)\right\rangle \hat{\rho}(t-\varepsilon^\alpha s,k)\mathrm{d}s,$$

hence evaluating at time $t = t_{n+1}$ leads to

$$\hat{\rho}(t_{n+1},k) = \hat{A}_0(t_{n+1},k) + \sum_{j=0}^{n}\int_{\frac{t_j}{\varepsilon^\alpha}}^{\frac{t_{j+1}}{\varepsilon^\alpha}} \mathrm{e}^{-s}\left\langle \mathrm{e}^{-\mathrm{i}\varepsilon s k\cdot v} M_\beta\right\rangle \hat{\rho}(t_{n+1}-\varepsilon^\alpha s,k)\mathrm{d}s, \tag{1.3.18}$$

where $\hat{A}_0$ is defined by (1.2.4). We perform a quadrature of order 2 in the integrals. Assuming that the time derivatives of $\hat{\rho}$ are uniformly bounded in ε, we have:
$\forall j \in [\![1, N-1]\!]$, $\forall s \in \left[\frac{t_j}{\varepsilon^\alpha}, \frac{t_{j+1}}{\varepsilon^\alpha}\right]$,

$$\hat{\rho}(t_{n+1}-\varepsilon^\alpha s,k) = a_j(\varepsilon,s)\hat{\rho}(t_{n+1}-t_j,k) + (1-a_j(\varepsilon,s))\hat{\rho}(t_{n+1}-t_{j+1},k) + O(\Delta t^2), \tag{1.3.19}$$

uniformly in ε, with $a_j(\varepsilon,s) = 1 - \frac{\varepsilon^\alpha s - t_j}{\Delta t}$. Inserting (1.3.19) in the integral term of (1.3.18) leads to

$$\begin{aligned}\int_{\frac{t_j}{\varepsilon^\alpha}}^{\frac{t_{j+1}}{\varepsilon^\alpha}} \mathrm{e}^{-s}\left\langle \mathrm{e}^{-\mathrm{i}\varepsilon s k\cdot v} M_\beta\right\rangle \hat{\rho}(t_{n+1}-\varepsilon^\alpha s,k)\mathrm{d}s &= c_j(k)\hat{\rho}(t_{n+1}-t_j,k)\\ &\quad + b_j(k)\hat{\rho}(t_{n+1}-t_{j+1},k) + O\left(\Delta t^2\right),\end{aligned} \tag{1.3.20}$$

uniformly in ε, where we used the following notations $\forall j \in [\![0, N]\!]$

$$b_j(k) = \int_{\frac{t_j}{\varepsilon^\alpha}}^{\frac{t_{j+1}}{\varepsilon^\alpha}} \frac{\varepsilon^\alpha s - t_j}{\Delta t}\mathrm{e}^{-s}\left\langle \mathrm{e}^{-\mathrm{i}\varepsilon s k\cdot v} M_\beta\right\rangle \mathrm{d}s, \tag{1.3.21}$$

$$c_j(k) = \int_{\frac{t_j}{\varepsilon^\alpha}}^{\frac{t_{j+1}}{\varepsilon^\alpha}} \left(1 - \frac{\varepsilon^\alpha s - t_j}{\Delta t}\right)\mathrm{e}^{-s}\left\langle \mathrm{e}^{-\mathrm{i}\varepsilon s k\cdot v} M_\beta\right\rangle \mathrm{d}s. \tag{1.3.22}$$

We use the quadrature (1.3.20) in (1.3.18) to write

$$\hat{\rho}(t_{n+1},k) = \hat{A}_0(t_{n+1},k) + \sum_{j=0}^{n}\left(c_j\hat{\rho}(t_{n+1-j},k) + b_j\hat{\rho}(t_{n-j},k) + O\left(\Delta t^2\right)\right), \tag{1.3.23}$$

and as $n\Delta t \leq T$ then $\sum_{j=0}^{n}\Delta t^2 = O(\Delta t)$ and we get a first order scheme that writes

$$\hat{\rho}^{n+1}(k) = \frac{\hat{A}_0(t_{n+1},k) + \sum_{j=1}^{n}\left(c_j\hat{\rho}^{n+1-j}(k) + b_j\hat{\rho}^{n-j}(k)\right) + b_0\hat{\rho}^n(k)}{1-c_0}. \tag{1.3.24}$$

In the case of diffusion or when the integrals in v of the coefficients b_j and c_j are computed exactly, this scheme enjoys the AP property . However, always because the high velocities cannot be taken into account in the numerical computations, it does not preserve the asymptotic in the case of the fractional diffusion limit with discrete integrations in v. Therefore, we have to suitably transform the integrals c_j and b_j before discretizing in velocity. We have

$$\begin{aligned}
b_j &= \int_{\frac{t_j}{\varepsilon^\alpha}}^{\frac{t_{j+1}}{\varepsilon^\alpha}} \frac{\varepsilon^\alpha s - t_j}{\Delta t} \mathrm{e}^{-s} \left\langle \left(\mathrm{e}^{-\mathrm{i}\varepsilon s k\cdot v} - 1 \right) M_\beta \right\rangle \mathrm{d}s + \int_{\frac{t_j}{\varepsilon^\alpha}}^{\frac{t_{j+1}}{\varepsilon^\alpha}} \frac{\varepsilon^\alpha s - t_j}{\Delta t} \mathrm{e}^{-s} \mathrm{d}s, \\
c_j &= \int_{\frac{t_j}{\varepsilon^\alpha}}^{\frac{t_{j+1}}{\varepsilon^\alpha}} \left(1 - \frac{\varepsilon^\alpha s - t_j}{\Delta t} \right) \mathrm{e}^{-s} \left\langle \left(\mathrm{e}^{-\mathrm{i}\varepsilon s k\cdot v} - 1 \right) M_\beta \right\rangle \mathrm{d}s \\
&\quad + \int_{\frac{t_j}{\varepsilon^\alpha}}^{\frac{t_{j+1}}{\varepsilon^\alpha}} \left(1 - \frac{\varepsilon^\alpha s - t_j}{\Delta t} \right) \mathrm{e}^{-s} \mathrm{d}s,
\end{aligned}$$

and in the velocity integrations we set $w = \varepsilon|k|v$ before discretizing the velocities as in (1.2.5), so when $M_\beta(v) = m/\left(1+|v|^\beta\right)$ we have with (1.3.4)

$$\begin{aligned}
b_j &= \varepsilon^\alpha |k|^\alpha \left\langle \frac{m}{(\varepsilon|k|)^\beta + |w|^\beta} \int_{\frac{t_j}{\varepsilon^\alpha}}^{\frac{t_{j+1}}{\varepsilon^\alpha}} \frac{\varepsilon^\alpha s - t_j}{\Delta t} \mathrm{e}^{-s} \left(\mathrm{e}^{-\mathrm{i}sw\cdot e} - 1 \right) \mathrm{d}s \right\rangle_{N_v} \\
&\quad + \int_{\frac{t_j}{\varepsilon^\alpha}}^{\frac{t_{j+1}}{\varepsilon^\alpha}} \frac{\varepsilon^\alpha s - t_j}{\Delta t} \mathrm{e}^{-s} \mathrm{d}s, \\
c_j &= \varepsilon^\alpha |k|^\alpha \left\langle \frac{m}{(\varepsilon|k|)^\beta + |w|^\beta} \int_{\frac{t_j}{\varepsilon^\alpha}}^{\frac{t_{j+1}}{\varepsilon^\alpha}} \left(1 - \frac{\varepsilon^\alpha s - t_j}{\Delta t} \right) \mathrm{e}^{-s} \left(\mathrm{e}^{-\mathrm{i}sw\cdot e} - 1 \right) \mathrm{d}s \right\rangle_{N_v} \\
&\quad + \int_{\frac{t_j}{\varepsilon^\alpha}}^{\frac{t_{j+1}}{\varepsilon^\alpha}} \left(1 - \frac{\varepsilon^\alpha s - t_j}{\Delta t} \right) \mathrm{e}^{-s} \mathrm{d}s,
\end{aligned}$$

with e any unitary vector. To ensure the AP property, the time integrations are computed exactly to get

$$\begin{aligned}
b_j &= \mathrm{e}^{-\frac{t_j}{\varepsilon^\alpha}} \left(\frac{1 - \mathrm{e}^{-\frac{\Delta t}{\varepsilon^\alpha}}}{\frac{\Delta t}{\varepsilon^\alpha}} - \mathrm{e}^{-\frac{\Delta t}{\varepsilon^\alpha}} \right) \left(1 - \varepsilon^\alpha |k|^\alpha \left\langle \frac{m}{(\varepsilon|k|)^\beta + |v|^\beta} \right\rangle_{N_v} \right) \qquad (1.3.25) \\
&\quad + \varepsilon^\alpha |k|^\alpha \left\langle \left(- \frac{\mathrm{e}^{-\frac{t_{j+1}}{\varepsilon^\alpha}(1+\mathrm{i}v\cdot e)}}{1+\mathrm{i}v\cdot e} + \frac{\varepsilon^\alpha}{\Delta t} \mathrm{e}^{-\frac{t_j}{\varepsilon^\alpha}(1+\mathrm{i}v\cdot e)} \frac{1 - \mathrm{e}^{-\frac{\Delta t}{\varepsilon^\alpha}(1+\mathrm{i}v\cdot e)}}{(1+\mathrm{i}v\cdot e)^2} \right) \frac{m}{(\varepsilon|k|)^\beta + |v|^\beta} \right\rangle_{N_v}, \\
c_j &= \mathrm{e}^{-\frac{t_j}{\varepsilon^\alpha}} \left(1 - \frac{1 - \mathrm{e}^{-\frac{\Delta t}{\varepsilon^\alpha}}}{\frac{\Delta t}{\varepsilon^\alpha}} \right) \left(1 - \varepsilon^\alpha |k|^\alpha \left\langle \frac{m}{(\varepsilon|k|)^\beta + |v|^\beta} \right\rangle_{N_v} \right) \qquad (1.3.26) \\
&\quad + \varepsilon^\alpha |k|^\alpha \left\langle \left(\frac{\mathrm{e}^{-\frac{t_j}{\varepsilon^\alpha}(1+\mathrm{i}v\cdot e)}}{1+\mathrm{i}v\cdot e} - \frac{\varepsilon^\alpha}{\Delta t} \mathrm{e}^{-\frac{t_j}{\varepsilon^\alpha}(1+\mathrm{i}v\cdot e)} \frac{1 - \mathrm{e}^{-\frac{\Delta t}{\varepsilon^\alpha}(1+\mathrm{i}v\cdot e)}}{(1+\mathrm{i}v\cdot e)^2} \right) \frac{m}{(\varepsilon|k|)^\beta + |v|^\beta} \right\rangle_{N_v}.
\end{aligned}$$

We have the following proposition

Proposition 1.6. *In case 1.2 (anomalous diffusion scaling), with the notations b_j and c_j defined in (1.3.25)-(1.3.26) and $\hat{A}_0$ defined in (1.2.4) and computed with* (1.3.4)*, we consider the following scheme defined for all k and for all time index $0 \leq n \leq N$ such that $N\Delta t = T$ by*

$$\hat{\rho}^{n+1}(k) = \frac{\hat{A}_0(t_{n+1},k) + \sum_{j=1}^{n} \left(c_j \hat{\rho}^{n+1-j}(k) + b_j \hat{\rho}^{n-j}(k) \right) + b_0 \hat{\rho}^n(k)}{1 - c_0},$$

with the initial condition $\hat{\rho}^0(k) = \hat{\rho}(0,k)$. This scheme has the following properties:

1. *The scheme is of order* 1 *and preserves the total mass*
$$\forall n \in [\![1, N]\!], \hat{\rho}^n(0) = \hat{\rho}^0(0).$$
2. *The scheme is AP: for a fixed Δt, the scheme solves the anomalous diffusion equation when ε goes to zero*
$$\frac{\hat{\rho}^{n+1}(k) - \hat{\rho}^n(k)}{\Delta t} = -\kappa |k|^\alpha \hat{\rho}^{n+1}(k),$$
where κ, defined by (1.1.6), is computed with (1.3.4)*.*
3. *Moreover, the semi-discrete-in-time scheme has uniform accuracy with respect to Δt, that is*
$$\|\hat{\rho}^n(\cdot) - \hat{\rho}(n\Delta t, \cdot)\|_{L^\infty} \leq C\Delta t,$$
with C independent of ε.

Remark 1.7. The numerical tests (see Fig. 1.6) suggest that, for all $\varepsilon > 0$, this scheme is of order 2 and degenerates into an order 1 scheme when ε becomes small. However, we are only able to prove the uniform order 1 of the scheme.

Proof. The conservation of the mass is obtained by induction, and the fact that it is of order 1 comes from the Taylor expansion we performed in the integrals. let us prove that for a fixed Δt the scheme solves the anomalous diffusion equation when ε goes to zero. From the exponential decay of A_0 and $b_j, c_j, j \geq 1$ we have when ε goes to zero

$$(1 - c_0)\, \hat{\rho}^{n+1}(k) = b_0(k) \hat{\rho}^n(k) + o(\varepsilon^\infty).$$

On the one side we have

$$b_0(k) = \frac{\varepsilon^\alpha}{\Delta t} + o(\varepsilon^\alpha),$$

and on the other side we have

$$\begin{aligned} c_0 &= \varepsilon^\alpha |k|^\alpha \left\langle \left(\frac{1}{1 + \mathrm{i} v \cdot e} - 1 \right) \frac{m}{(\varepsilon|k|)^\beta + |v|^\beta} \right\rangle_{N_v} + 1 - \frac{\varepsilon^\alpha}{\Delta t} + o(\varepsilon^\alpha) \\ &= -\varepsilon^\alpha |k|^\alpha \left\langle \frac{m}{|v|^\beta} \frac{(v \cdot e)^2}{1 + (v \cdot e)^2} \right\rangle_{N_v} + 1 - \frac{\varepsilon^\alpha}{\Delta t} + o(\varepsilon^\alpha) \\ &= -\varepsilon^\alpha |k|^\alpha \kappa + 1 - \frac{\varepsilon^\alpha}{\Delta t} + o(\varepsilon^\alpha). \end{aligned}$$

We deduce that when ε goes to zero, the scheme degenerates into

$$\frac{\hat{\rho}^{n+1}(k) - \hat{\rho}^n(k)}{\Delta t} = -\kappa |k|^\alpha \hat{\rho}^{n+1}(k),$$

where κ is defined by (1.1.6) and computed with (1.3.4). This is an implicit scheme for the anomalous diffusion equation (1.1.5).

Now, let us prove the uniform accuracy of the semi-discrete scheme. Here, we consider that all the velocity integrations are done continuously. Firstly, we need to precise the remainder $O(\Delta t^2)$ in (1.3.20). Taylor expansions of $\hat{\rho}(t_{n+1}-\varepsilon^\alpha s,k)$ leads to

$$\begin{aligned}\hat{\rho}(t_{n+1}-\varepsilon^\alpha s,k) &= a_j(\varepsilon,s)\hat{\rho}(t_{n+1}-t_j,k)+(1-a_j(\varepsilon,s))\hat{\rho}(t_{n+1}-t_{j+1})\\ &\quad - a_j(\varepsilon,s)\frac{(\varepsilon^\alpha s-t_j)^2}{2}\partial_t^2\hat{\rho}(t_{n+1}-\varepsilon^\alpha\xi_1(s),k)\\ &\quad - (1-a_j(\varepsilon,s))\frac{(\varepsilon^\alpha s-t_{j+1})^2}{2}\partial_t^2\hat{\rho}(t_{n+1}-\varepsilon^\alpha\xi_2(s),k),\end{aligned}$$

with $s\in\left[\frac{t_j}{\varepsilon^\alpha},\frac{t_{j+1}}{\varepsilon^\alpha}\right]$, $\xi_1(s)\in\left[\frac{t_j}{\varepsilon^\alpha},s\right]$, $\xi_2(s)\in\left[s,\frac{t_{j+1}}{\varepsilon^\alpha}\right]$ and $a_j=1-\frac{\varepsilon^\alpha s-t_j}{\Delta t}$. Hence, (1.3.18) rewrites

$$\hat{\rho}(t_{n+1},k)=\hat{A}_0(t_{n+1},k)+\sum_{j=0}^{n}c_j\hat{\rho}(t_{n+1}-t_j)+b_j\hat{\rho}(t_{n+1}-t_{j+1})+\Delta t^2F, \tag{1.3.27}$$

where

$$\begin{aligned}F=-\frac{1}{2}\sum_{j=0}^{n}\int_{\frac{t_j}{\varepsilon^\alpha}}^{\frac{t_{j+1}}{\varepsilon^\alpha}}&\left(a_j(\varepsilon,s)\left(\frac{\varepsilon^\alpha s-t_j}{\Delta t}\right)^2\partial_t^2\hat{\rho}(t_{n+1}-\varepsilon^\alpha\xi_1(s),k)\right.\\ &\left.+(1-a_j(\varepsilon,s))\left(\frac{t_{j+1}-\varepsilon^\alpha s}{\Delta t}\right)^2\partial_t^2\hat{\rho}(t_{n+1}-\varepsilon^\alpha\xi_2(s),k)\right)\mathrm{e}^{-s}\left\langle\mathrm{e}^{-\mathrm{i}\varepsilon sk\cdot v}M_\beta\right\rangle\mathrm{d}s,\end{aligned} \tag{1.3.28}$$

and with b_j and c_j defined in (1.3.21)-(1.3.22). As $a_j(\varepsilon,s)\geq 0$ and $1-a_j(\varepsilon,s)\geq 0$ for $s\in\left[\frac{t_j}{\varepsilon^\alpha},\frac{t_{j+1}}{\varepsilon^\alpha}\right]$, we have

$$\begin{aligned}|F|&\leq\mathcal{C}\sum_{j=0}^{n}\int_{\frac{t_j}{\varepsilon^\alpha}}^{\frac{t_{j+1}}{\varepsilon^\alpha}}\left(a_j(\varepsilon,s)\left(\frac{\varepsilon^\alpha s-t_j}{\Delta t}\right)^2+(1-a_j(\varepsilon,s))\left(\frac{t_{j+1}-\varepsilon^\alpha s}{\Delta t}\right)^2\right)\mathrm{e}^{-s}\mathrm{d}s\\ &\leq\mathcal{C}\sum_{j=0}^{n}\int_{\frac{t_j}{\varepsilon^\alpha}}^{\frac{t_{j+1}}{\varepsilon^\alpha}}\left(\frac{\varepsilon^\alpha s-t_j}{\Delta t}\right)\left(1-\frac{\varepsilon^\alpha s-t_j}{\Delta t}\right)\mathrm{e}^{-s}\mathrm{d}s\\ &\leq\mathcal{C}\sum_{j=0}^{n}\int_{\frac{t_j}{\varepsilon^\alpha}}^{\frac{t_{j+1}}{\varepsilon^\alpha}}\left(\frac{\varepsilon^\alpha s-t_j}{\Delta t}\right)\mathrm{e}^{-s}\mathrm{d}s,\end{aligned}$$

where we denoted $\mathcal{C}=\frac{1}{2}\sup_{t,k}\|\partial_t^2\hat{\rho}\|$ and remarked that $\frac{\varepsilon^\alpha s-t_j}{\Delta t}\in[0,1]$.

Now, let us denote $E_n=\hat{\rho}(t_n,k)-\hat{\rho}^n(k)$ and suppose that $E_0=0$. From (1.3.24) and (1.3.27), there is a relation linking the E_j

$$(1-c_0)\,E_{n+1}=b_0E_n+\sum_{j=1}^{n}(c_jE_{n+1-j}+b_jE_{n-j})+\Delta t^2F. \tag{1.3.29}$$

To obtain a bound of E_{n+1}, we will need two different estimates of $1/(1-c_0)$. On the one hand, we remark that with the expression of c_0 in (1.3.22) we have

$$|c_0|\leq\int_0^{\frac{\Delta t}{\varepsilon^\alpha}}\left(1-\frac{\varepsilon^\alpha s}{\Delta t}\right)\mathrm{e}^{-s}\mathrm{d}s. \tag{1.3.30}$$

On the other hand the inequality $0 \leq 1 - \frac{\varepsilon^\alpha s}{\Delta t} \leq 1$ for $s \in \left[0, \frac{\Delta t}{\varepsilon^\alpha}\right]$ also gives $|c_0| \leq 1 - \mathrm{e}^{-\frac{\Delta t}{\varepsilon^\alpha}}$, where we remark that in particular $|c_0| \leq 1$. Eventually, the inequality $|1 - c_0| \geq 1 - |c_0|$ implies the two following bounds

$$\left|\frac{1}{1-c_0}\right| \leq \frac{1}{1 - \displaystyle\int_0^{\frac{\Delta t}{\varepsilon^\alpha}} \left(1 - \frac{\varepsilon^\alpha s}{\Delta t}\right) \mathrm{e}^{-s} \mathrm{d}s} \quad \text{and} \quad \left|\frac{1}{1-c_0}\right| \leq \frac{1}{\mathrm{e}^{-\frac{\Delta t}{\varepsilon^\alpha}}}. \tag{1.3.31}$$

In (1.3.29) let us focus on the term containing F. It writes

$$\left|\frac{F}{1-c_0}\right| \leq \frac{\|\partial_t^2 \hat{\rho}\|_\infty}{2} \frac{\displaystyle\int_0^{\frac{\Delta t}{\varepsilon^\alpha}} \left(\frac{\varepsilon^\alpha s}{\Delta t}\right) \mathrm{e}^{-s} \mathrm{d}s}{|1-c_0|} + \frac{\|\partial_t^2 \hat{\rho}\|_\infty}{2} \frac{\displaystyle\sum_{j=1}^{n} \int_{\frac{t_j}{\varepsilon^\alpha}}^{\frac{t_{j+1}}{\varepsilon^\alpha}} \left(\frac{\varepsilon^\alpha s - t_j}{\Delta t}\right) \mathrm{e}^{-s} \mathrm{d}s}{|1-c_0|}, \tag{1.3.32}$$

using (1.3.31) we find an upper bound for the first term of (1.3.32)

$$\frac{\displaystyle\int_0^{\frac{\Delta t}{\varepsilon^\alpha}} \left(\frac{\varepsilon^\alpha s}{\Delta t}\right) \mathrm{e}^{-s} \mathrm{d}s}{|1-c_0|} \leq \frac{\displaystyle\int_0^{\frac{\Delta t}{\varepsilon^\alpha}} \mathrm{e}^{-s} \mathrm{d}s - \int_0^{\frac{\Delta t}{\varepsilon^\alpha}} \left(1 - \frac{\varepsilon^\alpha s}{\Delta t}\right) \mathrm{e}^{-s} \mathrm{d}s}{1 - \displaystyle\int_0^{\frac{\Delta t}{\varepsilon^\alpha}} \left(1 - \frac{\varepsilon^\alpha s}{\Delta t}\right) \mathrm{e}^{-s} \mathrm{d}s} \leq 1, \tag{1.3.33}$$

and reminding that $\frac{\varepsilon^\alpha s - t_j}{\Delta t} \leq 1$ for $s \in \left[\frac{t_j}{\varepsilon^\alpha}, \frac{t_{j+1}}{\varepsilon^\alpha}\right]$, the second term of (1.3.32) reads, using (1.3.31)

$$\frac{\displaystyle\sum_{j=1}^{n} \int_{\frac{t_j}{\varepsilon^\alpha}}^{\frac{t_{j+1}}{\varepsilon^\alpha}} \left(\frac{\varepsilon^\alpha s - t_j}{\Delta t}\right) \mathrm{e}^{-s} \mathrm{d}s}{|1-c_0|} \leq \frac{\displaystyle\sum_{j=1}^{n} \int_{\frac{t_j}{\varepsilon^\alpha}}^{\frac{t_{j+1}}{\varepsilon^\alpha}} \mathrm{e}^{-s} \mathrm{d}s}{|1-c_0|} \leq \frac{\displaystyle\int_{\frac{\Delta t}{\varepsilon^\alpha}}^{+\infty} \mathrm{e}^{-s} \mathrm{d}s}{|1-c_0|} \leq 1. \tag{1.3.34}$$

Eventually, (1.3.33) and (1.3.34) give the following upper bound for $\frac{F}{1-c_0}$

$$\left|\frac{F}{1-c_0}\right| \leq 2\mathcal{C}. \tag{1.3.35}$$

Let us focus now on the remaining term in the right hand side of (1.3.29) and denote $\mathcal{E}_n = \max_{\substack{j=0\cdots n \\ \varepsilon \in (0,1]}} |E_j|$. We have from (1.3.21) and (1.3.22)

$$\begin{aligned}
\left| b_0 E_n + \sum_{j=1}^{n} (c_j E_{n+1-j} + b_j E_{n-j}) \right| &\leq \int_0^{\frac{\Delta t}{\varepsilon^\alpha}} \frac{\varepsilon^\alpha s}{\Delta t} \mathrm{e}^{-s} \left| \left\langle \mathrm{e}^{-\mathrm{i}\varepsilon s k \cdot v} M_\beta \right\rangle E_n \right| \mathrm{d}s \\
&+ \sum_{j=1}^{n} \left(\int_{\frac{t_j}{\varepsilon^\alpha}}^{\frac{t_{j+1}}{\varepsilon^\alpha}} \left(1 - \frac{\varepsilon^\alpha s - t_j}{\Delta t}\right) \mathrm{e}^{-s} \left| \left\langle \mathrm{e}^{-\mathrm{i}\varepsilon s k \cdot v} M_\beta \right\rangle E_{n+1-j} \right| \mathrm{d}s \right. \\
&\left. + \int_{\frac{t_j}{\varepsilon^\alpha}}^{\frac{t_{j+1}}{\varepsilon^\alpha}} \frac{\varepsilon^\alpha s - t_j}{\Delta t} \mathrm{e}^{-s} \left| \left\langle \mathrm{e}^{-\mathrm{i}\varepsilon s k \cdot v} M_\beta \right\rangle E_{n-j} \right| \mathrm{d}s \right) \\
&\leq \left(\int_0^{\frac{\Delta t}{\varepsilon^\alpha}} \frac{\varepsilon^\alpha s}{\Delta t} \mathrm{e}^{-s} \mathrm{d}s + \sum_{j=1}^{n} \int_{\frac{t_j}{\varepsilon^\alpha}}^{\frac{t_{j+1}}{\varepsilon^\alpha}} \mathrm{e}^{-s} \mathrm{d}s \right) \mathcal{E}_n
\end{aligned}$$

$$\leq \left(1 - \int_0^{\frac{\Delta t}{\varepsilon^\alpha}} \left(1 - \frac{\varepsilon^\alpha s}{\Delta t}\right) \mathrm{e}^{-s} \mathrm{d}s\right) \mathcal{E}_n,$$

where we have used $\langle M_\beta \rangle = 1$. Hence, using (1.3.31), we get

$$\left| \frac{b_0 E_n + \sum_{j=1}^{n} (c_j E_{n+1-j} + b_j E_{n-j})}{1 - c_0} \right| \leq \mathcal{E}_n. \tag{1.3.36}$$

Eventually, we have the following estimate for E_{n+1} using (1.3.29), (1.3.35) and (1.3.36)

$$E_{n+1} \leq \mathcal{E}_n + 2\mathcal{C}\Delta t^2.$$

This implies that $\mathcal{E}_{n+1} \leq \mathcal{E}_n + 2\mathcal{C}\Delta t^2$, which gives, knowing that $\mathcal{E}_0 = 0$,

$$\mathcal{E}_{n+1} \leq 2\mathcal{C}(n+1)\Delta t^2.$$

Denoting T the final time of the algorithm and N such that $\Delta t = \frac{T}{N}$, we have for all $0 \leq n \leq N-1$, $n+1 \leq T/\Delta t$, and this ends the proof of the uniform accuracy. □

Remark 1.8. The previous scheme of Prop. 1.6 can be modified into a numerical scheme which degenerates into a second order time approximation of the asymptotic model. Indeed, we can modify (1.3.23) to get the following scheme

$$\begin{aligned}\hat{\rho}^{n+1}(k) = A_0(t_{n+1}, k) + b_0 \hat{\rho}^n(k) + \sum_{j=1}^{n} \left(c_j \hat{\rho}^{n+1-j}(k) + b_j \hat{\rho}^{n-j}(k)\right) \\ + (c_0 + b_0 - 1)\frac{\hat{\rho}^{n+1}(k) + \hat{\rho}^n(k)}{2} + (1 - b_0)\hat{\rho}(t_{n+1}, k).\end{aligned}$$

By construction, this scheme degenerates when ε goes to zero, into a Crank-Nicolson numerical scheme for the diffusion or anomalous diffusion equations.

Remark 1.9. The scheme of Prop. 1.6 is an expression closed on ρ. It implies that it is not necessary to solve the equation for f to compute the approximated value of ρ at each time step. Since ρ does not depend of the velocities, this improves the computational time. However, it is still possible to recover the values of the distribution function f from ρ. As an example, this can be done using the expression for $\hat{f}$ of the implicit scheme we described in the beginning of this section.
Note that a very similar approach, based on an integration of (1.1.2) between the times t_n and t_{n+1} provides a one-step first order scheme which enjoys AP property and that is of order 1 uniformly in ε. With this scheme, the storage of all the previous values of the density $\hat{\rho}$ is no longer necessary, but this gain of computational time is counterbalanced by the fact that it is now necessary to solve the equation for $\hat{f}$. Hence, the complexity coming from the number of terms in the sum of the expression of $\hat{\rho}$ disappears but we must now deal with the velocity space and perform numerical velocities integrations at each time step.

1.4 Numerical results

In this part, we present the numerical tests for the implicit scheme, the micro-macro scheme and the scheme based on the Duhamel formulation of the kinetic equation in the case of anomalous diffusion. In the sequel, we will denote by ISD (resp. ISA) the implicit schemes set in (1.3.5)-(1.3.8) (resp. in Prop. 1.3) in the diffusion case (resp. anomalous diffusion case); we will call MMSA the micro-macro scheme in Prop. 1.4 in the anomalous diffusion case. Eventually, the acronym DSA will refer to the scheme based on Duhamel Formulation in the Prop. 1.6. Finally, adiff denotes the numerical scheme of the anomalous diffusion equation given in (1.3.9).

In this part, we will consider $t > 0, x \in [-1, 1], v \in \mathbb{R}$ and the following initial data

$$f_0(x, v) = (1 + \sin(\pi x))M_\beta(v),$$

and periodic boundary conditions are imposed in x. In the fractional diffusion case, we will consider the equilibrium

$$M_\beta(v) = \frac{m}{1 + |v|^\beta},$$

with m chosen such that $\langle M_\beta(v)\rangle_{N_v} = 1$. In the sequel, unless other discretizations are mentioned, the following numerical parameters will hold:

1. time: the final time will be set $T = 0.1$ and $\Delta t = 10^{-3}$.

2. space: we will consider a uniform mesh in x considering $N_x = 64$ points. We will use (1.3.2) for the Fourier variable and (1.3.1) for the original space variable.

3. velocity: an uniform velocity grid of the truncated domain $[-v_{\max}, v_{\max}]$ is considered, with $2N_v + 1$ points. Here, we will consider $v_{\max} = 50$ and $N_v = 100$. The discretization (1.3.3) ensures that $\langle vM_\beta(v)\rangle_{N_v} = 0$, with $\langle\cdot\rangle_{N_v}$ defined in (1.3.4).

In the tests for the anomalous diffusion, we will consider $\alpha = 1.5$.

As we are testing three different schemes, it is worth checking whether, at least for large ε, they all agree to give close numerical solutions of the kinetic equation. Indeed, in the case of fractional diffusion, we plot the densities given by the three schemes at time $T = 0.1$ for $\varepsilon = 1$ and $\varepsilon = 0.1$ with the previous parameters. The results in Fig. 1.1 show that the three scheme give the same solution.

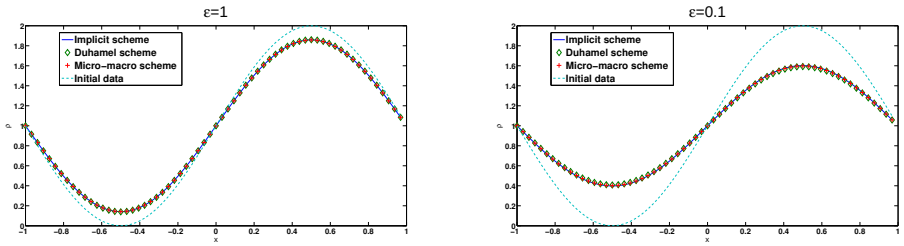

Figure 1.1: For $\Delta t = 10^{-3}$, the densities $\rho(t = 0.1, x)$ obtained with the three schemes. Left: for $\varepsilon = 1$. Right: for $\varepsilon = 0.1$.

To get more precise results, in the sequel, we will be interested in the relative error. The relative error is defined by the difference between a reference solution (obtained by a scheme

using a refined mesh) and the solution obtained by the tested scheme through the following formula

$$\text{Error}(T) = \frac{\|\rho_{\text{reference}}(T) - \rho_{\text{scheme}}(T)\|_2}{\|\rho_{\text{reference}}(T)\|_2}, \tag{1.4.1}$$

where $\|\cdot\|_2$ denotes the discrete L^2 norm and the reference scheme will be precised in each case.

1.4.1 The implicit scheme in the case of the anomalous diffusion limit

In this section, we test the ISA scheme. We check that it is of order 1 for a fixed value of ε and the AP property when ε goes to 0 for a fixed value of Δt.

Firstly, we remark that the scheme (1.3.5)-(1.3.8) does not preserve the asymptotic of anomalous diffusion: the left hand side of Fig. 1.2 shows that for $\varepsilon = 10^{-6}$ the implicit scheme returns a result very different from the result given by (1.3.9). Indeed, when $\varepsilon \ll 1$, (1.3.5)-(1.3.8) produces a stationary solution. So it appears that the change of variables in the velocity integrals is necessary to capture the anomalous diffusion limit, as shown in the right hand side of Fig. 1.2.

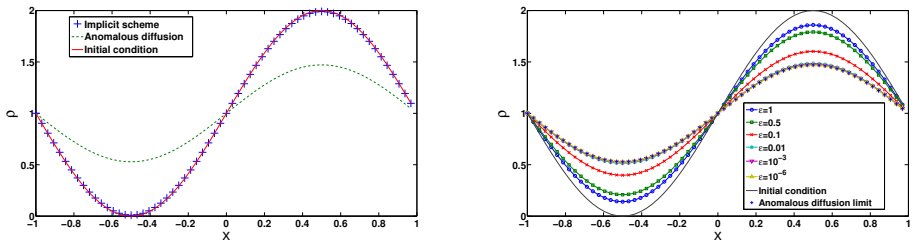

Figure 1.2: For $\Delta t = 10^{-3}$, the densities $\rho(t = 0.1, x)$. Left: scheme defined in (1.3.5)-(1.3.8) (with $\varepsilon = 10^{-6}$), by the adiff scheme and the initial data. Right: ISA scheme for different values of ε and the adiff scheme.

The left hand side of Fig. 1.3 shows the error between the reference scheme (defined as the adiff scheme) and the ISA scheme as a function of ε, for $\alpha = 0.8, 1, 1.5$. We observe that the convergence of the kinetic equation to the anomalous diffusion when ε goes to zero arises with a speed α. Theorically, the convergence to the anomalous diffusion equation arises with a speed $\varepsilon^{\min(\alpha, 2-\alpha)}$, but as we consider a finite domain for v in the tests, the convergence rate always appears to be ε^{α}. This result will be proved in [18].

However the convergence in time of the ISA scheme to the DSA scheme is not uniform with respect to ε. Setting $\Delta t = \varepsilon^{\alpha}$ in the scheme and letting Δt go to 0 shows that the densities does not converge to the density given by the anomalous diffusion equation. On the right hand side of Fig. 1.3, we plot the error in time between the adiff scheme as reference and the ISA scheme computed for different time steps satisfying $\Delta t = \varepsilon^{\alpha}$. We observe that the error does not converge to 0 when Δt goes to 0, illustrating the lack of uniformity.

1.4.2 The micro-macro scheme

In this part, we focus on the MMSA scheme in the case of the kinetic equation with anomalous diffusion limit. As it does not use only the Fourier variable, we must consider a grid for the space variable. Here we will take $x \in [-1, 1]$ discretized with $N_x = 32$ points. Following

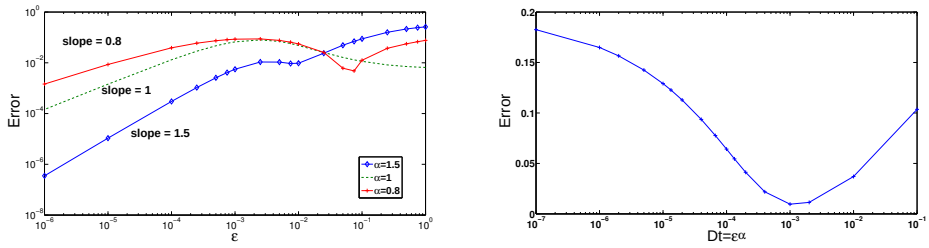

Figure 1.3: Left: For $\Delta t = 10^{-3}$ and $\alpha = 0.8, 1, 1.5$, the error as a function of ε between the reference adiff scheme and the ISA scheme (log scale). Right: The error between the ISA scheme for a range of $\Delta t = \varepsilon^\alpha$ and the adiff scheme as a function of Δt, which is fixed equal to ε^α (log scale).

Remark 1.5, we could have used (1.1.9) to compute the term giving the fractional diffusion for small ε in the macro part of (1.3.17) in the original space variable. For a sake of simplicity, we decided to treat it in Fourier variable, using (1.3.2). All the other space derivatives in this scheme are treated with a classical order 1 upwind scheme, using (1.3.1). Eventually, we use (1.3.3) for the velocities. As we solve the transport of the micro part in an explicit way, a CFL condition has to be imposed; then the time step is chosen small enough.

We start by testing the consistency of the scheme. We fix $\alpha = 1.5$ and for a decreasing range of time steps, we compute the solution given by the MMSA scheme. Then, for $\varepsilon = 1, 0.5$, we compare it to the reference solution given by MMSA with $\Delta t = 10^{-6}$. For $\varepsilon = 10^{-7}, 10^{-8}$, we compare to the solution given by the adiff scheme. Fig. 1.4 shows the error curves obtained for different values of ε. It appears that the MMSA scheme is of order 1 in time.

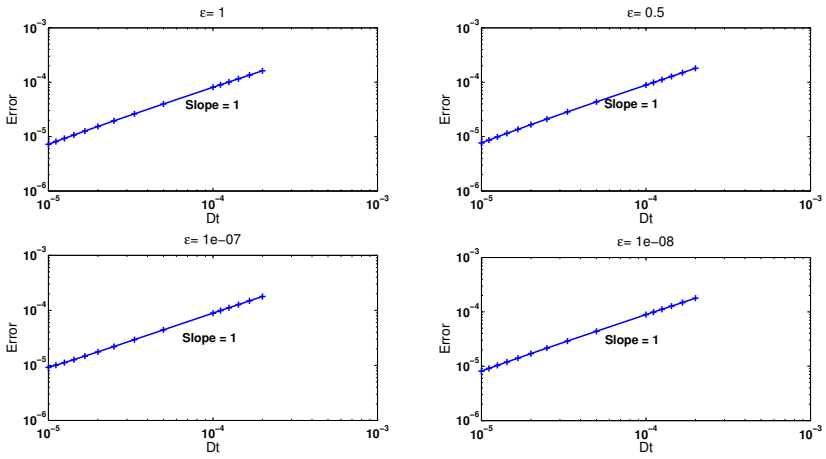

Figure 1.4: For $\varepsilon = 1, 0.5, 10^{-7}, 10^{-8}$, the error in time between the MMSA scheme computed for a range of Δt and the reference scheme computed with $\Delta t = 10^{-6}$ (log scale).

Let us recall that the micro-macro scheme we propose enjoys the AP property but has no uniform order 1 of accuracy. In order to show that the scheme preserves the asymptotic of anomalous diffusion we compute the densities $\rho(t = 0.1, x)$ obtained by the MMSA scheme for a range of ε; we compare them to the density obtained by the adiff scheme computed with the

same Δt. In order to respect the CFL condition, we took $\Delta t = 10^{-4}$ for $\varepsilon = 1, 0.5, 0.1, 0.01$ and $\Delta t = 10^{-3}$ for the smallest ε.The left hand side of Fig. 1.5 shows these densities in the case $\alpha = 1.5$, we observe that they are very close to the anomalous diffusion limit for small ε. On the right hand side of Fig. 1.5, the errors associated to this latter study are displayed in the cases $\alpha = 0.8, \alpha = 1$ and $\alpha = 1.5$, the adiff scheme being considered as reference. We observe that the convergence happens with speed α, as expected.

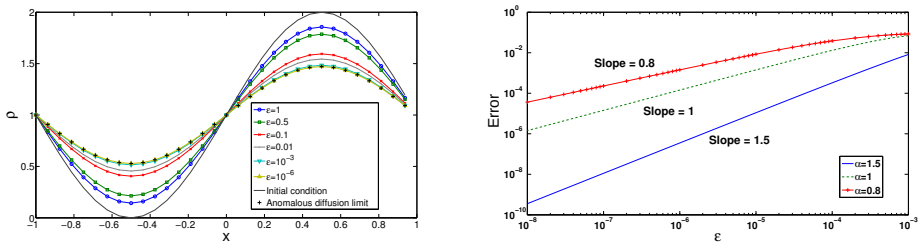

Figure 1.5: The densities $\rho(t = 0.1, x)$. Left: MMSA scheme for different values of ε and the diff scheme. Right: For $\Delta t = 10^{-3}$ and $\alpha = 0.8, 1, 1.5$, the error with respect to ε between the reference adiff scheme and the MMSA scheme (log scale).

1.4.3 The integral formulation based scheme

In this section, we test the Duhamel formulation based scheme DSA in anomalous diffusion regime. We put its properties of consistency, AP character and uniformity with respect to ε, written in Prop. 1.6, in evidence in this case.

The first thing we check is the convergence of the algorithm when Δt goes to zero. We compare the results given by the DSA scheme to the results given by the DSA scheme computed with a smaller time step, to make the consistency of the scheme appear. Considering different values of ε, we compute a reference solution with the scheme DSA with $\Delta t = 10^{-5}$ and we compare it to the results given by the DSA scheme for some larger time steps. Fig. 1.6 show error study of the convergence of the densities obtained. We observe that for $\varepsilon = 1, 0.5$ the scheme seems to be of order 2 whereas it is of order 1 for smaller values of ε.

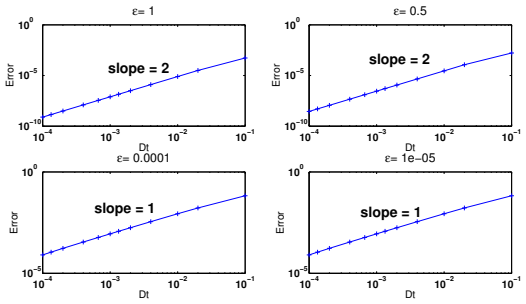

Figure 1.6: For $\varepsilon = 1, 0.1, 10^{-4}, 10^{-5}$, the error as a function of Δt between the DSA scheme and the DSA scheme computed for $\Delta t = 10^{-5}$ (log scale).

Then, we can study the AP character of the DSA scheme. The time step being fixed to $\Delta t = 10^{-3}$, we check that the results given by the DSA scheme converge to the result given

by the adiff scheme when ε goes to 0. Fig. 1.7 presents the densities $\rho(t = 0.1, x)$ obtained by these two schemes for different values of ε and then, the error as a function of ε is plotted for $\alpha = 0.8, 1, 1.5$. As previously, the expected numerical speed of the convergence to the anomalous diffusion is recovered.

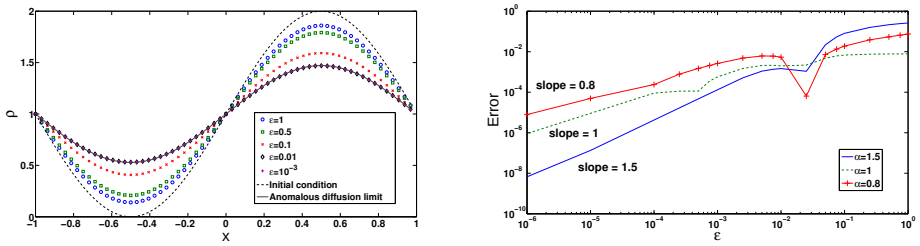

Figure 1.7: Left: For $\Delta t = 10^{-3}$ the densities $\rho(t = 0.1, x)$ given by the DSA scheme for different values of ε and the adiff scheme. Right: For $\Delta t = 10^{-3}$ and $\alpha = 0.8, 1, 1.5$, the error in ε between the reference adiff scheme and the DSA scheme (log scale).

To highlight the fact that the scheme is first order in time uniformly in ε, we compare the results given by the DSA scheme with $\Delta t = 10^{-5}$ to the results given by the same DSA scheme for a range of Δt. These errors are displayed in the left hand side of Fig. 1.8 as a function of ε where we observe that the error curves are stratified with respect to Δt, showing the uniformity of the scheme with respect to ε. As for the case of diffusion limit, the right hand side of Fig. 1.8 presents the error between the DSA scheme computed for $\Delta t = \varepsilon^\alpha$ and the limit adiff scheme computed for $\Delta t = 10^{-7}$. Since the DSA scheme is of order 1 uniformly in ε, this error tends to zero when Δt and ε go to zero.

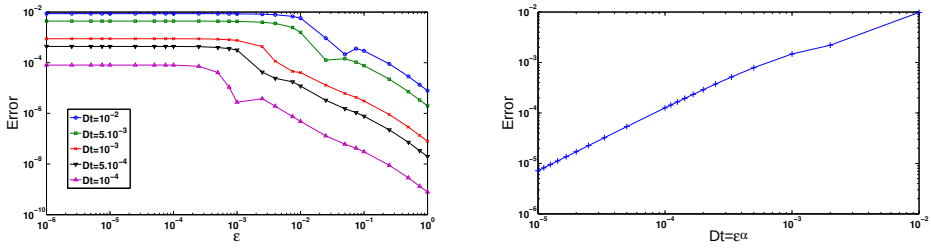

Figure 1.8: Left: The difference between the DSA scheme computed for $\Delta t = 10^{-5}$ and the DSA scheme computed for a range of Δt as a function of ε (log scale). Right: The difference between the DSA scheme computed for $\Delta t = \varepsilon^\alpha$ and the DSA scheme computed for $\Delta t = 10^{-7}$ as a function of Δt (log scale).

1.5 Conclusion

In this paper, we have first presented a formal derivation of anomalous diffusion asymptotics from a BGK kinetic equation. This analysis enables us to understand the role of the large velocities induced by the heavy-tailed equilibrium in the anomalous diffusion asymptotics. Moreover, this formal derivation paves the way to construct three different numerical schemes

for the kinetic equation, which all enjoy the asymptotic preserving property in the anomalous diffusion regimes.

The asymptotic preserving character in the case of anomalous diffusion comes from the fact that we managed to take into account the effect of large velocities of the equilibrium. As we saw in the simplest case of a direct fully implicit scheme, the asymptotic is not preserved when these large velocities are truncated. The schemes using the micro-macro formulation as well as the Duhamel formulation of the equations require the use of the same trick on the velocities. Moreover, this last scheme enjoys a uniform accuracy property.

In the near future, we aim at extending this work to more general context, considering higher dimensions, non periodic boundary conditions. The case of singular collision frequency also may generate anomalous diffusion (see [4]) and this also deserves a numerical study that we plan to do in a forthcoming work [18].

1.6 Appendix: General expression of the anomalous diffusion in the Fourier variable

In this part, we will show the following proposition

Proposition 1.10. *In case 2 (anomalous diffusion scaling), the equilibrium M_β satisfies*

$$\left\langle \left(\mathrm{e}^{-\mathrm{i}\varepsilon s k\cdot v}-1\right) M_\beta(v)\right\rangle \underset{\substack{\varepsilon\to 0\\ s\to 0\\ independently}}{=} (\varepsilon|k|)^{\beta-d}\mathcal{C}(s)+(\varepsilon s|k|)^{\beta-d}R(\varepsilon,s,k),$$

with $C(s)$ defined by

$$\mathcal{C}(s)=\int_{\mathbb{R}^d}\left(\mathrm{e}^{-\mathrm{i}se\cdot w}-1\right)\frac{m}{|w|^\beta}\mathrm{d}w, \tag{1.6.1}$$

and where $R(\varepsilon,s,k)$ is bounded and tends to 0 for small ε and s with an explicit form given by

$$R(\varepsilon,s,k)=\int_{w\in\mathbb{R}^d}\left(\mathrm{e}^{-\mathrm{i}w\cdot e}-1\right)\left(\frac{1}{(\varepsilon s|k|)^\beta}M_\beta\left(\frac{w}{\varepsilon s|k|}\right)-\frac{m}{|w|^\beta}\right)\mathrm{d}w.$$

Proof. Since we supposed that $M_\beta(v)\underset{\varepsilon\to 0}{\sim}\frac{m}{|v|^\beta}$, there exists a continuous bounded function ℓ and a positive constant K such that

$$\ell(v)\underset{|v|\to+\infty}{\to}0 \quad\text{and}\quad M_\beta(v)-\frac{m}{|v|^\beta}=\ell(v)\frac{m}{|v|^\beta}\ \text{if}\ |v|>K. \tag{1.6.2}$$

Hence we have

$$\left\langle \left(\mathrm{e}^{-\mathrm{i}\varepsilon s k\cdot v}-1\right) M_\beta(v)\right\rangle = I_1+I_2+I_3,$$

with

$$\begin{aligned}
I_1&=\int_{|v|\le K}\left(\mathrm{e}^{-\mathrm{i}\varepsilon s k\cdot v}-1\right)M_\beta(v)\mathrm{d}v,\\
I_2&=\int_{|v|>K}\left(\mathrm{e}^{-\mathrm{i}\varepsilon s k\cdot v}-1\right)\left(M_\beta(v)-\frac{m}{|v|^\beta}\right)\mathrm{d}v,\\
I_3&=\int_{|v|>K}\left(\mathrm{e}^{-\mathrm{i}\varepsilon s k\cdot v}-1\right)\frac{m}{|v|^\beta}\mathrm{d}v.
\end{aligned}$$

In the sequel, we consider separately the equivalents of these three integrals to obtain the fractional diffusion term. Using the fact that M_β is even, we can use a Taylor expansion for the exponential in the integral I_1

$$\begin{aligned}
|I_1|=\left|\int_{|v|\le K}\left(\mathrm{e}^{-\mathrm{i}\varepsilon s k\cdot v}-1\right)M_\beta(v)\mathrm{d}v\right| &= \left|\int_{|v|\le K}\left(\mathrm{e}^{-\mathrm{i}\varepsilon s k\cdot v}-1+\mathrm{i}\varepsilon s k\cdot v\right)M_\beta(v)\mathrm{d}v\right|\\
&\le \frac{\varepsilon^2 s^2}{2}\int_{|v|\le K}(k\cdot v)^2 M_\beta(v)\mathrm{d}v\\
&\le \frac{|k|^2|K|^2\varepsilon^2 s^2}{2}=o(\varepsilon^\alpha).
\end{aligned}$$

For the integral I_2, we perform the change of variables $w=\varepsilon|k|v$ for a nonzero k and use the function ℓ in (1.6.2)

$$I_2=\int_{|v|>K}\left(\mathrm{e}^{-\mathrm{i}\varepsilon s k\cdot v}-1\right)\left(M_\beta(v)-\frac{m}{|v|^\beta}\right)\mathrm{d}v=\int_{|v|>K}\left(\mathrm{e}^{-\mathrm{i}\varepsilon s k\cdot v}-1\right)\ell(v)\frac{m}{|v|^\beta}\mathrm{d}v$$

$$
\begin{aligned}
&= (\varepsilon|k|)^{\beta-d} \int_{|w|\geq \varepsilon K|k|} \left(\mathrm{e}^{-isw\cdot\frac{k}{|k|}} - 1\right) \ell\left(\frac{w}{\varepsilon|k|}\right) \frac{m}{|w|^\beta} \mathrm{d}w \\
&= (\varepsilon|k|)^{\beta-d} \int_{w\in\mathbb{R}^d} \left(\mathrm{e}^{-isw\cdot\frac{k}{|k|}} - 1\right) \ell\left(\frac{w}{\varepsilon|k|}\right) \frac{m}{|w|^\beta} \mathrm{d}w \\
&+ (\varepsilon|k|)^{\beta-d} \int_{|w|<\varepsilon K|k|} \left(\mathrm{e}^{-isw\cdot\frac{k}{|k|}} - 1\right) \ell\left(\frac{w}{\varepsilon|k|}\right) \frac{m}{|w|^\beta} \mathrm{d}w.
\end{aligned}
$$

With the choice of $\beta = \alpha + d$, we know that those two integrals are well defined; indeed in a neighborhood of zero, the integrand is equivalent to $C|w|^{2-\beta}$ and at infinity we can dominate it by $\frac{C}{|w|^\beta}$. Since $\ell(v) \underset{|v|\to\infty}{\to} 0$, the dominated convergence theorem enables to write

$$
I_2 \underset{\varepsilon\to 0}{=} o(\varepsilon^{\beta-d}).
$$

We perform the same changes of variables in the integral I_3

$$
\begin{aligned}
I_3 = \int_{|v|>K} \left(\mathrm{e}^{-\mathrm{i}\varepsilon sk\cdot v} - 1\right) \frac{m}{|v|^\beta} \mathrm{d}v &= (\varepsilon|k|)^{\beta-d} \int_{|w|\geq\varepsilon K|k|} \left(\mathrm{e}^{-isw\cdot\frac{k}{|k|}} - 1\right) \frac{m}{|w|^\beta} \mathrm{d}w \\
&= (\varepsilon|k|)^{\beta-d} \int_{w\in\mathbb{R}^d} \left(\mathrm{e}^{-isw\cdot\frac{k}{|k|}} - 1\right) \frac{m}{|w|^\beta} \mathrm{d}w \\
&+ (\varepsilon|k|)^{\beta-d} \int_{|w|<\varepsilon K|k|} \left(\mathrm{e}^{-isw\cdot\frac{k}{|k|}} - 1\right) \frac{m}{|w|^\beta} \mathrm{d}w.
\end{aligned}
$$

With the same arguments as for I_2, the second integral tends to zero as ε goes to zero. The first one has rotational symmetry with respect to k so, for any unitary vector e of $\mathbb{R}^d$, we have

$$
\begin{aligned}
I_3 &\underset{\varepsilon\to 0}{\sim} (\varepsilon|k|)^{\beta-d} \int_{w\in\mathbb{R}^d} \left(\mathrm{e}^{-isw\cdot e} - 1\right) \frac{m}{|w|^\beta} \mathrm{d}w \\
&= \varepsilon^{\beta-d}|k|^{\beta-d}\mathcal{C}(s).
\end{aligned}
$$

We finally get

$$
\left\langle \left(\mathrm{e}^{-\mathrm{i}\varepsilon sk\cdot v} - 1\right) M_\beta(v) \right\rangle \underset{\varepsilon\to 0}{\sim} \varepsilon^{\beta-d}|k|^{\beta-d} \int_{w\in\mathbb{R}^d} \left(\mathrm{e}^{-isw\cdot e} - 1\right) \frac{m}{|w|^\beta} \mathrm{d}w = \varepsilon^{\beta-d}|k|^{\beta-d}\mathcal{C}(s),
$$

with $C(s)$ defined in (1.6.1). We also need an estimation of the remainder in this equivalent when ε tends to zero and when s is small (independently). We already have an upper bound for I_1; in order to get one for all the terms smaller than the equivalent we must specify the remainders in the integrals arising in the study of I_2 and I_3. Firstly, let us consider the second term at the end of the computation of I_2

$$
\begin{aligned}
(\varepsilon|k|)^{\beta-d} \int_{|w|<\varepsilon K|k|} &\left(\mathrm{e}^{-isw\cdot\frac{k}{|k|}} - 1\right) l\left(\frac{w}{\varepsilon|k|}\right) \frac{m}{|w|^\beta} \mathrm{d}w \\
&\leq c(\varepsilon|k|)^{\beta-d} \int_{|w|<\varepsilon K|k|} \left(\mathrm{e}^{-isw\cdot\frac{k}{|k|}} - 1\right) \frac{m}{|w|^\beta} \mathrm{d}w \\
&\leq c(\varepsilon|k|)^{\beta-d} s^2 \int_{|w|<\varepsilon K|k|} |w|^{2-\beta} \mathrm{d}w \\
&\leq c(\varepsilon|k|)^{\beta-d} s^2 \int_0^{\varepsilon K|k|} r^{d-1} r^{2-\beta} \mathrm{d}r
\end{aligned}
$$

$$\leq cs^2\varepsilon^2|k|^2,$$

where c is a constant depending on the upper bound of ℓ, the constants m and β, the dimension d and K. We notice that the remainder in the integral I_3 can be bounded exactly in the same way, so it remains to consider the following term on which we perform the change of variable $w \to ws$

$$\begin{aligned}(\varepsilon|k|)^{\beta-d}\int_{w\in\mathbb{R}^d}\left(\mathrm{e}^{-isw\cdot\frac{k}{|k|}}-1\right)\ell\left(\frac{w}{\varepsilon|k|}\right)\frac{m}{|w|^\beta}\mathrm{d}w \\ = (\varepsilon s|k|)^{\beta-d}\int_{w\in\mathbb{R}^d}\left(\mathrm{e}^{-\mathrm{i}w\cdot\frac{k}{|k|}}-1\right)\ell\left(\frac{w}{\varepsilon s|k|}\right)\frac{m}{|w|^\beta}\mathrm{d}w.\end{aligned}$$

Using the same argument of dominated convergence, the integral has null limit for small ε and s, hence we get

$$\left\langle\left(\mathrm{e}^{-\mathrm{i}\varepsilon sk\cdot v}-1\right)M_\beta(v)\right\rangle \underset{\substack{\varepsilon\to0\\ s\to0\\ \text{independently}}}{=} (\varepsilon|k|)^{\beta-d}\mathcal{C}(s)+(\varepsilon s|k|)^{\beta-d}R(\varepsilon,s,k),$$

where $R(\varepsilon,s,k)$ is bounded and tends to 0 for small ε and s with an explicit form given by

$$R(\varepsilon,s,k)=\int_{w\in\mathbb{R}^d}\left(\mathrm{e}^{-\mathrm{i}w\cdot e}-1\right)\left(\frac{1}{(\varepsilon s|k|)^\beta}M_\beta\left(\frac{w}{\varepsilon s|k|}\right)-\frac{m}{|w|^\beta}\right)\mathrm{d}w.$$

□

1.7 Appendix: General expression of the anomalous diffusion in the original space variable

In this part, we will show the following proposition which enables to derive the anomalous diffusion limit of the kinetic equation with the original space variable in the general case.

Proposition 1.11. *Considering an equilibrium $M_\beta(v)$ in the case 2 (anomalous diffusion scaling), the following function $a(\varepsilon,z)$*

$$a(\varepsilon,z)=\int_0^{\frac{t}{\varepsilon^\alpha}}|z|^\beta\frac{\mathrm{e}^{-s}}{(\varepsilon s)^d}M_\beta\left(\frac{z}{\varepsilon s}\right)\mathrm{d}s.$$

satisfies

$$a(\varepsilon,z)\underset{\varepsilon\to0}{\sim}m\varepsilon^{\beta-d}\int_0^{+\infty}s^{\beta-d}\mathrm{e}^{-s}\mathrm{d}s,$$

and

$$a(\varepsilon,z)-m\varepsilon^{\beta-d}\int_0^{+\infty}s^{\beta-d}\mathrm{e}^{-s}\mathrm{d}s\underset{\varepsilon\to0}{\leq}C\varepsilon^{\beta-d},$$

where C is a constant independent of ε.

Proof. We start with the equality

$$a(\varepsilon,z)=\int_0^{+\infty}|z|^\beta\frac{\mathrm{e}^{-s}}{(\varepsilon s)^d}M_\beta\left(\frac{z}{\varepsilon s}\right)\mathrm{d}s-\int_{\frac{t}{\varepsilon^\alpha}}^{+\infty}|z|^\beta\frac{\mathrm{e}^{-s}}{(\varepsilon s)^d}M_\beta\left(\frac{z}{\varepsilon s}\right)\mathrm{d}s,$$

and as M_β is bounded by a constant C, we have

$$\left| \int_{\frac{t}{\varepsilon^\alpha}}^{+\infty} |z|^\beta \frac{\mathrm{e}^{-s}}{(\varepsilon s)^d} M_\beta\left(\frac{z}{\varepsilon s}\right) \mathrm{d}s \right| \leq C\,|z|^\beta \frac{1}{\varepsilon^d} \int_{\frac{t}{\varepsilon^\alpha}}^{+\infty} \frac{\mathrm{e}^{-s}}{s^d} \mathrm{d}s \underset{\varepsilon\to 0}{=} O(\varepsilon^\infty).$$

Hence, we obtain

$$\frac{1}{\varepsilon^{\beta-d}} \left| \int_{\frac{t}{\varepsilon^\alpha}}^{+\infty} |z|^\beta \frac{\mathrm{e}^{-s}}{(\varepsilon s)^d} M_\beta\left(\frac{z}{\varepsilon s}\right) \mathrm{d}s \right| \underset{\varepsilon\to 0}{\longrightarrow} 0,$$

and there exists a constant C_1 such that

$$\left| \int_{\frac{t}{\varepsilon^\alpha}}^{+\infty} |z|^\beta \frac{\mathrm{e}^{-s}}{(\varepsilon s)^d} M_\beta\left(\frac{z}{\varepsilon s}\right) \mathrm{d}s \right| \leq \varepsilon^{\beta-d} C_1.$$

As we did in the previous appendix, we consider a function $\ell(v)$ satisfying (1.6.2). Considering that, for a nonzero z,

$$\left|\frac{z}{\varepsilon s}\right| > K \Leftrightarrow s < \frac{|z|}{\varepsilon K},$$

$a(\varepsilon, z)$ becomes

$$\begin{aligned} a(\varepsilon,z) = &\int_0^{+\infty} |z|^\beta \frac{\mathrm{e}^{-s}}{(\varepsilon s)^d} \frac{m}{\left|\frac{z}{\varepsilon s}\right|^\beta} \mathrm{d}s + \int_0^{\frac{|z|}{\varepsilon K}} |z|^\beta \frac{\mathrm{e}^{-s}}{(\varepsilon s)^d} \left(M_\beta\left(\frac{z}{\varepsilon s}\right) - \frac{m}{\left|\frac{z}{\varepsilon s}\right|^\beta} \right) \mathrm{d}s \\ &+ \int_{\frac{|z|}{\varepsilon K}}^{+\infty} |z|^\beta \frac{\mathrm{e}^{-s}}{(\varepsilon s)^d} M_\beta\left(\frac{z}{\varepsilon s}\right) \mathrm{d}s - \int_{\frac{|z|}{\varepsilon K}}^{+\infty} |z|^\beta \frac{\mathrm{e}^{-s}}{(\varepsilon s)^d} \frac{m}{\left|\frac{z}{\varepsilon s}\right|^\beta} \mathrm{d}s \\ &- \int_{\frac{t}{\varepsilon^\alpha}}^{+\infty} |z|^\beta \frac{\mathrm{e}^{-s}}{(\varepsilon s)^d} M_\beta\left(\frac{z}{\varepsilon s}\right) \mathrm{d}s. \end{aligned} \tag{1.7.1}$$

Now we consider separately these five integrals of (1.7.1). The first one is exactly the equivalent we are looking for

$$\int_0^{+\infty} |z|^\beta \frac{\mathrm{e}^{-s}}{(\varepsilon s)^d} \frac{m}{\left|\frac{z}{\varepsilon s}\right|^\beta} \mathrm{d}s = m\varepsilon^{\beta-d} \int_0^{+\infty} s^{\beta-d} \mathrm{e}^{-s} \mathrm{d}s,$$

so we must prove that the other terms of (1.7.1) are small. For the second integral of (1.7.1), we use the function ℓ introduced in (1.6.2)

$$\begin{aligned} \int_0^{\frac{|z|}{\varepsilon K}} |z|^\beta \frac{\mathrm{e}^{-s}}{(\varepsilon s)^d} \left(M_\beta\left(\frac{z}{\varepsilon s}\right) - \frac{m}{\left|\frac{z}{\varepsilon s}\right|^\beta} \right) \mathrm{d}s &= \int_0^{\frac{|z|}{\varepsilon K}} |z|^\beta \frac{\mathrm{e}^{-s}}{(\varepsilon s)^d} \ell\left(\frac{z}{\varepsilon s}\right) \frac{m}{\left|\frac{z}{\varepsilon s}\right|^\beta} \mathrm{d}s \\ &= \varepsilon^{\beta-d} \int_0^{+\infty} s^{\beta-d} \mathrm{e}^{-s} \ell\left(\frac{z}{\varepsilon s}\right) \mathbf{1}_{\left[0,\frac{|z|}{\varepsilon K}\right]}(s) \mathrm{d}s. \end{aligned}$$

As $\ell(v) \underset{|v|\to+\infty}{\longrightarrow} 0$, we have

$$s^{\beta-d} \mathrm{e}^{-s} \ell\left(\frac{z}{\varepsilon s}\right) \mathbf{1}_{\left[0,\frac{|z|}{\varepsilon K}\right]}(s) \mathrm{d}s \underset{\varepsilon\to 0}{\longrightarrow} 0,$$

and

$$\left| s^{\beta-d} \mathrm{e}^{-s} \ell\left(\frac{z}{\varepsilon s}\right) \mathbf{1}_{\left[0,\frac{|z|}{\varepsilon K}\right]}(s) \mathrm{d}s \right| \leq C s^{\beta-d} \mathrm{e}^{-s},$$

where the constant C denotes the maximum of ℓ. So, by the dominated convergence theorem

$$\frac{1}{\varepsilon^{\beta-d}}\int_0^{\frac{|z|}{\varepsilon K}}|z|^\beta\,\frac{\mathrm{e}^{-s}}{(\varepsilon s)^d}\left(M_\beta\left(\frac{z}{\varepsilon s}\right)-\frac{m}{\left|\frac{z}{\varepsilon s}\right|^\beta}\right)\mathrm{d}s\underset{\varepsilon\to 0}{\longrightarrow}0,$$

and there exists a constant C_2 such that

$$\left|\int_0^{\frac{|z|}{\varepsilon K}}|z|^\beta\,\frac{\mathrm{e}^{-s}}{(\varepsilon s)^d}\left(M_\beta\left(\frac{z}{\varepsilon s}\right)-\frac{m}{\left|\frac{z}{\varepsilon s}\right|^\beta}\right)\mathrm{d}s\right|\leq C_2\varepsilon^{\beta-d}.$$

Then, we remark that the third and fourth integral in (1.7.1) are exponentially small

$$\begin{aligned}&\left|\int_{\frac{|z|}{\varepsilon K}}^{+\infty}|z|^\beta\,\frac{\mathrm{e}^{-s}}{(\varepsilon s)^d}M_\beta\left(\frac{z}{\varepsilon s}\right)\mathrm{d}s-\int_{\frac{|z|}{\varepsilon K}}^{+\infty}|z|^\beta\,\frac{\mathrm{e}^{-s}}{(\varepsilon s)^d}\frac{m}{\left|\frac{z}{\varepsilon s}\right|^\beta}\mathrm{d}s\right|\\&\leq C\frac{|z|^\beta}{\varepsilon^d}\int_{\frac{|z|}{\varepsilon K}}^{+\infty}\frac{\mathrm{e}^{-s}}{s^d}\mathrm{d}s+\varepsilon^{\beta-d}m\int_{\frac{|z|}{\varepsilon K}}^{+\infty}\mathrm{e}^{-s}s^{\beta-d}\mathrm{d}s\\&=O(\varepsilon^\infty),\end{aligned}$$

where C denotes the maximum of M_β. Hence, we deduce

$$\frac{1}{\varepsilon^{\beta-d}}\left(\int_{\frac{|z|}{\varepsilon K}}^{+\infty}|z|^\beta\,\frac{\mathrm{e}^{-s}}{(\varepsilon s)^d}M_\beta\left(\frac{z}{\varepsilon s}\right)\mathrm{d}s-\int_{\frac{|z|}{\varepsilon K}}^{+\infty}|z|^\beta\,\frac{\mathrm{e}^{-s}}{(\varepsilon s)^d}\frac{m}{\left|\frac{z}{\varepsilon s}\right|^\beta}\mathrm{d}s\right)\underset{\varepsilon\to 0}{\longrightarrow}0$$

and there exists a constant C_3 such that

$$\left|\int_{\frac{|z|}{\varepsilon K}}^{+\infty}|z|^\beta\,\frac{\mathrm{e}^{-s}}{(\varepsilon s)^d}M_\beta\left(\frac{z}{\varepsilon s}\right)\mathrm{d}s-\int_{\frac{|z|}{\varepsilon K}}^{+\infty}|z|^\beta\,\frac{\mathrm{e}^{-s}}{(\varepsilon s)^d}\frac{m}{\left|\frac{z}{\varepsilon s}\right|^\beta}\mathrm{d}s\right|\leq\varepsilon^{\beta-d}C_3.$$

Since the last integral of (1.7.1) has already been treated, this conclude the proof.

□

Chapter 2

Numerical schemes for kinetic equations in the anomalous diffusion limit: the case of degenerate collision frequency

2.1 Introduction

The theoretical and numerical study of particle system equations has major applications in plasma physics, galactic dynamics, chemotaxis or biological models. Depending on the physical properties of the system, different scales can be considered to describe it. When the mean free path of the particles is large compared to a typical length, a kinetic description of the system is required. Kinetic equations describe the time evolution of a distribution of particles depending on the time, the space and the velocity. This distribution of particles represents the probability for a particle to be at a given point of the phase space (x, v) at the time t. When the mean free path of the particles is small, a macroscopic description can be used. In this regime, the former distribution function is close to an equilibrium and can be averaged in the velocity variable. The relevant quantity is then the density of the particles, which only depends on the time and the space.

The passage from the microscopic to the macroscopic scale is mathematically performed by asymptotic analysis. From a numerical point of view, the small mean free path limit corresponds to a singular perturbation problem which is known to be difficult to simulate (although a lot of works has already been achieved in this context). Indeed, this limit induces the presence of multiple scales in the system, so that the numerical parameters have to solve the smallest ones for stability reasons. As a consequence, the construction of efficient schemes in this context is of great interest.

In this work, we are interested in the time evolution of the distribution function f which depends on the time $t > 0$, the space variable $x \in \Omega \subset \mathbb{R}^d$ and the velocity $v \in V \subset \mathbb{R}^d$ with $d = 1, 2, 3$. If f stands for a distribution of particles, they undergo the effect of collisions which are modelized here by a linear operator L acting on f through

$$L(f)(t, x, v) = \nu(v) \left(\rho_\nu(t, x)M(v) - f(t, x, v)\right),$$

where

$$\rho_\nu(t, x) = \frac{\langle \nu(v) f(t, x, v)\rangle_V}{\langle \nu(v)M(v)\rangle_V} =: \frac{\int_V \nu(v) f(t, x, v)\mathrm{d}v}{\int_V \nu(v)M(v)\mathrm{d}v}, \tag{2.1.1}$$

is not the usual density $\rho(t, x) = \langle f(t, x, v)\rangle_V$ but has been modified to ensure the mass conservation for L: $\langle L(f)\rangle_V = 0$. In the sequel, we will always denote by brackets the integration over v. The equilibrium $M(v)$ will be taken constant on $V = \{v, |v| \leq \delta\}$ (we choose $\delta = 1$ in the sequel)

$$M(v) = M_0, \ |v| \leq 1, \ \ M_0 > 0, \tag{2.1.2}$$

such that $\langle M(v)\rangle_V = 1$ and we will consider the case of a degenerate collision frequency

$$\nu(v) = \nu_0 |v|^{d+2+\beta}, \ |v| \leq 1, \tag{2.1.3}$$

for a given $\beta > 0$. Hence, the second order moment of M is not finite

$$D = \int_{|v|\leq 1} \frac{v \otimes v}{\nu(v)} M(v)\mathrm{d}v = +\infty. \tag{2.1.4}$$

In order to capture a nontrivial asymptotic model, a suitable scaling has to be considered (see for instance [4]). We consider the kinetic equation

$$\varepsilon^\alpha \partial_t f + \varepsilon v \cdot \nabla_x f = L(f), \text{ with } \alpha = \frac{2d + 2 + \beta}{d + 1 + \beta} \in (1, 2), \tag{2.1.5}$$

where $\varepsilon > 0$ is the Knudsen number, which is proportional to the mean free path of the particles. Equation (2.1.5) has to be supplemented with an initial condition $f(0,x,v) = f_0(x,v)$ and spatial periodic boundary conditions are considered.

Considering $\alpha = 2$, an equilibrium function M and a collision frequency ν such that the integral (2.1.4) is finite, (2.1.5) degenerates into a diffusion equation for ρ

$$\partial_t \rho(t,x) - \nabla_x \cdot (D\nabla_x)\rho(t,x) = 0,$$

when ε goes to zero. There is a huge literature on this subject, we refer for example to [48, 70, 7, 22] for details. When the diffusion coefficient (2.1.4) is no longer finite, this asymptotic breaks down which can be interpreted by saying that the time scale $t \sim \varepsilon^{-2}$ is too long. Then, it is necessary to consider an appropriate scaling to get a nontrivial limit for (2.1.5). For instance, it is known (see [55, 53, 5]) that when the collision frequency is not degenerated for small velocities and when the equilibrium M is an heavy-tailed function (equivalent to a power of v for large velocities) (2.1.5) degenerates into a fractional diffusion equation when ε goes to zero. As the scaling ε^α is not an integer power of ε this fractional diffusion limit is called an anomalous diffusion limit. This scaling arises in the study of granular media (see [27, 9, 8]), plasmas (see [23]) or even economy ([46]). The case with degenerate collision frequency we are considering has been studied in [4]. It does not correspond to a particles dynamics physical situation but rather to the modelization of some chains of oscillators, see [36, 54].

When ε goes to 0, the solution of (2.1.5) converges to $\rho(t,x)M(v)$ where ρ is the solution of the fractional diffusion equation that can be written in Fourier variable

$$\partial_t \hat{\rho}(t,k) = -\kappa |k|^\alpha \hat{\rho}(t,k), \tag{2.1.6}$$

where $\hat{\rho}$ stands for the space Fourier transform of ρ, k is the Fourier variable and κ is a constant which depends on M, ν and α and is defined by

$$\kappa = \frac{M_0 \nu_0^{1-\alpha}}{d+1+\beta} \left\langle \frac{1}{|v|^{d+\alpha}} \frac{(v\cdot e)^2}{1+(v\cdot e)^2} \right\rangle_{\mathbb{R}^d}, \tag{2.1.7}$$

for any $e \in \mathbb{R}^d$ such that $|e| = 1$ (note that κ does not depend on e). The fractional diffusion equation can also be written in the space variable

$$\partial_t \rho(t,x) = -\frac{1}{c_{d,\alpha}} \frac{M_0 \nu_0^{1-\alpha} \Gamma(\alpha+1)}{d+1+\beta} \left(-\Delta_x\right)^{\frac{\alpha}{2}} \rho(t,x), \tag{2.1.8}$$

where Γ is the usual Gamma function defined by $\Gamma(x) = \int_0^{+\infty} t^{x-1} \mathrm{e}^{-t} \mathrm{d}t$ and $c_{d,\alpha}$ is a normalization constant given by $c_{d,\alpha} = \frac{\alpha \Gamma\left(\frac{d+\alpha}{2}\right)}{2\pi^{\frac{d}{2}+\alpha} \Gamma\left(1-\frac{\alpha}{2}\right)}$. The fractional Laplacian $\left(-\Delta_x\right)^{\frac{\alpha}{2}}$ can be defined with its Fourier variable

$$\left(\widehat{\left(-\Delta_x\right)^{\frac{\alpha}{2}} \rho} \right)(k) = |k|^\alpha \hat{\rho}(k),$$

but has also an integral definition

$$\left(-\Delta_x\right)^{\frac{\alpha}{2}} \rho(x) = c_{d,\alpha} P.V. \int_{\mathbb{R}^d} \frac{\rho(x+y) - \rho(x)}{|y|^{d+\alpha}} \mathrm{d}y,$$

where *P.V.* is the principal value distribution.

From a numerical point of view, the presence of ε makes the numerical simulations challenging. Indeed, if one uses a naive approach, a relation linking the space and time numerical parameters to the stiffness ε (typically $\Delta t \sim \varepsilon^\alpha$, where Δt is the time step) is required for stability reasons, which implies a redhibitory cost when ε is small. The *Asymptotic Preserving* (AP) schemes are designed to overcome this strong restriction on the numerical parameters. Indeed, if we consider the continuous problem P_ε degenerating into P_0 when ε goes to zero, we ask the scheme S_ε^h to be consistent with the problem P_ε when the discretization parameter h tends to 0 and to degenerate into a scheme S_0^h solving the problem P_0 when $\varepsilon \to 0$. An AP scheme can also enjoy the stronger property of being *Uniformly Accurate* (UA). It means that the accuracy in h of the scheme does not depend of ε. Note that it is very desirable for an AP scheme to enjoyy the stronger property of being Uniformly Accurate but this is not automatic and is a difficult issue in general. For kinetic equations, AP scheme has already been developed (see [37]) and there is an important literature for the diffusion asymptotic, for example [41, 58, 57, 50, 52, 43, 12, 3]. In the case of a fractional diffusion scaling, the previous schemes do not enjoy the AP property. Indeed, as the velocities must be discretized with a finite number of points, the diffusion coefficient (2.1.4), which is an infinite integral in the case of the anomalous diffusion, appears to be always finite at the numerical level. Hence, the effects of the low velocities are missed and the approaches for the classical diffusion show only a numerical diffusion which does not match with the expected fractional diffusion.

In the case of the fractional diffusion induced by a heavy-tailed equilibrium, we set in a previous work ([17]) three numerical schemes enjoying the AP property. As the fractional diffusion limit did not naturally appear in the formulation of the schemes, we had to suitably modify them to make the fractional diffusion arise numerically. Let us remark that when $\alpha \in (1, 2)$, an alternative approach has been proposed in [69] for the case of heavy tail equilibria. In this paper, we present an extension of the strategy presented in [17] when the fractional diffusion comes from the degeneracy of the collision frequency. In addition to the technical difficulties which are inherent to the velocity dependency of ν there are many important differences with the heavy-tail case that we have to face. First, to numerically capture the important effects of the low velocities (instead of large velocities in the heavy-tail case). Second, in the present case, the renormalized density ρ_ν defined in (2.1.1) is different from the usual density ρ while these two quantities coincide in the heavy-tail case. This property induces an additional difficulty, as we will see, and a specific treatment is required in order to cover an asymptotic preserving property for the scheme. Lastly, the convergence rate to the fractional diffusion limit is very slow, so that the intermediate regime involves a large range of ε; as a consequence, the numerical validation turns out to be more difficult.

We will present three different Asymptotic Preserving schemes. First, we consider a fully implicit scheme for (2.1.5) in which Fourier space variable is considered. The delicate issue of the velocity discretization is highlighted to explain how the fractional diffusion arises. Then, a second scheme is proposed which allows to avoid, when desired, both the use of the space Fourier transform and that of a fully implicit scheme. A micro-macro formulation of (2.1.5) is then studied to write an semi-implicit scheme enjoying the AP property. Once again, the terms giving theoretically the anomalous diffusion limit will have to be treated with care to ensure the AP character of the scheme. Finally, a scheme based on a Duhamel formulation of (2.1.5) is proposed, which enjoys the stronger property of being uniformly accurate (UA) with respect to ε. These results were announced in [16]. Moreover, a proof of the convergence of the solution of (2.1.5) to the solution of (2.1.8) is given in [4]. We propose a formal derivation of the convergence rate in ε for this limit. This convergence rate is illustrated in the numerical

tests that we present in the last part.

The paper is organized as follows. In the next section, we will start by establishing a formal derivation of the fractional diffusion limit equation (2.1.8), and the rate of this convergence is formally derived (the related computation is postponed in the appendix). Then, in Section 3, we present the three asymptotic preserving schemes for (2.1.5). Eventually, we will present in the last section some numerical tests to highlight the properties of our schemes.

2.2 Formal derivation of the fractional diffusion limit

In this section, we formally derive the fractional diffusion (2.1.6) from the kinetic equation (2.1.5), where the computations are based on spatial Fourier transform. This will be the basis of the numerical methods proposed in Section 3. The proof has been done in [4].

We remind that $\hat{f}(t,k,v)$ (resp. $\hat{\rho}(t,k)$) denotes the spatial Fourier transform of $f(t,x,v)$ (resp. $\rho(t,x)$)

$$\hat{f}(t,k,v) = \int_{\mathbb{R}^d} e^{-\mathrm{i}k\cdot x} f(t,x,v)\mathrm{d}x.$$

Proposition 2.1. *Let $\hat{f}$ be the solution of (2.1.5) in the Fourier variable for a given initial condition $\hat{f}_0$. Then, when $\varepsilon \to 0$, $\hat{f}$ converges to $\hat{\rho}M$ with $\hat{\rho}$ solution of the fractional diffusion equation*

$$\partial_t \hat{\rho}(t,k) + \kappa |k|^\alpha \hat{\rho}(t,k) = 0,$$

with κ defined by (2.1.7) and with initial condition $\hat{\rho}(0,k) = \left\langle \hat{f}_0(k,v) \right\rangle_V$.

Proof. Considering the Fourier transform (in space) of (2.1.5), we get

$$\partial_t \hat{f} + \varepsilon^{-\alpha}(\nu + \mathrm{i}\varepsilon k\cdot v)\hat{f} = \varepsilon^{-\alpha}\nu\hat{\rho}_\nu M. \tag{2.2.1}$$

Integrating with respect to the velocity variable leads to

$$\partial_t \hat{\rho} + \mathrm{i}\varepsilon^{1-\alpha}\langle k\cdot v\hat{f}\rangle_V = 0. \tag{2.2.2}$$

From (2.2.1), we can write

$$\hat{f} = \frac{\nu\hat{\rho}_\nu M}{\nu + \mathrm{i}\varepsilon k\cdot v} - \varepsilon^\alpha \frac{\partial_t \hat{f}}{\nu + \mathrm{i}\varepsilon k\cdot v}, \tag{2.2.3}$$

so that $\hat{f} \underset{\varepsilon\to 0}{\longrightarrow} \hat{\rho}_\nu M$ and with an integration in v, $\hat{\rho} \underset{\varepsilon\to 0}{\sim} \hat{\rho}_\nu$, then (2.2.2) becomes

$$\partial_t \hat{\rho} + \mathrm{i}\varepsilon^{1-\alpha}\left\langle \frac{\nu k\cdot vM}{\nu + \mathrm{i}\varepsilon k\cdot v}\right\rangle_V \hat{\rho}_\nu = O(\varepsilon^\gamma), \gamma > 0. \tag{2.2.4}$$

The fact that the right hand side is negligible compared to the left hand side will be detailed in the Appendix. Then, the fractional diffusion operator is obtained by considering the limit $\varepsilon \to 0$ in the second term of the left hand side. Let us focus on this term in the sequel. First, since M and ν are even, we write

$$\mathrm{i}\varepsilon^{1-\alpha}\left\langle \frac{\nu k\cdot vM}{\nu + \mathrm{i}\varepsilon k\cdot v}\right\rangle_V = \varepsilon^{2-\alpha}\left\langle \frac{\nu(k\cdot v)^2 M}{\nu^2 + \varepsilon^2(k\cdot v)^2}\right\rangle_V.$$

We can remark that the limit $\varepsilon \to 0$ is not defined since the term into brackets goes to infinity when $\varepsilon \to 0$ because of the degeneracy of ν for small velocities. Then, to capture the effect of small velocities, we perform the change of variable $w = \varepsilon|k|v/\nu$ with

$$|w| = \tfrac{\varepsilon|k|}{\nu_0}|v|^{-(d+1+\beta)}, \quad \nu = \nu_0 \left(\tfrac{\varepsilon|k|}{\nu_0|w|}\right)^{\frac{d+2+\beta}{d+1+\beta}}, \quad \mathrm{d}v = \tfrac{1}{d+1+\beta}\left(\tfrac{\varepsilon|k|}{\nu_0|w|^{d+2+\beta}}\right)^{\frac{d}{d+1+\beta}} \mathrm{d}w,$$

to get

$$\begin{aligned}\lim_{\varepsilon\to 0} \mathrm{i}\varepsilon^{1-\alpha}\left\langle \frac{\nu k\cdot vM}{\nu+\mathrm{i}\varepsilon k\cdot v}\right\rangle_V &= \lim_{\varepsilon\to 0}\frac{\nu_0^{1-\alpha}M_0}{d+1+\beta}\left\langle \frac{(k/|k|\cdot w)^2}{1+(k/|k|\cdot w)^2}\frac{1}{|w|^{d+\alpha}}\right\rangle_{|w|\geq\varepsilon|k|/\nu_0} \\ &= \frac{M_0\nu_0^{1-\alpha}}{d+1+\beta}\left\langle \frac{1}{|w|^{d+\alpha}}\frac{(w\cdot e)^2}{1+(w\cdot e)^2}\right\rangle_{\mathbb{R}^d}|k|^\alpha = \kappa|k|^\alpha\end{aligned}$$

where e denotes any unitary vector, and κ has been defined in (2.1.7). Moreover, since when $\varepsilon \to 0$, we have $\hat{\rho} \to \hat{\rho}_\nu$, we then deduce the fractional diffusion asymptotic model from (2.2.4). □

Furthermore, we have the following result for the convergence rate (at the formal level). The proof is postponed to the Appendix.

Proposition 2.2. *Let $\hat{f}$ be the solution of* (2.1.5) *in the Fourier variable for a given initial condition $\hat{f}_0$. We get the following rate of convergence*

$$\hat{f} - \hat{\rho}M = O\left(\varepsilon^{\frac{d}{d+1+\beta}}\right) + O\left(\varepsilon^{\frac{\beta}{d+1+\beta}}\right).$$

2.3 Numerical schemes

In this section, we present three different numerical schemes, based respectively on a fully implicit scheme, a micro-macro formulation and an integral formulation of (2.1.5), designed to approximate the solution of (2.1.5). We will denote $t_n = n\Delta t, 0 \leq n \leq N$ the time discretization, such that $N\Delta t = T$ and we will set $f^n \simeq f(t_n)$. The space domain Ω is bounded and we consider periodic conditions, allowing the use of the Fourier variable. At the discrete level, we will use the discrete Fourier transform. The computation of the numerical solution requires the use of a velocity discretization. In the tests, we will consider a first order quadrature method based on a uniform fixed set of N_v points v_j, symmetrically distributed in the domain $|v| \leq 1$. In the sequel, we will denote by $\langle\cdot\rangle_{N_v,D}$ the discrete integration in v on a domain D :

$$\langle f\rangle_{N_v,D} = \Delta v \sum_{\substack{j\in[\![1,N_v]\!]\\ v_j\in D}} f(v_j). \tag{2.3.1}$$

We want these schemes to be Asymptotic Preserving (AP), indeed that for any initial condition f_0

1. when ε is fixed, the solution given by the numerical scheme is consistent with the solution of (2.1.5),
2. when the numerical parameters are fixed, the scheme degenerates into a scheme solving the anomalous diffusion equation (2.1.8) when ε tends to 0.

Since the fractional Laplacian of the asymptotic equation (2.1.6) comes from the small velocities of the degenerate collision frequency, it is necessary to take it into account in the schemes to ensure the AP property. One idea would be to consider an adaptive grid which is refined around $v = 0$ but this will impose to link the velocity discretization to ε, which breaks down the AP property. We propose a method based on an analytical modification of the terms degenerating into the fractional Laplacian in the scheme. This modification consists into applying a change of variable in some integrals in v of the scheme before discretizing them. Once it is done, we are able to show that the three schemes we propose preserve the asymptotic of fractional diffusion for a fixed set of numerical parameters.

2.3.1 Implicit scheme

The first idea to write a scheme for (2.1.5) which has the AP property is to use a fully implicit formulation of (2.1.5) in Fourier variable. It is well-known that in the case of the classical diffusion limit, such a scheme preserves the asymptotics, but here in the case of the fractional diffusion limit, it is not true, and a suitable modification of the scheme has to be performed to ensure the AP property.

We start with (2.1.5) written in Fourier variable and we consider a fully implicit time discretization

$$\frac{\hat{f}^{n+1}-\hat{f}^n}{\Delta t}+\frac{\nu}{\varepsilon^\alpha}\left(1+\mathrm{i}\frac{\varepsilon k\cdot v}{\nu}\right)\hat{f}^{n+1}=\frac{\nu}{\varepsilon^\alpha}\hat{\rho}_\nu^{n+1}M,$$

that is

$$\hat{f}^{n+1}=\frac{1-\lambda(v)}{1+\mathrm{i}\lambda(v)\frac{\varepsilon k\cdot v}{\nu}}\hat{f}^n+\frac{\lambda(v)}{1+\mathrm{i}\lambda(v)\frac{\varepsilon k\cdot v}{\nu}}\hat{\rho}_\nu^{n+1}M, \tag{2.3.2}$$

with $\lambda(v)=\Delta t\nu(v)/(\varepsilon^\alpha+\Delta t\nu(v))$. Remark that $0\le\lambda(v)\le 1$, λ goes to 1 when $\varepsilon\to 0$ and λ goes to 0 as $\Delta t\to 0$. So when $\varepsilon\to 0$ with fixed Δt, we get

$$\hat{f}^{n+1}=\hat{\rho}_\nu^{n+1}M, \tag{2.3.3}$$

which is the expected limit for $\hat{f}$. Now, it remains to find an expression for $\hat{\rho}_\nu^{n+1}$. To do so, we multiply (2.3.2) by ν and integrate in v to get

$$\hat{\rho}_\nu^{n+1}=\frac{\left\langle\frac{\frac{1}{\varepsilon^\alpha+\Delta t\nu}\nu\hat{f}^n}{1+\mathrm{i}\lambda(v)\frac{\varepsilon k\cdot v}{\nu}}\right\rangle_V}{\left\langle\frac{\frac{1}{\varepsilon^\alpha+\Delta t\nu}\nu M}{1+\mathrm{i}\lambda(v)\frac{\varepsilon k\cdot v}{\nu}}\right\rangle_V+I},\ \text{with}\ \ I=\frac{1}{\varepsilon^\alpha}\left\langle\frac{\nu M\lambda(v)^2\left(\frac{\varepsilon k\cdot v}{\nu}\right)^2}{1+\lambda(v)^2\left(\frac{\varepsilon k\cdot v}{\nu}\right)^2}\right\rangle_V. \tag{2.3.4}$$

At the continuous level, the term I gives the anomalous diffusion limit when ε goes to zero. Indeed, the change of variable $w=\varepsilon|k|v/\nu(v)$ in I enables to capture the small velocity effects so that $\lim_{\varepsilon\to 0} I=\kappa|k|^\alpha$, where κ has been defined in (2.1.7). However, the situation is completely different at the numerical level, namely when a discretization in velocity with N_v points has to be used. Indeed, a naive quadrature of I given by (2.3.4) would lead to

$$I\approx\varepsilon^{2-\alpha}\sum_{j=1}^{N_v}\frac{\nu(v_j)M(v_j)\Delta t^2(k\cdot v_j)^2}{(\varepsilon^\alpha+\Delta t\nu(v_j))^2+\varepsilon^2\Delta t^2(k\cdot v_j)^2}\underset{\varepsilon\to 0}{\sim}\varepsilon^{2-\alpha}\sum_{j=1}^{N_v}\frac{(k\cdot v_j)^2}{\nu(v_j)}M(v_j).$$

This implies that I goes to zero when ε goes to zero since the velocity discretization is fixed (remember that $\alpha<2$). Therefore, the asymptotic numerical scheme becomes $\hat{\rho}_\nu^{n+1}=\hat{\rho}_\nu^n$

when $\varepsilon \to 0$, which is not a consistent numerical scheme for the asymptotic model. To recover the correct asymptotic behavior, the main idea is to transform the expression of I at the continuous level before applying the discretization in order to make the anomalous diffusion operator appear in it. To do so, we perform a change of variables $w = \varepsilon|k|v/\nu(v)$ in I to get

$$I = \frac{|k|^\alpha \nu_0^{1-\alpha} M_0}{d+1+\beta} \int_{|w| \geq \frac{\varepsilon|k|}{\nu_0}} \frac{1}{|w|^{d+\alpha}} \frac{\left(\frac{\Delta t\varphi}{\varepsilon^\alpha + \Delta t\varphi}\right)^2 (w\cdot e)^2}{1 + \left(\frac{\Delta t\varphi}{\varepsilon^\alpha + \Delta t\varphi}\right)^2 (w\cdot e)^2} \mathrm{d}w,$$

where e denotes any unitary vector and $\varphi = \nu_0(\varepsilon|k|/(\nu_0|w|))^{\frac{d+2+\beta}{d+1+\beta}}$. Note that I does not depend on the choice of e. Once the change of variables has been done, the velocity discretization can be performed so that we get

$$I \approx \frac{|k|^\alpha \nu_0^{1-\alpha} M_0}{d+1+\beta} \left\langle \frac{1}{|w|^{d+\alpha}} \frac{\left(\frac{\Delta t\varphi}{\varepsilon^\alpha + \Delta t\varphi}\right)^2 (w\cdot e)^2}{1 + \left(\frac{\Delta t\varphi}{\varepsilon^\alpha + \Delta t\varphi}\right)^2 (w\cdot e)^2} \right\rangle_{N_v, |w_{\max}| \geq |w| \geq \frac{\varepsilon|k|}{\nu_0}} \tag{2.3.5}$$

where $\langle\cdot\rangle_{N_v,D}$ has been defined in (2.3.1). Let us remark that I is of magnitude Δt^2 for fixed ε and that when ε goes to zero, it degenerates towards

$$\frac{|k|^\alpha \nu_0^{1-\alpha} M_0}{d+1+\beta} \left\langle \frac{1}{|w|^{d+\alpha}} \frac{(w\cdot e)^2}{1+(w\cdot e)^2} \right\rangle_{N_v, |w| \leq |w_{\max}|} =: \bar{\kappa}|k|^\alpha, \tag{2.3.6}$$

which is a consistent approximation of κ given by (2.1.7). Let us remark that the numerical integration is done up to a maximum discrete velocity $|w_{\max}|$. Eventually, we have the following proposition

Proposition 2.3. *We consider the following scheme defined for all k and for all time indices $0 \leq n \leq N, N\Delta t = T$ by*

$$\hat{\rho}_\nu^{n+1} = \frac{\left\langle \frac{\frac{1}{\varepsilon^\alpha + \Delta t\nu} \nu \hat{f}^n}{1 + \mathrm{i}\lambda(v)\frac{\varepsilon k\cdot v}{\nu}} \right\rangle_{N_v,V}}{\left\langle \frac{\frac{1}{\varepsilon^\alpha + \Delta t\nu} \nu M}{1 + \mathrm{i}\lambda(v)\frac{\varepsilon k\cdot v}{\nu}} \right\rangle_{N_v,V} + I}, \quad \hat{f}^{n+1} = \frac{(1-\lambda(v))\hat{f}^n + \lambda(v)\hat{\rho}_\nu^{n+1} M}{1 + \mathrm{i}\lambda(v)\frac{\varepsilon k\cdot v}{\nu}}, \tag{2.3.7}$$

with I given by (2.3.5), $\hat{\rho}^{n+1} = \left\langle \hat{f}^{n+1} \right\rangle_{N_v,V}$, $\lambda(v) = \Delta t\nu(v)/(\varepsilon^\alpha + \Delta t\nu(v))$ and e is any unitary vector and with the initial condition $\hat{f}^0(k,v) = \hat{f}_0(k,v)$. This scheme has the following properties:

1. *The scheme is of order 1 for any fixed ε and preserves the total mass.*
2. *The scheme is AP: for a fixed Δt, the scheme solves the anomalous diffusion equation when ε goes to zero*

$$\frac{\hat{\rho}^{n+1}(k) - \hat{\rho}^n(k)}{\Delta t} = -\bar{\kappa}|k|^\alpha \hat{\rho}^{n+1}(k), \text{ with } \bar{\kappa} \text{ given by (2.3.6).} \tag{2.3.8}$$

Remark 2.4. We can go further, modifying the approximation (2.3.5) of I by

$$I \approx \frac{\Delta t^2}{(\varepsilon^{\alpha - \frac{d+2+\beta}{d+1+\beta}} + \Delta t)^2} \bar{\kappa},$$

where $\bar{\kappa}$ is defined in (2.3.6). The so-obtained scheme enjoys the same properties stated in the above proposition.

Proof. The first point of (i) is a direct consequence of the use of a fully implicit Euler scheme for (2.1.5). For the conservation of the total mass, let us write (2.3.7) for $k = 0$ and integrate with respect to v

$$\left\langle \frac{\nu M}{\varepsilon^\alpha + \Delta t \nu} \right\rangle_{N_v,V} \hat{\rho}_\nu^{n+1}(0) = \left\langle \frac{\nu}{\varepsilon^\alpha + \Delta t \nu} \hat{f}^n(0) \right\rangle_{N_v,V}, \tag{2.3.9}$$

$$\hat{\rho}^{n+1}(0) = \hat{\rho}^n(0) - \Delta t \left\langle \frac{\nu}{\varepsilon^\alpha + \Delta t \nu} \hat{f}^n(0) \right\rangle_{N_v,V} + \left\langle \frac{\Delta t \nu}{\varepsilon^\alpha + \Delta t \nu} M \right\rangle_{N_v,V} \hat{\rho}_\nu^{n+1}(0). \tag{2.3.10}$$

Injecting (2.3.9) in (2.3.10) leads to the result.

For the AP character of the scheme (ii), letting ε to 0 with fixed Δt in the first equation of (2.3.7) leads to

$$\frac{\hat{\rho}_\nu^{n+1} - \hat{\rho}^n}{\Delta t} = -\bar{\kappa}|k|^\alpha \hat{\rho}_\nu^{n+1}$$

and with (2.3.3) we have $\hat{\rho}^n = \hat{\rho}_\nu^n, \forall n \geq 1$ when $\varepsilon \to 0$. It implies that (2.3.7) degenerates into (2.3.8). □

2.3.2 Micro-macro decomposition based scheme

In the previous part, we presented a fully implicit scheme designed to solve (2.1.5); however the use of Fourier transform may be restrictive in some cases and one may have to use the original space variable. Therefore, making the transport part implicit in time may induce high computational cost especially in the multidimensional case. Here we write a scheme based on a micro-macro decomposition of the distribution function f in which the transport part is explicit. As for the previous scheme, suitable modifications have to be done to ensure the AP character.

Denoting $f(t,x,v) = \rho(t,x)M(v) + g(t,x,v)$ such that $\langle g \rangle_V = 0$, we insert this decomposition into (2.1.5) before integrating in v to get

$$\partial_t \rho + \varepsilon^{1-\alpha} \langle v \cdot \nabla_x g \rangle_V = 0. \tag{2.3.11}$$

Then we multiply this last equality by M and subtract it from (2.1.5) to write an expression for g

$$\partial_t g + \varepsilon^{1-\alpha} v \cdot \nabla_x \rho M + \varepsilon^{1-\alpha} \left(v \cdot \nabla_x g - \langle v \cdot \nabla_x g \rangle_V M \right) = -\frac{1}{\varepsilon^\alpha} \nu \left(g - \frac{\langle \nu g \rangle_V M}{\langle \nu M \rangle_V} \right). \tag{2.3.12}$$

From (2.3.11) and (2.3.12) we can write the following semi-discrete micro-macro scheme (see [52, 50])

$$\begin{cases} \dfrac{\rho^{n+1} - \rho^n}{\Delta t} + & \varepsilon^{1-\alpha} \left\langle v \cdot \nabla_x g^{n+1} \right\rangle_V = 0 \\ \dfrac{g^{n+1} - g^n}{\Delta t} + & \varepsilon^{1-\alpha} v \cdot \nabla_x \rho^n M + \varepsilon^{1-\alpha} \left(v \cdot \nabla_x g^n - \langle v \cdot \nabla_x g^n \rangle_V M \right) \\ & = -\dfrac{1}{\varepsilon^\alpha} \nu \left(g^{n+1} - \dfrac{\left\langle \nu g^{n+1} \right\rangle_V}{\langle \nu M \rangle_V} M \right). \end{cases} \tag{2.3.13}$$

As previously, if the velocity integrations are done directly using the approximation $\langle \cdot \rangle_V \approx \langle \cdot \rangle_{N_v,V}$ where the discrete bracket $\langle \cdot \rangle_{N_v,V}$ is given by (2.3.1), the so-obtained scheme does not

enjoy the AP property. Indeed, as g^{n+1} goes to zero when ε goes to zero, we have

$$\varepsilon v\cdot\nabla_x\rho^n M=-\nu\left(g^{n+1}-\frac{\left\langle\nu g^{n+1}\right\rangle_{N_v,V}}{\langle\nu M\rangle_{N_v,V}}M\right)+o(\varepsilon),$$

that is, for nonzero v

$$g^{n+1}=\frac{\left\langle\nu g^{n+1}\right\rangle_{N_v,V}}{\langle\nu M\rangle_{N_v,V}}M-\frac{\varepsilon}{\nu}v\cdot\nabla_x\rho^n M+o(\varepsilon).$$

Then, we insert this expression in the first line of (2.3.13), reminding that M is even, to get

$$\frac{\rho^{n+1}-\rho^n}{\Delta t}-\varepsilon^{2-\alpha}\left\langle\frac{M}{\nu}v\cdot\nabla_x\left(v\cdot\nabla_x\rho^n\right)\right\rangle_{N_v,V}=o(\varepsilon).$$

As in the previous part, the term into brackets is finite although it is not finite at the continuous level. Hence, when $\varepsilon\to 0$, (2.3.13) degenerates into $\rho^{n+1}=\rho^n$ which of course does not solve the fractional diffusion equation. To obtain the right asymptotic scheme, we must modify (2.3.13) to make the anomalous diffusion limit appear. To do so, we first express the term $\left\langle v\cdot\nabla_x g^{n+1}\right\rangle_V=\left\langle v\cdot\nabla_x f^{n+1}\right\rangle_V$ appearing in the first line of (2.3.13) with a semi-discrete implicit formulation of (2.1.5)

$$f^{n+1}=\lambda(v)\left(I+\varepsilon\frac{\lambda(v)}{\nu}v\cdot\nabla_x\right)^{-1}\rho_\nu^{n+1}M+(1-\lambda(v))\left(I+\varepsilon\frac{\lambda(v)}{\nu}v\cdot\nabla_x\right)^{-1}f^n,$$

with $\lambda(v)=\Delta t\nu(v)/(\varepsilon^\alpha+\Delta t\nu(v))$. The first line of (2.3.13) then reads

$$\begin{aligned}\frac{\rho^{n+1}-\rho^n}{\Delta t}&+\frac{1}{\varepsilon^\alpha}\left\langle\varepsilon\lambda(v)v\cdot\nabla_x\left(I+\frac{\varepsilon\lambda(v)}{\nu}v\cdot\nabla_x\right)^{-1}\rho_\nu^{n+1}M\right\rangle_V\\&+\varepsilon^{1-\alpha}\left\langle(1-\lambda(v))v\cdot\nabla_x\left[\left(I+\varepsilon\frac{\lambda(v)}{\nu}v\cdot\nabla_x\right)^{-1}f^n\right]\right\rangle_V=0,\end{aligned}\tag{2.3.14}$$

and can be simplified in a consistent way. Indeed, since the scheme is first order accurate, it is possible to remove terms of order Δt in (2.3.14) with no incidence on its global accuracy. Hence, we decide to keep the first line unchanged, as it plays a role in the AP character of the scheme and, in the second line of (2.3.14), the inverse of the transport operator is approximated by

$$\left(I+\varepsilon\frac{\lambda(v)}{\nu}v\cdot\nabla_x\right)^{-1}=I+O\left(\Delta t\right),$$

as $\lambda(v)$ is of magnitude Δt for fixed ε. Eventually, the first line of (2.3.13) becomes

$$\begin{aligned}\frac{\rho^{n+1}-\rho^n}{\Delta t}&+\frac{1}{\varepsilon^\alpha}\left\langle\varepsilon\lambda(v)v\cdot\nabla_x\left(I+\frac{\varepsilon\lambda(v)}{\nu}v\cdot\nabla_x\right)^{-1}\rho_\nu^{n+1}M\right\rangle_V\\&+\varepsilon^{1-\alpha}\left\langle(1-\lambda(v))\,v\cdot\nabla_x g^n\right\rangle_V=0,\end{aligned}\tag{2.3.15}$$

because $\langle(1-\lambda(v))v\cdot\nabla_x f^n\rangle_V=\langle(1-\lambda(v))v\cdot\nabla_x g^n\rangle_V$. As the anomalous diffusion limit comes from the second term of (2.3.15), we have to rewrite it in order to make the fractional

Laplacian appear. First, we have to express ρ_ν in terms of ρ; to do that, we inject the decomposition $f = \rho M + g$ in the definition of ρ_ν

$$\rho_\nu = \frac{\langle \nu f \rangle_V}{\langle \nu M \rangle_V} = \frac{\langle \nu(\rho M + g) \rangle_V}{\langle \nu M \rangle_V} = \rho + \frac{\langle \nu g \rangle_V}{\langle \nu M \rangle_V}.$$

Then, using space Fourier transform, we rewrite (2.3.15) as

$$\frac{\rho^{n+1} - \rho^n}{\Delta t} + \mathcal{F}^{-1}\left(\mathcal{I}\hat{\rho}^{n+1}\right) + \mathcal{F}^{-1}\left(\mathcal{I}\frac{\left\langle \nu \hat{g}^{n+1} \right\rangle_V}{\langle \nu M \rangle_V}\right) + \varepsilon^{1-\alpha} \left\langle (1 - \lambda(v))\, v \cdot \nabla_x g^n \right\rangle_V = 0, \quad (2.3.16)$$

where $\mathcal{F}^{-1}$ denotes the inverse Fourier transform and

$$\mathcal{I} = \varepsilon^{1-\alpha} \left\langle \frac{\mathrm{i}\lambda(v) k \cdot v M(v)}{1 + \mathrm{i}\frac{\varepsilon\lambda(v)}{\nu} k \cdot v} \right\rangle_V = \varepsilon^{-\alpha} \left\langle \frac{\lambda(v)^2 \frac{(\varepsilon k \cdot v)^2}{\nu} M}{1 + \lambda(v)^2 \left(\frac{\varepsilon k \cdot v}{\nu}\right)^2} \right\rangle_V.$$

Let us remark that for $k = 0$, we have $\mathcal{I} = 0$. For $k \neq 0$, the change of variables $w = \varepsilon|k|v/\nu(v)$ is performed in $\mathcal{I}$ before applying the discretization $\langle\cdot\rangle_{N_v,V}$ (using the definitions (2.1.2) and (2.1.3) of M and ν). Then, we have

$$\mathcal{I} = \frac{|k|^\alpha \nu_0^{1-\alpha} M_0}{d + 1 + \beta} \left\langle \frac{1}{|w|^{d+\alpha}} \frac{\left(\frac{\Delta t \nu_0 |k|^p}{\varepsilon^q (\nu_0 |w|)^p + \Delta t \nu_0 |k|^p}\right)^2 (w \cdot e)^2}{\left(\frac{\Delta t \nu_0 |k|^p}{\varepsilon^q (\nu_0 |w|)^p + \Delta t \nu_0 |k|^p}\right)^2 (w \cdot e)^2 + 1} \right\rangle_{N_v, |w_{\max}| \geq |w| \geq \frac{\varepsilon|k|}{\nu_0}},$$

where $p = \frac{d+2+\beta}{d+1+\beta}$ and $q = \frac{d}{d+1+\beta}$. Since $\mathcal{I}$ is of order Δt^2 when ε is fixed, it can be modified consistently into

$$\mathcal{I} \approx \left(\frac{\Delta t}{\varepsilon^q + \Delta t}\right)^2 \frac{|k|^\alpha \nu_0^{1-\alpha} M_0}{d + 1 + \beta} \left\langle \frac{1}{|w|^{d+\alpha}} \frac{(w \cdot e)^2}{(w \cdot e)^2 + 1} \right\rangle_{N_v, |w_{\max}| \geq |w| \geq \frac{\varepsilon|k|}{\nu_0}}. \quad (2.3.17)$$

Note that this approximation conserves the degeneracy rate in ε of $\mathcal{I}$ to the fractional diffusion coefficient $\bar{\kappa}$ defined in (2.3.6).

To compute (ρ^{n+1}, g^{n+1}) recursively with the second line of (2.3.13) and (2.3.16), we need to determine $\left\langle \nu g^{n+1} \right\rangle_{N_v,V}$. To do that, we start with the with the second line of (2.3.13) which gives an expression for g^{n+1}

$$g^{n+1} = \frac{g^n - \frac{\Delta t}{\varepsilon^\alpha}\mathcal{T}^n}{1 + \frac{\Delta t}{\varepsilon^\alpha}\nu} + \frac{\Delta t \nu M}{\langle \nu M \rangle_{N_v} (\varepsilon^\alpha + \Delta t \nu)} \left\langle \nu g^{n+1} \right\rangle_{N_v,V},$$

with

$$\mathcal{T}^n = \varepsilon v \cdot \nabla_x \rho^n M + \varepsilon \left(v \cdot \nabla_x g^n - \langle v \cdot \nabla_x g^n \rangle_{N_v,V} M \right). \quad (2.3.18)$$

Multiplying the expression for g^{n+1} by ν and integrating it using $\langle\cdot\rangle_{N_v,V}$, we find an expression for $\left\langle \nu g^{n+1} \right\rangle_{N_v,V}$

$$\left\langle \nu g^{n+1} \right\rangle_{N_v,V} = \frac{\left\langle \frac{\nu g^n}{1 + \frac{\Delta t}{\varepsilon^\alpha}\nu(v)} \right\rangle_{N_v,V} - \frac{\Delta t}{\varepsilon^\alpha} \left\langle \frac{\nu \mathcal{T}^n}{1 + \frac{\Delta t}{\varepsilon^\alpha}\nu} \right\rangle_{N_v,V}}{1 - \frac{\Delta t}{\varepsilon^\alpha \langle \nu M \rangle_{N_v,V}} \left\langle \frac{\nu^2 M}{1 + \frac{\Delta t}{\varepsilon^\alpha}\nu} \right\rangle_{N_v,V}}.$$

Finally, we have the following proposition.

Proposition 2.5. *We consider the following scheme (discretized in time and velocity) defined for all $x \in \mathbb{R}^d, v \in V$ and all time indices $0 \le n \le N$ with $N\Delta t = T (T > 0)$, by*

$$\begin{cases} \left\langle \nu g^{n+1} \right\rangle_{N_v,V} = & \langle \nu M \rangle_{N_v,V} \dfrac{\left\langle \dfrac{\nu g^n + \mathcal{T}^n}{\varepsilon^\alpha + \Delta t \nu} \right\rangle_{N_v,V}}{\left\langle \dfrac{\nu^2 M}{\varepsilon^\alpha + \Delta t \nu} \right\rangle_{N_v,V}} \\ \dfrac{g^{n+1} - g^n}{\Delta t} + & \mathcal{T}^n = -\dfrac{1}{\varepsilon^\alpha} \nu \left(g^{n+1} - \dfrac{\left\langle \nu g^{n+1} \right\rangle_{N_v,V}}{\langle \nu M \rangle_{N_v,V}} M \right) \\ \dfrac{\rho^{n+1} - \rho^n}{\Delta t} + & \mathcal{F}^{-1}\left(\mathcal{I} \hat{\rho}^{n+1/2} \right) + \mathcal{F}^{-1}\left(\mathcal{I} \dfrac{\langle \nu \hat{g}^{n+1} \rangle_{N_v,V}}{\langle \nu M \rangle_{N_v,V}} \right) \\ & + \varepsilon^{1-\alpha} \left\langle (1 - \lambda(v))\, v \cdot \nabla_x g^n \right\rangle_{N_v,V} = 0, \end{cases} \tag{2.3.19}$$

with $\mathcal{T}^n$ defined in (2.3.18)*, $\lambda(v) = \Delta t \nu(v)/(\varepsilon^\alpha + \Delta t \nu(v))$, where $\mathcal{F}^{-1}$ denotes the inverse Fourier transform in space and with the initial conditions $\rho^0(x) = \rho(0,x) = \langle f_0(x,v) \rangle_{N_v,V}$ and $g^0(x,v) = f_0(x,v) - \rho(0,x) M(v)$. The quantity $\hat{\rho}^{n+1/2}$ can be chosen equal to $\hat{\rho}^n$ or to $\hat{\rho}^{n+1}$ depending on the desired asymptotic scheme (explicit or implicit in time) and $\mathcal{I}$ is given by* (2.3.17)*. This scheme has the following properties:*

1. *The scheme is of order* 1 *for any fixed ε and preserves the total mass.*
2. *The scheme is AP: for a fixed Δt, it solves the anomalous diffusion equation when ε goes to zero*
$$\frac{\hat{\rho}^{n+1}(k) - \hat{\rho}^n(k)}{\Delta t} = -\bar{\kappa} |k|^\alpha \hat{\rho}^{n+1/2}(k),$$
where $\bar{\kappa}$ is defined by (2.3.6)*.*

Remark 2.6. Assuming that the space and velocity discretizations have been fixed, (ρ^n, g^n) are computed recursively with (2.3.19). The first line of the scheme enables to compute $\left\langle \nu g^{n+1} \right\rangle_{N_v,V}$ which is reported in the second and third lines to compute g^{n+1} and ρ^{n+1}.

As the term $\mathcal{I}$ defined in (2.3.17) has been precomputed to make the anomalous diffusion operator clearly appear, the velocity discretization is not a difficult issue anymore. Once it is defined, the integrals in v are computed with any quadrature method, such as rectangle formula. Finally, a standard upwind scheme is used to approximate the spatial derivative appearing in the term $\mathcal{T}^n$ defined in (2.3.18).

Remark 2.7. To guarantee the structure of the micro-macro model, it is important that the scheme satisfies $\left\langle g^{n+1} \right\rangle_{N_v,V} = 0$. To do that, g^{n+1} is modified consistently as $g^{n+1} \leftarrow g^{n+1} - \left\langle g^{n+1} \right\rangle_{N_v,V} M$.

Remark 2.8. As in the fully implicit scheme, we can go further by approximating consistently $\mathcal{I}$ given by (2.3.17) as

$$\mathcal{I} = \frac{\Delta t^2}{\Delta t^2 + \varepsilon^q (\Delta t + \varepsilon^q)} |k|^\alpha \bar{\kappa},$$

where $\bar{\kappa}$ is given by (2.3.6) and $q = d/(d + 1 + \beta)$. The so-obtained micro-macro based scheme still enjoys the same properties stated in the above proposition.

Proof. The proof of (i) is immediate from the derivation of the scheme, let us prove (ii). At first, we remark that $\mathcal{T}^n$ goes to 0 as $\varepsilon \to 0$, then the first line of (2.3.19) gives that $\left\langle \nu(v) g^{n+1} \right\rangle_{N_v,V}$

goes to 0 as $\varepsilon \to 0$ because $\langle g^n \rangle_{N_v} = 0$. After that, the second line of (2.3.19) implies that $g^{n+1} = o(1)$. When reported in the fourth line of (2.3.19), as $\varepsilon^{1-\alpha}(1-\lambda(v)) = O(\varepsilon)$, we get

$$\frac{\rho^{n+1}-\rho^n}{\Delta t} + \mathcal{F}^{-1}\left(\mathcal{I}\hat{\rho}^{n+1/2}\right) = o(1).$$

Finally, $\mathcal{I}$ is equivalent to $\bar{\kappa}|k|^\alpha$ for small ε, with $\bar{\kappa}$ given by (2.3.6). □

2.3.3 Scheme based on an integral formulation of the equation (2.1.5)

In the previous parts, we wrote two AP schemes solving (2.1.5). In this section, in the spirit of [17], we present a scheme based on an integral formulation of (2.1.5). However, the presence of the collision frequency ν requires specific developments to ensure the AP property. In particular, for general initial data, the strategy proposed in [17] leads to an AP scheme for ρ_ν instead of ρ (which are different if f is not at equilibrium). Then, the present section is decomposed into two parts: first, the case of equilibrium initial data is tackled, for which the scheme is proved to be uniformly accurate, and second the more delicate case of general initial data is studied, for which the scheme is proved to be AP.

Equilibrium initial data

We start from the Duhamel form for $\hat{f}$

$$\hat{f}(t,k,v) = \mathrm{e}^{-\frac{t}{\varepsilon^\alpha}(\nu+\mathrm{i}\varepsilon k\cdot v)}\hat{f}_0(k,v) + \nu M\int_0^{\frac{t}{\varepsilon^\alpha}} \mathrm{e}^{-s(\nu+\mathrm{i}\varepsilon k\cdot v)}\hat{\rho}_\nu(t-\varepsilon^\alpha s,k)\mathrm{d}s, \tag{2.3.20}$$

which we multiply by ν, integrate in v and evaluate at $t = t^{n+1}$ to get

$$K\hat{\rho}_\nu(t^{n+1},k) = \hat{A}_0(t^{n+1},k) + \int_0^{\frac{t^{n+1}}{\varepsilon^\alpha}} \left\langle \nu^2 M\mathrm{e}^{-s(\nu+\mathrm{i}\varepsilon k\cdot v)}\right\rangle_V \hat{\rho}_\nu(t^{n+1}-\varepsilon^\alpha s,k)\mathrm{d}s, \tag{2.3.21}$$

where

$$K = \langle \nu M\rangle_V, \text{ and } \hat{A}_0(t,k) = \left\langle \nu \mathrm{e}^{-\frac{t}{\varepsilon^\alpha}(\nu+\mathrm{i}\varepsilon k\cdot v)}\hat{f}_0(k,v)\right\rangle_V. \tag{2.3.22}$$

Then, we get

$$K\hat{\rho}_\nu(t_{n+1},k) = \sum_{j=0}^{n}\int_{\frac{t_j}{\varepsilon^\alpha}}^{\frac{t_{j+1}}{\varepsilon^\alpha}} \left\langle \nu^2 M\mathrm{e}^{-s(\nu+\mathrm{i}\varepsilon k\cdot v)}\right\rangle_V \hat{\rho}_\nu(t_{n+1}-\varepsilon^\alpha s,k)\mathrm{d}s + \hat{A}_0(t_{n+1},k), \tag{2.3.23}$$

where $\hat{A}_0$ and K are defined in (2.3.22). We perform a quadrature of order 2 in the integrals in s. Assuming that the time derivatives of $\hat{\rho}_\nu$ are uniformly bounded in ε, we have $\forall j \in [\![0, N-1]\!], \forall s \in \left[\frac{t_j}{\varepsilon^\alpha}, \frac{t_{j+1}}{\varepsilon^\alpha}\right]$,

$$\hat{\rho}_\nu(t_{n+1}-\varepsilon^\alpha s,k) = \left(1-\frac{\varepsilon^\alpha s - t_j}{\Delta t}\right)\hat{\rho}_\nu(t_{n+1-j},k) + \frac{\varepsilon^\alpha s - t_j}{\Delta t}\hat{\rho}_\nu(t_{n-j},k) + O\left(\Delta t^2\right). \tag{2.3.24}$$

Inserting this expression in the integral terms of (2.3.23) leads to

$$\int_{\frac{t_j}{\varepsilon^\alpha}}^{\frac{t_{j+1}}{\varepsilon^\alpha}} \left\langle \nu^2 M\mathrm{e}^{-s(\nu+\mathrm{i}\varepsilon k\cdot v)}\right\rangle_V \hat{\rho}_\nu(t_{n+1}-\varepsilon^\alpha s,k)\mathrm{d}s = c_j(\varepsilon,k)\hat{\rho}_\nu(t_{n+1}-t_j,k)$$

$$+ b_j(\varepsilon,k)\hat{\rho}_\nu(t_{n+1}-t_{j+1},k) + O(\Delta t^2), \tag{2.3.25}$$

where the remainder is bounded independently of ε and where we denoted

$$b_j(\varepsilon,k) = \int_{\frac{t_j}{\varepsilon^\alpha}}^{\frac{t_{j+1}}{\varepsilon^\alpha}} \frac{\varepsilon^\alpha s - t_j}{\Delta t} \left\langle \nu^2 M \mathrm{e}^{-s(\nu+\mathrm{i}\varepsilon k\cdot v)} \right\rangle_V \mathrm{d}s, \tag{2.3.26}$$

$$c_j(\varepsilon,k) = \int_{\frac{t_j}{\varepsilon^\alpha}}^{\frac{t_{j+1}}{\varepsilon^\alpha}} \left(1 - \frac{\varepsilon^\alpha s - t_j}{\Delta t}\right) \left\langle \nu^2 M \mathrm{e}^{-s(\nu+\mathrm{i}\varepsilon k\cdot v)} \right\rangle_V \mathrm{d}s. \tag{2.3.27}$$

Then, we use the quadrature (2.3.25) in (2.3.23) to write (using the obvious notations $b_j := b_j(\varepsilon,k)$) and $c_j := c_j(\varepsilon,k)$)

$$\hat{\rho}_\nu(t_{n+1},k) = \frac{1}{K}\sum_{j=0}^{n} \left[c_j\hat{\rho}_\nu(t_{n+1-j},k) + b_j\hat{\rho}_\nu(t_{n-j},k) + O(\Delta t^2)\right] + \frac{1}{K}\hat{A}_0(t_{n+1},k).$$

As $N\Delta t = T$, then $n\Delta t^2 \le T\Delta t$ and the last expression permits to write a first order scheme for $\hat{\rho}_\nu$ that writes

$$\hat{\rho}_\nu^{n+1}(k) = \frac{\hat{A}_0(t_{n+1},k) + \sum_{j=1}^{n}\left(c_j\hat{\rho}_\nu^{n+1-j}(k) + b_j\hat{\rho}_\nu^{n-j}(k)\right) + b_0\hat{\rho}_\nu^n(k)}{K - c_0}. \tag{2.3.28}$$

To ensure the AP property for this scheme, the discretization of the terms b_j and c_j is crucial: as in the previous cases, their limit as ε goes to zero makes the anomalous diffusion operator appear, but when computed numerically it does not arise because of the effects of the low velocities missed with the discretization. Indeed, we consider the velocity integration appearing in (2.3.26)-(2.3.27)

$$\left\langle \nu^2 M \mathrm{e}^{-s(\nu+\mathrm{i}\varepsilon k\cdot v)} \right\rangle_V = \left\langle \nu^2 M \left(\mathrm{e}^{-s(\nu+\mathrm{i}\varepsilon k\cdot v)} - \mathrm{e}^{-\nu(v)s}\right)\right\rangle_V + \left\langle \nu^2 M \mathrm{e}^{-\nu(v)s}\right\rangle_V. \tag{2.3.29}$$

At the continuous level, the first term in the right hand side gives the anomalous diffusion when ε goes to zero. Indeed, with M and ν defined by (2.1.2) and (2.1.3), the change of variables $w = \varepsilon|k|v/\nu$ in the integral in v reads

$$\begin{aligned}&\left\langle \nu^2 M \left(\mathrm{e}^{-s(\nu+\mathrm{i}\varepsilon k\cdot v)} - \mathrm{e}^{-\nu(v)s}\right)\right\rangle_V \\ &= \frac{\varepsilon^\alpha|k|^\alpha\nu_0^{1-\alpha}M_0}{d+1+\beta}\left\langle \varphi\frac{1}{|w|^{d+\alpha}}\left(\mathrm{e}^{-\varphi s(1+\mathrm{i}w\cdot e)} - \mathrm{e}^{-s\varphi}\right)\right\rangle_{|w|\ge\frac{\varepsilon|k|}{\nu_0}},\end{aligned} \tag{2.3.30}$$

with $\varphi = \nu_0\left(\frac{\varepsilon|k|}{\nu_0|w|}\right)^{\frac{d+2+\beta}{d+1+\beta}}$ and where e denotes any unitary vector. Here, the fractional diffusion limit clearly appears. We then inject (2.3.30) computed with discrete brackets $\langle\cdot\rangle_{N_v,|w_{\max}|\ge|w|\ge\varepsilon|k|/\nu_0}$ in (2.3.29) and eventually compute explicitly the integrals in s of (2.3.26)-(2.3.27) to get the following expression of b_j and c_j

$$\begin{aligned}b_j(\varepsilon,k) &= \frac{\varepsilon^\alpha}{\Delta t}\left\langle M\mathrm{e}^{-\frac{t_j}{\varepsilon^\alpha}\nu}\left(1-\mathrm{e}^{-\frac{\Delta t}{\varepsilon^\alpha}\nu}\right)\right\rangle_{N_v,V} - \left\langle \nu M\mathrm{e}^{-\frac{t_{j+1}}{\varepsilon^\alpha}\nu}\right\rangle_{N_v,V} \\ &+ \frac{\varepsilon^\alpha|k|^\alpha\nu_0^{1-\alpha}M_0}{d+1+\beta}\left\langle\frac{1}{|w|^{d+\alpha}}\left[\mathrm{e}^{-\frac{t_{j+1}}{\varepsilon^\alpha}\varphi} - \frac{\mathrm{e}^{-\frac{t_{j+1}}{\varepsilon^\alpha}\varphi(1+\mathrm{i}w\cdot e)}}{1+\mathrm{i}w\cdot e}\right.\right.\end{aligned} \tag{2.3.31}$$

$$
\begin{aligned}
&+\frac{\varepsilon^\alpha}{\Delta t}\left(\frac{\mathrm{e}^{-\frac{t_j}{\varepsilon^\alpha}\varphi(1+\mathrm{i}w\cdot e)}\left(1-\mathrm{e}^{-\frac{\Delta t}{\varepsilon^\alpha}\varphi(1+\mathrm{i}w\cdot e)}\right)}{\varphi(1+\mathrm{i}w\cdot e)^2}-\frac{\mathrm{e}^{-\frac{t_j}{\varepsilon^\alpha}\varphi}\left(1-\mathrm{e}^{-\frac{\Delta t}{\varepsilon^\alpha}\varphi}\right)}{\varphi}\right)\Bigg]\Bigg\rangle_{N_v,\mathcal{W}}\\
c_j(\varepsilon,k)&=\left\langle \nu M\mathrm{e}^{-\frac{t_j}{\varepsilon^\alpha}\nu}\right\rangle_{N_v,V}-\frac{\varepsilon^\alpha}{\Delta t}\left\langle M\mathrm{e}^{-\frac{t_j}{\varepsilon^\alpha}\nu}\left(1-\mathrm{e}^{-\frac{\Delta t}{\varepsilon^\alpha}\nu}\right)\right\rangle_{N_v,V}\\
&+\frac{\varepsilon^\alpha|k|^\alpha\nu_0^{1-\alpha}M_0}{d+1+\beta}\left\langle\frac{1}{|w|^{d+\alpha}}\left[\frac{\mathrm{e}^{-\frac{t_j}{\varepsilon^\alpha}\varphi(1+\mathrm{i}w\cdot e)}}{1+\mathrm{i}w\cdot e}-\mathrm{e}^{-\frac{t_j}{\varepsilon^\alpha}\varphi}\right.\right.\\
&-\frac{\varepsilon^\alpha}{\Delta t}\left(\frac{\mathrm{e}^{-\frac{t_j}{\varepsilon^\alpha}\varphi(1+\mathrm{i}w\cdot e)}\left(1-\mathrm{e}^{-\frac{\Delta t}{\varepsilon^\alpha}\varphi(1+\mathrm{i}w\cdot e)}\right)}{\varphi(1+\mathrm{i}w\cdot e)^2}-\frac{\mathrm{e}^{-\frac{t_j}{\varepsilon^\alpha}\varphi}\left(1-\mathrm{e}^{-\frac{\Delta t}{\varepsilon^\alpha}\varphi}\right)}{\varphi}\right)\Bigg]\Bigg\rangle_{N_v,\mathcal{W}},
\end{aligned}
\tag{2.3.32}
$$

with $\mathcal{W}=\left\{w\in\mathbb{R}^d,|w_{\max}|\geq|w|\geq\varepsilon|k|/\nu_0\right\}$. The so-obtained scheme (2.3.28) for $\hat\rho_\nu$ where b_j,c_j are given by (2.3.31)-(2.3.32) enables us to find a way to recover the distribution function $\hat f$ in Fourier variable. Indeed, with a Duhamel formulation of (2.1.5) integrated between t_n and t_{n+1} it is possible to write an expression for $\hat f(t_{n+1},k,v)$

$$
\hat f(t_{n+1},k,v)=\mathrm{e}^{-\frac{\Delta t}{\varepsilon^\alpha}(\nu+\mathrm{i}\varepsilon k\cdot v)}\hat f(t_n,k,v)+\int_0^{\frac{\Delta t}{\varepsilon^\alpha}}\mathrm{e}^{-s(\nu+\mathrm{i}\varepsilon k\cdot v)}\hat\rho_\nu(t_{n+1}-\varepsilon^\alpha s,k)\mathrm{d}s\;\nu M. \tag{2.3.33}
$$

Then, the quadrature (2.3.24) leads to

$$
\hat f(t_{n+1},k,v)=\mathrm{e}^{-\frac{\Delta t}{\varepsilon^\alpha}(\nu+\mathrm{i}\varepsilon k\cdot v)}\hat f(t_n,k,v)+\nu M\left(\gamma\hat\rho_\nu(t_{n+1},k)+\beta\hat\rho_\nu(t_n,k)\right)+O(\Delta t^2),
$$

where

$$
\gamma=\int_0^{\frac{\Delta t}{\varepsilon^\alpha}}\left(1-\frac{\varepsilon^\alpha s}{\Delta t}\right)\mathrm{e}^{-s(\nu+\mathrm{i}\varepsilon k\cdot v)}\mathrm{d}s,\quad \beta=\int_0^{\frac{\Delta t}{\varepsilon^\alpha}}\frac{\varepsilon^\alpha s}{\Delta t}\mathrm{e}^{-s(\nu+\mathrm{i}\varepsilon k\cdot v)}\mathrm{d}s. \tag{2.3.34}
$$

This provides a first order scheme for $\hat f$ using the values $\hat\rho_\nu^n$ determined with (2.3.28)

$$
\hat f^{n+1}=\mathrm{e}^{-\frac{\Delta t}{\varepsilon^\alpha}(\nu+\mathrm{i}\varepsilon k\cdot v)}\hat f^n+\nu M\left(\gamma\hat\rho_\nu^{n+1}+\beta\hat\rho_\nu^n\right),
$$

with the values of β and γ computed exactly to ensure the AP property of the scheme

$$
\gamma=\frac{1}{\nu+\mathrm{i}\varepsilon k\cdot v}-\frac{\varepsilon^\alpha}{\Delta t}\frac{1-\mathrm{e}^{-\frac{\Delta t}{\varepsilon^\alpha}(\nu+\mathrm{i}\varepsilon k\cdot v)}}{(\nu+\mathrm{i}\varepsilon k\cdot v)^2},\quad \beta=\frac{\varepsilon^\alpha}{\Delta t}\frac{1-\mathrm{e}^{-\frac{\Delta t}{\varepsilon^\alpha}(\nu+\mathrm{i}\varepsilon k\cdot v)}}{(\nu+\mathrm{i}\varepsilon k\cdot v)^2}-\frac{\mathrm{e}^{-\frac{\Delta t}{\varepsilon^\alpha}(\nu+\mathrm{i}\varepsilon k\cdot v)}}{\nu+\mathrm{i}\varepsilon k\cdot v}. \tag{2.3.35}
$$

A simple integration of $\hat f^{n+1}$ with $\langle\cdot\rangle_{N_v,V}$ gives an expression for $\hat\rho^{n+1}$. Eventually, we have the following proposition.

Proposition 2.9. *We consider the following scheme defined for all k and for all time index $0\leq n\leq N, N\Delta t=T$ by*

$$
\begin{cases}
\hat\rho_\nu^{n+1}(k)=\dfrac{\hat A_0(t_{n+1},k)+\sum_{j=1}^n\left(c_j\hat\rho_\nu^{n+1-j}(k)+b_j\hat\rho_\nu^{n-j}(k)\right)+b_0\hat\rho_\nu^n(k)}{K-c_0}\\[2ex]
\hat f^{n+1}=\mathrm{e}^{-\frac{\Delta t}{\varepsilon^\alpha}(\nu+\mathrm{i}\varepsilon k\cdot v)}\hat f^n+\nu M\left(\gamma\hat\rho_\nu^{n+1}+\beta\hat\rho_\nu^n\right),
\end{cases}
\tag{2.3.36}
$$

with $K,\hat A_0,b_j,c_j,\gamma$ and β defined in (2.3.22)-(2.3.31)-(2.3.32) *and* (2.3.35). *For an initial data $\hat f_0(k,v)$ at equilibrium, this scheme enjoys the following properties:*

1. *The scheme is first order in time and preserves the total mass.*

2. *The scheme is AP: for a fixed Δt, it solves the anomalous diffusion equation when ε goes to zero*
$$\frac{\hat\rho^{n+1}(k)-\hat\rho^n(k)}{\Delta t} = -\bar\kappa|k|^\alpha\hat\rho^{n+1}(k),$$
where $\hat\rho^n = \left\langle \hat f^n\right\rangle_{Nv,V}$ and $\bar\kappa$ is defined by (2.3.6).

3. *Moreover, the semi-discrete-in-time scheme enjoys the UA property: it is first order uniformly in ε*
$$\exists C>0,\ \sup_{\varepsilon\in(0,1]} \|\hat f^N(\cdot,\cdot)-\hat f(T,\cdot,\cdot)\|_{L^\infty_{k,v}} \le C\Delta t.$$

Remark 2.10. The numerical tests (see Fig. 2.3) suggests that this scheme is of order 2 for a fixed value of ε and of order 1 uniformly in ε.

Proof. For the mass conservation (i), we integrate (at the discrete level) with respect to v the second equation of (2.3.36) and evaluate it at $k=0$. For an initial data at equilibrium, we have $\hat\rho^0_\nu(k=0)=\hat\rho^0(k=0)$ so that

$$\hat\rho^1 = \left\langle e^{-\Delta t/\varepsilon^\alpha\nu}M\right\rangle_{N_v,V}\hat\rho^0 + \langle\nu M\gamma\rangle_{N_v,V}\hat\rho^1_\nu + \langle\nu M\beta\rangle_{N_v,V}\hat\rho^0_\nu,\ \text{ for } k=0.$$

From the first equation of (2.3.36), we easily get $\hat\rho^1_\nu(k=0)=\hat\rho^0(k=0)$ so that the previous equation leads to $\hat\rho^1(k=0)=\hat\rho^0(k=0)$. The mass conservation is deduced by induction, assuming that $\hat\rho^\ell_\nu(k=0)=\hat\rho^\ell(k=0)$ for $\ell=0,\dots,n$.

For the AP character (ii), let us remark that with (2.3.31) and (2.3.32), the formula for $\hat\rho_\nu$ in (2.3.36) degenerates into

$$\frac{\hat\rho^{n+1}_\nu(k)-\hat\rho^n_\nu(k)}{\Delta t} = -\bar\kappa|k|^\alpha\hat\rho^{n+1}_\nu(k).$$

Moreover, the second line of (2.3.36) gives $\hat f^{n+1}=\hat\rho^{n+1}_\nu M(v)$ for $n\ge 0$ when $\varepsilon\to 0$, that implies $\hat\rho^{n+1}=\hat\rho^{n+1}_\nu$ for small ε. As the initial condition is at equilibrium, we also have $\hat\rho^0=\hat\rho^0_\nu$. Eventually, when $\varepsilon\to 0$, (2.3.36) degenerates into

$$\frac{\hat\rho^{n+1}(k)-\hat\rho^n(k)}{\Delta t} = -\bar\kappa|k|^\alpha\hat\rho^{n+1}(k),$$

for all $n\le N$, which proves the AP property.

Now, let us prove that the semi-discrete (in time) scheme is first order accurate uniformly in ε (iii). Using the notations (2.3.31)-(2.3.32), (2.3.23) writes

$$\hat\rho_\nu(t_{n+1},k) = \frac{1}{K}\hat A_0(t_{n+1},k) + \frac{1}{K}\sum_{j=0}^n c_j\hat\rho_\nu(t_{n+1-j},k) + b_j\hat\rho_\nu(t_{n-j},k) + \frac{\Delta t^2}{K}F, \tag{2.3.37}$$

where the remainder F is given by

$$F = -\frac12\sum_{j=0}^n \int_{\frac{t_j}{\varepsilon^\alpha}}^{\frac{t_{j+1}}{\varepsilon^\alpha}} \left(\left(1-\frac{\varepsilon^\alpha s-t_j}{\Delta t}\right)\left(\frac{\varepsilon^\alpha s-t_j}{\Delta t}\right)^2 \partial_t^2\hat\rho_\nu(t_{n+1}-\varepsilon^\alpha\xi_1(s),k)\right. \tag{2.3.38}$$

$$+\frac{\varepsilon^\alpha s - t_j}{\Delta t}\left(\frac{t_{j+1}-\varepsilon^\alpha s}{\Delta t}\right)^2 \partial_t^2\hat\rho_\nu(t_{n+1}-\varepsilon^\alpha\xi_2(s),k)\Big)\left\langle \nu^2 M \mathrm{e}^{-s(\nu+\mathrm{i}\varepsilon k\cdot v)}\right\rangle_V \mathrm{d}s,$$

with $\xi_1(s),\xi_2(s)\in(0,\Delta t/\varepsilon^\alpha)$. As $1\geq\left(1-\frac{\varepsilon^\alpha s-t_j}{\Delta t}\right)\geq 0$ and $1\geq\frac{\varepsilon^\alpha s-t_j}{\Delta t}\geq 0$ for $s\in\left[\frac{t_j}{\varepsilon^\alpha},\frac{t_{j+1}}{\varepsilon^\alpha}\right]$, we have

$$\begin{aligned}|F| &\leq \frac{\|\partial_t^2\hat\rho_\nu\|_\infty}{2}\sum_{j=0}^n\int_{\frac{t_j}{\varepsilon^\alpha}}^{\frac{t_{j+1}}{\varepsilon^\alpha}}\left(\left(1-\frac{\varepsilon^\alpha s-t_j}{\Delta t}\right)\left(\frac{\varepsilon^\alpha s-t_j}{\Delta t}\right)^2\right.\\ &\quad\left.+\frac{\varepsilon^\alpha s-t_j}{\Delta t}\left(\frac{t_{j+1}-\varepsilon^\alpha s}{\Delta t}\right)^2\right)\left\langle\nu^2 M\mathrm{e}^{-s\nu}\right\rangle_V\mathrm{d}s\\ &\leq \frac{\|\partial_t^2\hat\rho_\nu\|_\infty}{2}\sum_{j=0}^n\int_{\frac{t_j}{\varepsilon^\alpha}}^{\frac{t_{j+1}}{\varepsilon^\alpha}}\left(\frac{\varepsilon^\alpha s-t_j}{\Delta t}\right)\left\langle\nu^2 M\mathrm{e}^{-s\nu}\right\rangle_V\mathrm{d}s. \end{aligned}\tag{2.3.39}$$

Now, let us denote $E_n=\hat\rho_\nu(t_n,k)-\hat\rho_\nu^n(k)$ and suppose that $E_0=0$. From (2.3.28) and (2.3.37) we have

$$\left(1-\frac{c_0}{K}\right)E_{n+1}=\frac{b_0}{K}E_n+\frac{1}{K}\sum_{j=1}^n(c_jE_{n+1-j}+b_jE_{n-j})+\frac{\Delta t^2}{K}F.\tag{2.3.40}$$

In the sequel, to get an estimate for E_{n+1}, we will need two different bounds for $(1-\frac{c_0}{K})^{-1}=K/(K-c_0)$. From the definition (2.3.27) of c_0, we directly get

$$|c_0|\leq\int_0^{\frac{\Delta t}{\varepsilon^\alpha}}\left(1-\frac{\varepsilon^\alpha s}{\Delta t}\right)\left\langle\nu^2M\mathrm{e}^{-s\nu}\right\rangle_V\mathrm{d}s$$

from which we deduce the first estimate for $|K/(K-c_0)|$

$$\left|\frac{K}{K-c_0}\right|\leq\frac{K}{\langle\nu M\rangle_V-\int_0^{\frac{\Delta t}{\varepsilon^\alpha}}\left(1-\frac{\varepsilon^\alpha s}{\Delta t}\right)\left\langle\nu^2M\mathrm{e}^{-s\nu}\right\rangle_V\mathrm{d}s}.\tag{2.3.41}$$

Now, using $0\leq 1-\frac{\varepsilon^\alpha s}{\Delta t}\leq 1$ for $s\in\left[0,\frac{\Delta t}{\varepsilon^\alpha}\right]$, we get

$$|c_0|\leq\left\langle\nu^2M\int_0^{\frac{\Delta t}{\varepsilon^\alpha}}\mathrm{e}^{-s\nu}\mathrm{d}s\right\rangle_V\leq K-\left\langle\nu M\mathrm{e}^{-\frac{\Delta t}{\varepsilon^\alpha}\nu}\right\rangle_V$$

so that we deduce the second estimate for $|K/(K-c_0)|$

$$\left|\frac{K}{K-c_0}\right|\leq K\left\langle\nu M\mathrm{e}^{-\frac{\Delta t}{\varepsilon^\alpha}\nu}\right\rangle_V^{-1}.\tag{2.3.42}$$

In (2.3.40) let us focus on the term containing F. From (2.3.39), we have

$$\left|\frac{\frac{1}{K}F}{1-\frac{c_0}{K}}\right|=\left|\frac{F}{K-c_0}\right|\leq\frac{\|\partial_t^2\hat\rho_\nu\|_\infty}{2}\frac{\displaystyle\int_0^{\frac{\Delta t}{\varepsilon^\alpha}}\left(\frac{\varepsilon^\alpha s}{\Delta t}\right)\left\langle\nu^2M\mathrm{e}^{-s\nu}\right\rangle_V\mathrm{d}s}{|K-c_0|}$$

$$+\frac{\|\partial_t^2\hat{\rho}_\nu\|_\infty}{2}\frac{\displaystyle\sum_{j=1}^{n}\int_{\frac{t_j}{\varepsilon^\alpha}}^{\frac{t_{j+1}}{\varepsilon^\alpha}}\left(\frac{\varepsilon^\alpha s-t_j}{\Delta t}\right)\left\langle\nu^2 M\mathrm{e}^{-s\nu}\right\rangle_V \mathrm{d}s}{|K-c_0|}, \tag{2.3.43}$$
$$=:\frac{\|\partial_t^2\hat{\rho}_\nu\|_\infty}{2}(T_1+T_2).$$

To find an estimate for T_1, we use (2.3.41) to write

$$T_1\le\frac{\displaystyle\int_0^{\frac{\Delta t}{\varepsilon^\alpha}}\left\langle\nu^2 M\mathrm{e}^{-s\nu(v)}\right\rangle_V \mathrm{d}s-\int_0^{\frac{\Delta t}{\varepsilon^\alpha}}\left(1-\frac{\varepsilon^\alpha s}{\Delta t}\right)\left\langle\nu^2 M\mathrm{e}^{-s\nu}\right\rangle_V \mathrm{d}s}{K-\displaystyle\int_0^{\frac{\Delta t}{\varepsilon^\alpha}}\left(1-\frac{\varepsilon^\alpha s}{\Delta t}\right)\left\langle\nu^2 M\mathrm{e}^{-s\nu}\right\rangle_V \mathrm{d}s}, \tag{2.3.44}$$

that implies that the first line of (2.3.43) is bounded by $\|\partial_t^2\hat{\rho}_\nu\|_\infty/2$. Now, using (2.3.42), T_2 can be estimated as

$$T_2\le\int_{\frac{\Delta t}{\varepsilon^\alpha}}^{\frac{t_{n+1}}{\varepsilon^\alpha}}\left\langle\nu^2 M\mathrm{e}^{-s\nu}\right\rangle_V \mathrm{d}s\,|K-c_0|^{-1}\le 1. \tag{2.3.45}$$

Eventually, (2.3.44) and (2.3.45) give

$$\left|\frac{F}{K-c_0}\right|\le\|\partial_t^2\hat{\rho}_\nu\|_\infty. \tag{2.3.46}$$

Now, for the other terms in (2.3.40), we introduce $\mathcal{E}_n=\max\limits_{\substack{j=0\cdots n\\ \varepsilon\in(0,1]}}|E_j|$. From the definition (2.3.31) and (2.3.32), we have for the first two terms of the right hand side of (2.3.40)

$$\begin{aligned}
&\frac{1}{K}\left|b_0E_n+\sum_{j=1}^{n}(c_jE_{n+1-j}+b_jE_{n-j})\right|\\
&\le\frac{1}{K}\int_0^{\frac{\Delta t}{\varepsilon^\alpha}}\frac{\varepsilon^\alpha s}{\Delta t}\left|\left\langle\nu^2 M\mathrm{e}^{-s(\nu+\mathrm{i}\varepsilon k\cdot v)}\right\rangle_V E_n\right|\mathrm{d}s\\
&+\sum_{j=1}^{n}\left(\int_{\frac{t_j}{\varepsilon^\alpha}}^{\frac{t_{j+1}}{\varepsilon^\alpha}}\left(1-\frac{\varepsilon^\alpha s-t_j}{\Delta t}\right)\left|\left\langle\nu^2 M\mathrm{e}^{-s(\nu+\mathrm{i}\varepsilon k\cdot v)}\right\rangle_V E_{n+1-j}\right|\mathrm{d}s\right.\\
&\left.+\int_{\frac{t_j}{\varepsilon^\alpha}}^{\frac{t_{j+1}}{\varepsilon^\alpha}}\frac{\varepsilon^\alpha s-t_j}{\Delta t}\left|\left\langle\nu^2 M\mathrm{e}^{-s(\nu+\mathrm{i}\varepsilon k\cdot v)}\right\rangle_V E_{n-j}\right|\mathrm{d}s\right)\\
&\le\frac{1}{K}\left(K-\int_0^{\frac{\Delta t}{\varepsilon^\alpha}}\left(1-\frac{\varepsilon^\alpha s}{\Delta t}\right)\left\langle\nu^2 M\mathrm{e}^{-\nu s}\right\rangle_V \mathrm{d}s\right)\mathcal{E}_n.
\end{aligned}$$

Hence, using (2.3.41), we get

$$|b_0E_n+\sum_{j=1}^{n}(c_jE_{n+1-j}+b_jE_{n-j})|\;\;|K-c_0|^{-1}\le\mathcal{E}_n. \tag{2.3.47}$$

Eventually (2.3.40) gives, using (2.3.46) and (2.3.47), $E_{n+1} \leq \mathcal{E}_n + \|\partial_t^2 \hat{\rho}_\nu\|_\infty \Delta t^2$. Hence $\mathcal{E}_{n+1} \leq \mathcal{E}_n + \|\partial_t^2 \hat{\rho}_\nu\|_\infty \Delta t^2$. As we supposed $\mathcal{E}_0 = 0$, it writes

$$\mathcal{E}_{n+1} \leq \|\partial_t^2 \hat{\rho}_\nu\|_\infty T \Delta t, \tag{2.3.48}$$

where $T = N\Delta t$ is the final time. This proves that the scheme in $\hat{\rho}_\nu$ is first order accurate uniformly in ε.

Now, to prove that the scheme in $\hat{f}$ is first order uniformly in ε we consider the Duhamel formulation for $\hat{f}$

$$\hat{f}(t_{n+1}, k, v) = \mathrm{e}^{-\frac{\Delta t}{\varepsilon^\alpha}(\nu + \mathrm{i}\varepsilon k\cdot v)} \hat{f}(t_n, k, v) + \nu M \int_0^{\frac{\Delta t}{\varepsilon^\alpha}} \mathrm{e}^{-s(\nu+\mathrm{i}\varepsilon k\cdot v)} \hat{\rho}_\nu(t_{n+1} - \varepsilon^\alpha s, k) \mathrm{d}s,$$

and with the same Taylor expansion as previously, we have

$$\hat{f}(t_{n+1}, k, v) = \nu M \left(\gamma \hat{\rho}_\nu(t_{n+1}, k) + \beta \hat{\rho}_\nu(t_n, k)\right) + \nu M \Delta t^2 G + \mathrm{e}^{-\frac{\Delta t}{\varepsilon^\alpha}(\nu+\mathrm{i}\varepsilon k\cdot v)} \hat{f}(t_n, k, v),$$

with β and γ defined in (2.3.34) and

$$\begin{aligned} G = -\frac{1}{2} \int_0^{\frac{\Delta t}{\varepsilon^\alpha}} \Bigg[& \left(1 - \frac{\varepsilon^\alpha s}{\Delta t}\right) \left(\frac{\varepsilon^\alpha s}{\Delta t}\right)^2 \partial_t^2 \hat{\rho}_\nu(t_{n+1} - \varepsilon^\alpha \xi_1(s), k) \\ & + \left(\frac{\varepsilon^\alpha s}{\Delta t}\right) \left(1 - \frac{\varepsilon^\alpha s}{\Delta t}\right)^2 \partial_t^2 \hat{\rho}_\nu(t_{n+1} - \varepsilon^\alpha \xi_2(s), k) \Bigg] \mathrm{e}^{-s(\nu+\mathrm{i}\varepsilon k\cdot v)} \mathrm{d}s, \end{aligned} \tag{2.3.49}$$

where $\xi_1(s), \xi_2(s) \in (0, \Delta t/\varepsilon^\alpha)$. As previously, we can estimate $|\nu MG|$

$$\begin{aligned} |\nu\ MG| &\leq \nu M \frac{\|\partial_t^2 \hat{\rho}_\nu\|_\infty}{2} \int_0^{\frac{\Delta t}{\varepsilon^\alpha}} \Bigg[\left(1 - \frac{\varepsilon^\alpha s - t_j}{\Delta t}\right) \left(\frac{\varepsilon^\alpha s - t_j}{\Delta t}\right)^2 \\ &\quad + \frac{\varepsilon^\alpha s - t_j}{\Delta t} \left(\frac{\varepsilon^\alpha s - t_{j+1}}{\Delta t}\right)^2 \Bigg] \left|\mathrm{e}^{-s(\nu+\mathrm{i}\varepsilon k\cdot v)}\right| \mathrm{d}s \\ &\leq \nu M \frac{\|\partial_t^2 \hat{\rho}_\nu\|_\infty}{2} \int_0^{\frac{\Delta t}{\varepsilon^\alpha}} \mathrm{e}^{-s\nu} \mathrm{d}s \leq C \left(1 - \mathrm{e}^{-\frac{\Delta t}{\varepsilon^\alpha}\nu}\right). \end{aligned}$$

One can now look at the truncation error $E_n^f = \hat{f}(t_n, k, v) - \hat{f}^n(k, v)$ which satisfies

$$E_{n+1}^f = \mathrm{e}^{-\frac{\Delta t}{\varepsilon^\alpha}(\nu+\mathrm{i}\varepsilon k\cdot v)} E_n^f + \nu M \left(\gamma E_{n+1} + \beta E_n\right) + \nu M \Delta t^2 G. \tag{2.3.50}$$

The term $\nu M(\gamma E_{n+1} + \beta E_n)$ can be estimated by (using definition (2.3.34))

$$\left|\nu M(\gamma E^{n+1} + \beta E^n)\right| \leq \nu M \int_0^{\frac{\Delta t}{\varepsilon^\alpha}} \mathrm{e}^{-s\nu} \mathrm{d}s\ \mathcal{E}_{n+1} \leq C \left(1 - \mathrm{e}^{-\frac{\Delta t}{\varepsilon^\alpha}\nu}\right) \Delta t,$$

where we used (2.3.48) for the last inequality. Hence, denoting $\Lambda_n = \max_{v\neq 0, k, \varepsilon \in (0,1]} |E_n^f|$ we get from (2.3.50): $\Lambda_{n+1} \leq \mathrm{e}^{-\frac{\Delta t}{\varepsilon^\alpha}\nu} \Lambda_n + C \left(1 - \mathrm{e}^{-\frac{\Delta t}{\varepsilon^\alpha}\nu}\right) \left(\Delta t^2 + \Delta t\right)$. With $\Lambda_0 = 0$, it finally comes that

$$\Lambda_{n+1} \leq C \left(1 - \mathrm{e}^{-\frac{\Delta t}{\varepsilon^\alpha}\nu}\right) \left(\Delta t + \Delta t^2\right) \sum_{j=0}^{n} \mathrm{e}^{-j\frac{\Delta t}{\varepsilon^\alpha}\nu} \leq C \Delta t.$$

□

General initial data

In the previous subsection, we observed that the asymptotic scheme of (2.3.36) as $\varepsilon \to 0$ writes

$$\frac{\hat{\rho}_\nu^{n+1}(k) - \hat{\rho}_\nu^n(k)}{\Delta t} = -\bar{\kappa}|k|^\alpha \hat{\rho}_\nu^{n+1}(k), \forall n \geq 0,$$

and moreover, we have $\hat{\rho}^{n+1} = \hat{\rho}_\nu^{n+1}$ for all $n \geq 0$. But, for general initial data, since $\hat{\rho}_\nu^0$ is different from $\hat{\rho}^0$, the asymptotic scheme is not the correct one because of this initial mismatch. Then when the initial data is not at equilibrium, the previous scheme is not AP and a suitable modification has to be done to recover the AP property. To do so, we modify (2.3.36) to ensure that the first step of the asymptotic scheme writes (when $\varepsilon \to 0$)

$$\frac{\hat{\rho}_\nu^1(k) - \hat{\rho}^0(k)}{\Delta t} = -\bar{\kappa}|k|^\alpha \hat{\rho}_\nu^1.$$

Hence, we have to find an expression for the term $\hat{\rho}_\nu^0$ appearing in the first equation of (2.3.36) for $n = 0$. Starting from (2.3.33) for $n = 0$, we get, up to first order

$$\hat{\rho}^1(k) = \left\langle \mathrm{e}^{-\frac{\Delta t}{\varepsilon^\alpha}(\nu + \mathrm{i}\varepsilon k\cdot v)} \hat{f}^0 \right\rangle_{N_v,V} + d\hat{\rho}_\nu^0(k),$$

where d is given by

$$d = \left\langle \frac{1 - \mathrm{e}^{-\frac{\Delta t}{\varepsilon^\alpha}(\nu + \mathrm{i}\varepsilon k\cdot v)}}{\nu + \mathrm{i}\varepsilon k \cdot v} \nu M \right\rangle_{N_v,V}. \tag{2.3.51}$$

Up to an error of order Δt, it is possible to replace $\hat{\rho}^1$ by $\hat{\rho}^0$ so that $\hat{\rho}_\nu^0$ becomes

$$\hat{\rho}_\nu^0 = \frac{1}{d}\left(\hat{\rho}^0 - \left\langle \mathrm{e}^{-\frac{\Delta t}{\varepsilon^\alpha}(\nu + \mathrm{i}\varepsilon k\cdot v)} \hat{f}^0 \right\rangle_{N_v,V}\right). \tag{2.3.52}$$

This expression is injected in (2.3.36) for $n = 0$ to compute $\hat{\rho}_\nu^1$. Then, for any ε, (2.3.52) is a consistent approximation and when ε goes to zero, $\hat{\rho}_\nu^0$ tends to $\hat{\rho}^0$ which ensures the AP property for any initial data.

Another defect in the previous scheme (2.3.36) is that, for a general initial data, it does not preserve the total mass. To overcome this, we add the following consistent step for $\hat{f}^{n+1}$

$$\hat{f}^{n+1}(k=0) \leftarrow \hat{f}^{n+1}(k=0) - \left\langle \hat{f}^{n+1}(k=0) \right\rangle_{N_v,V} M + \left\langle \hat{f}^0(k=0) \right\rangle_{N_v,V} M. \tag{2.3.53}$$

Eventually, for a general initial condition, we have the following proposition

Proposition 2.11. *We consider the scheme defined for all k and all time indices $1 \leq n \leq N, n\Delta t = T$ by* (2.3.36)-(2.3.53) *and for the first step by*

$$\begin{cases} \hat{\rho}_\nu^1(k) = \dfrac{1}{K - c_0}\left[\hat{A}_0(t_1,k) + \dfrac{b_0}{d}\left(\hat{\rho}^0 - \left\langle \mathrm{e}^{-\frac{\Delta t}{\varepsilon^\alpha}(\nu + \mathrm{i}\varepsilon k\cdot v)} \hat{f}^0 \right\rangle_{N_v,V}\right)\right] \\ \hat{f}^1(k,v) = \mathrm{e}^{-\frac{\Delta t}{\varepsilon^\alpha}(\nu + \mathrm{i}\varepsilon k\cdot v)} \hat{f}^0(k,v) + \nu M\left(\gamma\hat{\rho}_\nu^1(k) + \beta\hat{\rho}_\nu^0(k)\right) \\ \hat{f}^1(0,v) := \hat{f}^1(0,v) - \left\langle \hat{f}^1(0,v) \right\rangle_{N_v,V} M + \left\langle \hat{f}^0(0,v) \right\rangle_{N_v,V} M, \end{cases} \tag{2.3.54}$$

with $K, \hat{A}_0, b_0, c_0, \gamma, \beta$ and d defined in (2.3.22)-(2.3.31)-(2.3.32)-(2.3.35) *and* (2.3.51). *This scheme has the following properties:*

1. *The scheme is first order in time and preserves the total mass.*

2. *The scheme is AP: for a fixed Δt, the scheme solves the anomalous diffusion equation when ε goes to* 0
$$\frac{\hat\rho^{n+1}(k)-\hat\rho^n(k)}{\Delta t} = -\bar\kappa|k|^\alpha\hat\rho^{n+1}(k),$$
where $\bar\kappa$ is defined in (2.3.6).

Remark 2.12. for a general initial data, the time derivatives at $t=0$ are not bounded uniformly in ε. Hence, the uniform accuracy of the scheme is not a relevant property to be considered. However, the numerical tests tends to suggest that the consistency error is of order Δt uniformly in ε.

Proof. To prove that the scheme is first order in time, we have to show that when ε is fixed
$$\|\hat\rho_\nu(t_1,\cdot)-\hat\rho^1_\nu(\cdot)\|_\infty \le C_\varepsilon\Delta t,$$
where C_ε is a constant when ε is fixed. We will then be able to use the proof of Prop. 2.9. At the continuous level, (2.3.33) gives
$$\hat\rho(t_1,k) = \left\langle \mathrm{e}^{-\frac{\Delta t}{\varepsilon^\alpha}(\nu+\mathrm{i}\varepsilon k\cdot v)}\hat f_0(k,v)\right\rangle_V + \int_0^{\frac{\Delta t}{\varepsilon^\alpha}}\left\langle \nu M\mathrm{e}^{-s(\nu+\mathrm{i}\varepsilon k\cdot v)}\right\rangle_V\hat\rho_\nu(t_1-\varepsilon^\alpha s,k)\mathrm{d}s.$$
Denoting by $G(s)=\int_0^{t_1-\varepsilon^\alpha s}\partial_t\hat\rho_\nu(u)\mathrm{d}u$ and $H=-\int_0^{\Delta t}\partial_t\hat\rho(u)\mathrm{d}u$ the remainders of the Taylor expansions of $\hat\rho_\nu(t_1-\varepsilon^\alpha s,k)$ and $\hat\rho(t_1,k)$, we have
$$\begin{aligned}\hat\rho(t_0,k) = &\left\langle \mathrm{e}^{-\frac{\Delta t}{\varepsilon^\alpha}(\nu+\mathrm{i}\varepsilon k\cdot v)}\hat f_0(k,v)\right\rangle_V + d\hat\rho_\nu(t_0,k)+H\\ &+\int_0^{\frac{\Delta t}{\varepsilon^\alpha}}\left\langle \nu M\mathrm{e}^{-s(\nu+\mathrm{i}\varepsilon k\cdot v)}\right\rangle_V G(s)\mathrm{d}s,\end{aligned}$$
with d defined in (2.3.51). Hence, the error made by replacing $\hat\rho_\nu(t_0,k)$ by its approximation (2.3.52) in the first iteration of (2.3.36) is of magnitude
$$\frac{1}{d}\left(H+\int_0^{\frac{\Delta t}{\varepsilon^\alpha}}\left\langle \nu M\mathrm{e}^{-s(\nu+\mathrm{i}\varepsilon k\cdot v)}\right\rangle_V G(s)\mathrm{d}s\right).$$
Eventually, the error done in the first iteration of (2.3.54) writes
$$\begin{aligned}\|\hat\rho_\nu(t_1,\cdot)-\hat\rho^1_\nu(\cdot)\|_\infty \le &\left|\frac{1}{d}\frac{b_0}{K-c_0}\left(H+\int_0^{\frac{\Delta t}{\varepsilon^\alpha}}\left\langle \nu M\mathrm{e}^{-s(\nu+\mathrm{i}\varepsilon k\cdot v)}\right\rangle_V G(s)\mathrm{d}s\right)\right| \\ &+\left|\frac{F}{K-c_0}\right|\Delta t^2,\end{aligned} \tag{2.3.55}$$
with K, b_0, c_0 defined in (2.3.22)-(2.3.26)-(2.3.27) and F in (2.3.38) for $n=0$. The proof of Prop. 2.9 gives estimates for $1/(K-c_0)$ and $F/(K-c_0)$ in (2.3.42) and (2.3.46). Moreover, since
$$|b_0| \le \left|\int_0^{\frac{\Delta t}{\varepsilon^\alpha}}\left\langle \nu^2 M\mathrm{e}^{-s(\nu+\mathrm{i}\varepsilon k\cdot v)}\right\rangle_V\mathrm{d}s\right|,$$

an exact computation of this integral shows that when ε is fixed, the term b_0/d is bounded. Assuming that the time derivatives of $\hat{\rho}$ and $\hat{\rho}_\nu$ are bounded, there exists a constant C_ε depending *a priori* of ε such that $\|\hat{\rho}_\nu(t_1,\cdot) - \hat{\rho}^1_\nu(\cdot)\|_\infty \leq C_\varepsilon \Delta t$. The proof of Prop. 2.9 can then be used to show that the scheme is of order 1.

To show that (2.3.54) enjoys the AP property, we freeze Δt and let ε go to 0 in the expression of the scheme. The first iteration degenerates into

$$\frac{\hat{\rho}^1_\nu(k) - \hat{\rho}^0(k)}{\Delta t} = -\bar{\kappa}|k|^\alpha \hat{\rho}^1_\nu(k), \quad \hat{\rho}^1(k,v) = \hat{\rho}^1_\nu(k) M,$$

then, when ε goes to zero $\hat{\rho}^1(k) = \hat{\rho}^1_\nu(k)$ which ensures that the first iteration of the scheme enjoys the AP property. As the following iterations are the same as in Prop. 2.9, this proves (ii). □

2.4 Numerical results

In this section, we present some numerical tests to validate the three schemes we proposed in Section 2.3. For simplicity, we denote by IS the the implicit scheme, MMS the micro-macro scheme and DS the scheme based on the Duhamel formulation of the kinetic equation. Eventually, the implicit Euler scheme for the anomalous diffusion equation (2.3.8) is denoted adiff. We use the equilibrium (2.1.2), the collision frequency (2.1.3) and the initial data

$$f_0(x,v) = (1 + \sin(\pi x)) M_0, \tag{2.4.1}$$

for $x \in [-1,1]$ and $v \in V = [-1,1]$ and $w_{\max} = 1$ for the computation of the terms in $\langle\cdot\rangle_{N_v,w}$ of the schemes. The normalization constant M_0 is chosen such that $\langle M\rangle_{N_v,V} = 1$ and ν_0 is fixed $\nu_0 = 1$. We consider periodic conditions for the space, then the discretization used for the space variable uses $N_x + 1$ points and is given by

$$x_i = -1 + i\Delta x, \quad 0 \leq i \leq N_x, \tag{2.4.2}$$

where $\Delta x = \frac{2}{N_x}$. This space discretization is linked to the Fourier modes we use for the discrete Fourier transform in the numerical computations, that are the integers k such that $-N_x/2 \leq k \leq N_x/2$. The uniform discretization of the velocities is done with $N_v = 2N_v'$ points symmetrically distributed to ensure that the property $\langle vM\rangle_{N_v,V} = 0$ is conserved at the discrete level. Denoting $\Delta v = 1/N_v'$, we set

$$v_j = -1 + \frac{\Delta v}{2} + j\Delta v, \quad 0 \leq j \leq 2N_v' - 1. \tag{2.4.3}$$

Since the schemes do not require a refined velocity grid to enjoy the AP property, we fix $N_v' = 10$ in all the following tests. All the tests are performed using a final time $T = 1$ and $\beta = 1$, the time step Δt being specified in each case.

2.4.1 The implicit scheme (IS)

In this part, we test the properties of the IS scheme. To highlight its AP character, we present in the left hand side of Fig. 2.1 the densities $\rho(T,x)$ obtained by IS for $\Delta t = 10^{-1}$, $N_x = 32$ and a range of ε. For this figure, we compare our results to the anomalous diffusion limit given by the adiff scheme with the same time step. It appears that the densities converge slowly

to the anomalous diffusion limit when ε goes to 0. In the right part of Fig. 2.1, we plot the L^∞ norm (in space) of the error between $\rho(T,x)$ given by IS and $\rho_{\text{adiff}}(T,x)$ given by adiff as a function of ε (in log scale). Then, we can compare our numerical results to the rate of convergence computed in Prop. 2.2. We observe that the numerical rate 0.334 is in a very good agreement with the theoretical rate $d/(d+1+\beta) \approx 0.333$. Let us remark that we showed in Prop. 2.2 that theoretically, the convergence happens rather with rate $\varepsilon^{\min\left(\frac{d}{d+1+\beta}, \frac{\beta}{d+1+\beta}\right)}$, but the terms (2.5.1)-(2.5.2) giving the $O(\varepsilon^{\frac{\beta}{d+1+\beta}})$ do not arise numerically. Indeed, it is given by a divergent integral multiplied by a power of ε. As we use a bounded domain for v and we did not apply a specific treatment for these terms, this divergent integral is numerically finite and then it vanishes when ε becomes small.

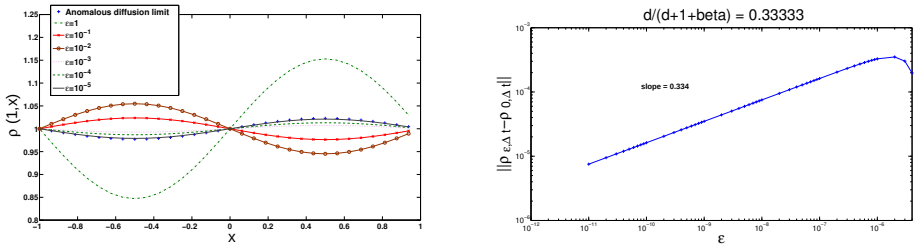

Figure 2.1: Left: For $\Delta t = 10^{-1}$, the densities given by IS for a range of ε and by adiff. Right: For $\Delta t = 10^{-1}$, the error between the densities given by IS and by adiff as a function of ε (log scale).

2.4.2 Micro-macro based scheme (MMS)

In this part, we test the properties of MMS. In the left hand side of Fig. 2.2 we present the densities $\rho(T,x)$ obtained with the MMS scheme for a range of ε and we compare it to the anomalous diffusion limit given by adiff. We used $N_x = 32$ points to discretize the space. We use Fourier variable for the equation on ρ (macro part), but the space derivatives of the micro part are discretized with a classical first order upwind scheme. Hence, a CFL condition has to respected so that $\Delta t = 10^{-3}$. When ε goes to zero, the densities obtained by MMS converges towards the density obtained by adiff. On the right hand side of Fig. 2.2, we plot the L^∞ norm (in space) of the error between $\rho(T,x)$ obtained by MMS and $\rho_{\text{adiff}}(T,x)$ obtained by adiff (using $\Delta t = 10^{-3}$), as a function of ε. We can observe that the convergence happens with a rate 0.337 which is very close to the theoretical value $\varepsilon^{\frac{d}{d+1+\beta}} = 0.333$.

2.4.3 The integral formulation scheme (DS)

In this section, we test the properties of the DS scheme. First of all, we remark that for $\varepsilon = 1$ the scheme appears to be of second order, as suggested by Fig. 2.3. For this test, we consider $N_x = 8$ and we consider the L^∞ norm (in space) of the error between the densities given by DS for a range of $\Delta t \in [2 \times 10^{-3}, 0.5]$ and the density given by DS for $\Delta t = 10^{-3}$ (which is the reference).

Then, we study the AP character of the scheme, fixing $\Delta t = 10^{-1}$, considering a range of ε. As previously, on the left hand side of Fig. 2.4, the densities $\rho(T,x)$ obtained by DS and by adiff (using $\Delta t = 10^{-1}$) are plotted as a function of space with $N_x = 32$. On the right

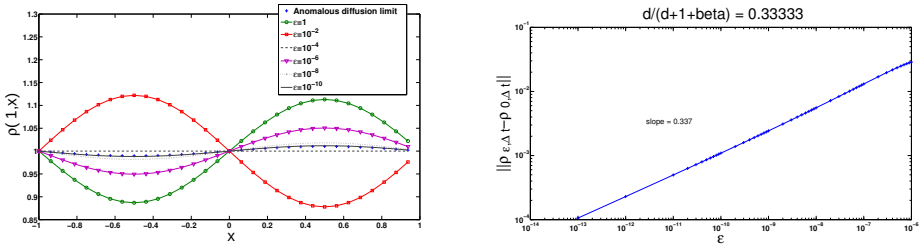

Figure 2.2: left: For $\Delta t = 10^{-3}$, the densities given by the MMS scheme for a range of ε and the anomalous diffusion limit given by the adiff scheme. Right: For $\Delta t = 10^{-3}$, the error between the MMS scheme and the DSA scheme as a function of ε (log scale).

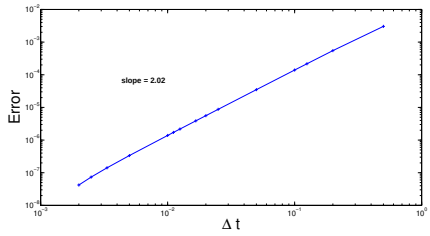

Figure 2.3: For $\varepsilon = 1$, the error between DS computed for $\Delta t = 10^{-3}$ and DS computed for a range of $\Delta t \in [2 \times 10^{-3}, 0.5]$ (log scale).

hand side of Fig. 2.4, the L^∞ norm (in space) of the error between $\rho(T,x)$ obtained by DS and $\rho_{\text{adiff}}(T,x)$ obtained by adiff (using $\Delta t = 10^{-1}$) is plotted as a function of ε, for $N_x = 8$. As in the previous cases, we observe that the numerical convergence rate is close to the theoretical one $\varepsilon^{\frac{d}{d+1+\beta}}$.

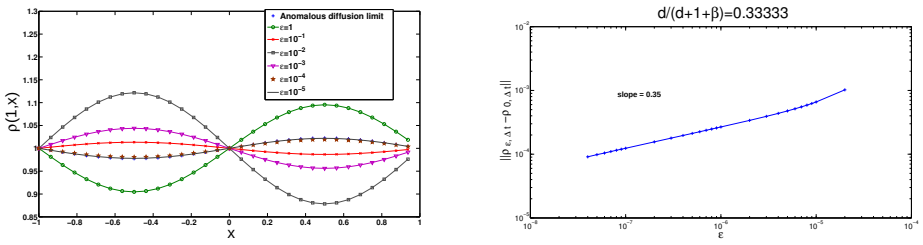

Figure 2.4: Left: For $\Delta t = 10^{-1}$, the densities given by DS for a range of ε and by adiff. Right: For $\Delta t = 10^{-1}$, the error between DS and the adiff as a function of ε (log scale).

Eventually, we illustrate that DS is first order in time uniformly in ε. Indeed, the left hand side of Fig. 2.5 displays the L^∞ error (in space)

$$E(\varepsilon, \Delta t) = \|\rho^\varepsilon_{\Delta t}(T,\cdot) - \rho^\varepsilon_{\Delta t = 10^{-3}}(T,\cdot)\|_\infty, \tag{2.4.4}$$

where $\rho^\varepsilon_{\Delta t = 10^{-3}}(T,x)$ is obtained by DS with $\Delta t = 10^{-3}$ and $\rho^\varepsilon_{\Delta t}(T,\cdot)$ is obtained by DS using larger Δt. The error $E(\varepsilon, \Delta t)$ is computed for a range of $\Delta t \in [5\times 10^{-3}, 0.5]$ and of $\varepsilon \in [10^{-7}, 1]$.

For this test, we fixed $N_x = 8$. These errors are stratified with respect to Δt, confirming the uniform accuracy of DS with respect to ε.

We now consider the following non equilibrium initial data

$$f_0(x,v) = (1+\sin(\pi x))\mathrm{e}^{-|v|}, \tag{2.4.5}$$

and the same numerical parameters as in the last test. As previously, we also look at (2.4.4) (see the right hand side of Fig. 2.5). It turns out that even if the initial condition is out of equilibrium, the Duhamel based scheme is uniformly accurate. As a consequence, considering the maximum with respect to $\varepsilon \in [10^{-7}, 1]$ of $E(\varepsilon, \Delta t)$ enables to highlight that DS is of order 1 uniformly in ε (obviously, the same occurs for the well-prepared initial data). Note that when this test is applied to the IS and MMS methods, the resulting error curves are not stratified.

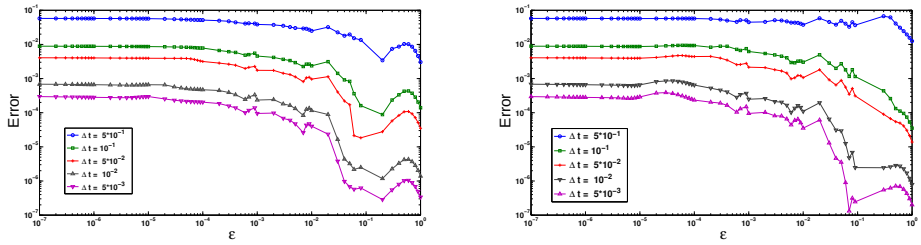

Figure 2.5: The error between DS computed for $\Delta t = 10^{-3}$ and DS computed for a range of Δt, as functions of ε (log scale). Left: equilibrium initial data (2.4.1). Right: non equilibrium initial data (2.4.5).

2.5 Appendix

In this section, we deal with the proof of Prop. 2.1.

The proof is a direct consequence of the following lemma:

Lemma 2.13. *Let $\hat{f}$ be the solution of (2.1.5) in the Fourier variable for a given initial condition $\hat{f}_0$ and let $t > 0$ be fixed. Then its modified density $\hat{\rho}_\nu$ satisfies formally*

$$\partial_t \hat{\rho}_\nu(t,k) + |k|^\alpha \kappa \hat{\rho}_\nu(t,k) = O\left(\varepsilon^{\frac{d}{d+1+\beta}}\right) + O\left(\varepsilon^{\frac{\beta}{d+1+\beta}}\right),$$

with κ given by (2.1.7) and with the initial condition $\hat{\rho}_\nu(0,k) = \left\langle \nu \hat{f}_0(k,v)\right\rangle_V / \langle \nu M\rangle_V$. Furthermore, the density and modified density $\hat{\rho}$ and $\hat{\rho}_\nu$ satisfy formally $\hat{\rho}(t,k) = \hat{\rho}_\nu(t,k) + O\left(\varepsilon^{\alpha-\gamma}\right)$, for all $0 < \gamma < \alpha$.

Proof. (Lemma 2.13) The proof relies on the integral formulation (2.3.20) which gives the expression (2.3.21) after an integration in $v \in V$. Using the notations K and $\hat{A}_0$ defined in (2.3.22), let us rewrite (2.3.21) at time t as follows

$$K\hat{\rho}_\nu(t,k) = \hat{A}_0(t,k) + \int_0^{\frac{t}{\varepsilon^\alpha}} \left\langle \nu^2 M \mathrm{e}^{-\nu s}\right\rangle_V \left(\hat{\rho}_\nu(t-\varepsilon^\alpha s,k) - \hat{\rho}_\nu(t,k)\right) \mathrm{d}s \tag{2.5.1}$$

$$+ \int_0^{\frac{t}{\varepsilon^\alpha}} \left\langle \nu^2 M \left(e^{-s(\nu+\mathrm{i}\varepsilon k\cdot v)} - \mathrm{e}^{-\nu s}\right)\right\rangle_V \left(\hat{\rho}_\nu(t-\varepsilon^\alpha s,k) - \hat{\rho}_\nu(t,k)\right) \mathrm{d}s \tag{2.5.2}$$

$$+\int_0^{\frac{t}{\varepsilon^\alpha}}\left\langle \nu^2 M\left(e^{-s(\nu+\mathrm{i}\varepsilon k\cdot v)}-\mathrm{e}^{-\nu s}\right)\right\rangle_V \mathrm{d}s\hat{\rho}_\nu(t,k) \tag{2.5.3}$$

$$+\int_0^{\frac{t}{\varepsilon^\alpha}}\left\langle \nu^2 M\mathrm{e}^{-\nu s}\right\rangle_V \mathrm{d}s\hat{\rho}_\nu(t,k), \tag{2.5.4}$$

and consider each line separately. First of all, let us remark that in (2.5.4), the integral in s can be directly computed and that the initial layer term $\hat{A}_0$ in (2.5.1) is exponentially small. Let us denote $\mathcal{I}_1$ the integral term appearing in (2.5.1) and show that is equivalent to $-\varepsilon^\alpha\partial_t\hat{\rho}_\nu(t,k)$ for small ε up to a rest of order $O\left(\varepsilon^{\alpha+\frac{\alpha d}{d+2+\beta}}\right)$. We rewrite $\mathcal{I}_1$ as

$$\mathcal{I}_1=-\int_0^{\frac{t}{\varepsilon^\alpha}}\left\langle \nu^2 M\mathrm{e}^{-\nu s}\right\rangle_V\left(\int_{t-\varepsilon^\alpha s}^t\partial_t\hat{\rho}_\nu(\xi,k)\mathrm{d}\xi\right)\mathrm{d}s,$$

and we permute the integrals before computing exactly the integral in s to get

$$\mathcal{I}_1=-\int_0^t\partial_t\hat{\rho}_\nu(t-\xi,k)\left\langle \nu M\mathrm{e}^{-\nu\frac{\xi}{\varepsilon^\alpha}}\right\rangle_V\mathrm{d}\xi+O(\varepsilon^\infty).$$

Hence, up to an exponentially small error in ε, $\mathcal{I}_1$ reads

$$\mathcal{I}_1=-\varepsilon^\alpha\partial_t\hat{\rho}_\nu(t,k)-\varepsilon^\alpha\int_0^{\frac{t}{\varepsilon^\alpha}}\left\langle \nu M\mathrm{e}^{-\nu(v)\xi}\right\rangle_V\left(\partial_t\hat{\rho}_\nu(t-\varepsilon^\alpha\xi,k)-\partial_t\hat{\rho}_\nu(t,k)\right)\mathrm{d}\xi.$$

It remains to show that the second term appearing in $\mathcal{I}_1$ is smaller that ε^α. Indeed in the brackets we do the change of variables $w=(\nu_0\xi)^{\frac{1}{d+2+\beta}}v$ to make appear a fractional time derivative. Then with the change of variables $\xi\to\varepsilon^\alpha\xi$ in the integral in ξ, $\mathcal{I}_1$ writes

$$\begin{aligned}\mathcal{I}_1&=-\varepsilon^\alpha\partial_t\hat{\rho}_\nu(t,k)+O\left(\varepsilon^\infty\right)\\&-\varepsilon^{\alpha\left(\frac{2d+2+\beta}{d+2+\beta}\right)}M_0\nu_0^{-\frac{d}{d+2+\beta}}\int_0^t\left\langle|w|^{d+2+\beta}\mathrm{e}^{-|w|^{d+2+\beta}}\right\rangle_{|w|\le\tilde{\delta}}\frac{\partial_t\hat{\rho}_\nu(t-\xi,k)-\partial_t\hat{\rho}_\nu(t,k)}{\xi^{\frac{2d+2+\beta}{d+2+\beta}}}\mathrm{d}\xi\end{aligned}$$

where $\tilde{\delta}=\left(\frac{\nu_0\xi}{\varepsilon^\alpha}\right)^{\frac{1}{d+2+\beta}}$ and $\langle\cdot\rangle_{|w|\le\tilde{\delta}}$ denotes the integration in w on the domain $|w|\le\tilde{\delta}$. The term into brackets is integrable on $\mathbb{R}^d$ and $\frac{2d+2+\beta}{d+2+\beta}=1+\frac{d}{d+2+\beta}\in(1,2)$. Supposing that $\hat{\rho}_\nu$ is regular, the integral in ξ is well defined and is bounded by a constant for any fixed t. Hence

$$\mathcal{I}_1=-\varepsilon^\alpha\partial_t\hat{\rho}_\nu(t,k)+O\left(\varepsilon^{\alpha+\frac{\alpha d}{d+2+\beta}}\right). \tag{2.5.5}$$

Now, let us denote $\mathcal{I}_2$ the term (2.5.2) and remark that it vanishes for $k=0$. We want to show that it is of magnitude $O\left(\varepsilon^{\alpha+\frac{d}{d+1+\beta}}\right)$ when ε goes to 0. For nonzero k we apply the change of variable $w=\frac{\varepsilon|k|v}{\nu(v)}$, such that $v=\left(\frac{\varepsilon|k|}{\nu_0|w|^{d+2+\beta}}\right)^{\frac{1}{d+1+\beta}}w$ and $\mathrm{d}v=\frac{1}{d+1+\beta}\left(\frac{\varepsilon|k|}{\nu_0|w|^{d+2+\beta}}\right)^{\frac{d}{d+1+\beta}}\mathrm{d}w$, to make the limit appear in the brackets. Then, with a Taylor expansion of $\hat{\rho}_\nu$, $\mathcal{I}_2$ writes

$$\mathcal{I}_2=-\varepsilon^\alpha C\int_0^{\frac{t}{\varepsilon^\alpha}}\left\langle\frac{\varphi}{|w|^{d+\alpha}}\left(\mathrm{e}^{-s\varphi(1+\mathrm{i}w\cdot e)}-\mathrm{e}^{-s\varphi}\right)\right\rangle_{|w|\ge\Delta}\left(\int_{t-\varepsilon^\alpha s}^t\partial_t\hat{\rho}_\nu(\xi,k)\mathrm{d}\xi\right)\mathrm{d}s,$$

where $C=\frac{|k|^\alpha M_0\nu_0^{1-\alpha}}{d+1+\beta}$, $\varphi=\nu_0\left(\frac{\varepsilon|k|}{\nu_0|w|}\right)^{\frac{d+2+\beta}{d+1+\beta}}$, $\Delta=\frac{\varepsilon|k|}{\nu_0}$ and where e denotes any unitary vector. As for $\mathcal{I}_1$, we permute the integrals before computing the integral in s to get the following expression of $\mathcal{I}_2$

$$\mathcal{I}_2=\varepsilon^{2\alpha}C\mathcal{I}_2^1+\varepsilon^\alpha C\partial_t\hat{\rho}_\nu(t,k)\mathcal{I}_2^2+O\left(\varepsilon^\infty\right), \tag{2.5.6}$$

with

$$\mathcal{I}_2^1 = \int_0^{\frac{t}{\varepsilon^\alpha}} \left\langle \frac{1}{|w|^{d+\alpha}} \left(\frac{\mathrm{e}^{-\xi\varphi(1+\mathrm{i}w\cdot e)}}{1+\mathrm{i}w\cdot e} - \mathrm{e}^{-\xi\varphi} \right) \right\rangle_{|w|\geq\Delta} (\partial_t\hat{\rho}_\nu(t-\varepsilon^\alpha\xi,k) - \partial_t\hat{\rho}_\nu(t,k))\,\mathrm{d}\xi \quad (2.5.7)$$

$$\mathcal{I}_2^2 = \int_0^{t} \left\langle \frac{1}{|w|^{d+\alpha}} \left(\frac{\mathrm{e}^{-\frac{\xi}{\varepsilon^\alpha}\varphi(1+\mathrm{i}w\cdot e)}}{1+\mathrm{i}w\cdot e} - \mathrm{e}^{-\frac{\xi}{\varepsilon^\alpha}\varphi} \right) \right\rangle_{|w|\geq\Delta} \mathrm{d}\xi. \quad (2.5.8)$$

The exact computation of the integral in ξ leads to

$$\mathcal{I}_2^2 = O\left(\varepsilon^{\frac{d}{d+1+\beta}}\right), \quad (2.5.9)$$

and we now focus on $\mathcal{I}_2^1$. In the brackets we do the change of variables $v = \frac{\nu_0}{|k|\varepsilon}(\xi\nu_0)^{-\frac{d+1+\beta}{d+2+\beta}}$ such that $\xi\varphi = \frac{1}{|v|^{\frac{d+2+\beta}{d+1+\beta}}}$, to get

$$\begin{aligned}
&\left\langle \frac{1}{|w|^{d+\alpha}} \left(\frac{\mathrm{e}^{-\frac{\xi}{\varepsilon^\alpha}\varphi(1+\mathrm{i}w\cdot e)}}{1+\mathrm{i}w\cdot e} - \mathrm{e}^{-\frac{\xi}{\varepsilon^\alpha}\varphi} \right) \right\rangle_{|w|\geq\Delta} \\
&= \frac{\nu_0^{\frac{\alpha}{d+2+\beta}}}{\varepsilon^\alpha|k|^\alpha} \frac{1}{\xi^{\alpha\frac{d+1+\beta}{d+2+\beta}}} \left\langle \frac{1}{|v|^{d+\alpha}} \left(\frac{\mathrm{e}^{-\frac{1}{|v|^{\frac{d+2+\beta}{d+1+\beta}}}(1+\mathrm{i}\psi(v)\cdot e)}}{1+\mathrm{i}\psi(v)\cdot e} - \mathrm{e}^{-\frac{1}{|v|^{\frac{d+2+\beta}{d+1+\beta}}}} \right) \right\rangle_{|v|\geq\tilde{\Delta}},
\end{aligned}$$

with $\psi(v) = \frac{\varepsilon|k|}{\nu_0}(\xi\nu_0)^{\frac{d+1+\beta}{d+2+\beta}} v$ and $\tilde{\Delta} = \frac{\nu_0}{\varepsilon|k|}(\xi\nu_0)^{-\frac{d+1+\beta}{d+2+\beta}}\Delta$. This last expression gives the following upper bound for $\mathcal{I}_2^1$

$$\left|\varepsilon^\alpha\mathcal{I}_2^1\right| \leq C\int_0^{\frac{t}{\varepsilon^\alpha}} \frac{|\partial_t\hat{\rho}_\nu(t-\varepsilon^\alpha\xi,k) - \partial_t\hat{\rho}_\nu(t,k)|}{|\xi|^{\alpha\frac{d+1+\beta}{d+2+\beta}}}\mathrm{d}\xi,$$

we then apply the change of variables $\xi \to \varepsilon^\alpha\xi$ to get $\varepsilon^\alpha\mathcal{I}_2^1 = O\left(\varepsilon^{\frac{\alpha d}{d+2+\beta}}\right)$, which combined with (2.5.9) in (2.5.6) leads to

$$\mathcal{I}_2 = O\left(\varepsilon^{\alpha+\frac{d}{d+1+\beta}}\right) + O\left(\varepsilon^{\alpha+\frac{\alpha d}{d+2+\beta}}\right) = O\left(\varepsilon^{\alpha+\frac{d}{d+1+\beta}}\right). \quad (2.5.10)$$

It remains to consider (2.5.3), let us denote

$$\mathcal{I}_3 = \int_0^{\frac{t}{\varepsilon^\alpha}} \left\langle \nu^2 M\left(\mathrm{e}^{-s(\nu+\mathrm{i}\varepsilon k\cdot v)} - \mathrm{e}^{-\nu s}\right)\right\rangle_V \mathrm{d}s,$$

that writes after the change of variables $w = \frac{\varepsilon|k|v}{\nu(v)}$ and an exact integration in s

$$\mathcal{I}_3 = -\frac{\varepsilon^\alpha|k|^\alpha\nu_0^{1-\alpha}M_0}{d+1+\beta} \left\langle \frac{1}{|w|^{d+\alpha}} \frac{(w\cdot e)^2}{1+(w\cdot e)^2} \right\rangle_{|w|\geq\Delta} + O(\varepsilon^\infty),$$

where we see the anomalous diffusion coefficient appear. Eventually, we get the following equivalent for $\mathcal{I}_3$

$$\mathcal{I}_3 = -\varepsilon^\alpha\kappa + O\left(\varepsilon^{\alpha+\frac{\beta}{d+1+\beta}}\right), \quad (2.5.11)$$

with κ given by (2.1.7). Finally replacing the lines (2.5.1)-(2.5.2)-(2.5.3)-(2.5.4) with their equivalents leads to the result

$$\partial_t \hat{\rho}_\nu + |k|^\alpha \kappa \hat{\rho}_\nu = O\left(\varepsilon^{\frac{d}{d+1+\beta}}\right) + O\left(\varepsilon^{\frac{\beta}{d+1+\beta}}\right). \tag{2.5.12}$$

□

Chapter 3

Numerical schemes for kinetic equations with diffusion limit and anomalous time scale

3.1 Introduction

The modeling of a large amount of particles, from a theoretical or numerical point of view, is a very active field of research. The direct application of Newton's laws leads to a large system of coupled equations, one for each particle of the system. Since such a huge number of unknowns is beyond the reach of numerical computations, the so-called microscopic scale is not adapted to the numerical analysis of these systems. Instead, an approach based on statistical physics is preferred, where the distribution function of particles $f_\varepsilon(t,x,v)$ depending on the time $t \geq 0$, the position $x \in \mathbb{R}^d$, and the velocity $v \in \mathbb{R}^d$ is considered. The parameter $\varepsilon \in (0,1]$ denotes here the Knudsen number, which is proportional to the mean free path of the particle.

Provided an initial condition $f(0,x,v) = f_{in}(x,v)$, we consider the following kinetic equation for f_ε

$$\Theta(\varepsilon)\partial_t f_\varepsilon + \varepsilon v \cdot \nabla_x f_\varepsilon = L(f_\varepsilon). \tag{3.1.1}$$

The quantity $\Theta(\varepsilon) = \varepsilon^2 (1 + \ln(\varepsilon))$, is a suitable scaling parameter to be chosen according to the nature of L, in order to capture a non-trivial dynamic when ε goes to 0. The linear operator L describes the collisions of the particles. We will consider the particular case of the BGK operator

$$L(f_\varepsilon) = \rho_\varepsilon M - f_\varepsilon, \tag{3.1.2}$$

with

$$\rho_\varepsilon(t,x) = \int_{\mathbb{R}^d} f_\varepsilon(t,x,v)\mathrm{d}v =: \langle f_\varepsilon \rangle (t,x).$$

Here, the equilibrium function M is even, positive and normalized to 1

$$M(-v) = M(v) > 0 \quad \text{for all} \quad v \in \mathbb{R}^d \quad \text{and} \quad \langle M \rangle = 1.$$

In the last part of this chapter, we will extend our numerical methods to the case of a more general collision operator. In what follows, the integral in v of f on a domain $\mathcal{D}$ will always be denoted $\langle f \rangle_{\mathcal{D}}$. The integral is on the whole space $\mathbb{R}^d$ when no domain is specified.

The asymptotic analysis of (3.1.1) when $\varepsilon \to 0$ can be found in [55]. Our aim in this paper is to construct numerical schemes for (3.1.1) that fits with this asymptotic analysis. The properties of the equilibrium function M, and the scaling $\Theta(\varepsilon)$ of (3.1.1) make various asymptotic behaviors arise. For instance, considering the scaling $\Theta(\varepsilon) = \varepsilon$ with a local Maxwellian equilibrium in (3.1.1) and the Boltzmann operator instead of the linear collision operator L, leads when ε goes to 0 to a fluid limit for (3.1.1) (see [1, 2]). With the BGK collision operator, the scaling $\Theta(\varepsilon) = \varepsilon^2$, and a global Maxwellian equilibrium $M(v) = (2\pi)^{-d/2}\mathrm{e}^{-v^2/2}$, the solution f_ε of (3.1.1) degenerates when $\varepsilon \to 0$ to a distribution at equilibrium $f = \rho M$, where ρ solves a diffusion equation

$$\partial_t \rho - \nabla_x \cdot (D \nabla_x \rho) = 0,$$

with initial condition $\rho_{in} = \langle f_{in} \rangle$. A rigorous derivation of diffusion-type equations in this last case was first investigated in [70, 3, 7, 22]. When M is a Maxwellian and $\Theta(\varepsilon) = \varepsilon^2$, the diffusion coefficient D is finite because of the exponential decay of M for large v, and is given by

$$D = \langle v \otimes v M \rangle . \tag{3.1.3}$$

However, for non Maxwellian equilibrium, it may happen in many situations that the coefficient D becomes infinite. An important example is the case of a so-called heavy-tailed function

$M(v) \sim 1/|v|^{d+\alpha}$ for large v, $\alpha \in (0,2)$. In this case, the scaling $\Theta(\varepsilon) = \varepsilon^2$ is not the suitable choice and does not lead to a non trivial dynamics when ε goes to 0. It is well-known that, in this case, the time scale $\Theta(\varepsilon)$ should be modified according to α in order to capture a non-trivial dynamics, which turns out to be a fractional diffusion model [55, 5]. Heavy-tailed equilibria arise in the study of granular media (see [27, 9, 8]), astrophysical plasmas (see [56, 68]), tokamaks (see [23]) or in economy (see [46]). Usually, the fractional diffusion equation describes the motion of the particles driven by a Levy process (see [21, 20]), while the classical diffusion is governed by a Brownian process.

From a numerical point of view, the case $\alpha \in (0,2)$ has been treated in [17, 16, 69]. In this paper, we consider the so-called critical case $\alpha = 2$, of the above heavy-tailed equilibrium, which induces a different asymptotic behavior when ε goes to 0. For a sake of simplicity we will consider here the following particular case

$$M(v) = \begin{cases} m & |v| < 1 \\ m/|v|^{d+2} & |v| \geq 1, \end{cases} \tag{3.1.4}$$

where m is such that $\langle M \rangle = 1$. With this assumption, it has been shown in [55] that if $\Theta(\varepsilon) \sim \varepsilon^2 |\ln(\varepsilon)|$ in (3.1.1) the solution f_ε of (3.1.1) converges weakly when $\varepsilon \to 0$ to $\rho_0 M$, where ρ_0 solves a classical diffusion equation

$$\begin{cases} \partial_t \rho_0 - c_d m \Delta \rho_0 = 0, \\ \rho_0(0,x) = \rho_{in}(x) = \langle f_{in} \rangle (x). \end{cases} \tag{3.1.5}$$

Here c_d is a coefficient that only depends on the dimension d ($c_1 = 2, c_2 = \pi$, and $c_3 = 8\pi/3$). To have a non-vanishing of $\Theta(\varepsilon)$ for $\varepsilon = 1$, we shall consider

$$\Theta(\varepsilon) = \varepsilon^2 \left(1 + |\ln(\varepsilon)|\right). \tag{3.1.6}$$

In this work, we prove that when the initial data f_{in} is at equilibrium, the convergence when $\varepsilon \to 0$ of the solution f_ε of (3.1.1) to the solution of (3.1.5) is very slow. However, we will show that f_ε approaches much faster an intermediate equilibrium $\tilde{\rho}_\varepsilon M$, where $\tilde{\rho}_\varepsilon$ is the solution of the following equation (in Fourier variable)

$$\begin{cases} \partial_t \hat{\tilde{\rho}}_\varepsilon + a_\varepsilon(k) \hat{\tilde{\rho}}_\varepsilon = 0, & t > 0, k \in \mathbb{R}^d \\ \hat{\tilde{\rho}}_\varepsilon(0,k) = \hat{\rho}_{in}(k), & k \in \mathbb{R}^d, \end{cases} \tag{3.1.7}$$

and

$$a_\varepsilon(k) = \frac{1}{\Theta(\varepsilon)} \left\langle \frac{\varepsilon^2 (k \cdot v)^2}{1 + \varepsilon^2 (k \cdot v)^2} M \right\rangle, \tag{3.1.8}$$

where $\hat{\tilde{\rho}}_\varepsilon$ is the space Fourier transform of $\tilde{\rho}_\varepsilon$.

The main goal of this work is to construct numerical schemes for (3.1.1) which do not need to be refined in order to capture the right asymptotic behavior, when ε goes to 0. There are, in fact, some stiffness in the problem (3.1.1). First, the smallness of ε imposes severe conditions on the numerical parameters, if a naive approach is used. We will follow an *Asymptotic Preserving* (AP) strategy [37, 43, 44] to overcome this difficulty. Namely, if we consider a problem P_ε which degenerates into a problem P_0 when ε tends to 0, then an AP scheme S_ε^h should enjoy the following properties:

1. at fixed ε, S_ε^h must be consistent with P_ε when the discretization parameter h tends to 0.

2. S_ε^h must degenerate into a scheme S_0^h consistent with P_0 when ε goes to 0.

An AP scheme can even enjoy the stronger property of being *Uniformly Accurate* (UA), meaning that its accuracy does not depend on ε.

The construction of AP schemes for the case of classical diffusion with classical time scale $\Theta(\varepsilon) = \varepsilon^2$ has been widely investigated (see [37, 40, 40, 41, 43, 11, 12, 52, 50]), but the heavy-tail of the equilibrium brings an additional stiffness, which is not usual in the classical cases. Indeed, the anomalous time scale (3.1.6) in (3.1.1) is designed to capture the effect of the high velocities in the asymptotic analysis. From a numerical point of view, taking into account these high velocities is then crucial to ensure the AP property of the scheme. In previous works (see [16, 17, 18]), we investigated AP schemes for kinetic equations in the fractional diffusion limit. In the critical case, the same methodology can not be applied since the resulting schemes do not respect the dynamics of the convergence towards the diffusion equation (3.1.1). This is due to the slow convergence in this critical case, and a specific study will be performed to capture the right asymptotic behavior.

Three numerical schemes will be investigated in this paper. The first one is based on a fully implicit in time scheme for (3.1.1) using a Fourier variable in space. A suitable modification is introduced in this case, and its AP behavior is proved. Then, a scheme based on a micro-macro decomposition of the distribution function f_ε is presented. It allows to avoid, if needed, the use of the Fourier transform and of the time implicit character of the previous scheme. Moreover, it can be adapted to deal with more general collision operators in (3.1.1). Once again, the convergence towards (3.1.7) has to be treated with care to ensure the good asymptotic behavior of the scheme. Eventually, we propose an approach based on an integral formulation of (3.1.1) in Fourier variable, which enjoys the stronger UA property. To summarize, we will show that (3.1.1) approaches (3.1.7) with a rate $\varepsilon\sqrt{1+|\ln(\varepsilon)|}$, while (3.1.7) approaches the limit model (3.1.5) with the slower rate $1/\left(1+|\ln(\varepsilon)|\right)$, and we will construct numerical schemes which respect this asymptotic behavior. This can be illustrated by the following diagram

$$\begin{array}{ccccc} P_\varepsilon : (3.1.1) & \xrightarrow[\varepsilon\sqrt{1+|\ln(\varepsilon)|}]{} & \tilde{P}_\varepsilon : (3.1.7) & \xrightarrow[1/(1+|\ln(\varepsilon)|)]{} & P_0 : (3.1.5) \\ \uparrow{\scriptstyle h\to 0} & & \uparrow{\scriptstyle h\to 0} & & \uparrow{\scriptstyle h\to 0} \\ S_\varepsilon^h & \xrightarrow[\varepsilon\sqrt{1+|\ln(\varepsilon)|}]{} & \tilde{S}_\varepsilon^h & \xrightarrow[1/(1+|\ln(\varepsilon)|)]{} & S_0^h \end{array} \tag{3.1.9}$$

The schemes S_ε^h and $\tilde{S}_\varepsilon^h$ are respectively consistent with the problems P_ε and $\tilde{P}_\varepsilon$ when $\varepsilon > 0$ is fixed, and S_0^h is consistent with P_0. The scheme S_ε^h approaches $\tilde{S}_\varepsilon^h$ with rate $\varepsilon\sqrt{1+|\ln(\varepsilon)|}$ while $\tilde{S}_\varepsilon^h$ approaches S_0 with rate $1/\left(1+|\ln(\varepsilon)|\right)$ when the discretization parameter h is fixed and when ε goes to 0. The asymptotic behavior $P_\varepsilon \to \tilde{P}_\varepsilon \to P_0$ will be proved in suitable functional spaces and illustrated by several numerical tests.

The paper is organized as follows. In the next section, we will start by establishing the convergence rates of (3.1.1) towards (3.1.5), and of (3.1.7) to (3.1.5). Then, in Section 3.3, we present an asymptotic preserving scheme for (3.1.7), and the three asymptotic preserving schemes for (3.1.1), which are tested in Section 3.5. Eventually, we will present in the last section an extension of the micro-macro scheme to the case of more general collision operators.

3.2 Degeneracy to the diffusion limit in the case of a BGK operator

In this section, we show that the convergence of (3.1.1) towards the diffusion limit (3.1.5) can be quantified by two steps as described by the diagram (3.1.9). This will be the basis of the numerical methods proposed in Section 3.3. In what follows, the space Fourier transform will be often used. We will denote $\hat{f}(t,k,v)$ (resp. $\hat{\rho}(t,k)$) the space Fourier transform of $f(t,x,v)$ (resp. $\rho(t,x)$)

$$\hat{f}(t,k,v) = \int_{\mathbb{R}^d} \mathrm{e}^{-ik\cdot x} f(t,x,v)\mathrm{d}x.$$

We will use the following weighted L^2 norm

$$\|f(x,v)\|^2_{L^2_{M^{-1}}} = \int_{\mathbb{R}^d}\int_{\mathbb{R}^d} |f(x,v)|^2 \frac{1}{M(v)}\mathrm{d}v\mathrm{d}x, \tag{3.2.1}$$

where M is given by (3.1.4). We have the following propositions:

Proposition 3.1. *Let $f_\varepsilon \in L^\infty\left(0,T;L^2_{M^{-1}}\right)$ be the solution of (3.1.1) with initial condition $f_{in}(x,v) = \rho_{in}(x)M(v)$, with $\rho_{in} \in H^{N_d}\left(\mathbb{R}^d\right)$ ($N_1 = 3, N_2 = N_3 = 6$), where $H^{N_d}\left(\mathbb{R}^d\right)$ denotes the usual Sobolev space, and let $T > 0$. Then, there exists a constant C such that*

$$\|f_\varepsilon - \tilde{\rho}_\varepsilon M\|_{L^\infty\left(0,T;L^2_{M^{-1}}\right)} \leq CT\varepsilon\sqrt{1+|\ln(\varepsilon)|}\|\rho_{in}\|_{H^{N_d}}, \tag{3.2.2}$$

where $\tilde{\rho}_\varepsilon \in L^\infty\left(0,T;L^2\right)$ solves (3.1.7) with initial condition ρ_{in}, and with M defined in (3.1.4).

Proposition 3.2. *Assume that the previous assumptions hold, and let $\tilde{\rho}_\varepsilon \in L^\infty\left(0,T;L^2(\mathbb{R}^d)\right)$ be the solution of (3.1.7) with $\rho_{in} \in H^{M_d}\left(\mathbb{R}^d\right)$ ($M_1 = 2, M_2 = M_3 = 4$), and let $T > 0$. Then, there exists a constant C such that*

$$\|\tilde{\rho}_\varepsilon - \rho_0\|_{L^\infty\left(0,T;L^2(\mathbb{R}^d)\right)} \leq \frac{CT}{1+|\ln(\varepsilon)|}\|\rho_{in}\|_{H^{M_d}}, \tag{3.2.3}$$

where $\rho_0 \in L^\infty\left(0,T;L^2(\mathbb{R}^d)\right)$ solves (3.1.5), with initial condition ρ_{in}.

These two propositions establish that the convergence $\varepsilon \to 0$ of (3.1.1) makes appear two dynamics with very different rates in ε. Indeed, in a first step, the solution f_ε approaches (relatively) quickly a distribution function at equilibrium $\tilde{\rho}_\varepsilon(t,x)M(v)$, with $\tilde{\rho}_\varepsilon$ solution of (3.1.7). Then, in a second step, this density $\tilde{\rho}_\varepsilon$ goes much more slowly to the solution ρ_0 of the limit diffusion equation (3.1.5). Hence, the approximation of f_ε by its diffusion limit (3.1.5) is valid only for very small ε. At the numerical level, it implies that a large range of ε may stay out of reach if no appropriate strategy is used in the numerical schemes. The next parts present numerical methods for (3.1.1) degenerating when ε to 0 into numerical methods solving (3.1.7). In particular, the schemes enjoy the AP property that is

- when ε is fixed, the scheme is consistent with (3.1.1),
- the difference between the numerical scheme S^h_ε for (3.1.1) and the numerical scheme $\tilde{S}^h_\varepsilon$ for (3.1.7) converges to 0 when ε goes to 0.

Afterwards, letting ε go to zero in the scheme $\tilde{S}^h_\varepsilon$ for (3.1.7) makes it degenerate in a scheme S^h_0 solving the limit diffusion equation (3.1.5). This approach enables to capture numerically the two scales of convergence of the solution of (3.1.1) to its diffusion limit, as described by (3.1.9).

The proofs of Prop. 3.1 and Prop. 3.2 follows the ideas developed in [5] in the case of a fractional diffusion limit for kinetic equation, coming from a heavy-tailed equilibrium function. We start by proving the following lemma, which gives the limit of a_ε when ε goes to 0.

Lemma 3.3. *Considering a_ε defined in* (3.1.8)*, there exists a constant C such that, $\forall k \in \mathbb{R}^d$*

1. *If $d = 1$,*
$$\left|a_\varepsilon(k) - 2mk^2\right| \leq \frac{C}{1+|\ln(\varepsilon)|}\left(1+k^2\right). \tag{3.2.4}$$
2. *If $d = 2, 3$,*
$$|a_\varepsilon(k) - c_d m|k|^2| \leq \frac{C}{1+|\ln(\varepsilon)|}\left(1+|k|^4\right) \tag{3.2.5}$$
with $c_2 = \pi$ and $c_3 = \frac{8\pi}{3}$.

Proof of Lemma 3.3. In the 1-dimensional case, with the change of variables $w = \varepsilon v$, the coefficient a_ε reads

$$a_\varepsilon(k) = \frac{m}{1+|\ln(\varepsilon)|}\left\langle \frac{k^2v^2}{1+\varepsilon^2k^2v^2}\right\rangle_{|v|<1} + \frac{m}{1+|\ln(\varepsilon)|}\left\langle \frac{k^2w^2}{1+k^2w^2}\frac{1}{|w|^3}\right\rangle_{|w|\geq\varepsilon}, \tag{3.2.6}$$

where the last term in (3.2.6) can be computed for nonzero k with the change of variables $u = 1/w$

$$\frac{m}{1+|\ln(\varepsilon)|}\left\langle \frac{k^2w^2}{1+k^2w^2}\frac{1}{|w|^3}\right\rangle_{|w|\geq\varepsilon} = 2mk^2 + \frac{2mk^2}{1+|\ln(\varepsilon)|}\left(\frac{1}{2}\ln\left(\varepsilon^2+\frac{1}{k^2}\right)-1\right),$$

and the first term is bounded by $Ck^2/(1+|\ln(\varepsilon)|)$. Eventually the inequality $\ln(x)/2 \leq 1+x$ for $x > 0$, gives (3.2.4).

When $d = 2, 3$, with the change of variables $w = \varepsilon|k|v$ for nonzero k, (3.1.8) reads

$$a_\varepsilon(k) = \frac{m}{1+|\ln(\varepsilon)|}\left\langle \frac{(k\cdot v)^2}{1+\varepsilon^2(k\cdot v)^2}\right\rangle_{|v|\leq1} + \frac{m|k|^2}{1+|\ln(\varepsilon)|}\left\langle \frac{(w\cdot e)^2}{1+(w\cdot e)^2}\frac{1}{|w|^{d+2}}\right\rangle_{|w|\geq\varepsilon|k|}, \tag{3.2.7}$$

where e denotes any unitary vector. The first term is lower than $C|k|^2$, it remains to consider the second one. Depending on the dimension, a change of variables in polar or spherical coordinates can be applied in it. Since no additional difficulty arise when $d = 3$, we treat here the case of polar coordinates, when $d = 2$. Choosing e such that $w \cdot e = |w|\cos(\theta)$, it can be rewritten as

$$\left\langle \frac{(w\cdot e)^2}{1+(w\cdot e)^2}\frac{1}{|w|^{d+2}}\right\rangle_{|w|\geq\varepsilon|k|} = I_1 + I_2 + I_3,$$

with

$$I_1 = \int_{\theta=0}^{2\pi}\int_{r=\varepsilon|k|}^{1} r^2\cos^2(\theta)\frac{1}{r^3}\mathrm{d}r\mathrm{d}\theta, \tag{3.2.8}$$

$$I_2 = \int_{\theta=0}^{2\pi}\int_{r=\varepsilon|k|}^{1} r^2\cos^2(\theta)\left(\frac{1}{1+r^2\cos^2(\theta)}-1\right)\frac{1}{r^3}\mathrm{d}r\mathrm{d}\theta \tag{3.2.9}$$

$$I_3 = \int_{\theta=0}^{2\pi}\int_{r=1}^{\infty}\frac{r^2\cos^2(\theta)}{1+r^2\cos^2(\theta)}\frac{1}{r^3}\mathrm{d}r\mathrm{d}\theta. \tag{3.2.10}$$

At this stage, the last two integrals can be bounded

$$|I_2| \leq \int_{\theta=0}^{2\pi}\int_{r=\varepsilon|k|}^{1}\frac{r^4\cos^4(\theta)}{1+r^2\cos^2(\theta)}\frac{1}{r^3}\mathrm{d}r\mathrm{d}\theta \leq \int_{\theta=0}^{2\pi}\int_{r=\varepsilon|k|}^{1} r\cos^4(\theta)\mathrm{d}r\mathrm{d}\theta \leq C(1+|k|^2)$$

$$|I_3| \leq \int_{0}^{2\pi}\int_{r=1}^{\infty}\frac{1}{r^3}\mathrm{d}r\mathrm{d}\theta \leq C,$$

and the first one can be computed explicitly

$$I_1 = -\pi\ln(|k|) - \pi\ln(\varepsilon).$$

Eventually, the inequality $\ln(|k|) \leq |k|$ yields (3.2.5). □

Remark 3.4. The proof of Lemma 3.3 provides, for nonzero k, a rewriting of a_ε in which the diffusion limit clearly appears. In dimension 1, it is

$$a_\varepsilon^{d=1}(k) = 2mk^2 + \frac{m}{1+|\ln(\varepsilon)|}\left\langle\frac{k^2v^2}{1+\varepsilon^2k^2v^2}\right\rangle_{|v|<1} + \frac{2mk^2}{1+|\ln(\varepsilon)|}\left(\frac{1}{2}\ln\left(\varepsilon^2+\frac{1}{k^2}\right)-1\right), \tag{3.2.11}$$

and in dimension 2 it reads

$$a_\varepsilon^{d=2}(k) = \pi m|k|^2 + \frac{m}{1+|\ln(\varepsilon)|}\left\langle\frac{(k\cdot v)^2}{1+\varepsilon^2(k\cdot v)^2}\right\rangle_{|v|\geq 1} - \frac{m|k|^2}{1+|\ln(\varepsilon)|}\pi\left(1+\ln(|k|)\right) \tag{3.2.12}$$

$$+\frac{m|k|^2}{1+|\ln(\varepsilon)|}\left(-\int_{\theta=0}^{2\pi}\int_{r=\varepsilon|k|}^{1}\frac{r\cos^4(\theta)}{1+r^2\cos^2(\theta)}\mathrm{d}r\mathrm{d}\theta + \int_{\theta=0}^{2\pi}\int_{r=1}^{\infty}\frac{\cos^2(\theta)}{1+r^2\cos^2(\theta)}\frac{1}{r}\mathrm{d}r\mathrm{d}\theta\right).$$

Eventually, a change of variables in spherical coordinates provides the case of dimension 3

$$a_\varepsilon^{d=3}(k) = \frac{8\pi}{3}m|k|^2 + \frac{m}{1+|\ln(\varepsilon)|}\left\langle\frac{(k\cdot v)^2}{1+\varepsilon^2(k\cdot v)^2}\right\rangle_{|v|\geq 1} - \frac{m|k|^2}{1+|\ln(\varepsilon)|}\frac{8\pi}{3}\left(\ln(|k|)+1\right) \tag{3.2.13}$$

$$+\frac{2\pi m|k|^2}{1+|\ln(\varepsilon)|}\left(-\int_{\theta=0}^{\pi}\int_{r=\varepsilon|k|}^{1}\frac{r\sin^5(\theta)}{1+r^2\sin^2(\theta)}\mathrm{d}r\mathrm{d}\theta + \int_{\theta=0}^{\pi}\int_{r=1}^{\infty}\frac{\sin^2(\theta)}{1+r^2\sin^2(\theta)}\frac{1}{r}\mathrm{d}r\mathrm{d}\theta\right).$$

Proof of Prop. 3.2. Denoting $\hat\rho_0$ and $\hat{\tilde\rho}_\varepsilon$ the solutions of (3.1.5) and (3.1.7) in space Fourier variable, with initial condition $\hat\rho_{in}$, and $a_0(k) = c_d m k^2$, $\hat\rho_0$ and $\hat{\tilde\rho}_\varepsilon$ satisfy

$$\hat{\tilde\rho}_\varepsilon(t,k) = \mathrm{e}^{-ta_\varepsilon(k)}\hat\rho_{in}(k),$$
$$\hat\rho_0(t,k) = \mathrm{e}^{-ta_0(k)}\hat\rho_{in}(k).$$

Since $a_\varepsilon(k) \geq 0$ and $a_0(k) \geq 0$, the inequality $|\mathrm{e}^{-x} - \mathrm{e}^{-y}| \leq |x-y|$ for $x \geq 0, y \geq 0$ yields

$$\begin{cases} |\hat\rho_0 - \hat{\tilde\rho}_\varepsilon| \leq \dfrac{Ct}{1+|\ln(\varepsilon)|}\left(1+k^2\right)|\hat\rho_{in}| & \text{if } d=1, \\ |\hat\rho_0 - \hat{\tilde\rho}_\varepsilon| \leq \dfrac{Ct}{1+|\ln(\varepsilon)|}\left(1+|k|^2\right)^2|\hat\rho_{in}| & \text{if } d=2,3, \end{cases}$$

and gives (3.2.3). □

The convergence of the solution of (3.1.7) to the solution of (3.1.5) is very slow in ε, but Prop. 3.1 states that the degeneracy of (3.1.1) to (3.1.7) happens much faster. The proof of Prop. 3.1 is based on the proof of the similar result stated in [5] for the case of a kinetic equation with heavy-tailed equilibrium degenerating to a fractional diffusion equation. It uses the following properties of the collision operator, established in [22] and [55] in a more general case:

Proposition 3.5. *The collision operator L given by* (3.1.2) *has the following properties*

1. *The operator L is bounded in $L^2_{M^{-1}}(\mathbb{R}^d \times \mathbb{R}^d)$.*
2. *There exists a constant $C > 0$ such that*
$$\forall f \in L^2_{M^{-1}},\ \int_{\mathbb{R}^d} L(f)\frac{f}{M}\mathrm{d}v \leq -\frac{1}{2}\int_{\mathbb{R}^d} |f - \langle f\rangle M|^2 \frac{1}{M}\mathrm{d}v.$$
3. *For $h \in L^2_{M^{-1}}$, the equation $L(g) = h$ has a solution if and only if $\langle h\rangle = 0$. If $\langle g\rangle = 0$, this solution is unique.*

Proof of Prop. 3.1. As in [5], the proof relies on the following Hilbert expansion of the solution f_ε of (3.1.1)
$$f_\varepsilon = \tilde{\rho}_\varepsilon M + g_1 + g_2 + r,$$
where ρ, g_1, g_2 and r solve
$$(1 + \varepsilon v\cdot\nabla_x)\, g_1 = -\varepsilon v\cdot\nabla_x \tilde{\rho}_\varepsilon M \tag{3.2.14}$$
$$\langle g_2\rangle M - g_2 = -\langle g_1\rangle M + \Theta(\varepsilon)\partial_t\tilde{\rho}_\varepsilon M \tag{3.2.15}$$
$$\partial_t r + \frac{\varepsilon}{\Theta(\varepsilon)} v\cdot\nabla_x r = \frac{1}{\Theta(\varepsilon)}\left(\langle r\rangle M - r\right) - \partial_t g_1 - \left(\partial_t g_2 + \frac{\varepsilon}{\Theta(\varepsilon)} v\cdot\nabla_x g_2\right) \tag{3.2.16}$$
with initial condition $\tilde{\rho}_\varepsilon(0,x) = \rho_{in}(x), g_1(0,x,v) = g_2(0,x,v) = r(0,x,v) = 0$. Considering (3.2.14) in Fourier variable leads to
$$\hat{g}_1 = -\frac{\mathrm{i}\varepsilon k\cdot v}{1 + \mathrm{i}\varepsilon k\cdot v}\hat{\tilde{\rho}}_\varepsilon M. \tag{3.2.17}$$
Furthermore, the left-hand side of (3.2.15) is such that $\langle\langle g_2\rangle M - g_2\rangle = 0$. Still in Fourier variable, (3.2.15) then reads $-\langle g_1\rangle + \Theta(\varepsilon)\partial_t\tilde{\rho}_\varepsilon = 0$, that is using (3.2.17) and the symmetry of M
$$\partial_t\hat{\tilde{\rho}}_\varepsilon(t,k) + a_\varepsilon(k)\hat{\tilde{\rho}}_\varepsilon(t,k) = 0,$$
with a_ε defined in (3.1.8). Note that solving this equation leads to
$$\hat{\tilde{\rho}}_\varepsilon(t,k) = \mathrm{e}^{-a_\varepsilon(k)t}\hat{\rho}_{in}(k),\ \ \partial_t\hat{\tilde{\rho}}_\varepsilon(t,k) = -a_\varepsilon(k)\mathrm{e}^{-a_\varepsilon(k)t}\hat{\rho}_{in}(k). \tag{3.2.18}$$
As $\hat{\rho}$ solves (3.1.7), the proof of the proposition relies on establishing estimates for $\|g_1\|_{L^\infty(0,T;L^2_{M^{-1}})}$, $\|g_2\|_{L^\infty(0,T;L^2_{M^{-1}})}$ and $\|r\|_{L^\infty(0,T;L^2_{M^{-1}})}$. Since $a_\varepsilon \geq 0$, (3.2.18) and the expression of $\hat{g}_1$ in (3.2.17) give
$$\int_{\mathbb{R}^d} |\hat{g}_1|^2 \frac{\mathrm{d}v}{M} \leq \Theta(\varepsilon)a_\varepsilon(k)|\hat{\rho}_{in}|^2,$$
with $\Theta(\varepsilon)$ defined in (3.1.6). The estimation of a_ε given by Lemma 3.3 yields
$$\|g_1\|_{L^\infty(0,T;L^2_{M^{-1}})} \leq C\varepsilon\sqrt{1 + |\ln(\varepsilon)|}\|\rho_{in}\|_{H^{N_d}}, \tag{3.2.19}$$

with $N_1 = 1$, and $N_2 = N_3 = 2$.

The solution g_2 of (3.2.15) is unique if $\langle g_2 \rangle = 0$. It can be rewritten as

$$-g_2 = -\langle g_1 \rangle M + \Theta(\varepsilon)\partial_t \tilde{\rho}_\varepsilon M,$$

and (3.2.17) and (3.1.7) imply $g_2 = 0$. The estimation of r can be done with (3.2.16) integrated on the characteristic curves, multiplied by r/M and integrated in velocity. Since $g_2 = 0$ and the term in $\langle r \rangle M - r$ gives a negative integral with the second point of Prop. 3.5, it reads

$$\frac{1}{2}\frac{\mathrm{d}}{\mathrm{d}t}\int_{\mathbb{R}^d} \frac{r^2(t, X(t), v)}{M}\mathrm{d}v \leq -\int_{\mathbb{R}^d} \partial_t g_1\left(t, X(t), v\right)\frac{r(t, X(t), v)}{M}\mathrm{d}v,$$

where $X(t) = x + \frac{\varepsilon}{\Theta(\varepsilon)}tv$. After an integration in time and space, and using a Cauchy-Schwarz inequality, it eventually writes

$$\frac{1}{2}\|r\|_{L^\infty(0,T;L^2_{M^{-1}})} \leq \|\partial_t g_1\|_{L^1(0,T;L^2_{M^{-1}})},$$

so that an upper bound for the right-hand side is needed to complete the proof of the proposition. A differentiation in time of (3.2.17), together with (3.2.18), gives

$$\|\partial_t g_1\|^2_{L^2_{M^{-1}}} \leq \Theta(\varepsilon)\int_{\mathbb{R}^d} a_\varepsilon(k)^3 \mathrm{e}^{-a_\varepsilon(k)t}|\hat{\rho}_{in}|^2\mathrm{d}k,$$

hence, using Lemma 3.3

$$\|\partial_t g_1\|_{L^1(0,T;L^2_{M^{-1}})} \leq CT\varepsilon\sqrt{1 + |\ln(\varepsilon)|}\|\rho_{in}\|_{H^{N_d}},$$

which completes the proof. □

3.3 Numerical schemes in the case of the BGK operator

This section presents three numerical schemes designed to approximate the solution of (3.1.1), and to respect the asymptotic behavior of Prop. 3.1 and Prop. 3.2 when ε becomes small. These schemes are based respectively on an implicit formulation of (3.1.1) in Fourier variable, a micro-macro decomposition, and an integral formulation of (3.1.1). These three strategies have been investigated in [17, 18] in the case of the fractional diffusion limit of the kinetic equation, $\alpha \in (0, 2)$. Here we extend them to the case $\alpha = 2$. In this critical case, we required that not only the limit equation (3.1.5), but the asymptotic behavior (3.1.7) of the numerical solution is prescribed.

In what follows, we will denote by $t_n = n\Delta t, 0 \leq n \leq N$, such that $N\Delta t = T$ the time discretization, and we will set $f^n \approx f(t_n)$. All the numerical tests will be performed at time $T = 0.1$, the time step Δt being specified in each case. The schemes require a velocity discretization, we will denote

$$\langle f \rangle_{N_v, D} = \Delta v \sum_{\substack{j=1 \\ v_j \in D}}^{N_v} f(v_j), \tag{3.3.1}$$

the quadrature formula for the integration in velocity on the domain D. When no domain is specified, the integration is for all the index $1 \leq j \leq N_v$. In the tests, we will consider a uniform discretization of the domain $|v| \leq 10$, with N_v points symmetrically distributed on

both sides of the origin to ensure that $\langle vM\rangle_{N_v} = 0$. Namely, we will consider $N_v = 2N_v'$ with $N_v' = 100$ and use the grid

$$v_j = -10 + \frac{\Delta v}{2} + j\Delta v, \;\; 0 \leq j \leq 2N_v' - 1, \tag{3.3.2}$$

with $\Delta v = 10/N_v'$. The normalization constant m of the equilibrium M is chosen such that $\langle M\rangle_{N_v} = 1$. The space domain is bounded, and we consider periodic conditions, allowing the use of the Fourier variable. At the discrete level, the discrete Fourier variable will be used. In the tests, we will consider $x \in [-1, 1]$, discretized with N_x points such that

$$x_i = -1 + (i-1)\Delta x, \;\; 1 \leq i \leq N_x, \tag{3.3.3}$$

where $\Delta x = 2/N_x$. This space discretization is linked to the Fourier modes we use for the computation of the discrete Fourier transform, that are the integers k such that $-N_x/2 \leq k \leq N_x/2$. At the discrete level, the usual L^2 norm in space, and the norm $L^2_{M^{-1}}$ defined in (3.2.1) will be computed using the space and velocity discretization

$$\|\rho\|^2_{L^2_{N_x}} = \Delta x \sum_{i=1}^{N_x} |\rho(x_i)|^2, \quad \|f\|^2_{L^2_{M^{-1},N_x,N_v}} = \Delta x \Delta v \sum_{i=1}^{N_x}\sum_{j=1}^{N_v} \frac{|f(x_i,v_j)|^2}{M(v_j)}. \tag{3.3.4}$$

Eventually, in the following numerical tests, we will take $N_x = 32$ and consider the initial condition

$$f_{in}(x,v) = (1 + \sin(\pi x))M(v). \tag{3.3.5}$$

We want our schemes to enjoy a stronger property than the AP one. Indeed, they respect the two steps of the convergence of (3.1.1) towards (3.1.5) following the diagram (3.1.9).

The peculiar asymptotic behavior of (3.1.1) comes from the effect of the high velocities in the equilibrium function M. Indeed, its heavy-tailed character makes the usual diffusion coefficient (3.1.3) be infinite. The anomalous scaling $\Theta(\varepsilon)$ is chosen to counterbalance the weight of M for large velocities. It is then necessary to take them into account in the numerical computations. One idea would be to consider an adaptive grid for large velocities, to use as much large velocities as needed. However, linking the stiffness ε and the discretization parameters is not in the spirit of AP strategies. We propose a method based on analytical modifications of the terms degenerating into (3.1.8) in the schemes. These modifications are done consistently in the schemes, and (3.1.8) is carefully discretized to ensure the degeneracy to the limit equation (3.1.5). Once it is done, we are able to prove that the schemes respect the asymptotic behavior of (3.1.1).

3.3.1 Discretization of a_ε

Since the degeneracy of (3.1.1) to the diffusion limit (3.1.5) goes through the equation (3.1.7), it is necessary to handle the degeneracy of (3.1.7) to (3.1.5) numerically to design AP schemes for (3.1.1). In Fourier variable, both (3.1.5) and (3.1.7) are differential equations, which can be solved analytically, and that can also be solved with classical schemes. For instance, a semidiscrete-in-time implicit scheme for (3.1.7) reads

$$\frac{\hat{\bar{\rho}}_\varepsilon^{n+1} - \hat{\bar{\rho}}_\varepsilon^{n}}{\Delta t} + a_\varepsilon(k)\hat{\bar{\rho}}_\varepsilon^{n+1} = 0, \tag{3.3.6}$$

and it degenerates into a scheme solving (3.1.5) if $a_\varepsilon(k) \to a_0(k) = mc_d|k|^2$ when ε goes to 0. If the velocity integrations are done continuously, this is ensured thanks to (3.2.4). Unfortunately,

the discrete velocity integration breaks this property. Indeed, with (3.3.1) the discrete version of $a_\varepsilon(k)$ writes

$$\frac{1}{\Theta(\varepsilon)}\left\langle \frac{\varepsilon^2 k^2 v^2}{1+\varepsilon^2 k^2 v^2} M \right\rangle_{N_v} = \frac{\Delta v}{1+|\ln(\varepsilon)|}\sum_{j=1}^{N_v} \frac{k^2 v_j^2}{1+\varepsilon^2 k^2 v_j^2} M(v_j) \underset{\varepsilon\to 0}{\sim} \frac{\Delta v}{1+|\ln(\varepsilon)|}\sum_{j=1}^{N_v} k^2 v_j^2 M(v_j). \tag{3.3.7}$$

Since the quadrature uses a finite number of points, the sum above is finite whilst its continuous version is infinite. Then, the naive numerical version of $a_\varepsilon(k)$ tends to 0 when $\varepsilon \to 0$, which is not satisfactory. Consequently, it is necessary to modify analytically a_ε before applying the discretization (3.3.1), to ensure the correct asymptotic behavior of a_ε. In Remark 3.4, the expressions $a_\varepsilon(k)$ rewritten in (3.2.11)-(3.2.12)-(3.2.13) make the limit behavior of a_ε clearly appear. Hence, at the discrete level, we rather use a discrete version of these terms, where the integrals are computed with an usual quadrature (3.3.1). It ensures the discrete version $a_\varepsilon^{N_v}$ of a_ε to degenerate to the expected diffusion coefficient when ε tends to 0. To do so, in dimension 1, we use the following discrete version of a_ε, from (3.2.11)

$$a_\varepsilon^{N_v}(k) = \begin{cases} \dfrac{m}{1+|\ln(\varepsilon)|}\left\langle \dfrac{k^2 v^2}{1+\varepsilon^2 k^2 v^2}\right\rangle_{N_v,|v|\le 1} + 2m|k|^2\left(1+\dfrac{\frac{1}{2}\ln\left(\varepsilon^2+\frac{1}{|k|^2}\right)-1}{1+|\ln(\varepsilon)|}\right), & k\neq 0 \\ 0, & k=0, \end{cases} \tag{3.3.8}$$

which respects the estimates (3.2.4) at the discrete level. Eventually, with $a_\varepsilon^{N_v}$, the Euler scheme for (3.1.7) degenerates when ε goes to 0, to a Euler scheme for (3.1.5).

The numerical tests highlight this behavior. Indeed, Fig. 3.1 displays the solutions given by the scheme (3.3.6), with a_ε computed with the discretizations (3.3.7) and (3.3.8). The solutions are computed with $\Delta t = 10^{-2}$, for a range of ε. We also plot the numerical solution of the limit model approximated by

$$\frac{\hat\rho_0^{n+1}-\hat\rho_0^n}{\Delta t} + 2m|k|^2\hat\rho_0^{n+1} = 0. \tag{3.3.9}$$

When a_ε is computed directly with (3.3.7), we observe that the solution of (3.3.6) does not tend to the limit diffusion when ε goes to 0, but to the initial condition $\rho_{in} = \langle f_{in}\rangle_{N_v}$, with f_{in} defined in (3.3.5). Conversely, the solution of (3.3.6) with a_ε computed with (3.3.8), comes close to the solution of (3.3.9) when ε goes to 0. Moreover, Fig. 3.2 suggests that this convergence in ε happens with the speed $1/(1+|\ln(\varepsilon)|)$, proved in Prop. 3.2. To obtain this figure, we computed the solution $\rho_{\varepsilon,\Delta t}$ of (3.3.6) with (3.3.8), and the solution $\rho_{\Delta t}$ of (3.3.9), with $\Delta t = 10^{-2}$. Then, we plotted the relative error

$$Error(\varepsilon) = \frac{\|\rho_{\varepsilon,\Delta t} - \rho_{\Delta t}\|_{L^2_{N_x}}}{\|\rho_{\Delta t}\|_{L^2_{N_x}}},$$

with $\|\cdot\|_{L^2_{N_x}}$ defined in (3.3.4), as a function of $\varepsilon \in (0,1)$.

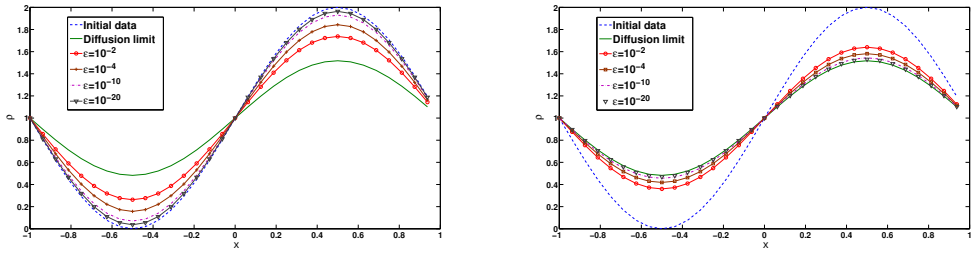

Figure 3.1: For $\Delta t = 10^{-2}$, the solutions of (3.3.9) and (3.3.6) at time $T = 0.1$ for different values of ε. Left: when a_ε is computed with (3.3.7). Right: when a_ε is computed with (3.3.8).

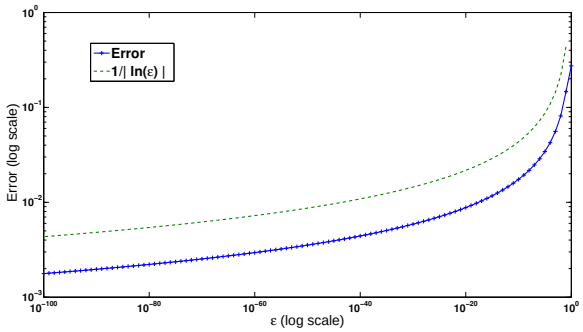

Figure 3.2: For $\Delta t = 10^{-2}$, the relative error between the solution of the scheme (3.3.6) and the limit scheme (3.3.9) at time $T = 0.1$, in function of ε (log scale).

3.3.2 Implicit scheme (IS)

The first idea to write a scheme for (3.1.1) which enjoys the AP property is to use a fully implicit scheme for (3.1.1) written in Fourier variable. Indeed, it is well-known that in the case of the classical diffusion limit, such a scheme degenerates when $\varepsilon \to 0$ into a scheme solving the limit equation. In our case, such an approach does not work, due to the effects of large velocities. Then, it is necessary to suitably write the scheme to make this degeneracy appear. We start with (3.1.1) written in space Fourier variable, and we consider a fully implicit time discretization

$$\frac{\hat{f}^{n+1} - \hat{f}^n}{\Delta t} + \frac{1}{\Theta(\varepsilon)} \left(1 + \mathrm{i}\varepsilon k \cdot v\right) \hat{f}^{n+1} = \frac{1}{\Theta(\varepsilon)} \hat{\rho}^{n+1} M, \tag{3.3.10}$$

where the dependance in ε of f^{n+1}, f^n and ρ^{n+1} has been omitted to simplify the notations. This scheme degenerates when $\varepsilon \to 0$ into

$$\hat{f}^{n+1} = \hat{\rho}^{n+1} M.$$

Therefore, provided that the density $\hat{\rho}^{n+1}$ is known, the scheme (3.3.10) enjoys the AP property, and $\hat{f}^{n+1}$ reads

$$\hat{f}^{n+1} = \frac{\Theta(\varepsilon)\hat{f}^n + \Delta t\ \hat{\rho}^{n+1} M}{\Theta(\varepsilon) + \Delta t + \mathrm{i}\varepsilon \Delta t\ k \cdot v}. \tag{3.3.11}$$

An expression for $\hat{\rho}^{n+1}$ is given by a fully implicit time discretization of (3.1.1) integrated in velocity

$$\frac{\hat{\rho}^{n+1} - \hat{\rho}^n}{\Delta t} + \frac{1}{\Theta(\varepsilon)} \left\langle \mathrm{i}\varepsilon k \cdot v \hat{f}^{n+1} \right\rangle = 0,$$

which writes, using the expression of $\hat{f}^{n+1}$ in (3.3.11)

$$\frac{\hat{\rho}^{n+1} - \hat{\rho}^n}{\Delta t} + \left\langle \frac{\mathrm{i}\varepsilon k \cdot v \hat{f}^n}{\Theta(\varepsilon) + \Delta t + \mathrm{i}\Delta t \varepsilon k \cdot v} \right\rangle + \frac{\Delta t}{\Theta(\varepsilon)} \left\langle \frac{\mathrm{i}\varepsilon k \cdot v M}{\Theta(\varepsilon) + \Delta t + \mathrm{i}\varepsilon \Delta t k \cdot v} \right\rangle \hat{\rho}^{n+1} = 0. \tag{3.3.12}$$

Using the symmetry of M, the last term of the previous expression can be rewritten as

$$\frac{\Delta t}{\Theta(\varepsilon)} \left\langle \frac{\mathrm{i}\varepsilon k \cdot v M}{\Theta(\varepsilon) + \Delta t + \mathrm{i}\varepsilon \Delta t k \cdot v} \right\rangle \hat{\rho}^{n+1} = \frac{\Delta t^2}{\Theta(\varepsilon)} \left\langle \frac{\varepsilon^2 (k \cdot v)^2}{\left(\Theta(\varepsilon) + \Delta t\right)^2 + \varepsilon^2 \Delta t^2 \left(k \cdot v\right)^2} M \right\rangle \hat{\rho}^{n+1} \tag{3.3.13}$$

$$= \frac{1}{\Theta(\varepsilon)} \left\langle \frac{\varepsilon^2 \left(k \cdot v\right)^2}{\left(\frac{\Theta(\varepsilon) + \Delta t}{\Delta t}\right)^2 + \varepsilon^2 \left(k \cdot v\right)^2} M \right\rangle \hat{\rho}^{n+1}. \tag{3.3.14}$$

The expression (3.3.13) indicates that the term is of order Δt^2 for fixed ε, and thus can be removed or modified with no incidence on the accuracy of the scheme. The expression (3.3.14) shows that it degenerates into the coefficient $a_\varepsilon(k)$ when ε decreases. Since the second term of (3.3.12) vanishes for small ε, if the integrations in velocity are done continuously, the scheme degenerates when ε to 0 into a scheme solving (3.1.7). To ensure the AP property at the fully discrete level, (3.3.14) can be approximated by

$$\left(\frac{\Delta t}{\Theta(\varepsilon) + \Delta t}\right)^2 \frac{1}{\Theta(\varepsilon)} \left\langle \frac{\varepsilon^2 (k \cdot v)^2}{1 + \varepsilon^2 (k \cdot v)^2} M \right\rangle \hat{\rho}^{n+1/2} = \left(\frac{\Delta t}{\Theta(\varepsilon) + \Delta t}\right)^2 a_\varepsilon(k) \hat{\rho}^{n+1/2},$$

where $\hat{\rho}^{n+1/2}$ can be taken equal to $\hat{\rho}^n$ or $\hat{\rho}^{n+1}$, depending on the desired limit scheme (implicit or explicit). Then the coefficient a_ε is numerically approximated as in Section 3.3.1 to ensure the AP property. Eventually, we have the following proposition

Proposition 3.6. *We consider the following scheme defined for all k and all time indices $0 \leq n \leq N, N\Delta t = T$ by*

$$\begin{cases} \dfrac{\hat{f}^{n+1} - \hat{f}^n}{\Delta t} + \dfrac{1}{\Theta(\varepsilon)} \left(1 + \mathrm{i}\varepsilon k \cdot v\right) \hat{f}^{n+1} = \dfrac{1}{\Theta(\varepsilon)} \hat{\rho}^{n+1} M \\ \dfrac{\hat{\rho}^{n+1} - \hat{\rho}^n}{\Delta t} + \left\langle \dfrac{\mathrm{i}\varepsilon k \cdot v \hat{f}^n}{\Theta(\varepsilon) + \Delta t + \mathrm{i}\Delta t \varepsilon k \cdot v} \right\rangle_{N_v} + \left(\dfrac{\Delta t}{\Delta t + \Theta(\varepsilon)} \right)^2 a_\varepsilon^{N_v}(k) \hat{\rho}^{n+1/2} = 0, \end{cases} \tag{3.3.15}$$

with $\Theta(\varepsilon)$ and $a_\varepsilon^{N_v}$ defined in (3.1.6) *and* (3.3.8)*, and with initial condition $\hat{f}^0(k,v) = \hat{f}_{in}(k,v), \hat{\rho}^0(k) = \left\langle \hat{f}^0(k,\cdot) \right\rangle_{N_v}$. The quantity $\hat{\rho}^{n+1/2}$ can be chosen equal to $\hat{\rho}^n$ or $\hat{\rho}^{n+1}$ depending on the desired asymptotic scheme (implicit or explicit in time). This scheme has the following properties:*

1. *The scheme is of order* 1 *for fixed $\varepsilon > 0$ and preserves the total mass.*

2. *The scheme is AP: for a fixed Δt, the scheme solves the diffusion equation* (3.1.5) *when ε goes to* 0

$$\frac{\hat{\rho}^{n+1} - \hat{\rho}^n}{\Delta t} + m c_d |k|^2 \hat{\rho}^{n+1/2} = 0, \tag{3.3.16}$$

with $c_1 = 2, c_2 = \pi, c_3 = \frac{8\pi}{3}$ and where m has been defined in (3.1.4)*.*

Remark 3.7. The degeneracy of (3.3.15) to a scheme solving (3.1.5) respects the two dynamics discussed in the diagram (3.1.9). Indeed, the numerical tests show that (3.3.15) degenerates with speed $\varepsilon\sqrt{1 + |\ln(\varepsilon)|}$ to

$$\frac{\hat{\rho}^{n+1} - \hat{\rho}^n}{\Delta t} + a_\varepsilon^{N_v}(k) \hat{\rho}^{n+1/2} = 0, \tag{3.3.17}$$

which solves (3.1.7). Then letting ε going to 0 in the previous scheme makes it degenerate to (3.3.16) with speed $1/(1 + |\ln(\varepsilon)|)$.

Proof. The first point of Prop. 3.6 is a direct consequence of the fact that we used an Euler scheme for (3.1.1), and that the modifications we applied to it were done consistently. Taking $k = 0$ in the second line of (3.3.15) yields the conservation of the total mass. Eventually, with the modification of the term (3.3.14), the AP character is straightforward. Indeed, letting ε becomes small with fixed Δt in (3.3.15) leads to

$$\begin{cases} \hat{f}^{n+1} = \hat{\rho}^{n+1} M \\ \dfrac{\hat{\rho}^{n+1} - \hat{\rho}^n}{\Delta t} + a_\varepsilon^{N_v}(k) \hat{\rho}^{n+1/2} = 0, \end{cases}$$

which degenerates into a scheme solving (3.1.5) when $\varepsilon \to 0$. □

3.3.3 Micro-macro scheme (MMS)

In the previous part, we proposed an implicit scheme for (3.1.1), which has the same behavior as the solution of (3.1.1) when ε goes to 0. However, the use of the Fourier variable may be restrictive in some cases, and its extension to more general collision operators seems difficult. Moreover, the implicit treatment of the transport operator induces high computational cost, especially in multi-dimensional cases. We propose here a scheme based on a micro-macro decomposition of the distribution function f_ε, which respects the behavior of f_ε when $\varepsilon \to 0$. It treats the transport terms explicitly, and can be extended to the case of general collision operators of [55] with a strategy similar to [49].

Denoting $\rho_\varepsilon = \langle f_\varepsilon \rangle$, we consider the decomposition $f_\varepsilon(t,x,v) = \rho_\varepsilon(t,x)M(v) + g_\varepsilon(t,x,v)$, such that $\langle g_\varepsilon \rangle = 0$. Inserting it in (3.1.1) and integrating in velocity gives

$$\partial_t \rho_\varepsilon + \frac{\varepsilon}{\Theta(\varepsilon)} \langle v \cdot \nabla_x g_\varepsilon \rangle = 0. \tag{3.3.18}$$

Then, we multiply (3.3.18) by M and we subtract it from (3.1.1) to get an equation for g_ε

$$\partial_t g_\varepsilon + \frac{\varepsilon}{\Theta(\varepsilon)} v \cdot \nabla_x \rho_\varepsilon M + \frac{\varepsilon}{\Theta(\varepsilon)} \left(v \cdot \nabla_x g_\varepsilon - \langle v \cdot \nabla_x g_\varepsilon \rangle M \right) = -\frac{1}{\Theta(\varepsilon)} g_\varepsilon. \tag{3.3.19}$$

A semi-discrete-in-time numerical scheme can be designed following [52], in which we implicit the stiffest terms

$$\begin{cases} \dfrac{g^{n+1} - g^n}{\Delta t} + \dfrac{\varepsilon}{\Theta(\varepsilon)} v \cdot \nabla_x \rho^n M + \dfrac{\varepsilon}{\Theta(\varepsilon)} \left(v \cdot \nabla_x g^n - \langle v \cdot \nabla_x g^n \rangle M \right) = -\dfrac{1}{\Theta(\varepsilon)} g^{n+1} \\ \dfrac{\rho^{n+1} - \rho^n}{\Delta t} + \dfrac{\varepsilon}{\Theta(\varepsilon)} \left\langle v \cdot \nabla_x g^{n+1} \right\rangle = 0. \end{cases} \tag{3.3.20}$$

Here, the dependence in ε of ρ^n and g^n is omitted to simplify the notations. For fixed ε, it is a consistent scheme, it remains to check wether it preserves the correct asymptotic. With the first line of (3.3.20), $g^{n+1} = O(\varepsilon)$ when Δt is fixed, and then $g^{n+1} = -\varepsilon v \cdot \nabla_x \rho^n M + o(\varepsilon)$. When reported in the second line of (3.3.20), this gives the following limit scheme for ρ

$$\frac{\rho^{n+1} - \rho^n}{\Delta t} - \frac{1}{1 + |\ln(\varepsilon)|} \langle v \cdot \nabla_x \left(v \cdot \nabla_x \rho^n M \right) \rangle = 0, \tag{3.3.21}$$

which does not corresponds to the expected diffusion limit. Indeed, the term into brackets is infinite when the integration in velocity is done continuously, but it is finite when the discretization (3.3.1) is applied. Hence, in this latter case, when $\varepsilon \to 0$, the limit scheme is $\rho^{n+1} = \rho^n$, which is not consistent with (3.1.5). It is then necessary to modify (3.3.20) to ensure the correct asymptotic behavior. To do so, we modify the macro equation by making appear the inverse of the transport operator. We first remark that $\left\langle v \cdot \nabla_x g^{n+1} \right\rangle = \left\langle v \cdot \nabla_x f^{n+1} \right\rangle$, we then use a semi discrete implicit formulation of f as in the previous part (see (3.3.10) for instance)

$$f^{n+1} = \frac{\Theta(\varepsilon)}{\Theta(\varepsilon) + \Delta t} \left(I + \frac{\Delta t}{\Theta(\varepsilon) + \Delta t} \varepsilon v \cdot \nabla_x \right)^{-1} f^n + \frac{\Delta t}{\Theta(\varepsilon) + \Delta t} \left(I + \frac{\Delta t}{\Theta(\varepsilon) + \Delta t} \varepsilon v \cdot \nabla_x \right)^{-1} \rho^{n+1} M.$$

This expression is injected in the flux of the macro equation of (3.3.20) to get

$$\frac{\rho^{n+1} - \rho^n}{\Delta t} + \frac{\varepsilon}{\Theta(\varepsilon) + \Delta t} \left\langle v \cdot \nabla_x \left(\left(I + \frac{\Delta t}{\Theta(\varepsilon) + \Delta t} \varepsilon v \cdot \nabla_x \right)^{-1} f^n \right) \right\rangle \tag{3.3.22}$$

$$+\frac{\varepsilon}{\Theta(\varepsilon)}\frac{\Delta t}{\Theta(\varepsilon)+\Delta t}\left\langle v\cdot\nabla_x\left(\left(I+\frac{\Delta t}{\Theta(\varepsilon)+\Delta t}\varepsilon v\cdot\nabla_x\right)^{-1}\rho^{n+1}M\right)\right\rangle=0. \quad (3.3.23)$$

Since the scheme is first order in time, the bracket in (3.3.22) can be simplified consistently in $\langle v\cdot\nabla_x f^n\rangle$ to avoid the inversion of a differential operator. For the same reason, we could remove (3.3.23) with no incidence on the consistency of the scheme; however, it degenerates when $\varepsilon\to 0$ to the diffusion of (3.1.5). Therefore, this term is kept to ensure the AP property of the scheme, but it must be treated with care to take correctly the effects of the high velocities into account. In Fourier variable, and using the evenness of M, (3.3.23) reads

$$\frac{1}{\Theta(\varepsilon)}\left(\frac{\Delta t}{\Theta(\varepsilon)+\Delta t}\right)^2\left\langle\frac{\varepsilon^2(k\cdot v)^2}{1+\left(\frac{\Delta t}{\Theta(\varepsilon)+\Delta t}\right)^2\varepsilon^2(k\cdot v)^2}M\right\rangle\hat\rho^{n+1}.$$

This term is of order Δt^2 when ε is fixed, and it degenerates to $a_\varepsilon(k)\hat\rho^{n+1}$ (with a_ε defined in (3.1.8)) when ε becomes small with Δt fixed. Thus, (3.3.23) can be modified consistently in $\Delta t^2/(\Theta(\varepsilon)+\Delta t)^2 a_\varepsilon(k)\hat\rho^{n+1/2}$, which ensures both the AP character of the scheme, and the fact that the numerical solution solves (3.1.7) when ε belongs to the intermediate regime in which the solution f_ε of (3.1.1) solves (3.1.7). Here, $\hat\rho^{n+1/2}$ can be chosen equal to $\hat\rho^n$ or $\hat\rho^{n+1}$.

The passage from the semi-discrete-in-time scheme to the fully discretized scheme can then be done with the quadrature (3.3.1), and the suitable discretization of a_ε defined in (3.1.8), as in section 3.3.1. The derivatives in space are treated with a classical first order upwind scheme; for a sake of simplicity in the notations, we still write here the spatial derivatives as continuous. Eventually, we have the following proposition.

Proposition 3.8. *We consider the following scheme (discretized in time and velocity) defined for all $x\in\mathbb{R}^d$, $v_j, 1\le j\le N_v$ and all time indices $0\le n\le N, N\Delta t=T>0$ by*

$$\begin{cases}\dfrac{g^{n+1}-g^n}{\Delta t}+\dfrac{\varepsilon}{\Theta(\varepsilon)}v\cdot\nabla_x\rho^n M+\dfrac{\varepsilon}{\Theta(\varepsilon)}\left(v\cdot\nabla_x g^n-\langle v\cdot\nabla_x g^n\rangle_{N_v}M\right)=-\dfrac{1}{\Theta(\varepsilon)}g^{n+1}\\ \dfrac{\rho^{n+1}-\rho^n}{\Delta t}+\dfrac{\varepsilon}{\Theta(\varepsilon)+\Delta t}\langle v\cdot\nabla_x g^n\rangle_{N_v}+\left(\dfrac{\Delta t}{\Theta(\varepsilon)+\Delta t}\right)^2\mathcal{F}^{-1}\left(a_\varepsilon^{N_v}\hat\rho^{n+1/2}\right)=0,\end{cases} \quad (3.3.24)$$

with $\Theta(\varepsilon)$ and $a_\varepsilon^{N_v}$ defined in (3.1.6) and in (3.3.8), where $\mathcal{F}^{-1}$ denotes the inverse of the Fourier transform, and with initial condition $\rho^0=\langle f_{in}\rangle_{N_v}$, and $g^0=f_{in}-\rho^0 M$. The quantity $\hat\rho^{n+1/2}$ can be chosen equal to $\hat\rho^n$ or $\hat\rho^{n+1}$ depending on the desired asymptotic scheme (implicit or explicit in time). This scheme has the following properties:

1. *The scheme is of first order in time for any fixed $\varepsilon>0$ and preserves the total mass.*
2. *The scheme is AP: for a fixed Δt, the scheme solves the diffusion equation (3.1.5) when ε goes to 0*
$$\frac{\hat\rho^{n+1}-\hat\rho^n}{\Delta t}+mc_d|k|^2\hat\rho^{n+1/2}=0, \quad (3.3.25)$$
with $c_1=2, c_2=\pi, c_3=\frac{8\pi}{3}$, and where m has beed defined in (3.1.4).

Remark 3.9. As in the case of the implicit scheme, this scheme enjoys a property stronger than being AP, since it respects the diagram (3.1.9). Hence, it respects the dynamics of the convergence to the solution of the diffusion equation (3.1.5) when $\varepsilon\to 0$. Indeed, the numerical

tests show that (3.3.24) degenerates with speed $\varepsilon\sqrt{1+|\ln(\varepsilon)|}$ to the scheme (3.3.17), which solves (3.1.7). The degeneracy to the limit scheme (3.3.25) happens much more slowly, with speed $1/(1+|\ln(\varepsilon)|)$.

Remark 3.10. If we want to avoid the use of Fourier variable, we can replace $\mathcal{F}^{-1}\left(a_\varepsilon^{N_v}\hat{\rho}^{n+1/2}\right)$ by $-mc_d\Delta_x\rho^{n+1/2}$. This modification is consistent with (3.1.1), and still enjoys the AP property, but the convergence to the limit scheme does not make a scheme for (3.1.7) arise in the intermediate regime in ε.

Proof. Since the first point comes immediately from the derivation of the scheme, let us prove the second point. The first line of (3.3.24) gives that $g^{n+1}=o(1)$ when $\varepsilon\to 0$. Once injected in the second line, it yields

$$\frac{\rho^{n+1}-\rho^n}{\Delta t}+\mathcal{F}^{-1}\left(a_\varepsilon^{N_v}\hat{\rho}^{n+1/2}\right)=o(1),$$

which is a consistent approximation of (3.1.7). Finally, $a_\varepsilon^{N_v}$ tends to $mc_d|k|^2$ when $\varepsilon\to 0$, which concludes the proof. □

3.3.4 Integral formulation based scheme (DS)

In the previous parts, we proposed two numerical schemes solving (3.1.1), which in addition respect the asymptotic behavior of the continuous solution when ε goes to 0. They enjoy the AP property, but their precision is not uniform in ε. In this section, we propose a scheme based on an integral formulation of (3.1.1) in Fourier variable. This approach was investigated in [17]-[18] in the case of the fractional diffusion limit. This scheme was shown to be uniformly accurate (UA) : its precision does not depend on the stiffness parameter ε. A similar strategy is performed here, to deal with the diffusion case with an anomalous scaling.

We start from the Duhamel form for $\hat{f}_\varepsilon$, solution of (3.1.1) in space Fourier variable

$$\hat{f}_\varepsilon(t,k,v)=A_0(t,k,v)+\int_0^{\frac{t}{\Theta(\varepsilon)}}\mathrm{e}^{-s(1+\mathrm{i}\varepsilon k\cdot v)}\hat{\rho}_\varepsilon(t-\Theta(\varepsilon)s,k)M(v)\mathrm{d}s,$$

where

$$A_0(t,k,v)=\mathrm{e}^{-t(1+\mathrm{i}\varepsilon k\cdot v)}\hat{f}_{in}(k,v). \tag{3.3.26}$$

Evaluating at time t_{n+1} and integrating in velocity, we get

$$\hat{\rho}_\varepsilon(t_{n+1},k)=\langle A_0(t_{n+1},k,\cdot)\rangle+\sum_{j=0}^{n}\int_{\frac{t_j}{\Theta(\varepsilon)}}^{\frac{t_{j+1}}{\Theta(\varepsilon)}}\left\langle\mathrm{e}^{-s(1+\mathrm{i}\varepsilon k\cdot v)}M\right\rangle\hat{\rho}_\varepsilon(t_{n+1}-\Theta(\varepsilon)s,k)\mathrm{d}s. \tag{3.3.27}$$

To write a scheme on $\hat{\rho}_\varepsilon$, we perform a quadrature of order 2 in the integral in s; we have $\forall j\in[\![0,n]\!],\forall s\in\left[\frac{t_j}{\Theta(\varepsilon)},\frac{t_{j+1}}{\Theta(\varepsilon)}\right]$,

$$\hat{\rho}_\varepsilon(t_{n+1}-\Theta(\varepsilon)s,k)=\left(1-\frac{\Theta(\varepsilon)s-t_j}{\Delta t}\right)\hat{\rho}_\varepsilon\left(t_{n+1}-t_j\right)+\frac{\Theta(\varepsilon)s-t_j}{\Delta t}\hat{\rho}_\varepsilon(t_{n+1}-t_{j+1})+O(\Delta t^2). \tag{3.3.28}$$

Assuming that the time derivatives of $\hat{\rho}_\varepsilon$ are uniformly bounded in ε, the remainder is uniformly bounded by a term of magnitude $O\left(\Delta t^2\right)$ independently of ε. Inserting (3.3.28) in (3.3.27) yields the following scheme for $\hat{\rho}_\varepsilon$

$$\hat{\rho}_\varepsilon^{n+1}=\langle A_0(t_{n+1},k,\cdot)\rangle+\sum_{j=0}^{n}b_j\hat{\rho}_\varepsilon^{n-j}+c_j\hat{\rho}_\varepsilon^{n+1-j}, \tag{3.3.29}$$

where the coefficients $b_j, c_j, 0 \leq j \leq n$ are given by

$$b_j = \int_{\frac{t_j}{\Theta(\varepsilon)}}^{\frac{t_{j+1}}{\Theta(\varepsilon)}} \frac{\Theta(\varepsilon)s - t_j}{\Delta t} \left\langle \mathrm{e}^{-s(1+\mathrm{i}\varepsilon k\cdot v)} M \right\rangle \mathrm{d}s$$
$$c_j = \int_{\frac{t_j}{\Theta(\varepsilon)}}^{\frac{t_{j+1}}{\Theta(\varepsilon)}} \left(1 - \frac{\Theta(\varepsilon)s - t_j}{\Delta t}\right) \left\langle \mathrm{e}^{-s(1+\mathrm{i}\varepsilon k\cdot v)} M \right\rangle \mathrm{d}s.$$

The consistency of this scheme comes directly from its derivation, but the discretization of the integrals in velocity appearing in b_j and c_j is crucial to ensure the AP property. Indeed, as in the previous parts, their continuous limit when ε goes to 0 makes the diffusion (3.1.5) appear. But the effects of the high velocities are not captured if (3.3.1) is used. Therefore, it is necessary to modify analytically b_j and c_j before applying the velocity discretization. The velocity integration of b_j and c_j can be rewritten as

$$\left\langle \mathrm{e}^{-s(1+\mathrm{i}\varepsilon k\cdot v)} M \right\rangle = \mathrm{e}^{-s} + \left\langle \left(\mathrm{e}^{-s(1+\mathrm{i}\varepsilon k\cdot v)} - \mathrm{e}^{-s}\right) M \right\rangle_{|v|<1} + \left\langle \left(\mathrm{e}^{-s(1+\mathrm{i}\varepsilon k\cdot v)} - \mathrm{e}^{-s}\right) M \right\rangle_{|v|\geq 1},$$

because $\langle M \rangle = 1$. After that, the change of variables $w = \varepsilon v$ is performed in the last term to capture the high velocity effects, and the integrals in s of b_j and c_j are computed exactly to get

$$\begin{aligned} b_j = {} & -\mathrm{e}^{-\frac{t_{j+1}}{\Theta(\varepsilon)}} + \frac{\Theta(\varepsilon)}{\Delta t}\mathrm{e}^{-\frac{t_j}{\Theta(\varepsilon)}}\left(1 - \mathrm{e}^{-\frac{\Delta t}{\Theta(\varepsilon)}}\right) + m\left\langle \mathrm{e}^{-\frac{t_{j+1}}{\Theta(\varepsilon)}} - \frac{\mathrm{e}^{-\frac{t_{j+1}}{\Theta(\varepsilon)}(1+\mathrm{i}\varepsilon k\cdot v)}}{1+\mathrm{i}\varepsilon k\cdot v}\right\rangle_{|v|<1} \qquad (3.3.30) \\ & + \frac{\Theta(\varepsilon)}{\Delta t} m\left\langle \mathrm{e}^{-\frac{t_j}{\Theta(\varepsilon)}(1+\mathrm{i}\varepsilon k\cdot v)} \frac{1 - \mathrm{e}^{-\frac{\Delta t}{\Theta(\varepsilon)}(1+\mathrm{i}\varepsilon k\cdot v)}}{(1+\mathrm{i}\varepsilon k\cdot v)^2} - \mathrm{e}^{-\frac{t_j}{\Theta(\varepsilon)}}\left(1 - \mathrm{e}^{-\frac{\Delta t}{\Theta(\varepsilon)}}\right)\right\rangle_{|v|<1} \\ & + \varepsilon^2 m\left\langle \frac{1}{|w|^{d+2}}\left(\mathrm{e}^{-\frac{t_{j+1}}{\Theta(\varepsilon)}} - \frac{\mathrm{e}^{-\frac{t_{j+1}}{\Theta(\varepsilon)}(1+\mathrm{i}k\cdot w)}}{1+\mathrm{i}k\cdot w}\right)\right\rangle_{|w|\geq\varepsilon} \\ & + \frac{\Theta(\varepsilon)}{\Delta t}\varepsilon^2 m\left\langle \frac{1}{|w|^{d+2}}\left(\mathrm{e}^{\frac{t_j}{\Theta(\varepsilon)}(1+\mathrm{i}k\cdot w)} \frac{1 - \mathrm{e}^{-\frac{\Delta t}{\Theta(\varepsilon)}(1+\mathrm{i}k\cdot w)}}{(1+\mathrm{i}k\cdot w)^2} - \mathrm{e}^{-\frac{t_j}{\Theta(\varepsilon)}}(1 - \mathrm{e}^{-\frac{\Delta t}{\Theta(\varepsilon)}})\right)\right\rangle_{|w|\geq\varepsilon}, \end{aligned}$$

$$\begin{aligned} c_j = {} & \mathrm{e}^{-\frac{t_j}{\Theta(\varepsilon)}} - \frac{\Theta(\varepsilon)}{\Delta t}\mathrm{e}^{-\frac{t_j}{\Theta(\varepsilon)}}\left(1 - \mathrm{e}^{-\frac{\Delta t}{\Theta(\varepsilon)}}\right) \qquad (3.3.31) \\ & - \frac{\Theta(\varepsilon)}{\Delta t} m\left\langle \mathrm{e}^{-\frac{t_j}{\Theta(\varepsilon)}(1+\mathrm{i}\varepsilon k\cdot v)} \frac{1 - \mathrm{e}^{-\frac{\Delta t}{\Theta(\varepsilon)}(1+\mathrm{i}\varepsilon k\cdot v)}}{(1+\mathrm{i}\varepsilon k\cdot v)^2} - \mathrm{e}^{-\frac{t_j}{\Theta(\varepsilon)}}\left(1 - \mathrm{e}^{-\frac{\Delta t}{\Theta(\varepsilon)}}\right)\right\rangle_{|v|<1} \\ & + m\left\langle \frac{\mathrm{e}^{-\frac{t_j}{\Theta(\varepsilon)}(1+\mathrm{i}\varepsilon k\cdot v)}}{1+\mathrm{i}\varepsilon k\cdot v} - \mathrm{e}^{-\frac{t_j}{\Theta(\varepsilon)}}\right\rangle_{|v|<1} + \varepsilon^2 m\left\langle \frac{1}{|w|^{d+2}}\left(\frac{\mathrm{e}^{-\frac{t_j}{\Theta(\varepsilon)}(1+\mathrm{i}k\cdot w)}}{1+\mathrm{i}k\cdot w} - \mathrm{e}^{-\frac{t_j}{\Theta(\varepsilon)}}\right)\right\rangle_{|w|\geq\varepsilon} \qquad (3.3.32) \\ & - \frac{\Theta(\varepsilon)}{\Delta t}\varepsilon^2 m\left\langle \frac{1}{|w|^{d+2}}\left(\mathrm{e}^{-\frac{t_j}{\Theta(\varepsilon)}(1+\mathrm{i}k\cdot w)} \frac{1 - \mathrm{e}^{-\frac{\Delta t}{\Theta(\varepsilon)}(1+\mathrm{i}k\cdot w)}}{(1+\mathrm{i}k\cdot w)^2} - \mathrm{e}^{-\frac{t_j}{\Theta(\varepsilon)}}\left(1 - \mathrm{e}^{-\frac{\Delta t}{\Theta(\varepsilon)}}\right)\right)\right\rangle_{|w|\geq\varepsilon}. \end{aligned}$$

However, it is still not sufficient to ensure the AP character of the scheme when the integrals

are discretized since, when $j=0$, the term (3.3.32) reads

$$\Theta(\varepsilon)\left(\frac{m}{1+|\ln(\varepsilon)|}\left\langle\frac{(k\cdot v)^2}{1+\varepsilon^2(k\cdot v)^2}\right\rangle_{|v|<1}+\frac{m}{1+|\ln(\varepsilon)|}\left\langle\frac{1}{|w|^{d+2}}\frac{(k\cdot w)^2}{1+(k\cdot w)^2}\right\rangle_{|w|\geq\varepsilon}\right),$$

which is equal to $\Theta(\varepsilon)a_\varepsilon$, with a_ε defined in (3.1.8) and rewritten in (3.2.6) (note that the equality (3.2.6) is valid for any dimension). In Section 3.3.1, we established that the discretization of this term is crucial to ensure the AP property of our schemes. Following the strategy presented previously, we then replace (3.3.32) by an appropriate discretization $\Theta(\varepsilon)a_\varepsilon^{N_v}$ defined in (3.3.8) when $j=0$. Eventually, c_0 rewrites

$$c_0=\Theta(\varepsilon)a_\varepsilon^{N_v}(k)+1-\frac{\Theta(\varepsilon)}{\Delta t}\left(1-\mathrm{e}^{-\frac{\Delta t}{\Theta(\varepsilon)}}\right)-\frac{\Theta(\varepsilon)}{\Delta t}m\left\langle\frac{1-\mathrm{e}^{-\frac{\Delta t}{\Theta(\varepsilon)}(1+\mathrm{i}\varepsilon k\cdot v)}}{(1+\mathrm{i}\varepsilon k\cdot v)^2}-1+\mathrm{e}^{-\frac{\Delta t}{\Theta(\varepsilon)}}\right\rangle_{|v|<1} \tag{3.3.33}$$

$$-\frac{\Theta(\varepsilon)}{\Delta t}m\varepsilon^2\left\langle\frac{1}{|w|^{d+2}}\left(\frac{1-\mathrm{e}^{-\frac{\Delta t}{\Theta(\varepsilon)}(1+\mathrm{i}k\cdot w)}}{(1+\mathrm{i}k\cdot w)^2}-1+\mathrm{e}^{-\frac{\Delta t}{\Theta(\varepsilon)}}\right)\right\rangle_{|w|\geq\varepsilon}.$$

The expressions b_j ($j\geq 0$), c_j ($j\geq 1$) and c_0, defined in (3.3.30)-(3.3.31)-(3.3.33), computed with the discretization (3.3.1) make the scheme (3.3.29) AP. Moreover, let us remark that the scheme only uses ρ and not f. It implies that the computation of the whole distribution f is not necessary, which represents a gain of computational cost, since the problem for f is of higher dimension than the problem on ρ. Let us note that f can even so be computed in Fourier variable with a scheme similar to (3.3.29). Indeed, Duhamel formula of (3.1.1) between the times t_n and t_{n+1} leads to

$$\hat f(t_{n+1},k,v)=\mathrm{e}^{-\frac{\Delta t}{\Theta(\varepsilon)}(1+\mathrm{i}\varepsilon k\cdot v)}\hat f(t_n,k,v)+\int_0^{\frac{\Delta t}{\Theta(\varepsilon)}}\mathrm{e}^{-s(1+\mathrm{i}\varepsilon k\cdot v)}\hat\rho(t_{n+1}-\Theta(\varepsilon)s,k)M(v)\mathrm{d}s. \tag{3.3.34}$$

As in the scheme for $\hat\rho$, we apply the quadrature (3.3.28) in the integral in s, and the scheme for $\hat f$ reads

$$\hat f^{n+1}=\mathrm{e}^{-\frac{\Delta t}{\Theta(\varepsilon)}(1+\mathrm{i}\varepsilon k\cdot v)}\hat f^n+\beta\hat\rho^nM+\gamma\hat\rho^{n+1}M,$$

with

$$\beta=\int_0^{\frac{\Delta t}{\Theta(\varepsilon)}}\frac{\Theta(\varepsilon)s}{\Delta t}\mathrm{e}^{-s(1+\mathrm{i}\varepsilon k\cdot v)}\mathrm{d}s=-\frac{\mathrm{e}^{-\frac{\Delta t}{\Theta(\varepsilon)}(1+\mathrm{i}\varepsilon k\cdot v)}}{1+\mathrm{i}\varepsilon k\cdot v}+\frac{\Theta(\varepsilon)}{\Delta t}\frac{1-\mathrm{e}^{-\frac{\Delta t}{\Theta(\varepsilon)}(1+\mathrm{i}\varepsilon k\cdot v)}}{(1+\mathrm{i}\varepsilon k\cdot v)^2} \tag{3.3.35}$$

$$\gamma=\int_0^{\frac{\Delta t}{\Theta(\varepsilon)}}\left(1-\frac{\Theta(\varepsilon)s}{\Delta t}\right)\mathrm{e}^{-s(1+\mathrm{i}\varepsilon k\cdot v)}\mathrm{d}s=\frac{1}{1+\mathrm{i}\varepsilon k\cdot v}-\frac{\Theta(\varepsilon)}{\Delta t}\frac{1-\mathrm{e}^{-\frac{\Delta t}{\Theta(\varepsilon)}(1+\mathrm{i}\varepsilon k\cdot v)}}{(1+\mathrm{i}\varepsilon k\cdot v)^2}. \tag{3.3.36}$$

Eventually, we have the following proposition.

Proposition 3.11. *Provided the initial condition* $\left(\hat f^0(k,v_j)\right)_{j=1,\dots,N_v}=\left(\hat f_{in}(k,v_j)\right)_{j=1,\dots,N_v}$, $\hat\rho^0(k)=\left\langle\hat f^0(k,\cdot)\right\rangle_{N_v}$, *we consider the following scheme, defined for all k and all time indices $0\leq n\leq N, N\Delta t=T$, by*

$$\begin{cases}\hat\rho^{n+1}(k)=\dfrac{\langle A_0(t_{n+1},k,v)\rangle_{N_v}+b_0\hat\rho^n(k)+\sum_{j=1}^n\left[b_j\hat\rho^{n-j}(k)+c_j\hat\rho^{n+1-j}(k)\right]}{1-c_0}\\ \hat f^{n+1}=\mathrm{e}^{-\frac{\Delta t}{\Theta(\varepsilon)}(1+\mathrm{i}\varepsilon k\cdot v)}\hat f^{n+1}+\beta\hat\rho^nM+\gamma\hat\rho^{n+1}M,\end{cases} \tag{3.3.37}$$

with A_0, β, γ defined in (3.3.26)-(3.3.35)-(3.3.36)*, and $b_j (j \geq 0), c_j (j \geq 1)$ and c_0 defined in* (3.3.30)-(3.3.31)-(3.3.33) *and computed with* (3.3.1)*. This scheme has the following properties:*

1. *The scheme is first order in time and preserves the total mass.*
2. *The scheme is AP: for a fixed Δt, it solves the diffusion equation* (3.1.5) *when ε goes to zero*
$$\frac{\hat{\rho}^{n+1} - \hat{\rho}^n}{\Delta t} + m c_d |k|^2 \hat{\rho}^{n+1} = 0,$$
with $c_1 = 2, c_2 = \pi, c_3 = \frac{3\pi}{8}$, and where m has been defined in (3.1.4)*.*
3. *Moreover, the semi-discrete-in-time scheme enjoys the UA property: it is first order uniformly in ε*
$$\exists C > 0, \ \sup_{\varepsilon \in (0,1]} \|\hat{f}^N(\cdot,\cdot) - \hat{f}(T,\cdot,\cdot)\|_{L^\infty_{k,v}} \leq C \Delta t.$$

Remark 3.12. The UA property of the scheme ensures that it respects the dynamics of the convergence towards the diffusion equation (3.1.5).

Proof. The conservation of the mass can be proved by induction on the expression of $\hat{\rho}^{n+1}$ for $k = 0$. Moreover, since the proof of the third point of Prop. 3.11 is very similar to the one presented in [17]-[18] in the case of the fractional diffusion limit, we just prove the AP character of the scheme (3.3.37). First of all, let us remark that A_0,b_j and c_j $(j \geq 1)$ defined in (3.3.26)-(3.3.30)-(3.3.31) are exponentially small when ε goes to 0. The expressions (3.3.30) and (3.3.33) then give the following equivalents for b_0 and c_0

$$b_0 = \frac{\Theta(\varepsilon)}{\Delta t} + \Theta(\varepsilon) o(1), \quad c_0 = \Theta(\varepsilon) a_\varepsilon^{N_v} + \frac{\Theta(\varepsilon)}{\Delta t} + \Theta(\varepsilon) o(1).$$

Hence the scheme for $\hat{\rho}$ degenerates when ε goes to 0 into

$$\frac{\hat{\rho}^{n+1} - \hat{\rho}^n}{\Delta t} + a_\varepsilon^{N_v} \hat{\rho}^{n+1} = 0.$$

The asymptotic behavior of $a_\varepsilon^{N_v}$ has already been studied, it remains to consider the limit of the expression of $\hat{f}^{n+1}$ when ε goes to 0. From (3.3.35) and (3.3.36), we have

$$\beta = O(\Theta(\varepsilon)), \ \ \gamma = 1 + O(\Theta(\varepsilon)),$$

and eventually the scheme for $\hat{f}^{n+1}$ degenerates for small ε into $\hat{f}^{n+1} = \hat{\rho}^{n+1} M$. □

3.4 Numerical tests

In this section, we propose numerical tests in dimension 1 to validate the schemes of the previous parts. For simplicity, we will denote IS the implicit scheme of Prop. 3.6, MMS the micro-macro scheme of Prop. 3.8, and DS the integral formulation based scheme of Prop. 3.11. The implicit Euler scheme (3.3.17) for the equation (3.1.7), with a_ε computed with (3.3.8), will be denoted *quasi-diff.* Eventually, the scheme (3.3.16) for the limit diffusion equation (3.1.5) will be denoted *diff.* To highlight the consistency of the schemes, we will compare their

solutions to the solution of a reference scheme which is an explicit Euler scheme in Fourier variable for (3.1.1)

$$\begin{cases} \dfrac{\hat{f}^{n+1}-\hat{f}^n}{\Delta t}+\dfrac{1}{\Theta(\varepsilon)}\left(1+\mathrm{i}\varepsilon kv\right)\hat{f}^n=\dfrac{1}{\Theta(\varepsilon)}\hat{\rho}^n M \\ \hat{\rho}^{n+1}=\left\langle \hat{f}^{n+1}\right\rangle_{N_v} \\ \hat{f}^0(k,v)=\hat{f}_{in}(k,v). \end{cases} \tag{3.4.1}$$

As detailed in the beginning of Section 3.3, all the tests are performed at time $T=0.1$, the time step being specified in each case. We will consider N_x points in space on the interval $[-1,1]$ with periodic boundary conditions, and the velocities are discretized with $N_v=199$ points symmetrically distributed on the interval $[-10,10]$. The initial condition is (3.3.5). In the DS scheme, the velocity integrations with the variable w in (3.3.30)-(3.3.31)-(3.3.33) are computed with the same grid as the integrals with the v variable.

3.4.1 Implicit scheme (IS)

In this section, we test the properties of the IS scheme. First of all, its consistency is tested. The left part of Fig. 3.3 shows that, for $\varepsilon=1$, its solution coincides with the solution of the explicit scheme (3.4.1). For this figure, the two solutions are computed with the time step $\Delta t=10^{-2}$. Then, the solution $\rho_{\Delta t}$ of the IS scheme for a range of Δt is compared to the solution $\rho_{\Delta t_{ref}=10^{-6}}$ of the IS scheme for $\Delta t_{ref}=10^{-6}$ at time $T=0.1$. The relative error between these densities

$$\mathrm{Error}_{\mathrm{consistency}}(\Delta t,\varepsilon)=\frac{\|\rho_{reference}-\rho_{\Delta t}\|_{L^2_{N_x}}}{\|\rho_{reference}\|_{L^2_{N_x}}}, \tag{3.4.2}$$

with $\|\cdot\|_{L^2_{N_x}}$ defined in (3.3.4), is displayed in the right-hand side of Fig. 3.3 in function of Δt. As it is a line with slope 0.98, the numerical order of the method is 1.

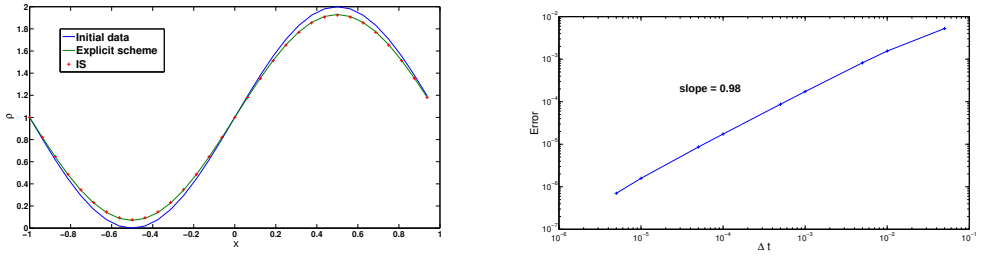

Figure 3.3: Left: for $\Delta t=10^{-2}$ and $\varepsilon=1$, the solutions of the IS scheme and of the explicit scheme (3.4.1). Right: The relative consistency error (3.4.2) for the IS scheme (log scale).

Then, the AP character of the IS scheme is tested. The dynamics of the convergence towards the diffusion limit (3.1.5) is highlighted in the left part of Fig. 3.4, where the densities obtained with the IS scheme are presented for a range of ε, and compared to the densities given by *quasi-diff* and *diff* schemes. These solutions are computed with $\Delta t=10^{-2}$. For intermediate ε, the solution of the IS scheme sticks to the solution of *quasi-diff*, and the two densities goes together to the solution of *diff* when ε tends to 0. The convergence towards the solution of *quasi-diff*

happens with speed $\varepsilon\sqrt{1+|\ln(\varepsilon)|}$, as suggested by the error study presented in the right-hand side of Fig. 3.4. Denoting by f the distribution function obtained with the IS scheme, and $\rho_{quasi-diff}$ the density obtained with the *quasi-diff* scheme for $\Delta t = 10^{-2}$, the quantity

$$\text{Error}_{\text{AP}}(\varepsilon) = \|f - \rho_{quasi-diff} M\|_{L^2_{M^{-1},N_x,N_v}}, \tag{3.4.3}$$

with $\|\cdot\|_{L^2_{M^{-1},N_x,N_v}}$ defined in (3.3.4), is displayed in function of ε. This numerical quantity decreases with the expected rate $\varepsilon\sqrt{1+|\ln(\varepsilon)|}$ stated in Prop. 3.1. Note that the numerical results of section 3.3.1 assure that the convergence of the solution of IS to the solution of *diff* happens with the speed $1/(1+|\ln(\varepsilon)|)$ proved in Prop. 3.2.

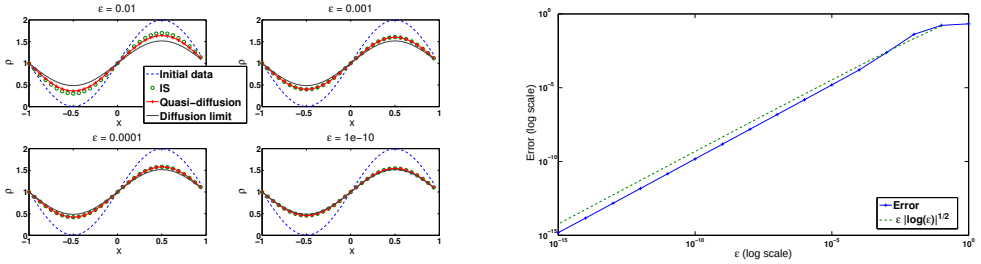

Figure 3.4: Left: for $\Delta t = 10^{-2}$, the solutions of IS, *quasi-diff* and *diff* schemes for different values of ε. Right: for $\Delta t = 10^{-2}$, the error (3.4.3) between the solution of IS and *quasi-diff* scheme in function of ε (log scale).

3.4.2 Micro-macro scheme (MMS)

In this section, we focus on the MMS scheme and we highlight its properties with the same tests as in the previous section. As the transport operator is treated with a classical upwind scheme in the MMS scheme, the CFL condition imposes to take time steps smaller than in the previous section. The left-hand side of Fig. 3.5 shows that the solutions of the MMS and explicit schemes with $\Delta t = 10^{-4}$ and $\varepsilon = 1$ coincide. The numerical order of the MMS scheme is studied in the right-hand side of Fig. 3.5, where the consistency error (3.4.2) for $\varepsilon = 1$ is displayed in function of Δt. For this figure, the density $\rho_{reference}$ is the density obtained with the MMS scheme for $\Delta t = 10^{-6}$ and $\rho_{\Delta t}$ are densities obtained with the MMS scheme for a range of Δt. As expected, the numerical order of the method is 1.

Concerning the AP character of the MMS scheme, the left-hand side of Fig. 3.6 shows, for a range of ε, the densities obtained with the MMS, *quasi-diff* and *diff* schemes with $\Delta t = 10^{-4}$. Once again, the solution of the MMS scheme first joins the solution of the *quasi-diff* scheme when ε becomes small and the two reach the solution of *diff* scheme together when ε tends to 0. The speed of the convergence towards the solution of *quasi-diff* scheme is $\varepsilon\sqrt{1+|\ln(\varepsilon)|}$ stated in Prop. 3.1. Indeed, the right-hand side of Fig. 3.6 displays the error (3.4.3), where $\rho_{quasi-diff}$, and the solution f given by the MMS scheme are computed with $\Delta t = 10^{-4}$.

3.4.3 Integral formulation based scheme (DS)

In this section, we test the integral formulation scheme DS. For $\varepsilon = 1$, we check in the left-hand side of Fig. 3.7, that the solutions of the explicit and DS schemes are close. This figure was

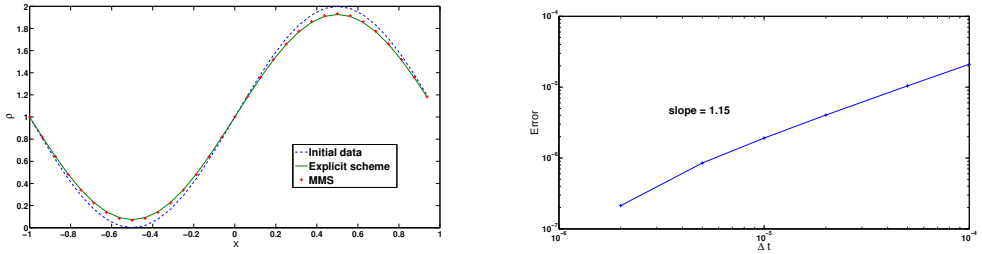

Figure 3.5: Left: for $\Delta t = 10^{-4}$ and $\varepsilon = 1$, the solutions of the MMS scheme and of the explicit scheme (3.4.1). Right: The relative consistency error (3.4.2) for the MMS scheme (log scale).

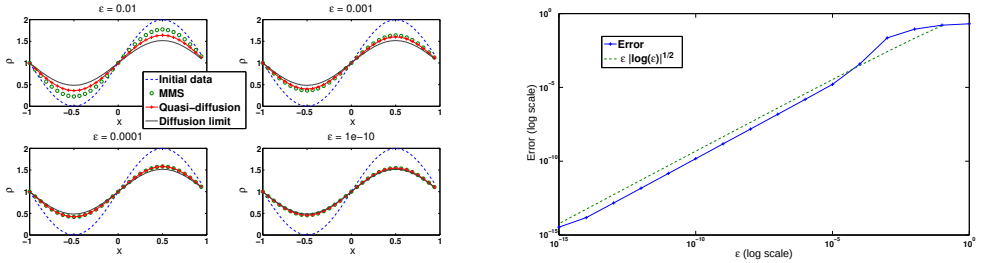

Figure 3.6: Left: for $\Delta t = 10^{-4}$, the solutions of MMS, *quasi-diff* and *diff* schemes for different values of ε. Right: for $\Delta t = 10^{-4}$, the error (3.4.3) between the solution of MMS and *quasi-diff* scheme in function of ε (log scale).

obtained with $\Delta t = 10^{-2}$. The order of accuracy of the DS scheme is studied in the right-hand side of Fig. 3.7. For $\varepsilon = 1$, it displays the error (3.4.2) between $\rho_{reference}$ defined as the solution of the DS scheme for $\Delta t = 5 \cdot 10^{-5}$, and the solution of the DS scheme $\rho_{\Delta t}$ for a range of Δt. In a logarithmic scale, the slope of the line obtained is close to 1, as expected.

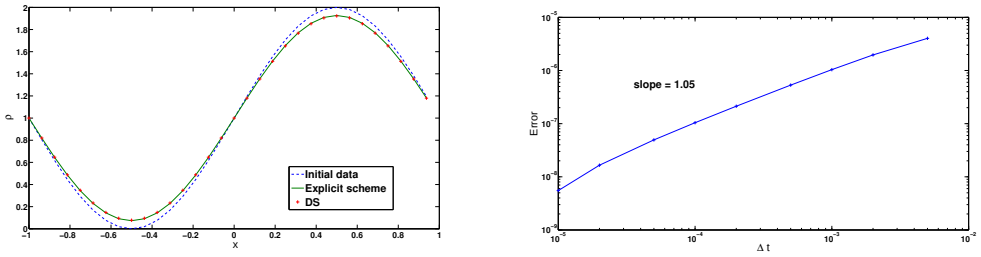

Figure 3.7: Left: for $\Delta t = 10^{-2}$ and $\varepsilon = 1$, the solutions of the DS scheme and of the explicit scheme (3.4.1). Right: The relative consistency error (3.4.2) for the DS scheme (log scale).

Then, we can study the AP character of the DS scheme. The dynamics of the convergence towards the diffusion limit (3.1.5) is highlighted in the left-hand side of Fig. 3.8. It presents the densities obtained with the DS, *quasi-diff* and *diff* schemes for $\Delta t = 10^{-2}$. The solution of the DS scheme has the right behavior, since it is very close to the solution of *quasi-diff* for intermediate ε, and remains stuck to it as it goes to the solution of *diff* when ε goes to 0. The right-hand side of Fig. 3.8 displays the error study of the convergence in ε of the solution of the DS scheme to the solution of the *quasi-diff* scheme. The error (3.4.3) is displayed in a logarithmic scale in this figure, where both $\rho_{quasi-diff}$ and the solution f of the DS scheme are computed with $\Delta t = 10^{-2}$. The convergence happens with the expected $\varepsilon\sqrt{1 + |\ln(\varepsilon)|}$ rate.

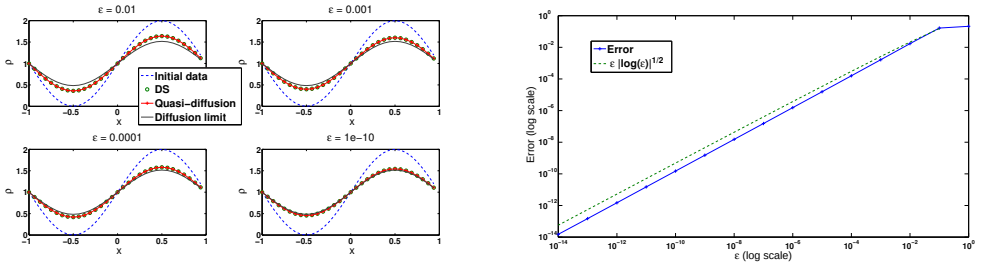

Figure 3.8: Left: for $\Delta t = 10^{-2}$, the solutions of DS, *quasi-diff* and *diff* schemes for different values of ε. Right: for $\Delta t = 10^{-2}$, the error (3.4.3) between the solution of DS and *quasi-diff* scheme in function of ε (log scale).

To highlight the fact that the DS scheme is of order 1 uniformly in ε, we compare the results given by the DS scheme for $\Delta t_{ref} = 5 \cdot 10^{-5}$ to the results given by the same DS scheme for different values of Δt and ε. With these densities, the error (3.4.2) is displayed in Fig. 3.9 as a function of ε. We observe that the error curves are stratified with respect to ε, showing the uniformity of the scheme with respect to ε.

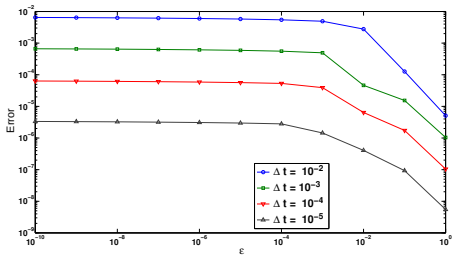

Figure 3.9: The error (3.4.2) as a function of ε. The density $\rho_{reference}$ is the density given by the DS scheme for $\Delta t_{ref} = 5 \cdot 10^{-5}$, and $\rho_{\Delta t}$ are the densities given by the DS scheme for different values of Δt (log scale).

3.5 Numerical schemes in the case of a more general collision operator

In the previous sections of this chapter, we proposed numerical schemes for (3.1.1) in the case of the BGK operator (3.1.2). With this particular collision operator, we were able to design three numerical schemes enjoying the AP property to solve (3.1.1). Two of them are based on the use of the spatial Fourier transform and strongly use the simple form of the collision operator. However, more general collision operator may have to be used. In this part, we propose an adaptation of the micro-macro scheme to the case of a general linear collision operator, as in [55]. Using a relaxation type method (as proposed in [49]) we will derive an AP scheme without requiring a costly inversion of L.

Provided an initial condition $f_{in}(x, v)$, we consider the kinetic equation (3.1.1). The linear operator L describes the collisions of the particles. Following the framework of [55] we consider

$$\begin{aligned} L(f_\varepsilon) &= \int_{\mathbb{R}^d} \left[\sigma(v, v') f_\varepsilon(v') - \sigma(v', v) f_\varepsilon(v)\right] \mathrm{d}v' \\ &= K(f_\varepsilon) - \nu f_\varepsilon, \end{aligned} \tag{3.5.1}$$

with

$$K(f_\varepsilon) = \int_{\mathbb{R}^d} \sigma(v, v') f_\varepsilon(v') \mathrm{d}v', \quad \nu(v) = \int_{\mathbb{R}^d} \sigma(v', v) \mathrm{d}v'. \tag{3.5.2}$$

To fit with [55] and [5], we make the following assumptions

1. The cross section σ is locally integrable on $\mathbb{R}^{2d}$, non negative and the collision frequency ν is locally integrable on $\mathbb{R}^d$ and satisfies

$$\nu(-v) = \nu(v) \geq \nu_1 > 0 \text{ for all } v \in \mathbb{R}^d.$$

2. There exists a function $M \geq 0$ in $L^1(\nu)$ such that $|v|^2 \nu(v)^{-1} M$ is locally integrable and such that $\ker L$ is spanned by M

$$\nu(v) M(v) = K(M)(v) = \int_{\mathbb{R}^d} \sigma(v, v') M(v') \mathrm{d}v'.$$

Furthermore, the function M is even, positive and normalized to 1

$$M(-v) = M(v) > 0 \quad \text{for all} \quad v \in \mathbb{R}^d \quad \text{and} \quad \int_{\mathbb{R}^d} M(v) \mathrm{d}v = 1.$$

3. We could have made the same assumptions of [55] concerning the behavior of M and ν for large $|v|$ but for a sake of simplicity in the computations we will consider the particular case

$$M(v) = \begin{cases} m & |v| < 1 \\ m/|v|^{d+\alpha} & |v| \geq 1 \end{cases}, \quad \nu(v) = \begin{cases} \nu_0 & |v| < 1 \\ \nu_0 |v|^{2-\alpha} & |v| \geq 1 \end{cases}, \quad 1 < \alpha \leq 2. \tag{3.5.3}$$

4. We assume that there exists a constant C such that

$$\int_{\mathbb{R}^d} M(v') \frac{\nu(v) M(v)}{\sigma(v,v')} \mathrm{d}v' + \left(\int_{\mathbb{R}^d} \frac{M(v')}{\nu(v')} \frac{\sigma(v,v')^2}{\nu(v)^2 M(v)^2} \mathrm{d}v' \right)^{1/2} \leq C, \quad \text{for all } v \in \mathbb{R}^d.$$

(Note that this assumption is fulfilled with the choice of $\sigma(v,v')$ made for the numerical applications of the last part.)

Under these assumptions, it has been shown in [55] that if $\Theta(\varepsilon) \sim \varepsilon^2 |\ln(\varepsilon)|$, the solution f_ε of (3.1.1) converges weakly when $\varepsilon \to 0$ to $\rho_0 M$ where ρ_0 solves a classical diffusion equation

$$\partial_t \rho_0 - \frac{c_d}{\alpha - 1} \frac{m}{\nu_0} \Delta \rho_0 = 0, \tag{3.5.4}$$

with initial condition $\rho_{in} = \langle f_{in} \rangle$. Here c_d is a coefficient that depends only on the dimension ($c_1 = 2, c_2 = \pi, c_3 = 8\pi/3$) and m is the normalization coefficient of the equilibrium M. To avoid the cancellation of $\Theta(\varepsilon)$ for $\varepsilon = 1$, we shall consider $\Theta(\varepsilon) = \varepsilon^2 (1 + |\ln(\varepsilon)|)$ defined in (3.1.6) in what follows.

3.5.1 Micro-macro scheme

We want to adapt the micro-macro scheme proposed in Section **??** to the case of the linear collision operator (3.5.1). As in section 3.3.3, we consider the decomposition $f_\varepsilon(t,x,v) = \rho_\varepsilon(t,x) M(v) + g_\varepsilon(t,x,v)$, such that $\langle g_\varepsilon \rangle = 0$. Inserting it in (3.1.1) gives the macro equation

$$\partial_t \rho_\varepsilon + \frac{\varepsilon}{\Theta(\varepsilon)} \langle v \cdot \nabla_x g_\varepsilon \rangle = 0, \tag{3.5.5}$$

and the micro equation

$$\partial_t g_\varepsilon + \frac{\varepsilon}{\Theta(\varepsilon)} v \cdot \nabla_x \rho_\varepsilon M + \frac{\varepsilon}{\Theta(\varepsilon)} (I - \Pi)(v \cdot \nabla_x g_\varepsilon) = \frac{1}{\Theta(\varepsilon)} L(g_\varepsilon), \tag{3.5.6}$$

where Π denotes the orthogonal projection on the kernel of L

$$\Pi(f) = \langle f \rangle M. \tag{3.5.7}$$

The micro equation

In the BGK case, the discretization of the micro equation was not a difficult issue. The strategy was to implicit the stiffest terms, *i.e.* the right hand side of the equation. Here the semi-discrete-in-time scheme would read

$$\frac{g^{n+1} - g^n}{\Delta t} + \frac{\varepsilon}{\Theta(\varepsilon)} v \cdot \nabla_x \rho^n M + \frac{\varepsilon}{\Theta(\varepsilon)} \left(v \cdot \nabla_x g^n - \langle v \cdot \nabla_x g^n \rangle M \right) = \frac{1}{\Theta(\varepsilon)} L(g^{n+1}),$$

where the dependence in ε of ρ and g is omitted to simplify the notations. Nevertheless, in this case, it is necessary to invert the operator $I - \Delta t / \Theta(\varepsilon) L$ to compute g^{n+1}, which may induce a

huge computational cost. To avoid such an inversion, we propose to use a relaxation strategy. It is based on the following rewriting of (3.5.6)

$$\partial_t g_\varepsilon + \frac{1}{\Theta(\varepsilon)} g_\varepsilon = \frac{1}{\Theta(\varepsilon)} \left[L(g_\varepsilon) + g_\varepsilon - \varepsilon v \cdot \nabla_x \rho_\varepsilon M - \varepsilon \left(I - \Pi \right) \left(v \cdot \nabla_x g_\varepsilon \right) \right],$$

that can be integrated in time between t_n and t_{n+1}

$$\begin{aligned} g(t_{n+1}, x, v) = & \frac{1}{\Theta(\varepsilon)} \int_{t_n}^{t_{n+1}} \mathrm{e}^{-\frac{t_{n+1}-s}{\Theta(\varepsilon)}} \left[L(g) + g - \varepsilon v \cdot \nabla_x \rho M - \varepsilon \left(I - \Pi \right) \left(v \cdot \nabla_x g \right) \right](s, x, v) \mathrm{d}s \\ & + \mathrm{e}^{-\frac{\Delta t}{\Theta(\varepsilon)}} g(t_n, x, v). \end{aligned} \tag{3.5.8}$$

We approximate the terms into brackets at time t^n to get

$$g^{n+1} = \mathrm{e}^{-\frac{\Delta t}{\Theta(\varepsilon)}} g^n + \frac{1}{\Theta(\varepsilon)} \left(\int_{t_n}^{t_{n+1}} \mathrm{e}^{-\frac{t_{n+1}-s}{\Theta(\varepsilon)}} \mathrm{d}s \right) \left[L(g^n) + g^n - \varepsilon v \cdot \nabla_x \rho^n M - \varepsilon \left(I - \Pi \right) \left(v \cdot \nabla_x g^n \right) \right], \tag{3.5.9}$$

which is consistent with (3.5.8) for all fixed $\varepsilon > 0$. To ensure the AP character of the scheme, g must vanish when ε goes to 0, so the remaining integral in time in (3.5.9) is approximated by a quadrature on the mid-point of the integral. This transformation is still consistent with (3.5.8), and in addition this ensures g^{n+1} to go to zero as ε becomes small. Eventually, we have a semi-discrete-in-time scheme for the micro equation (3.5.6)

$$g^{n+1} = \mathrm{e}^{-\frac{\Delta t}{\Theta(\varepsilon)}} g^n + \frac{\Delta t}{\Theta(\varepsilon)} \mathrm{e}^{-\frac{\Delta t}{2\Theta(\varepsilon)}} \left[L(g^n) + g^n - \varepsilon v \cdot \nabla_x \rho^n M - \varepsilon \left(I - \Pi \right) \left(v \cdot \nabla_x g^n \right) \right]. \tag{3.5.10}$$

The discretization in velocity is done by the use of (3.3.1) applied to the operators L and Π. It defines the numerical collision operator and the numerical projection on its kernel of L

$$L_{N_v}(f)(v_i) = \Delta v \sum_{j=1}^{N_v} (\sigma(v_i, v_j) f(v_j) - \sigma(v_j, v_i) f(v_i)), \quad \Pi_{Nv}(f)(v_i) = \langle f \rangle_{N_v} M(v_i). \tag{3.5.11}$$

The discretization in space is done with a classical upwind scheme for the gradient.

The macro equation

It remains to find a scheme for ρ from the macro equation (3.5.5). As in the BGK case, we implicit the must stiff term, which yield a semi-discrete-in time scheme for ρ

$$\frac{\rho^{n+1} - \rho^n}{\Delta t} + \frac{\varepsilon}{\Theta(\varepsilon)} \left\langle v \cdot \nabla_x g^{n+1} \right\rangle = 0, \tag{3.5.12}$$

but injecting directly the expression (3.5.10) in it does not ensure the AP character of the scheme. Indeed, as in the last parts, the numerical diffusion coefficient (3.1.3) is finite, which implies that the limit scheme for ρ is $\rho^{n+1} = \rho^n$ and not a scheme for (3.5.4). As in Section 3.3.3, we remark that $\langle v \cdot \nabla_x g \rangle = \langle v \cdot \nabla_x f \rangle$ and we rather inject an implicit formulation of f. Considering only a discretization in time, an implicit formulation of (3.1.1) writes

$$\Theta(\varepsilon) \frac{f^{n+1} - f^n}{\Delta t} + \varepsilon v \cdot \nabla_x f^{n+1} = K\left(f^{n+1} \right) - \nu f^{n+1}, \tag{3.5.13}$$

where K and ν have been defined in (3.5.2). This provides an expression for f^{n+1}

$$f^{n+1} = \frac{1}{\Theta(\varepsilon)+\Delta t\nu}\left[I + \frac{\Delta t}{\Theta(\varepsilon)+\Delta t\nu}\varepsilon v\cdot\nabla_x\right]^{-1}\left(\Delta t\rho^{n+1}\nu M + \Delta t K\left(g^{n+1}\right) + \Theta(\varepsilon)f^n\right),$$

that is injected in (3.5.12) to obtain

$$\frac{\rho^{n+1}-\rho^n}{\Delta t} + \frac{\varepsilon}{\Theta(\varepsilon)}\left\langle v\cdot\nabla_x\left(\frac{\Delta t}{\Theta(\varepsilon)+\Delta t\nu}\left[I+\frac{\Delta t}{\Theta(\varepsilon)+\Delta t\nu}\varepsilon v\cdot\nabla_x\right]^{-1}\rho^{n+1}\nu M\right)\right\rangle \tag{3.5.14}$$

$$+\frac{\varepsilon}{\Theta(\varepsilon)}\left\langle v\cdot\nabla_x\left(\frac{\Theta(\varepsilon)}{\Theta(\varepsilon)+\Delta t\nu}\left[I+\frac{\Delta t}{\Theta(\varepsilon)+\Delta t\nu}\varepsilon v\cdot\nabla_x\right]^{-1}f^n\right)\right\rangle \tag{3.5.15}$$

$$+\Delta t\frac{\varepsilon}{\Theta(\varepsilon)}\left\langle v\cdot\nabla_x\left(\frac{1}{\Theta(\varepsilon)+\Delta t\nu}\left[I+\frac{\Delta t}{\Theta(\varepsilon)+\Delta t\nu}\varepsilon v\cdot\nabla_x\right]^{-1}K\left(g^{n+1}\right)\right)\right\rangle = 0. \tag{3.5.16}$$

As in Section 3.3.3, this scheme for ρ can be simplified. Indeed, as (3.5.16) is of magnitude Δt in a scheme of order 1 in time, it can be removed. The line (3.5.15) can also be simplified in

$$\left\langle \frac{\varepsilon}{\Theta(\varepsilon)+\Delta t\nu}v\cdot\nabla_x f^{n+1}\right\rangle = \left\langle \frac{\varepsilon}{\Theta(\varepsilon)+\Delta t\nu}v\cdot\nabla_x g^{n+1}\right\rangle,$$

with the same argument. The second term of (3.5.14) could be removed as well, but it degenerates into the diffusion limit when ε goes to 0, it is then necessary to keep it. Moreover, it must be numerically treated with care to ensure the AP property of the scheme, since its naive numerical version degenerates to 0 when ε becomes small, as in the first parts of this chapter. Indeed, the second term of (3.5.14) writes, in Fourier variable

$$\begin{aligned}\frac{1}{\Theta(\varepsilon)}\left\langle \frac{\frac{\Delta t}{\Theta(\varepsilon)+\Delta t\nu}\,\varepsilon \mathrm{i}k\cdot v\,\nu M}{1+\frac{\Delta t}{\Theta(\varepsilon)+\Delta t\nu}\,\varepsilon \mathrm{i}k\cdot v}\right\rangle\hat\rho^{n+1} &= \frac{\Delta t^2}{\Theta(\varepsilon)}\left\langle \frac{\varepsilon^2(k\cdot v)^2\nu M}{(\Theta(\varepsilon)+\Delta t\nu)^2+\Delta t^2\varepsilon^2(k\cdot v)^2}\right\rangle\hat\rho^{n+1}\\ &= \frac{1}{\Theta(\varepsilon)}\left\langle \frac{\varepsilon^2(k\cdot v)^2\nu M}{\left(\frac{\Theta(\varepsilon)}{\Delta t}+\nu\right)^2+\varepsilon^2(k\cdot v)^2}\right\rangle\hat\rho^{n+1}.\end{aligned}$$

The first line indicates that it is of magnitude Δt^2. Therefore, any modification can be applied to it with no loss of consistency if it remains of the same order. The second line indicates that it is close from

$$\frac{1}{\Theta(\varepsilon)}\left\langle \frac{\varepsilon^2(k\cdot v)^2\nu M}{\nu^2+\varepsilon^2(k\cdot v)^2}\right\rangle\hat\rho^{n+1},$$

when ε goes to 0. As a consequence, we replace it consistently by $\Delta t^2/(\Delta t+\Theta(\varepsilon))^2\ \tilde a_\varepsilon(k)\hat\rho^{n+1/2}$ with

$$\tilde a_\varepsilon(k) = \frac{1}{\Theta(\varepsilon)}\left\langle \frac{\varepsilon^2(k\cdot v)^2\nu M}{\nu^2+\varepsilon^2(k\cdot v)^2}\right\rangle, \tag{3.5.17}$$

and where $\hat\rho^{n+1/2}$ can be chosen equal to $\hat\rho^n$ or $\hat\rho^{n+1}$ depending on the desired asymptotic scheme. Eventually, we have the following semi-discrete-in-time scheme for ρ

$$\frac{\rho^{n+1}-\rho^n}{\Delta t} + \left\langle \frac{\varepsilon}{\Theta(\varepsilon)+\Delta t\nu}v\cdot\nabla_x g^{n+1}\right\rangle + \left(\frac{\Delta t}{\Delta t+\Theta(\varepsilon)}\right)^2\mathcal{F}^{-1}\left(\tilde a_\varepsilon(k)\hat\rho^{n+1/2}\right) = 0,$$

where $\mathcal{F}^{-1}$ stands for the inverse Fourier transform. To set the AP property of this expression, it remains to remark that the continuous version of $\tilde{a}_\varepsilon$ degenerates when $\varepsilon \to 0$ to the diffusion coefficient of (3.5.4), and to find a numerical expression of $\tilde{a}_\varepsilon$ respecting this degeneracy. First of all, using (3.5.3) let us rewrite $\tilde{a}_\varepsilon$ as

$$\tilde{a}_\varepsilon(k) = \frac{1}{1+|\ln(\varepsilon)|}\left\langle \frac{(k\cdot v)^2}{\nu_0+\varepsilon^2\,(k\cdot v)^2}\nu_0 m\right\rangle_{|v|<1} + \frac{1}{\Theta(\varepsilon)}\left\langle \frac{\left(\frac{\varepsilon v}{\nu_0|v|^{2-\alpha}}\cdot k\right)^2}{1+\left(\frac{\varepsilon v}{\nu_0|v|^{2-\alpha}}\cdot k\right)^2}\nu_0|v|^{2-\alpha}\frac{m}{|v|^{d+\alpha}}\right\rangle_{|v|\geq 1},$$

and apply the change of variables $w = \varepsilon v/\left(\nu_0|v|^{2-\alpha}\right)$ in the second term, with

$$v = \left(\frac{\nu_0}{\varepsilon}\right)^{\frac{1}{\alpha-1}},\ \ |v| = \left(\frac{\nu_0}{\varepsilon}|w|\right)^{\frac{1}{\alpha-1}},\ \ \mathrm{d}v = \frac{1}{\alpha-1}\left(\frac{\nu_0}{\varepsilon}\right)^{\frac{d}{\alpha-1}}|w|^{d\frac{2-\alpha}{\alpha-1}},$$

to get

$$\tilde{a}_\varepsilon(k) = \frac{1}{1+|\ln(\varepsilon)|}\left\langle \frac{(k\cdot v)^2}{\nu_0+\varepsilon^2\,(k\cdot v)^2}\nu_0 m\right\rangle_{|v|<1} + \frac{1}{\alpha-1}\frac{m}{\nu_0}\frac{1}{1+|\ln(\varepsilon)|}\left\langle \frac{(k\cdot w)^2}{1+(k\cdot w)^2}\frac{1}{|w|^{d+2}}\right\rangle_{|w|\geq\frac{\varepsilon}{\nu_0}}.$$

In the 1-dimensional case, it is -up to a constant- the same expression as (3.2.6). Then, $\tilde{a}_\varepsilon$ writes for nonzero k

$$\begin{aligned}\tilde{a}_\varepsilon^{d=1}(k) = {}& \frac{2}{\alpha-1}\frac{m}{\nu_0}|k|^2 + \frac{1}{1+|\ln(\varepsilon)|}\left\langle \frac{(k\cdot v)^2}{\nu_0^2+\varepsilon^2(k\cdot v)^2}\nu_0 m\right\rangle_{|v|<1} \\ & + \frac{2}{\alpha-1}\frac{m}{\nu_0}\frac{|k|^2}{1+|\ln(\varepsilon)|}\left(\frac{1}{2}\ln\left(\varepsilon^2+\frac{\nu_0^2}{|k|^2}\right)-1\right).\end{aligned} \tag{3.5.18}$$

When the dimension is 2 or 3, the change of variables $u = |k|w$ yields an expression close to (3.2.7). In both cases, computations similar to the ones done in the proof of Lemma 3.3 give the following rewriting for $\tilde{a}_\varepsilon(k)$, when $k \neq 0$

$$\begin{aligned}\tilde{a}_\varepsilon^{d=2}(k) = {}& \frac{\pi}{\alpha-1}\frac{m}{\nu_0}|k|^2 + \frac{1}{1+|\ln(\varepsilon)|}\left\langle \frac{(k\cdot v)^2}{\nu_0^2+\varepsilon^2(k\cdot v)^2}\nu_0 m\right\rangle_{|v|<1} \\ & - \frac{\pi}{\alpha-1}\frac{m}{\nu_0}\frac{|k|^2}{1+|\ln(\varepsilon)|}\left(1+\ln\left(\frac{|k|}{\nu_0}\right)\right) \\ & - \frac{\pi}{\alpha-1}\frac{m}{\nu_0}\frac{|k|^2}{1+|\ln(\varepsilon)|}\int_{\theta=0}^{2\pi}\int_{r=\frac{\varepsilon|k|}{\nu_0}}^{1}\frac{r\cos^4(\theta)}{1+r^2\cos^2(\theta)}\mathrm{d}r\mathrm{d}\theta \\ & + \frac{\pi}{\alpha-1}\frac{m}{\nu_0}\frac{|k|^2}{1+|\ln(\varepsilon)|}\int_{\theta=0}^{2\pi}\int_{r=1}^{\infty}\frac{1}{r}\frac{\cos^2(\theta)}{1+r^2\cos^2(\theta)}\mathrm{d}r\mathrm{d}\theta,\end{aligned} \tag{3.5.19}$$

and, with a change of variable in spherical coordinates

$$\begin{aligned}\tilde{a}_\varepsilon^{d=3}(k) = {}& \frac{8\pi}{3}\frac{1}{\alpha-1}\frac{m}{\nu_0}|k|^2 + \frac{1}{1+|\ln(\varepsilon)|}\left\langle \frac{(k\cdot v)^2}{\nu_0^2+\varepsilon^2(k\cdot v)^2}\nu_0 m\right\rangle_{|v|<1} \\ & - \frac{8\pi}{3}\frac{1}{\alpha-1}\frac{m}{\nu_0}\frac{|k|^2}{1+|\ln(\varepsilon)|}\left(\ln\left(\frac{|k|}{\nu_0}\right)-1\right) \\ & - \frac{2\pi}{\alpha-1}\frac{m}{\nu_0}\frac{|k|^2}{1+|\ln(\varepsilon)|}\int_{\theta=0}^{\pi}\int_{r=\frac{\varepsilon|k|}{\nu_0}}^{1}\frac{r\sin^5(\theta)}{1+r^2\sin^2(\theta)}\mathrm{d}r\mathrm{d}\theta\end{aligned} \tag{3.5.20}$$

$$+\frac{2\pi}{\alpha-1}\frac{m}{\nu_0}\frac{|k|^2}{1+|\ln(\varepsilon)|}\int_{\theta=0}^{\pi}\int_{r=1}^{\infty}\frac{1}{r}\frac{\sin^3(\theta)}{1+r^2\sin^2(\theta)}\mathrm{d}r\mathrm{d}\theta.$$

This yields the limit of $\tilde{a}_\varepsilon$ when ε tends to 0

$$\tilde{a}_\varepsilon(k)\underset{\varepsilon\to 0}{\longrightarrow}\frac{c_d}{\alpha-1}\frac{m}{\nu_0}|k|^2,$$

with $c_1=2, c_2=\pi, c_3=8\pi/3$, that is the expected diffusion coefficient. To ensure the scheme enjoy the AP property, it is crucial to use a discretization of $\tilde{a}_\varepsilon$ that respects this limit. As in Section 3.3.1, the use of a naive quadrature of (3.5.17) does not ensure $\tilde{a}_\varepsilon^{N_v}$ to degenerate into the numerical diffusion coefficient when ε goes to 0. Indeed, it would write

$$\frac{1}{1+|\ln(\varepsilon)|}\left\langle\frac{(k\cdot v)^2}{\nu^2+(k\cdot v)^2}\nu M\right\rangle_{N_v}\underset{\varepsilon\to 0}{\sim}\frac{1}{1+|\ln(\varepsilon)|}\left\langle\frac{(k\cdot v)^2}{\nu}M\right\rangle_{N_v},$$

and since the discretization uses a finite number of points, the last term into brackets is finite instead of infinite. In this way, the naive numerical version of $\tilde{a}_\varepsilon$ tends to 0 when ε becomes small. We then use a quadrature based on the expressions (3.5.18)-(3.5.19)-(3.5.20), that respects the asymptotic behavior of $\tilde{a}_\varepsilon$. In the numerical tests in dimension 1, we will use the following discrete version of $\tilde{a}_\varepsilon$

$$\begin{aligned}\tilde{a}_\varepsilon^{N_v}(k)=&\frac{2}{\alpha-1}\frac{m}{\nu_0}|k|^2+\frac{1}{1+|\ln(\varepsilon)|}\left\langle\frac{(k\cdot v)^2}{\nu_0^2+\varepsilon^2(k\cdot v)^2}\nu_0 m\right\rangle_{N_v,|v|<1}\\&+\frac{2}{\alpha-1}\frac{m}{\nu_0}\frac{|k|^2}{1+|\ln(\varepsilon)|}\left(\frac{1}{2}\ln\left(\varepsilon^2+\frac{\nu_0^2}{|k|^2}\right)-1\right),\end{aligned}\tag{3.5.21}$$

when $k\neq 0$, and 0 otherwise. Eventually, we have the following proposition

Proposition 3.13. *We consider the following scheme (discretized in time and velocity) defined for all $x\in\mathbb{R}^d, v\in\mathbb{R}^d$ and all time indices $0\leq n\leq N, N\Delta t=T>0$ by*

$$\begin{cases} g^{n+1}=\mathrm{e}^{-\frac{\Delta t}{\Theta(\varepsilon)}}g^n+\dfrac{\Delta t}{\Theta(\varepsilon)}\mathrm{e}^{-\frac{\Delta t}{2\Theta(\varepsilon)}}\left[L_{N_v}(g^n)+g^n-\varepsilon v\cdot\nabla_x\rho^n M-\varepsilon\left(I-\Pi_{N_v}\right)(v\cdot\nabla_x g^n)\right]\\ \dfrac{\rho^{n+1}-\rho^n}{\Delta t}+\left\langle\dfrac{\varepsilon}{\Theta(\varepsilon)+\Delta t\nu}\,v\cdot\nabla_x g^{n+1}\right\rangle_{N_v}+\left(\dfrac{\Delta t}{\Delta t+\Theta(\varepsilon)}\right)^2\mathcal{F}^{-1}\left(\tilde{a}_\varepsilon^{N_v}(k)\hat{\rho}^{n+1/2}\right)=0,\end{cases}\tag{3.5.22}$$

with $\Theta(\varepsilon), L_{N_v}, \Pi_{N_v}$ in (3.1.6)-(3.5.11), where $\mathcal{F}^{-1}$ denotes the inverse of the Fourier transform, and where $\tilde{a}_\varepsilon^{N_v}$ has been defined in (3.5.21). The quantity $\hat{\rho}^{n+1/2}$ can be chosen equal to $\hat{\rho}^n$ or $\hat{\rho}^{n+1}$ depending on the desired asymptotic scheme. Provided an initial data $f^0(k,v)=f_{in}(k,v), \rho^0(k)=\left\langle f^0(k,\cdot)d\right\rangle_{N_v}$, and $g^0=f^0-\rho^0 M$, the scheme has the following properties:

1. *The scheme is of order 1 for fixed ε, and preserves the total mass.*
2. *The scheme is AP: for a fixed Δt, the scheme solves the diffusion equation (3.5.4) when ε goes to 0*
$$\frac{\hat{\rho}^{n+1}-\hat{\rho}^n}{\Delta t}+\frac{c_d}{\alpha-1}\frac{m}{\nu_0}|k|^2\hat{\rho}^{n+1/2}=0.$$

Remark 3.14. If one must use the space variable, it is possible to avoid the use of the Fourier transform in (3.5.22) by replacing $\mathcal{F}^{-1}\left(\tilde{a}_\varepsilon^{N_v}\hat{\rho}^{n+1/2}\right)$ by $-\frac{c_d}{\alpha-1}\frac{m}{\nu_0}\Delta_x\rho^{n+1/2}$.

Proof. The first point comes immediately from the construction of the scheme. For the second point, we remark that the expression for g^{n+1} in the first line of (3.5.22) ensures that g^{n+1} is exponentially small when ε tends to 0 with fixed Δt. Then, the term in g^{n+1} in the second line of (3.5.22) vanishes when ε is small. As we chose the quadrature of $\tilde{a}_\varepsilon^{N_v}$ to ensure that

$$\tilde{a}_\varepsilon^{N_v} \underset{\varepsilon\to 0}{\longrightarrow} \frac{c_d}{\alpha-1}\frac{m}{\nu_0}|k|^2,$$

the scheme for ρ degenerates into

$$\frac{\rho^{n+1}-\rho^n}{\Delta t} + \mathcal{F}^{-1}\left(\frac{c_d}{\alpha-1}\frac{m}{\nu_0}|k|^2\hat{\rho}^{n+1/2}\right) = 0,$$

which solves (3.5.4). □

3.5.2 Numerical tests

In this section, we test the properties of the micro-macro scheme presented in Prop. 3.13 with the collision operator (3.5.1). The equilibrium M and collision frequency ν we consider are written in (3.5.3), and the collision kernel σ we consider is given by $\sigma(v,v') = a(v)a(v')M(v)$, where

$$a(v) = \begin{cases} 1 & \text{if } |v| \le 1 \\ |v|^{2-\alpha} & \text{if } |v| > 1 \end{cases}.$$

We will take $\alpha = 1.5$ in what follows. As in Section 3.4, we will denote by *diff* the implicit Euler scheme in Fourier variable for the limit diffusion equation (3.5.4). All the tests are performed with the numerical parameters detailed in the beginning of Section 3.3, and the initial condition (3.3.5). Due to the CFL condition coming from the upwind scheme for the space derivatives in the micro-macro scheme, we will consider $\Delta t = 10^{-4}$.

To test the consistency of the micro-macro scheme, we compare its solution to the solution of an explicit Euler scheme for (3.1.1) with (3.5.1)

$$\begin{cases} \dfrac{f^{n+1}-f^n}{\Delta t} + \dfrac{\varepsilon}{\Theta(\varepsilon)} v\cdot\nabla_x f^n = \dfrac{1}{\Theta(\varepsilon)} L\left(f^n\right) \\ \rho^{n+1} = \left\langle f^{n+1}\right\rangle_{N_v} \\ f^0(k,v) = f_{in}(k,v) \end{cases}, \tag{3.5.23}$$

where the space derivatives, written continuously here in a sake of simplicity, are discretized with an upwind scheme. For $\varepsilon = 1$ and $N_x = 128$, the densities obtained with this scheme and with the micro-macro scheme are presented in the left-hand side of Fig. 3.10, showing that the two densities are very close. The right-hand side of Fig. 3.10 is a numerical order study of the micro-macro scheme. The error (3.4.2), where $\rho_{reference}$ is the density obtained with the micro-macro scheme with $\Delta t = 10^{-6}$, is plotted in function of Δt. The slope of the line we obtain is close to 1, as expected for a first order in time scheme.

To test the AP character of the micro-macro scheme, we fix $\Delta t = 10^{-4}, N_x = 32$, and we compare the obtained results with the result of the *diff* scheme. In the case of the general collision operator, the comparison with the results of the equation (3.1.7) is *a priori* not relevant. Indeed, the proof of the result of the rate of degeneracy of the solution of (3.1.1) to the solution of (3.1.7) in Prop. 3.1 is not valid in the case of the general collision operator. In addition, the rate of the degeneracy of the numerical solution of the micro-macro scheme towards the numerical solution of (3.1.7) is not conserved with the relaxation strategy used in

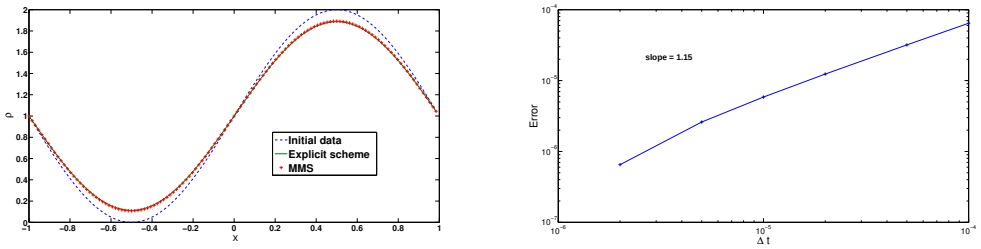

Figure 3.10: Left: for $\Delta t = 10^{-4}$ and $\varepsilon = 1$, the solutions of the micro-macro scheme and of the explicit scheme (3.5.23). Right: The relative consistency error (3.4.2) for the micro-macro scheme, computed with $\Delta t_{ref} = 10^{-6}$ (log scale).

the micro equation. Actually, with this method, g has an exponential decrease in ε, which does not even match with the degeneracy expected in the case of the BGK operator. The left-hand side of Fig. 3.11, presents the densities obtained with the micro-macro and *diff* scheme for a range of ε. It turns out that the degeneracy to the diffusion limit is slow. This is highlighted in the right-hand side of Fig. 3.11 where the error

$$Error(\varepsilon) = \frac{\|\rho^{\text{micro-macro}}_{\varepsilon,\Delta t} - \rho^{diff}_{\Delta t}\|_{L^2_{N_x}}}{\|\rho^{diff}_{\Delta t}\|_{L^2_{N_x}}}, \tag{3.5.24}$$

is displayed in function of ε. The numerical degeneracy rate we obtain is $1/(1 + |\ln(\varepsilon)|)$, as in the case of the BGK operator.

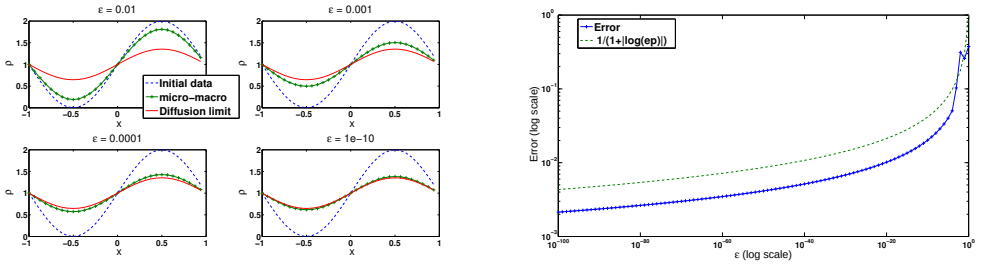

Figure 3.11: Left: for $\Delta t = 10^{-4}$, the solutions of the micro-macro and *diff* schemes, for a range of ε. Right: for $\Delta t = 10^{-4}$, the error (3.5.24) between the solution of the micro-macro and *diff* scheme in function of ε (log scale).

Chapter 4

A relaxed micro-macro scheme for kinetic equation with fractional diffusion scaling and non-local collision operators

4.1 Introduction

We are interested in numerical schemes for kinetic equation with fractional diffusion limit. Let $f(t,x,v)$ be the solution of the following kinetic equation

$$\varepsilon^\alpha \partial_t f + \varepsilon v \cdot \nabla_x f = L(f), \tag{4.1.1}$$

with $t > 0$, $x \in \mathbb{R}^d$ and $v \in \mathbb{R}^d$ and an initial condition $f(0,x,v) = f_0(x,v)$. The linear operator L models the collisions the particles are subject to, and is given by

$$L(f) = \int_{\mathbb{R}^d} \left[\sigma(x,v,v')f(v') - \sigma(x,v',v)f(v)\right] \mathrm{d}v', \tag{4.1.2}$$

where σ is the cross-section. This relaxed collision operator can be rewritten as

$$L(f) = K(f) - \nu f, \tag{4.1.3}$$

with

$$K(f) = \int_{\mathbb{R}^d} \sigma(x,v,v')f(v')\mathrm{d}v', \quad \nu(x,v) = \int_{\mathbb{R}^d} \sigma(x,v',v)\mathrm{d}v'. \tag{4.1.4}$$

We make the same assumptions as in [53, 5], that is: there exists a unique equilibrium function M, which is even, depends only on v, and such that

$$L(M) = 0, \quad \langle M(v)\rangle = 1, \tag{4.1.5}$$

where the integral in velocity is denoted $\langle\cdot\rangle$ such that

$$\langle M(v)\rangle = \int_{\mathbb{R}^d} M(v)\mathrm{d}v.$$

The $L^2\left(\frac{\mathrm{d}v}{M}\right)$-orthogonal projection on the kernel of L is defined by

$$\Pi(f) = \langle f\rangle M. \tag{4.1.6}$$

We suppose that M is a heavy-tailed equilibrium

$$M(v) \underset{|v|\to\infty}{\sim} \frac{m}{|v|^{d+\alpha}}, \alpha \in (0,2), \tag{4.1.7}$$

where m is a normalization coefficient. Moreover, the cross section σ is supposed non negative and locally integrable on $\mathbb{R}^{2d}$ for all x. It satisfies the following inequality

$$\nu_1 M(v) \le \sigma(x,v,v') \le \nu_2 M(v), \ \ \forall x \in \mathbb{R}^d, \ \forall v \in \mathbb{R}^d, \ \forall v' \in \mathbb{R}^d,$$

with $0 < \nu_1 \le \nu_2$. The collision frequency ν is then bounded

$$0 < \nu_1 \le \nu(x,v) \le \nu_2, \ \ \forall x \in \mathbb{R}^d, \forall v \in \mathbb{R}^d \tag{4.1.8}$$

we suppose that $\nu(x,v) = \nu(x,-v)$ for all $x \in \mathbb{R}^d, v \in \mathbb{R}^d$, and that there exists a function ν_0 such that

$$\nu(x,v) \underset{|v|\to+\infty}{\longrightarrow} \nu_0(x). \tag{4.1.9}$$

When the equilibrium M is a Maxwellian equilibrium and the collision frequency ν does not vanish at the origin, it has been shown that if $\alpha = 2$, the solution of (4.1.1) converges

when ε goes to 0 to an equilibrium distribution ρM, where ρ solves a diffusion equation (see for instance [7, 3, 22, 64]). In the case of the heavy-tailed equilibrium (4.1.7) we are considering here, this limit is not relevant. Indeed, the heavy-tail of the equilibrium makes the diffusion coefficient be infinite. The use of another scaling ε^α, with $0 < \alpha < 2$, is then necessary to make an asymptotic regime arise for (4.1.1). Under the assumptions that are done here, it has been shown in [53, 5] that under regularity conditions on the initial condition f_0, the solution f of (4.1.1) converges, when ε tends to 0, to an equilibrium distribution ρM with $\rho(t,x)$ solution of

$$\partial_t \rho + m\mathcal{L}(\rho) = 0, \tag{4.1.10}$$

where m is defined in (4.1.7), with initial condition $\rho(0,x) = \langle f_0(x,v)\rangle$. The operator $\mathcal{L}$ is given by

$$\mathcal{L}(\rho)(t,x) = P.V. \int_{\mathbb{R}^d} \gamma(x, x-y) \frac{\rho(t,x) - \rho(t,x-y)}{|y|^{d+\alpha}} \mathrm{d}y, \tag{4.1.11}$$

where *P.V.* stands for the principal value of the integral, and with

$$\gamma(x,y) = \nu_0(x)\nu_0(y) \int_0^{+\infty} z^\alpha \mathrm{e}^{-z\int_0^1 \nu_0((1-s)x+sy)\mathrm{d}s} \mathrm{d}z. \tag{4.1.12}$$

For $\gamma = 1$, the operator $\mathcal{L}$ reduces to a fractional Laplacian

$$(-\Delta)^{\alpha/2}\,\rho(x) = -c_{d,\alpha}\; P.V. \int_{\mathbb{R}^d} \frac{\rho(x) - \rho(x-y)}{|y|^{d+\alpha}} \mathrm{d}y, \tag{4.1.13}$$

where the normalization constant $c_{d,\alpha}$, which depends only on the dimension and α, is given by

$$c_{d,\alpha} = \frac{\alpha 2^{\alpha-1}\Gamma\left(\frac{\alpha+d}{2}\right)}{\pi^{d/2}\Gamma\left(\frac{2-\alpha}{2}\right)}, \tag{4.1.14}$$

where Γ denotes the usual Gamma function. When the cross-section σ in (4.1.2) does not depend on x, it has been shown in [55, 5] that (4.1.1) converges when ε goes to 0 to a fractional diffusion equation, written with the fractional Laplacian (4.1.13). Such a fractional diffusion limit also arises when the equilibrium M is Maxwellian, and the collision frequency vanishes at the origin (see [4]).

Since the fractional Laplacian (4.1.13) has a very simple expression in Fourier variable,

$$\mathcal{F}\left[(-\Delta)^{\alpha/2}\,\rho\right](k) = |k|^\alpha \mathcal{F}[\rho](k), \tag{4.1.15}$$

where $\mathcal{F}[\rho]$ denotes the Fourier transform in space of a given function ρ, the study of the convergence of (4.1.1) to the fractional diffusion limit writes more easily in Fourier variable. Roughly, it consists in taking account for the effects of the high velocities in the asymptotic analysis. However, in the case we are considering here, the operator $\mathcal{L}$ defined in (4.1.11) has no simple form in Fourier variable. Therefore, one has to consider the problem in the original space variable to perform the asymptotic analysis of (4.1.1), in addition to the effects of the high velocities that still have to be dealt with.

In the numerical computations, (4.1.1) becomes stiff when ε goes to 0, which complicates the resolution of (4.1.1). Indeed, a relation between the stiffness parameter ε and the discretization parameter often arises if a standard method is employed. From a computational time point of view, such schemes then become very costly when ε gets smaller, which makes the asymptotic regime unattainable. The Asymptotic Preserving (AP) schemes have been introduced in [43,

44, 37] to overcome this difficulty. Such schemes are consistent with (4.1.1) when ε is fixed and degenerate into schemes solving the limit model when ε goes to 0 with fixed discretization parameters. In the case of the classical diffusion limit, many AP schemes have been proposed (see for instance [58, 59, 41, 52, 50, 12, 28, 38, 39, 42, 45, 31, 32, 19, 11, 24]). However, they do not enjoy the AP property in the case of the fractional diffusion limit, since they do not deal correctly with the high velocities the slow decreasing equilibrium. In the case of a heavy-tailed equilibrium, and a simplified collision operator of BGK type, we proposed in [17] a strategy to construct AP schemes for (4.1.1) with fractional diffusion limit, by taking correctly into account the effect of high velocities. We then applied a similar method to construct AP schemes in the case where the anomalous diffusion limit comes from the degeneracy of the collision frequency at the origin (see [16, 18]). We also extended this study to the critical case $\alpha = 2$ in (4.1.7), in which the time scale ε^α in (4.1.1) should be replaced by $\varepsilon^2|\ln(\varepsilon)$ (see [33]). In this case, the asymptotic model is classical diffusion equation (see [55]). In all these studies, the use of the space Fourier variable in the numerical computations simplified the method, since the discretization of the limit equation was not a difficult issue. Here, as the limit operator (4.1.11) has no simple expression in Fourier variable, the discretization of the limit equation must be done in the original space variable, which induces an additional difficulty. Moreover, from a computational point of view, the collision operator L is costly to inverse numerically since it is a nonlocal operator. The strategy we present avoids this inversion by the use of a relaxation strategy, as in [49].

The chapter is organized as follows: in a first part, we write a scheme for (4.1.1) based on a micro-macro decomposition of the distribution function, and that enjoys the AP property for (4.1.10). The discretization of the operator $\mathcal{L}$ is then discussed in the second part, and eventually numerical tests are proposed to highlight the properties of the micro-macro scheme.

4.2 Micro-macro scheme

In this section, we propose a numerical scheme for (4.1.1) able to capture the solution of (4.1.10) when ε goes to 0. This scheme enjoys the Asymptotic Preserving (AP) property, that is that for any initial condition f_0

- it is consistent with the kinetic equation (4.1.1) when ε is fixed,
- it degenerates into a consistent numerical scheme solving the asymptotic equation (4.1.10) when the discretization parameters are fixed and ε tends to 0.

In the sequel, we will consider a time discretization $t_n = n\Delta t, n = 0, \dots, N$ such that $N\Delta t = T$, where T is the final time, and we will set $f^n \equiv f(t_n)$. The theoretical results of [53, 5] are valid on the whole space domain $\mathbb{R}^d$, and since the case of a bounded space domain generates a different limit equation (see [14]), we consider here the space domain $x \in [-1, 1]$ and periodic boundary conditions. In the numerical tests, the space domain will be discretized with N_x points

$$x_i = -1 + i\Delta x, \;\; 0 \leq i \leq N_x - 1, \tag{4.2.1}$$

where $\Delta x = 2/N_x$. Eventually, we will solve the problem for the velocities $|v| \leq 10$, with N_v points symmetrically distributed around the origin. We will consider $N_v = 2N_v'$ point, with $N_v' = 100$ and the grid

$$v_j = -10 + \frac{\Delta v}{2} + j\Delta v, \;\; 0 \leq j \leq 2N_v' - 1. \tag{4.2.2}$$

The discrete integrations in velocity will be denoted $\langle\cdot\rangle_{N_v}$, with

$$\langle f\rangle_{N_v} = \Delta v \sum_{j=0}^{2N_v'-1} f(v_j). \tag{4.2.3}$$

For a sake of simplicity in the computations, we consider the equilibrium

$$M(v) = \frac{m}{1+|v|^{d+\alpha}}, \tag{4.2.4}$$

with m chosen such that $\langle M\rangle = 1$, and $\alpha \in (0,2)$. Note that our strategy also works for any M satisfying the general assumptions (4.1.5)-(4.1.7).

We first decompose the solution of (4.1.1) as $f = \rho M + g$ with $\rho = \langle f\rangle$ and $\langle g\rangle = 0$. Inserting this decomposition in (4.1.1) leads, after an integration in velocity, to the following macro equation

$$\varepsilon^\alpha \partial_t \rho + \varepsilon \langle v\cdot\nabla_x g\rangle = 0. \tag{4.2.5}$$

Applying the operator $I-\Pi$, with Π defined in (4.1.6), to (4.1.1) leads to the micro equation

$$\varepsilon^\alpha \partial_t g + \varepsilon v\cdot\nabla_x \rho M + \varepsilon (I-\Pi)(v\cdot\nabla_x g) = L(g). \tag{4.2.6}$$

4.2.1 The micro scheme

To write a AP numerical approximation of (4.1.1), a suitable discretization of the micro-macro system (4.2.5)-(4.2.6) has to be derived. In this section, we discuss the discretization of the micro equation (4.2.6). Since we require the scheme to enjoy the AP property, the numerical approximation of g must vanish when ε goes to 0. In a first step, we construct a semi-discrete-in-time scheme for (4.2.6). To ensure the AP property of the scheme, one strategy would be to make implicit the stiffest term of the equation. Denoting $g^n \approx g(t_n)$, the semi-discrete-in-time scheme would read

$$\frac{g^{n+1}-g^n}{\Delta t} + \frac{\varepsilon}{\varepsilon^\alpha} v\cdot\nabla_x \rho^n M + \frac{\varepsilon}{\varepsilon^\alpha}(I-\Pi)(v\cdot\nabla_x g^n) = \frac{1}{\varepsilon^\alpha} L\left(g^{n+1}\right).$$

Unfortunately, solving this equation in g^{n+1} requires the inversion of the operator $I-\Delta t/\varepsilon^\alpha L$, which is non local. This inversion may induce a high computational cost in its numerical evaluation. To overcome this inversion, we follow the strategy of [49], and rewrite (4.2.6) as

$$\partial_t g + \frac{1}{\varepsilon^\alpha} g = \frac{1}{\varepsilon^\alpha}\left[L(g) + g - \varepsilon v\cdot\nabla_x \rho M - \varepsilon(I-\Pi)(v\cdot\nabla_x g)\right].$$

We then integrate this equality between the times t_n and t_{n+1} to obtain an expression of $g(t_{n+1},x,v)$

$$\begin{aligned} g(t_{n+1},x,v) = {} & \mathrm{e}^{-\frac{\Delta t}{\varepsilon^\alpha}} g(t_n,x,v) \\ & + \frac{1}{\varepsilon^\alpha}\int_{t_n}^{t_{n+1}} \mathrm{e}^{-\frac{t_{n+1}-s}{\varepsilon^\alpha}} \left[L(g) + g - \varepsilon v\cdot\nabla_x\rho M - \varepsilon(I-\Pi)(v\cdot\nabla_x g)\right](s,x,v)\mathrm{d}s. \end{aligned}$$

This allows to write a scheme for g in which the inversion of L is not necessary. Indeed, we use a suitable quadrature on the time integral, and we get the scheme

$$g^{n+1} = \mathrm{e}^{-\frac{\Delta t}{\varepsilon^\alpha}} g^n + \left(\frac{1}{\varepsilon^\alpha}\int_{t_n}^{t_{n+1}} \mathrm{e}^{-\frac{t_{n+1}-s}{\varepsilon^\alpha}}\mathrm{d}s\right)\left[L(g^n) + g^n - \varepsilon v\cdot\nabla_x\rho^n M - \varepsilon(I-\Pi)(v\cdot\nabla_x g^n)\right].$$

To ensure that g^{n+1} converges to 0 as ε goes to 0, we approximate the remaining integral by $\mathrm{e}^{-\Delta t/2\varepsilon^\alpha}$, which corresponds to a midpoint approximation. The fully discrete scheme is obtained by applying the discretization (4.2.1) in the space variable and using an upwind scheme for the transport terms in space. The velocities are discretized with (4.2.2) and the integrals in v are computed with (4.2.3). Eventually, still writing the gradients in x continuously for a sake of simplicity, the micro scheme writes

$$g^{n+1} = \mathrm{e}^{-\frac{\Delta t}{\varepsilon^\alpha}} g^n + \frac{\Delta t}{\varepsilon^\alpha} \mathrm{e}^{-\frac{\Delta t}{2\varepsilon^\alpha}} \left[L_{N_v}\left(g^n\right) + g^n - \varepsilon v \cdot \nabla_x \rho^n M - \varepsilon \left(I - \Pi_{N_v}\right)\left(v \cdot \nabla_x g^n\right) \right], \quad (4.2.7)$$

where L_{N_v} and Π_{N_v} denote the operators L and Π computed with the discrete integral (4.2.3)

$$\begin{aligned} L_{N_v}(f)(v_i) &= \Delta v \sum_{j=0}^{2N_v'-1} \left(\sigma(x, v_i, v_j) f(v_j) - \sigma(x, v_j, v_i) f(v_i)\right), \quad (4.2.8) \\ \Pi_{N_v}(f)(v_i) &= \langle f \rangle_{N_v} M(v_i). \end{aligned}$$

4.2.2 The macro scheme

In this section, we propose a discretization of the macro equation that is able to capture the limit (4.1.10) of (4.1.1). The simpler strategy, which consists in making implicit the stiffest term of the equation, is not sufficient to ensure the AP property of the scheme. Indeed, such a scheme would read

$$\frac{\rho^{n+1} - \rho^n}{\Delta t} + \frac{\varepsilon}{\varepsilon^\alpha} \left\langle v \cdot \nabla_x g^{n+1} \right\rangle = 0, \quad (4.2.9)$$

and, since the expression of g^{n+1} in (4.2.7) has exponential decay in ε when ε goes to 0, the scheme degenerates into $\rho^{n+1} = \rho^n$ when ε becomes small. Instead, we remark that because of the symmetry of M we have

$$\left\langle v \cdot \nabla_x g^{n+1} \right\rangle = \left\langle v \cdot \nabla_x f^{n+1} \right\rangle, \quad (4.2.10)$$

and we inject a fully implicit formulation of f in the above expression, to make appear explicitely the limit operator $\mathcal{L}$ arise in (4.2.9). More precisely, we proceed as follows We first write an implicit formulation of (4.1.1)-(4.1.2)

$$\varepsilon^\alpha \frac{f^{n+1} - f^n}{\Delta t} + \left(\nu + \varepsilon v \cdot \nabla_x\right) f^{n+1} = K\left(f^{n+1}\right),$$

where the decomposition (4.1.3)-(4.1.4) of L is employed. Since $K(M) = \nu M$, we have $K\left(f^{n+1}\right) = \nu \rho^{n+1} M + K\left(g^{n+1}\right)$, and the expression of f^{n+1} writes

$$\begin{aligned} f^{n+1} = &\frac{\varepsilon^\alpha}{\varepsilon^\alpha + \Delta t \nu} \left(I + \frac{\Delta t}{\varepsilon^\alpha + \Delta t \nu} \varepsilon v \cdot \nabla_x\right)^{-1} f^n \\ &+ \frac{\Delta t \nu}{\varepsilon^\alpha + \Delta t \nu} \left(I + \frac{\Delta t}{\varepsilon^\alpha + \Delta t \nu} \varepsilon v \cdot \nabla_x\right)^{-1} \rho^{n+1} M \\ &+ \frac{\Delta t}{\varepsilon^\alpha + \Delta t \nu} \left(I + \frac{\Delta t}{\varepsilon^\alpha + \Delta t \nu} \varepsilon v \cdot \nabla_x\right)^{-1} K\left(g^{n+1}\right), \end{aligned}$$

and it can be injected in (4.2.9)-(4.2.10) to get

$$\frac{\rho^{n+1} - \rho^n}{\Delta t} + \frac{\varepsilon}{\varepsilon^\alpha} \left\langle v \cdot \nabla_x \left[\frac{\varepsilon^\alpha}{\varepsilon^\alpha + \Delta t \nu} \left(I + \frac{\Delta t}{\varepsilon^\alpha + \Delta t \nu} \varepsilon v \cdot \nabla_x\right)^{-1} f^n \right] \right\rangle \quad (4.2.11)$$

$$+\frac{\varepsilon}{\varepsilon^\alpha}\left\langle v\cdot\nabla_x\left[\frac{\Delta t\nu}{\varepsilon^\alpha+\Delta t\nu}\left(I+\frac{\Delta t}{\varepsilon^\alpha+\Delta t\nu}\varepsilon v\cdot\nabla_x\right)^{-1}\rho^{n+1}M\right]\right\rangle \tag{4.2.12}$$

$$+\frac{\varepsilon}{\varepsilon^\alpha}\left\langle v\cdot\nabla_x\left[\frac{\Delta t}{\varepsilon^\alpha+\Delta t\nu}\left(I+\frac{\Delta t}{\varepsilon^\alpha+\Delta t\nu}\varepsilon v\cdot\nabla_x\right)^{-1}K\left(g^{n+1}\right)\right]\right\rangle=0. \tag{4.2.13}$$

Now, we shall make some simplifications by removing some terms in the fluxes which are of order Δt. First of all, since (4.2.13) is of magnitude Δt, it can be removed with no incidence on the accuracy of the scheme. Moreover, since

$$\begin{aligned}\frac{\varepsilon}{\varepsilon^\alpha}\left\langle v\cdot\nabla_x\left[\frac{\varepsilon^\alpha}{\varepsilon^\alpha+\Delta t\nu}\left(I+\frac{\Delta t}{\varepsilon^\alpha+\Delta t\nu}\varepsilon v\cdot\nabla_x\right)^{-1}f^n\right]\right\rangle&=\frac{\varepsilon}{\varepsilon^\alpha+\Delta t}\left\langle v\cdot\nabla_x f^n\right\rangle+O\left(\Delta t\right)\\&=\frac{\varepsilon}{\varepsilon^\alpha+\Delta t}\left\langle v\cdot\nabla_x g^n\right\rangle+O\left(\Delta t\right),\end{aligned}$$

the bracket in (4.2.11) can be replaced by $\varepsilon\left\langle v\cdot\nabla_x g^n\right\rangle/\left(\varepsilon^\alpha+\Delta t\right)$ up to terms of order Δt. However, we do not remove (4.2.12) although this term is also of order Δt. In fact, when ε goes to 0, it converges to $\mathcal{L}(\rho^{n+1})$. Indeed, we have

$$\frac{\Delta t\nu}{\varepsilon^\alpha+\Delta t\nu}\left(I+\frac{\Delta t}{\varepsilon^\alpha+\Delta t\nu}\varepsilon v\cdot\nabla_x\right)^{-1}=\frac{\Delta t\nu}{\varepsilon^\alpha+\Delta t\nu}\left(\nu+\frac{\Delta t\nu}{\varepsilon^\alpha+\Delta t\nu}\varepsilon v\cdot\nabla_x\right)^{-1}\nu,$$

which can be approximated by

$$\left(\nu+\varepsilon v\cdot\nabla_x\right)^{-1}\nu,$$

when ε goes to 0,up to ε^α terms. We make the following approximation that

$$\frac{\Delta t\nu}{\varepsilon^\alpha+\Delta t\nu}\left(I+\frac{\Delta t}{\varepsilon^\alpha+\Delta t\nu}\varepsilon v\cdot\nabla_x\right)^{-1}\approx\frac{\Delta t}{\varepsilon^\alpha+\Delta t}\left(\nu+\varepsilon v\cdot\nabla_x\right)^{-1}\nu.$$

This latter term produces the fractional Laplacian when ε goes to 0. The macro scheme can then we rewritten as

$$\begin{aligned}&\frac{\rho^{n+1}-\rho^n}{\Delta t}+\frac{\varepsilon}{\varepsilon^\alpha+\Delta t}\left\langle v\cdot\nabla_x g^n\right\rangle\\&\qquad+\frac{\Delta t}{\varepsilon^\alpha+\Delta t}\frac{1}{\varepsilon^\alpha}\left\langle\varepsilon v\cdot\nabla_x\left(\nu+\varepsilon v\cdot\nabla_x\right)^{-1}\nu\rho^{n+1}M\right\rangle=0,\end{aligned} \tag{4.2.14}$$

where $\left\langle\varepsilon v\cdot\nabla_x\left(\nu+\varepsilon v\cdot\nabla_x\right)^{-1}\nu\rho^{n+1}M\right\rangle$ converges to $\mathcal{L}(\rho^{n+1})$ when ε goes to 0. The formal proof of this convergence is proposed in Appendix. Since (4.2.14) is of magnitude Δt and converges to $\mathcal{L}\left(\rho^{n+1}\right)$ when ε goes to 0, it is then possible to replace it by

$$\frac{\Delta t}{\varepsilon^\alpha+\Delta t}m\mathcal{L}\left(\rho^n\right),$$

where $\mathcal{L}$ has been defined in (4.1.11), and where we replaced ρ^{n+1} by ρ^n to simplify the numerical computations. Eventually, a semi-discrete-in-time scheme for ρ writes

$$\frac{\rho^{n+1}-\rho^n}{\Delta t}+\frac{\varepsilon}{\varepsilon^\alpha+\Delta t}\left\langle v\cdot\nabla_x g^n\right\rangle+\frac{\Delta t}{\varepsilon^\alpha+\Delta t}m\mathcal{L}\left(\rho^n\right)=0, \tag{4.2.15}$$

and we have the following proposition

Proposition 4.1. *We consider the scheme discretized in time and velocity, defined for all $x \in \mathbb{R}^d, v \in \mathbb{R}^d$ and all time indices $0 \leq n \leq N, N\Delta t = T > 0$, by*

$$\begin{cases} g^{n+1} = \mathrm{e}^{-\frac{\Delta t}{\varepsilon^\alpha}} g^n + \dfrac{\Delta t}{\varepsilon^\alpha} \mathrm{e}^{-\frac{\Delta t}{2\varepsilon^\alpha}} \left[L_{N_v}\left(g^n\right) + g^n - \varepsilon v \cdot \nabla_x \rho^n M - \varepsilon \left(I - \Pi_{N_v}\right)\left(v \cdot \nabla_x g^n\right) \right] \\ \dfrac{\rho^{n+1} - \rho^n}{\Delta t} + \dfrac{\varepsilon}{\varepsilon^\alpha + \Delta t} \left\langle v \cdot \nabla_x g^n \right\rangle_{N_v} + \dfrac{\Delta t}{\varepsilon^\alpha + \Delta t} m \mathcal{L}\left(\rho^n\right) = 0, \end{cases} \tag{4.2.16}$$

with L_{N_v}, Π_{N_v} defined in (4.2.8)*, and with the initial data $f^0 = f_0(x,v)$, $\rho^0 = \left\langle f^0 \right\rangle_{N_v}$ and $g^0 = f^0 - \rho^0 M$. The scheme has the following properties:*

1. *The scheme is of order* 1 *for any fixed $\varepsilon > 0$.*
2. *The scheme is AP: for a fixed Δt, the scheme solves the limit equation* (4.1.10) *when ε goes to* 0
$$\frac{\rho^{n+1} - \rho^n}{\Delta t} + m\mathcal{L}\left(\rho^n\right) = 0, \tag{4.2.17}$$
where $\mathcal{L}$ has been defined in (4.1.11)*.*

Proof. The first point comes immediately from the derivation of the scheme, since all the manipulations we applied to the schemes were done consistently. For the second point, let us remark from its expression in the first line of (4.2.16), that g^{n+1} has exponential decay in ε. Since g^{n+1} vanishes when ε goes to 0, $f^{n+1} = \rho^{n+1} M + g^{n+1}$ tends to a distribution at equilibrium where ρ^{n+1} solves the limit scheme of the second line of (4.2.16)

$$\frac{\rho^{n+1} - \rho^n}{\Delta t} + m\mathcal{L}\left(\rho^n\right) = 0.$$

As the asymptotic scheme is first order in time, we conclude that the scheme (4.2.16) enjoys the AP property. □

Remark 4.2. The proposition above holds for the semi-discrete scheme in time and velocity. The discretization of the space variable can be done with a classical upwind scheme for the gradients, but in addition, a discretization in the real space of the operator $\mathcal{L}$ is necessary.

4.3 Discretization of the limit equation

In the previous section, we proposed a semi-discrete scheme in time and velocity which solves (4.1.1) and enjoys the AP property. However, the fully discrete scheme requires a discretization of the operator $\mathcal{L}$ defined in (4.1.11). From the expression of the integral, two difficulties arise when numerically computing it. First of all, since ρ and ν_0 are periodic functions, the integrand has a slow decay to 0. Therefore, it is necessary to truncate the integral far from the origin, to ensure that the discretization has a good accuracy. The second difficulty comes from the singularity of the integrand at the origin, that must be treated with care.

The discretization of heavy-tailed integrals arising in the integral formulation of the fractional Laplacian is an independent question from the derivation of AP schemes for (4.1.1). In the case of the fractional Laplacian, some efficient methods are presented in [65, 35]. However, because of the coefficient γ defined in (4.1.12) appearing in $\mathcal{L}$, they cannot be rendered word for word in our case. We propose here a very simple approach for the discretization of $\mathcal{L}$ in dimension $d = 1$, when $\alpha > 0.5$, based on a method proposed in [65]. The development of

an efficient numerical methods for $\mathcal{L}$ in the general case would be the topic of an independent task, and is not our main concern in this work.

To deal separately with the two difficulties arising in the numerical computation of $\mathcal{L}$, let δ and A be such that $0 < \delta < A < +\infty$. We decompose $\mathcal{L}$ as follows

$$\mathcal{L}(\rho)(x) = P.V. \int_{|y|\leq\delta} \gamma(x, x-y) \frac{\rho(x) - \rho(x-y)}{|y|^{1+\alpha}} \mathrm{d}y \tag{4.3.1}$$

$$+ \int_{\delta<|y|\leq A} \gamma(x, x-y) \frac{\rho(x) - \rho(x-y)}{|y|^{1+\alpha}} \mathrm{d}y \tag{4.3.2}$$

$$+ \int_{|y|>A} \gamma(x, x-y) \frac{\rho(x) - \rho(x-y)}{|y|^{1+\alpha}} \mathrm{d}y, \tag{4.3.3}$$

where γ has been defined in (4.1.12). A discretization of these three integrals must be chosen to ensure that $\mathcal{L}$ is computed with a good accuracy. First of all, A must be chosen large enough to ensure that (4.3.3) can be removed in the approximation of $\mathcal{L}$. As γ and ρ are bounded functions, there exists a constant C such that

$$\left| \int_{|y|>A} \gamma(x, x-y) \frac{\rho(x) - \rho(x-y)}{|y|^{d+\alpha}} \mathrm{d}y \right| \leq C \int_{|y|>A} \frac{1}{|y|^{1+\alpha}} \mathrm{d}y = \frac{2C}{\alpha} A^{-\alpha}. \tag{4.3.4}$$

It is then possible to choose A large enough to ensure that the error done when removing (4.3.3) in the computation of $\mathcal{L}(\rho)$ can be neglected. Therefore, we fix

$$A = C(\alpha \Delta x)^{-1/\alpha}, \tag{4.3.5}$$

with C chosen independently of the discretization parameters such that the estimate (4.3.4) is smaller than Δx. We will consider $C = 10$ in all the following numerical tests. Note that the value of A tends to infinity when α is small, that is why we consider only $\alpha > 1/2$ in the sequel.

The discretization of (4.3.2) can be done with a standard quadrature, such as the Simpson method. We propose to use a discretization of the intervals $[-A, -\delta)$ and $(\delta, A]$ with step Δx. The values of γ can be numerically computed on this grid, and those of ρ are interpolated with a good accuracy, from the values of ρ on the space grid (4.2.1), using the periodic boundary conditions of ρ. Note that it is necessary to use a quadrature precise enough, since the integration interval is large. Indeed, with the choice $\alpha > 1/2$, the integration interval can be of magnitude $C/\Delta x^2$. A quadrature of order at least 3 is then needed to ensure that (4.3.2) is computed with precision at least $O(\Delta x)$. In addition, the choice of δ plays an important role in the accuracy of the approximation of (4.3.2). Indeed, the error in the quadrature method is bounded by the derivative of the integrand. In the case of (4.3.2), this derivative may be large when y goes to 0. Hence, if δ is too small, the error done in the approximation of (4.3.2) is important because of the bound of the derivative.

Eventually, the discretization of the integral (4.3.1) yields the problems associated with the discretization of the integrals defined as principal values. To take into account the symmetry of the integral which is necessary to define the principal value, we expand the integrand

$$\gamma(x, x-y)\left[\rho(x) - \rho(x-y)\right],$$

around the origin. It reads

$$\gamma(x, x-y)\left[\rho(x) - \rho(x-y)\right] = -\sum_{j=1}^{q} c_j y^j + R, \tag{4.3.6}$$

where the remainder R is such that $|R| \leq C|y|^{q+1}$, and with

$$c_j = \sum_{i=1}^{j} (-1)^i \frac{1}{i!(j-i)!} \partial_y^{(j-i)} \gamma(x,x) \partial_x^{(i)} \rho(x).$$

Once injected in (4.3.1), the decomposition (4.3.6) reads

$$-\sum_{j=1}^{q} c_j \int_{-\delta}^{\delta} \frac{y^j}{|y|^{1+\alpha}} \mathrm{d}y + \int_{-\delta}^{\delta} \frac{R}{|y|^{1+\alpha}} \mathrm{d}y,$$

where the integrals can be explicitly computed, and vanish when j is odd. Eventually, denoting $p = \lfloor q/2 \rfloor$, we have

$$\int_{|y|\leq\delta} \gamma(x, x-y) \frac{\rho(x) - \rho(x-y)}{|y|^{1+\alpha}} \mathrm{d}y = -\sum_{j=1}^{p} c_{2j} \frac{2}{2j-\alpha} \delta^{2j-\alpha} + O(\delta^{2p+1-\alpha}). \tag{4.3.7}$$

Since δ cannot be chosen too small because of the computation of (4.3.2), the accuracy of this approximation depends on the number of terms considered in the Taylor expansion.

To check the accuracy of this numerical method for $\mathcal{L}$, we test it on the simple case of the fractional Laplacian, when $\gamma = c_{1,\alpha}$ is constant and we fix $\alpha = 1.5$. As the fractional Laplacian of the function ρ can be computed easily and with a good accuracy in Fourier variable, this provides a reference solution to which the current discretization can be compared. In the test presented in Fig. 4.1, we consider the periodic function defined by

$$\rho(x) = e^{-9x^2}, \quad x \in [-1, 1], \tag{4.3.8}$$

and $N_x = 64$ points for the discretization (4.2.1). The fractional Laplacian of ρ is computed with (4.1.15), where the Fourier modes k are chosen as the integers such that $-N_x/2 \leq k \leq N_x/2$. Using the discretization of $\mathcal{L}$ explained above with $\delta = 0.3$, and A defined in (4.3.5) with $C = 10$, Fig. 4.1 presents the quantities $\mathcal{L}(\rho)$ with (4.3.1) approximated up to the order 2 and 4 in δ. We observe that the solutions are close from the reference solution computed with the Fourier transform, and that the approximation with the order 4 in δ is more precise.

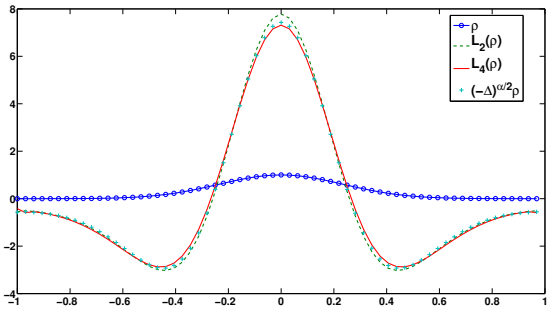

Figure 4.1: For $N_x = 64$ and ρ defined in (4.3.8), the function ρ, $(-\Delta)^{\alpha/2}\rho$ and $\mathcal{L}(\rho)$ computed up to the order 2 and 4 in δ.

However, we observed that the use of a larger order in δ in the approximation of (4.3.1) makes instabilities arise on the border of the domain. In what follows, we will use the above

approximation of $\mathcal{L}$ up to the order 2 in δ in the approximation of (4.3.1). The function γ defined in (4.1.12) is computed once for all, independently of ε with a fine quadrature of the integral in the exponential. After this quadrature, γ can be expressed in terms of an usual Γ function, which avoids another numerical computation of an integral. When the function γ is non constant, there is -up to our knowledge- no reference solution to which we can compare the discretization of $\mathcal{L}$. In the following numerical tests, we will highlight that the micro-macro scheme degenerates into a scheme for (4.1.10) when ε goes to 0, with the operator $\mathcal{L}$ computed with the method we proposed in this part. If a better discretization of $\mathcal{L}$ is available, one will just have to put it in place of $\mathcal{L}$ in the macro equation of the scheme (4.2.16), and observe that it is conserved in the limit equation.

4.4 Numerical tests

In this section, we test the properties of the micro-macro scheme of Prop. 4.1, using the discretization of $\mathcal{L}$ discussed in the previous part, with A defined in (4.3.5), and $C = 10$. In the discretization of $\mathcal{L}$, we fix $\delta = 0.3$ since this choice of δ made the method be precise for the fractional Laplacian. In the sequel we will consider the following cross-section

$$\sigma(x, v, v') = f_1(x) f_2(v) f_2(v') M(v), \tag{4.4.1}$$

where M has been defined in (4.2.4). The function f_1 is periodic and defined on $[-1, 1]$ by

$$f_1(x) = e^{-9x^2} + c_{1,\alpha},$$

and the function f_2 is given by

$$f_2(v) = 1 + \frac{1}{1 + |v|^{d+\alpha}}.$$

We will consider the following initial data for f

$$f_0(x, v) = (1 + \sin(\pi x))\, M(v), \tag{4.4.2}$$

and the time, space and velocity variables will be discretized as explained in the beginning of Section 4.2, with $v_{max} = 10$ and $N_v = 200$ for the velocities. All the computations will be done up to the final time $T = 0.1$, the number of time steps and space points will be specified in each case.

First of all, we compare the solution of the scheme (4.2.16) to the solution of a conventional scheme in time for (4.1.1). When $\varepsilon = 1$, since (4.1.1) is not stiff, it can be numerically solved with an explicit scheme, that writes

$$\begin{cases} \varepsilon^\alpha \dfrac{f^{n+1} - f^n}{\Delta t} + \varepsilon v \cdot \nabla_x f^n = L_{N_v}\left(f^n\right) \\ \rho^{n+1} = \left\langle f^{n+1} \right\rangle_{N_v}, \end{cases} \tag{4.4.3}$$

where L_{N_v} and $\langle \cdot \rangle_{N_v}$ are defined in (4.2.8)-(4.2.3), and with the gradient computed with an upwind scheme. The densities obtained with the schemes (4.2.16) and (4.4.3) for $\Delta t = 10^{-3}$ and $N_x = 64$ are displayed in Fig. 4.2. We observe that the density obtained with the micro-macro scheme is very close from the one obtained with the explicit scheme.

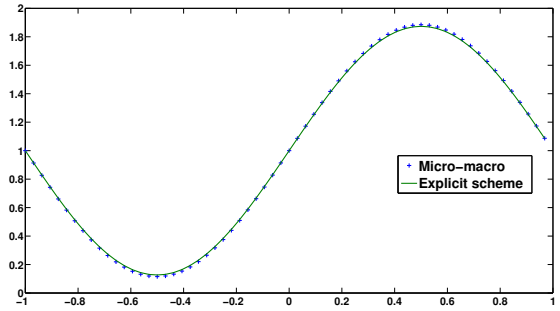

Figure 4.2: For $T = 0.1$, $\Delta t = 10^{-3}$, $N_x = 64$, and $\varepsilon = 1$, the densities obtained with the scheme (4.2.16) and (4.4.3).

To highlight the fact that the micro-macro scheme (4.2.16) is of order 1 when ε is fixed, we present in Fig. 4.3 a numerical order study of this scheme. To obtain this figure, we fixed the number of points in space $N_x = 64$ and we computed a reference solution with (4.2.16) and $\Delta t = 10^{-4}$. We then compared this reference solution with the solutions of (4.2.16) obtained with a range of larger Δt. The relative error

$$E(\Delta t) = \frac{\|\rho_{ref} - \rho_{\Delta t}\|_\infty}{\|\rho_{ref}\|_\infty},$$

is displayed as a function of Δt in Fig. 4.3. As it draws a line of slope slightly larger than 1, we conclude on the first order accuracy in time for the micro-macro scheme.

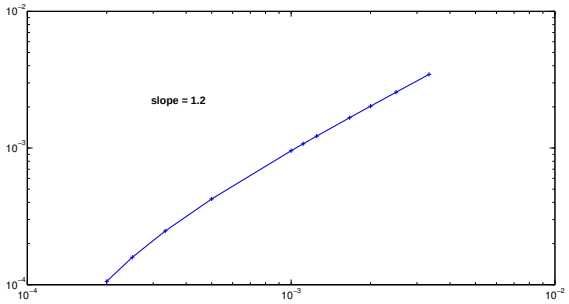

Figure 4.3: For $T = 0.1$, $N_x = 64$, and $\varepsilon = 1$, the relative error between the scheme (4.2.16) computed with $\Delta t = 10^{-4}$ and (4.2.16) computed with a range of larger Δt, in function of Δt (log scale).

To highlight the AP character of the micro-macro scheme, Fig. 4.4 displays the density obtained with the micro-macro scheme with $N_x = 64$, $\Delta t = 10^{-3}$, and $\varepsilon = 10^{-4}$, and the density obtained with the limit scheme (4.2.17) with the same parameters. As the two densities coincide, it shows that the micro-macro scheme degenerates into the scheme (4.2.17) when ε goes to 0.

Moreover, it is possible to show numerically that the solution of the micro-macro scheme converges with speed ε^α to the solution of the limit scheme (see [5]). To highlight this property, we fixed $N_x = 64$ and $\Delta t = 10^{-3}$, and we computed the relative error between the solution

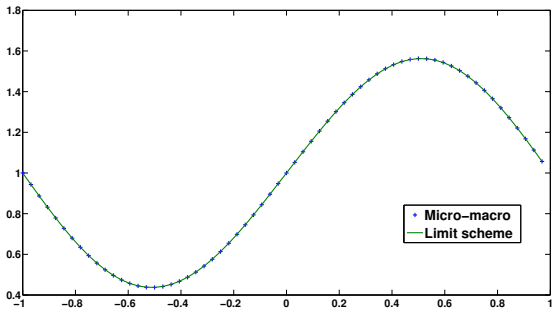

Figure 4.4: For $T = 0.1$, $\Delta t = 10^{-3}$, and $N_x = 64$ the densities obtained with the limit scheme and with the micro-macro scheme for $\varepsilon = 10^{-4}$.

ρ_{limit} of the limit scheme (4.2.17) and ρ_ε of the micro-macro scheme (4.2.16) for a range of ε. The error is defined by

$$E(\varepsilon) = \frac{\|\rho_\varepsilon - \rho_{limit}\|_\infty}{\|\rho_{limit}\|_\infty},$$

and is displayed in Fig. 4.5 in function of ε. In logarithmic scale, it is a line of slope α, which shows that the numerical decay rate of the micro-macro scheme towards the limit scheme is ε^α.

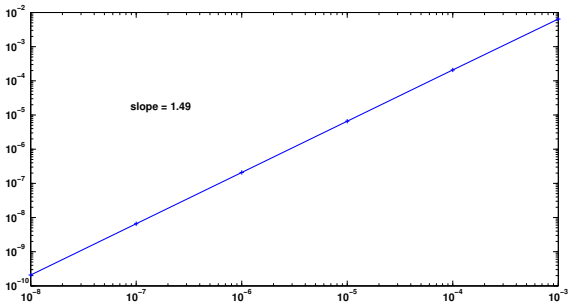

Figure 4.5: For $T = 0.1$, $\Delta t = 10^{-3}$, and $N_x = 64$, the relative error between the scheme (4.2.16) computed for a range of ε and the limit scheme (4.2.17) (log scale).

Remark 4.3. It is worth mentioning that the approximations we performed to design the micro-macro scheme make it less efficient in the intermediate regime compared to the regime $\varepsilon = 1$ and $\varepsilon << 1$. This is a common feature of AP schemes, which may suffer from order reduction when $\Delta t \approx \varepsilon^\alpha$ (see Chapters 1 and 2). This is highlighted in Fig. 4.6, where the densities obtained with the schemes (4.2.16) and (4.4.3) for $\varepsilon = 10^{-2}$ are displayed. We fixed $N_x = 64$, and the micro-macro schemes uses a time step $\Delta t = 10^{-4}$ while the explicit scheme is computed with a finer time step $\Delta t = 10^{-6}$. Contrary to the previous Figures, the density are not superimposed which emphasizes the lack of uniform accuracy of our scheme. However, since it is consistent, considering smaller Δt enables to recover the reference solution.

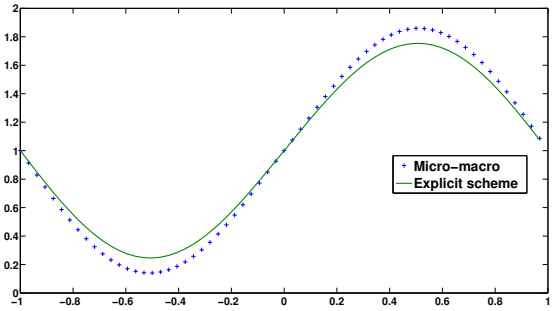

Figure 4.6: For $T = 0.1$, $\varepsilon = 10^{-2}$, and $N_x = 64$ the densities obtained with the explicit scheme for $\Delta t = 10^{-6}$ and with the micro-macro scheme for $\Delta t = 10^{-4}$.

4.5 Appendix

In this appendix, we formally prove that for a given density ρ, the quantity

$$\frac{1}{\varepsilon^\alpha}\left\langle \varepsilon v\cdot\nabla_x\left(\nu+\varepsilon v\cdot\nabla_x\right)^{-1}\nu M\right\rangle\rho, \tag{4.5.1}$$

converges to $\mathcal{L}(\rho)$ when ε goes to 0, with M given by (4.2.4), where $\mathcal{L}$ has been defined in (4.1.11), and ν fulfills (4.1.9). The inverse of the transport operator can be analytically solved. Indeed, following the computations of [5, 53], the solution χ of the equation

$$\left(\nu+\varepsilon v\cdot\nabla_x\right)\chi = \nu\rho M,$$

has an integral formulation

$$\chi(x,v) = \int_0^{+\infty} \mathrm{e}^{-\int_0^z \nu(x-\varepsilon v s,v)\mathrm{d}s}\nu(x-\varepsilon vz,v)\rho(x-\varepsilon vz)M(v)\mathrm{d}z, \tag{4.5.2}$$

that can be easily computed by solving the equation with the characteristics. The brackets in (4.5.1) makes the quantity $\varepsilon v\cdot\nabla_x\chi$ appear, which satisfies the equality

$$\varepsilon v\cdot\nabla_x\chi = \nu\left(\rho M-\chi\right),$$

and that can be rewritten using (4.5.2)

$$\begin{aligned}\rho M-\chi &= \rho M-\int_0^{+\infty}\mathrm{e}^{-\int_0^z \nu(x-\varepsilon v s,v)\mathrm{d}s}\nu(x-\varepsilon vz,v)\rho(x-\varepsilon vz)\mathrm{d}zM\\ &= \int_0^{+\infty}\mathrm{e}^{-\int_0^z \nu(x-\varepsilon v s,v)\mathrm{d}s}\nu(x-\varepsilon vz,v)\left[\rho(x)-\rho(x-\varepsilon vz)\right]\mathrm{d}zM,\end{aligned}$$

because (4.1.8) implies that

$$\int_0^{+\infty}\mathrm{e}^{-\int_0^z \nu(x-\varepsilon v s,v)\mathrm{d}s}\nu(x-\varepsilon vz,v)\mathrm{d}z = 1.$$

This provides an expression of $\varepsilon v\cdot\nabla_x\chi$ that makes the fractional diffusion limit appear once injected in (4.5.1). Indeed, (4.5.1) rewrites

$$\frac{1}{\varepsilon^\alpha}\left\langle\int_0^{+\infty}\mathrm{e}^{-\int_0^z \nu(x-\varepsilon v s,v)\mathrm{d}s}\nu(x-\varepsilon vs,v)\left[\rho(x)-\rho(x-\varepsilon vz)\right]\mathrm{d}zM\nu\right\rangle, \tag{4.5.3}$$

and the change of variables $w = \varepsilon v z$ in the integral in v makes the limit operator appear. Using (4.2.4), it writes

$$\int_{\mathbb{R}^d} \int_0^{+\infty} \nu\left(x, \frac{w}{\varepsilon z}\right) \frac{m z^\alpha}{\varepsilon^{d+\alpha} z^{d+\alpha} + |w|^{d+\alpha}} \nu\left(x - w, \frac{w}{\varepsilon z}\right) \mathrm{e}^{-z \int_0^1 \nu\left(x - ws, \frac{w}{\varepsilon z}\right) \mathrm{d}s} \\ [\rho(x) - \rho(x - w)] \, \mathrm{d}z \mathrm{d}w,$$

and using (4.1.9), it formally converges to

$$m \; P.V. \int_{\mathbb{R}^d} \left(\nu_0(x) \nu_0(x - w) \int_0^{+\infty} z^\alpha \mathrm{e}^{-z \int_0^1 \nu_0(x - ws) \mathrm{d}s} \mathrm{d}z \right) \frac{\rho(x) - \rho(x - w)}{|w|^{d+\alpha}} \mathrm{d}w,$$

when ε goes to 0, which is the expression of the limit operator (4.1.11) applied to ρ.

Conclusion

Dans cette thèse, nous avons construit plusieurs schémas numériques pour l'équation cinétique qui possèdent la propriété *Asymptotic Preserving* (AP) pour trois cas d'asymptotiques de diffusion anormale. En considérant une équation cinétique dont l'opérateur de collision a un équilibre à queue lourde, nous avons tout d'abord proposé trois schémas capables de capter la limite de diffusion fractionnaire de l'équation. Après avoir dressé le constat qu'une approche basée sur une formulation complètement implicite en temps de l'équation cinétique ne possédait pas la propriété AP pour la limite de diffusion fractionnaire, nous avons mis en place une stratégie pour prendre en compte les grandes vitesses dans les calculs numériques et assurer ainsi la propriété AP du schéma. En utilisant cette méthode, nous avons ensuite pu construire un schéma AP basé sur une décomposition micro-macro de la fonction de distribution qui est écrit en variable d'espace et où le transport est traité explicitement. Enfin, nous avons construit un schéma basé sur une formulation intégrale de l'équation cinétique en Fourier qui possède la propriété UA (pour *Uniform Accuracy*), plus forte que la propriété AP puisque la précision d'un tel schéma ne dépend pas de ε. Pour ces trois schémas, une attention particulière a été portée à la discrétisation en vitesse, puisqu'il est crucial de prendre en compte le poids à l'infini de l'équilibre dans les calculs numériques pour assurer la convergence des schémas vers des schémas qui résolvent l'équation de diffusion fractionnaire quand ε tend vers 0.

Nous avons ensuite appliqué cette méthodologie à un deuxième cas de limite de diffusion fractionnaire pour l'équation cinétique. En considérant un opérateur de collision dont la fréquence de collision présente une dégénérescence en $v = 0$, l'équation cinétique tend en effet vers une équation de diffusion fractionnaire quand ε tend vers 0. Nous avons adapté les trois schémas écrits pour le cas de l'équilibre à queue lourde en faisant en sorte que les petites vitesses soient correctement prises en compte dans les schémas numériques, et en adaptant la stratégie de construction des schémas à l'opérateur de collision.

En considérant le cas critique $\alpha = 2$ des équilibres à queue lourde de la première partie, nous avons adapté les trois schémas (implicite, micro-macro et basé sur une formulation intégrale de l'équation) à ce cas de limite de diffusion normale avec scaling anormal. En plus de l'importance des grandes vitesses dans le modèle asymptotique, la difficulté de l'écriture de schémas pour ce cas réside dans la lenteur de la convergence vers le modèle limite. En effet, nous avons montré que le modèle tend vers l'équation limite avec le taux $1/(1+|\ln(\varepsilon)|)$. Comme nous avons prouvé que cette convergence se fait en passant par un modèle intermédiaire vers lequel le modèle cinétique tend avec le taux $\varepsilon\,(1+|\ln(\varepsilon)|)$, nous avons construit les schémas de manière à ce qu'ils respectent la dynamique de la convergence. Cette stratégie permet de limiter l'étendue du régime intermédiaire. Nous avons ensuite écrit un schéma micro-macro pour l'équation cinétique avec un opérateur de collision général qui possède la propriété AP pour cette asymptotique de diffusion fractionnaire. Il utilise une stratégie dite relaxée pour l'équation micro, ce qui évite l'inversion de l'opérateur de collision.

Les trois familles de schémas (implicite, micro-macro et basé sur la formulation de Duhamel de l'équation) qui sont mises en place dans ce manuscrit sont d'ordre 1, donc de précision équivalente. Cependant, chacune possède des avantages particuliers par rapport aux autres. Grâce à leur simplicité, les schémas implicites peuvent facilement être mis en oeuvre. En dimension 1 leur coût de calcul est raisonnable, mais pas en dimension supérieure. Il est à noter que, du fait de la non-uniformité de la précision en ε, les régimes intermédiaires sont plus coûteux que les régimes $\varepsilon = 1$ et $\varepsilon << 1$. En termes de coûts de calcul, d'ordre et de comportement dans les régimes intermédiaires, les schémas micro-macro se comportent de la même manière. En revanche, le passage en dimension supérieure se fait a priori plus facilement que pour les schémas implicites. Un autre intérêt de l'approche micro-macro est qu'elle peut

s'adapter à des opérateurs de collision plus généraux que l'opérateur BGK, alors que les schémas implicite et Duhamel sont restreints à ce cas. En dernier lieu, comme les schémas basés sur la formulation de Duhamel de l'équation sont uniformément précis en ε, ils deviennent compétitifs en termes de coûts de calcul dans les régimes intermédiaires. De plus, comme il est possible de n'écrire qu'un schéma sur la densité macroscopique ρ, le passage en dimension supérieure se fait a priori de manière moins coûteuse que pour les deux précédentes classes de schémas, car il n'y a pas de stockage en vitesse nécessaire.

Enfin, nous avons traité dans la dernière partie le cas d'une limite de diffusion fractionnaire lorsque l'opérateur de collision est non-local en v avec la fréquence de collision dépendant de x et l'équilibre est à queue lourde. Dans ce cadre, inadapté à l'utilisation de la variable de Fourier en espace, nous avons construit un schéma micro-macro pour l'équation cinétique, dans lequel l'équation micro est traitée avec une approche relaxée qui permet de ne pas inverser l'opérateur de collision non local, et le caractère AP est assuré par la prise en compte des grandes vitesses et de l'inverse de l'opérateur de transport dans l'équation macro.

Pour continuer ce travail, il serait tout d'abord intéressant de réaliser des tests numériques des schémas écrits dans la thèse en dimension supérieure à 1. De plus, les schémas basés sur la formulation intégrale de l'équation cinétique nécessitent le calcul d'une convolution discrète à chaque pas de temps. Pour améliorer le temps de calcul, il faudrait optimiser son traitement, puisqu'elle est pour l'instant calculée avec une méthode directe. Une autre perspective de travail est d'utiliser les approches mises en place dans cette thèse pour construire des schémas d'ordre plus élevé en temps. Pour les schémas implicite et micro-macro, il faudrait utiliser un schéma semi-discret en temps d'ordre élevé avant de reprendre l'analyse préalable à la discrétisation en vitesse. En revanche, il semble qu'augmenter l'ordre de l'approche basée sur la formulation intégrale de l'équation cinétique est plus compliqué, puisque l'ordre de la discrétisation du modèle asymptotique peut être inférieur à l'ordre du schéma.

Concernant le dernier cas traité dans cette thèse, la limite de diffusion fractionnaire lorsque l'opérateur de collision est non local avec la section locale qui dépend de x, une discrétisation plus efficace et robuste de l'opérateur limite permettrait d'améliorer la résolution du système micro-macro. Ce problème, indépendant des questions liées à la discrétisation des équations cinétiques, est crucial pour disposer d'un schéma AP efficace pour l'équation cinétique dans ce cadre.

L'étude que nous proposons dans ce manuscrit pourrait être prolongée à la prise en compte d'autres opérateurs de collision, comme l'opérateur de Fokker-Planck avec équilibre à queue lourde [13] ou l'opérateur de Vlasov-Fokker-Planck fractionnaire [15] qui permettent d'établir une limite de diffusion fractionnaire pour l'équation cinétique. Notons cependant que la limite des modèles cinétiques lorsque l'équilibre de l'opérateur de collision est une fonction à queue lourde n'est pas connue pour tous les opérateurs de collision. Par exemple, dans des travaux récents, E. Nasreddine et M. Puel ont montré que l'équation cinétique avec opérateur de Fokker-Planck pouvait, sous certaines conditions sur l'équilibre à queue lourde, avoir une limite de diffusion normale [61]. Avec d'autres hypothèses sur l'équilibre à queue lourde, une limite de diffusion fractionnaire ou une limite de diffusion normale avec scaling anormal dans un cas critique apparaît [13]. En revanche, lorsque ces hypothèses ne sont pas vérifiées, l'analyse asymptotique du modèle est bien plus complexe. La généralisation des schémas proposés dans cette thèse à des opérateurs de collision plus généraux n'est envisageable que dans les cas pour lesquels la dérivation théorique des modèles asymptotiques a été effectuée.

Enfin, l'étude proposée dans cette thèse pourrait être prolongée à plus long terme en adaptant les schémas pour prendre en compte des conditions de bord autres que périodiques.

D'un point de vue mathématique, l'analyse asymptotique dans ce cadre est compliquée par la présence du bord et reste un problème ouvert dans bien des cas. En considérant l'équation cinétique munie d'un opérateur de Vlasov-Fokker-Planck fractionnaire sur un domaine borné avec des conditions de réflexion spéculaire aux bords, L. Cesbron a établi une limite de diffusion fractionnaire pour l'équation cinétique dans [14]. Cette limite s'écrit avec un opérateur intégral proche du laplacien fractionnaire, mais dont l'écriture prend en compte les conditions de bord imposées. Ainsi, comme les conditions imposées au bord changent la nature du modèle asymptotique, une étude spécifique est donc nécessaire pour établir des schémas AP dans ce cas.

Bibliography

[1] C. Bardos, F. Golse, and D. Levermore. Fluid dynamic limits of kinetic equations. i. formal derivations. *J. Stat. Phys.*, 63(1-2):323–344, 1991.

[2] C. Bardos, F. Golse, and D. Levermore. Fluid dynamic limits of kinetic equations. ii: Convergence proofs for the boltzmann equations. *Comm. on Pure and Appl. Math.*, XLVI:667–753, 1993.

[3] C. Bardos, R. Santos, and R. Sentis. Diffusion approximation and computation of the critical size. *Trans. Amer. Math. Soc.*, 284(2):617–649, 1984.

[4] N. Ben Abdallah, A. Mellet, and M. Puel. Anomalous diffusion limit for kinetic equations with degenerate collision frequency. *Math. Models Methods Appl. Sci.*, 21(11):2249–2262, 2011.

[5] N. Ben Abdallah, A. Mellet, and M. Puel. Fractional diffusion limit for collisional kinetic equations: A Hilbert expansion approach. *Kinet. Relat. Models*, 4(4):873–900, 2011.

[6] M. Bennoune, M. Lemou, and L. Mieussens. Uniformly stable numerical schemes for the Boltzmann equation preserving the compressible Navier Stokes asymptotics. *J. Comput. Phys.*, 227(8):3781 – 3803, 2008.

[7] A. Bensoussan, J.-L. Lions, and G. Papanicolaou. Boundary layers and homogenization of transport processes. *Publ. Res. Int. Math. Sci.*, 15:53–157, 1979.

[8] A.V. Bobylev, J.A. Carrillo, and I.M. Gamba. On some properties of kinetic and hydrodynamic equations for inelastic interactions. *J. Statist. Phys.*, 98:743–773, 2000.

[9] A.V. Bobylev and I.M. Gamba. Boltzmann equations for mixtures of Maxwell gases: Exact solutions and power like tails. *J. Statist. Phys.*, 124(2-4):497–516, 2006.

[10] C. Borgers, C. Greengard, and E. Thomann. The diffusion limit of free molecular flow in thin plane channels. *SIAM J. Appl. Math.*, 52(4):1057–1075, 1992.

[11] C. Buet and S. Cordier. Asymptotic preserving scheme and numerical methods for radiative hydrodynamic models. *C. R. Math. Acad. Sci. Paris*, 338(12):951 – 956, 2004.

[12] J.A. Carrillo, T. Goudon, P. Lafitte, and F. Vecil. Numerical schemes of diffusion asymptotics and moment closures for kinetic equations. *J. Sci. Comput.*, 36(1):113–149, 2008.

[13] P. Cattiaux, E. Nasreddine, and M. Puel. Diffusion or fractional diffusion limit for kinetic Fokker-Planck equation with heavy-tails equilibria. *Preprint*, 2016.

[14] L. Cesbron. Anomalous diffusion limit of kinetic equation on spatially bounded domains. *Preprint*, 2016.

[15] L. Cesbron, A. Mellet, and K. Trivisa. Anomalous transport of particles in plasma physics. *Applied Mathematics Letters*, 25(12):2344 – 2348, 2012.

[16] N. Crouseilles, H. Hivert, and M. Lemou. Multiscale numerical schemes for kinetic equations in the anomalous diffusion limit. *C. R. Math. Acad. Sci. Paris*, 353(8):755 – 760, 2015.

[17] N. Crouseilles, H. Hivert, and M. Lemou. Numerical schemes for kinetic equations in the anomalous diffusion limit. Part I: The case of heavy-tailed equilibrium. *SIAM, J. Sc. Comput.*, 38(2):A737–A764, 2016.

[18] N. Crouseilles, H. Hivert, and M. Lemou. Numerical schemes for kinetic equations in the anomalous diffusion limit. Part II: Degenerate collision frequency. *SIAM J. Sc. Comput.*, 38(4):A2464–A2491, 2016.

[19] N. Crouseilles and M. Lemou. An asymptotic preserving scheme based on a micro-macro decomposition for collisional Vlasov equations: diffusion and high-field scaling limits. *Kinet. Relat Models*, 4(2):441–477, 2011.

[20] S. De Moor. Fractional diffusion limit for a stochastic kinetic equation. *Stochastic Process. Appl.*, 124(3):1335 – 1367, 2014.

[21] S. De Moor. *Limites diffusives pour des équations cinétiques stochastiques*. PhD thesis, ENS Rennes, Rennes, France, 2014.

[22] P. Degond, T. Goudon, and F. Poupaud. Diffusion limit for non homogeneous and non-micro-reversible processes. *Indiana Univ. Math. J*, 49:1175–1198, 2000.

[23] D. del Castillo-Negrete, B. Carreras, and V. Lynch. Non-diffusive transport in plasma turbulence: A fractional diffusion approach. *Phys. Rev. Lett.*, 94:065003, Feb 2005.

[24] G. Dimarco and L. Pareschi. Exponential Runge-Kutta methods for stiff kinetic equations. *SIAM J. Numer. Anal.*, 49(5):2057–2077, 2011.

[25] C. Dogbé. Diffusion anormale pour le gaz de Knudsen. *Comptes Rendus de l'Académie des Sciences - Series I - Mathematics*, 326(8):1025 – 1030, 1998.

[26] C. Dogbé. Anomalous diffusion limit induced on a kinetic equation. *Journal of Statistical Physics*, 100(3-4):603–632, 2000.

[27] M.H. Ernst and R. Brito. Scaling solutions of inelastic Boltzmann equations with over-populated high energy tails. *J. Statist. Phys.*, 109(3-4):407–432, 2002.

[28] F. Filbet and S. Jin. A class of asymptotic-preserving schemes for kinetic equations and related problems with stiff sources. *J. Comput. Phys.*, 229(20):7625 – 7648, 2010.

[29] I. Gallagher, L. Saint-Raymond, and B. Texier. *From Newton to Boltzmann: Hard Spheres and Short-range Potentials*. Zurich Lectures in Advanced Mathematics. European Mathematical Society, 2014.

[30] F. Golse. Anomalous diffusion limit for the Knudsen gas. *Asymptotic Analysis*, 17(1):1–12, 1998.

[31] L. Gosse and G. Toscani. An asymptotic-preserving well-balanced scheme for the hyperbolic heat equations. *C. R. Math. Acad. Sci. Paris*, 334(4):337 – 342, 2002.

[32] L. Gosse and G. Toscani. Asymptotic-preserving & well-balanced schemes for radiative transfer and the Rosseland approximation. *Numerische Mathematik*, 98(2):223–250, 2004.

[33] H. Hivert. Numerical schemes for kinetic equations with diffusion limit and anomalous time scale. *Preprint*, 2016.

[34] M. Hochbruck and A. Ostermann. Exponential integrators. *Acta Numer.*, 19:209–286, 5 2010.

[35] Y. Huang and A. Oberman. Numerical methods for the fractional Laplacian: A finite difference-quadrature approach. *SIAM Journal on Numerical Analysis*, 52(6):3056–3084, 2014.

[36] M. Jara, T. Komorowski, and S. Olla. Limit theorems for additive functionals of a Markov chain. *Ann. Appl. Probab.*, 19(6):2270–2300, 12 2009.

[37] S. Jin. Efficient asymptotic-preserving (AP) schemes for some multiscale kinetic equations. *SIAM J. Sci. Comput.*, 21(2):441–454, 1999.

[38] S. Jin and D. Levermore. The discrete-ordinate method in diffusive regimes. *Transport Theory Stat. Phys.*, 20(5-6):413–439, 1991.

[39] S. Jin and D. Levermore. Numerical schemes for hyperbolic conservation laws with stiff relaxation terms. *J. Comput. Phys.*, 126(2):449 – 467, 1996.

[40] S. Jin and L. Pareschi. Discretization of the multiscale semiconductor Boltzmann equation by diffusive relaxation schemes. *J. Comput. Phys.*, 161(1):312–330, June 2000.

[41] S Jin, L. Pareschi, and G. Toscani. Uniformly accurate diffusive relaxation schemes for multiscale transport equations. *SIAM J. Numer. Anal.*, 38(3):913–936, 2000.

[42] S. Jin and Y. Shi. A micro-macro decomposition-based asymptotic-preserving scheme for the multispecies Boltzmann equation. *SIAM J. Sc. Comput.*, 31(6):4580–4606, 2010.

[43] A. Klar. An asymptotic-induced scheme for nonstationary transport equations in the diffusive limit. *SIAM J. Numer. Anal.*, 35(3):1073–1094, 1998.

[44] A. Klar. An asymptotic preserving numerical scheme for kinetic equations in the low Mach number limit. *SIAM J. Numer. Anal.*, 36(5):1507–1527, 1999.

[45] A. KLAR and C. SCHMEISER. Numerical passage from radiative heat transfer to nonlinear diffusion models. *Math. Models Methods Appl. Sci.*, 11(05):749–767, 2001.

[46] C. Kleiber and S. Kotz. *Statistical size distributions in economics and actuarial sciences*. John Wiley and Sons, Hoboken, NJ, 2003.

[47] O. E. Lanford. *Dynamical Systems, Theory and Applications: Battelle Seattle 1974 Rencontres*, chapter Time evolution of large classical systems, pages 1–111. Springer Berlin Heidelberg, Berlin, Heidelberg, 1975.

[48] E. W. Larsen and J. B. Keller. Asymptotic solution of neutron transport problems for small mean free paths. *J. Math. Phys*, 15:75–81, 1974.

[49] M. Lemou. Relaxed micro-macro schemes for kinetic equations. *C. R. Math. Acad. Sci. Paris*, 348(7-8):455 – 460, 2010.

[50] M. Lemou and F. Méhats. Micro-macro schemes for kinetic equations including boundary layers. *SIAM J. Sci. Comput.*, 34(6):734–760, 2012.

[51] M. Lemou, F. Méhats, and P. Raphaël. Orbital stability of spherical galactic models. *Inventiones mathematicae*, 187(1):145–194, 2012.

[52] M. Lemou and L. Mieussens. A new asymptotic preserving scheme based on micro-macro formulation for linear kinetic equations in the diffusion limit. *SIAM J. Sci. Comput.*, 31(1):334–368, 2008.

[53] A. Mellet. Fractional diffusion limit for collisional kinetic equations: A moments method. *Indiana Univ. Math. J.*, 59:1333–1360, 2010.

[54] A. Mellet and S. Merino-Aceituno. Anomalous energy transport in FPU-β chain. *Journal of Statistical Physics*, pages 1–39, 2015.

[55] A. Mellet, S. Mischler, and C. Mouhot. Fractional diffusion limit for collisional kinetic equations. *Arch. Ration. Mech. Anal.*, 199:493–525, 2011.

[56] D. A. Mendis and M. Rosenberg. Cosmic dusty plasma. *Annu. Rev. Astron. Astrophys.*, 32(1):419–463, 1994.

[57] L. Mieussens. On the asymptotic preserving property of the unified gas kinetic scheme for the diffusion limit of linear kinetic models. *J. Comput. Phys.*, 253:138–156, 2013.

[58] G. Naldi and L. Pareschi. Numerical schemes for kinetic equations in diffusive regimes. *Appl. Math. Lett.*, 11(2):29 – 35, 1998.

[59] G. Naldi and L. Pareschi. Numerical schemes for hyperbolic systems of conservation laws with stiff diffusive relaxation. *SIAM J. Numer. Anal.*, 37(4):1246–1270, 2000.

[60] G. Naldi, L. Pareschi, and G. Toscani, editors. *Mathematical Modeling of Collective Behavior in Socio-Economic and Life Sciences*. Birkhäuser Boston, Boston, 2010.

[61] E. Nasreddine and M. Puel. Diffusion limit of Fokker-Planck equation with heavy tail equilibria. *ESAIM: M2AN*, 49(1):1–17, 2015.

[62] L. Pareschi and G. Toscani. *Interacting Multiagent Systems: Kinetic equations and Monte Carlo methods*. Number 9780199655465 in OUP Catalogue. Oxford University Press, May 2013.

[63] V. Pareto. *Cours d'Économie Politique*. Lausanne and Paris, 1897.

[64] F. Poupaud. Diffusion approximation of the linear semiconductor Boltzmann equation: analysis of boundary layers. *J. Asympt. Anal.*, 4(4):293–317, 1991.

[65] C. Pozrikidis. *The Fractional Laplacian.* Chapman and Hall/CRC, 2016.

[66] M. Pulvirenti, C. Saffirio, and S. Simonella. On the validity of the Boltzmann equation for short range potentials. *Reviews in Mathematical Physics*, 26(02):1450001, 2014.

[67] J. Saragosti, V. Calvez, N. Bournaveas, B. Perthame, A. Buguin, and P. Silberzan. Directional persistence of chemotactic bacteria in a traveling concentration wave. *Proceedings of the National Academy of Sciences*, 108(39):16235–16240, 2011.

[68] D. Summers and R. M. Thorne. The modified plasma dispersion function. *Fluids B*, 3(8):1835–1847, 1991.

[69] L. Wang and B. Yan. An asymptotic-preserving scheme for linear kinetic equation with fractional diffusion limit. *J. Comput. Phys.*, 312:157 – 174, 2016.

[70] E. Wigner. *Nuclear reactor theory.* AMS, Providence, RI, 1961.

[71] K. Xu. A gas-kinetic BGK scheme for the Navier-Stokes equations and its connection with artificial dissipation and Godunov method. *J. Comput. Phys.*, 171:289–335, 2001.

Resumé

L'objet de cette thèse est la construction de schémas numériques pour les équations cinétiques dans différents régimes de diffusion anormale. Comme le modèle devient raide en s'approchant du modèle asymptotique, les méthodes numériques standard deviennent coûteuses dans ce régime. Les schémas *Asymptotic Preserving* (AP) ont été introduits pour pallier à cette difficulté. Ils sont en effet stables le long de la transition du régime mésoscopique au régime microscopique.

Dans le premier chapitre, nous considérons le cas d'une distribution d'équilibre qui est une fonction à queue lourde et dont le moment d'ordre 2 est infini. Le poids important des grandes vitesses de l'équilibre fait tomber la limite de diffusion usuelle en défaut, et on montre que le modèle asymptotique est une équation de diffusion fractionnaire. En nous basant sur une analyse asymptotique formelle de la convergence vers le modèle limite, nous construisons trois schémas AP pour le problème. La discrétisation en vitesse est discutée afin de prendre en compte correctement les grandes vitesses, et nous montrons que le troisième schéma est en outre uniformément précis au cours de la transition vers le régime microscopique.

Dans le chapitre 2, nous étendons ces résultats au cas d'une fréquence de collision dégénérée en 0 qui mène aussi à une équation de diffusion fractionnaire. Nous adaptons ensuite ces méthodes numériques au cas d'une limite de diffusion normale avec scaling en temps anormal dans l'équation cinétique dans le chapitre 3. Dans ce cadre, la lenteur de la convergence vers le modèle asymptotique rend nécessaire une adaptation de l'approche AP des chapitres précédents. Enfin, le chapitre 4 présente un schéma AP pour l'équation cinétique dans le cas heavy-tail du chapitre 1 lorsque l'opérateur de collision est non-local.

Abstract

In this thesis, we construct numerical schemes for kinetic equations in some anomalous diffusion regimes. As the model becomes stiff when reaching the asymptotic model, the standard numerical methods become costly in this regime. *Asymptotic Preserving* (AP) schemes have been designed to overcome this difficulty. Indeed, they are uniformly stable along the transition from the mesoscopic regime to the microscopic one.

In the first chapter, we study the case of a heavy-tailed equilibrium distribution, with infinite second order moment. The importance of the high velocities in the equilibrium makes the classical diffusion limit fail, and one can prove that the asymptotic model is a fractional diffusion equation. We construct three AP schemes for this problem, based on a formal asymptotic analysis of the convergence towards the limit model. The discretization of the velocities is then discussed to take into account the high velocities. Moreover, we prove that the third scheme enjoys the stronger property of being uniformly accurate along the convergence towards the microscopic regime.

In chapter 2, we extend these results to the case of a degenerated collision frequency, also leading to a fractional diffusion limit. In chapter 3, these methods are then adapted to the case of a classical diffusion limit with anomalous time scale in the kinetic equation. In this case, an adaptation of the AP approach of the previous chapter is needed, because of the slow convergence rate of the kinetic equation towards the limit model. Eventually, a AP scheme for kinetic equation with heavy-tailed equilibria and non local collision operator is presented in chapter 4.